

**THE PATHOGENESIS OF
CLASSICAL HODGKIN LYMPHOMA:
INVESTIGATION OF POSSIBLE VIRAL PATHOGENS
AND RECURRENT CHROMOSOMAL IMBALANCES**

Katherine Sarah Wilson BSc (Hons), MPhil

A thesis submitted in partial fulfilment of the requirements for the degree of:

Doctor of Philosophy

Institute of Comparative Medicine

University of Glasgow

August 2008

©Katherine Wilson 2008

DECLARATION

This thesis is my own work and has not been submitted in any previous application for a degree.

Sources of information have been specifically acknowledged.

Katherine S Wilson

ABSTRACT

Hodgkin lymphoma (HL) is a malignant lymphoma that is diagnosed mostly in young adults, and is the second most common malignancy to affect this age group. This disease is subdivided into two entities with different aetiologies: classical HL (cHL) (~95% of cases) and nodular lymphocyte-predominant HL. In Europe, ~82% of young adults with cHL are non-Epstein-Barr virus-associated and epidemiological studies have suggested that a common infectious agent may play a key role in the aetiology of these cases. The molecular biology of HL is not well understood, primarily due to the low number of Hodgkin and Reed-Sternberg (HRS) cells present within these tumours. However, recently developed techniques for the selection and micromanipulation of single HRS cells from tumours, and the development of molecular cytogenetic techniques (i.e. array-comparative genomic hybridisation (CGH)) are overcoming these difficulties.

To investigate a potential candidate virus, DNA samples from cHL biopsies were screened for the measles virus (MV) and polyomaviruses (PyV), using immunohistochemistry and highly sensitive PCR assays. Chromosomal imbalances in six well-established cHL-derived cell lines and a cHL case were analysed by array-CGH. To obtain sufficient DNA for array-CGH from the cHL case, single HRS cells were isolated using laser microdissection. DNA was extracted then amplified by degenerate oligonucleotide primer polymerase chain reaction.

MV and PyV genomes were not detected within cHL biopsies. Recurrent chromosomal imbalances were confirmed within the cHL-derived cell lines and cHL

case, in addition to several novel imbalances. This is the first time that a cHL case has been analysed by array-CGH.

ACKNOWLEDGEMENTS

I would like to express my gratitude to my supervisors Professor Ruth Jarrett (Leukemia Research Fund (LRF) Virus Centre, University of Glasgow) and Dr Sabrina Tosi (Brunel University) for allowing me the opportunity to undertake this degree, and for their guidance throughout my period of study at Glasgow University.

The completion of this investigation would not have been possible without the assistance of my colleagues at the LRF Virus Centre in Glasgow. I would particularly like to thank Dr Alice Gallagher, Mrs June Freeland and Miss Lesley Shield, for their invaluable knowledge and expertise on PCR techniques, immunohistochemistry and laser microdissection.

I performed all the array-CGH experiments at the Wellcome Trust Centre for Human Genetics in Oxford under the guidance of Dr Samantha Knight and Dr Regina Regan. I thoroughly enjoyed working in the Neurogenetics & Psychiatric Genetics Laboratory and would like to thank Sam and her group for making me feel so welcome during these visits.

To all my colleagues in the Glasgow office of CMG, I would like to express my thanks for all the encouragement and support they have given me throughout the writing up of this thesis.

Finally, a huge thank you to my family and friends who, throughout my studies, have provided encouragement, support, sustenance and laughter.

LIST OF CONTENTS

	Page number	
List of Figures	xii	
List of Tables	xiv	
Abbreviations	xvi	
CHAPTER 1	INTRODUCTION	1
1.1	Hodgkin Lymphoma	2
1.2	Classification of Hodgkin Lymphoma	4
1.2.1	NLPHL	5
1.2.2	NSHL	5
1.2.3	MCHL	6
1.2.4	LDHL	6
1.2.5	LRCHL	6
1.3	Origin and clonality of HRS cells	7
1.3.1	cHL-derived cell lines	7
1.3.2	The origin of HRS cells	7
1.3.3	The phenotype of HRS cells	11
1.3.4	Anti-apoptotic mechanism of the HRS cells	12
1.3.4.1	CD95 death receptor pathway	12
1.3.4.2	The NF κ B signalling pathway	13
1.4	Epstein-Barr Virus	15
1.4.1	Lytic and latent infection of EBV	16
1.4.2	EBV and HL	19
1.4.3	Epidemiology of HL	21
1.4.4	Epidemiology of EBV and HL	23
1.4.5	Non-EBV-associated HL cases	27
1.5	Classical cytogenetics	30
1.5.1	Chromosome banding techniques	30
1.5.2	Classical cytogenetics and HL	31
1.6	Molecular cytogenetics	32

1.6.1	In situ hybridisation	32
1.6.2	Flourescence in situ hybridisation	33
1.6.3	FICTION analysis	34
1.6.4	Comparative Genomic Hybridisation	35
1.6.4.1	Investigation of lymphoma using CGH	39
1.6.4.2	Limitations of CGH	40
1.6.5	Whole genome amplification	41
1.6.5.1	Linker-adaptor PCR	41
1.6.5.2	Primer-extension pre-amplification PCR	42
1.6.5.3	Degenerate oligonucleotide-primed-PCR	42
1.6.5.4	Multiple displacement amplification	43
1.6.6	Whole genome amplification, CGH and lymphomas	44
1.6.7	Laser microdissection and whole genome amplification	45
1.6.8	CGH analysis of classical HL	45
1.6.9	Array-CGH	49
1.7	Aims of thesis	51
CHAPTER 2	MATERIALS AND METHODS	52
2.1	Materials	53
2.2	Methods	53
2.2.1	Tissue collection	53
2.2.2	Tissue biopsy processing	54
2.2.3	Preparation of viable cell suspensions	54
2.2.4	Cell counting	55
2.2.5	Enrichment of mononuclear cells from lymph nodes	55
2.2.6	Storage of viable mononuclear cell suspensions	55
2.2.7	Cell lines	56
2.2.7.1	Recovery and maintenance of cell lines	56
2.2.8	Preparation of cytopsin slides	58
2.2.9	CD30-staining using the ABCComplex Method	58
2.2.10	Laser microdissection from cytopsin slides	59
2.2.11	Total RNA extraction	60
2.2.12	DNA extraction from tumour samples or cell lines	61

2.2.13	Ethanol precipitation of DNA	62
2.2.14	Quantification of nucleic acids	63
2.2.15	Polymerase chain reaction	63
2.2.15.1	DOP-PCR	63
2.2.16	Analysis of PCR products	66
2.2.16.1	Agarose gel electrophoresis	66
2.2.16.2	Polyacrylamide gel electrophoresis	67
2.2.17	Cloning and plasmid preparations	67
2.2.18	Nucleotide sequence analysis	68
CHAPTER 3	NO EVIDENCE FOR A DIRECT ASSOCIATION BETWEEN MEASLES VIRUS AND HODGKIN LYMPHOMA	69
3.1	Introduction	70
3.2	Materials and methods	76
3.2.1	Case selection	76
3.2.2	Immunohistochemistry	79
3.2.3	Reverse Transcription (RT)-PCR	80
3.2.4	Conventional PCR	81
3.2.5	Quantitative real-time PCR	84
3.3	Results	86
3.3.1	Epidemiology	86
3.3.2	Immunohistochemistry	86
3.3.3	Reverse Transcriptase (RT)-PCR	87
3.4	Discussion	93
CHAPTER 4	NO EVIDENCE OF POLYOMAVIRUS GENOMES IN HODGKIN LYMPHOMA	95
4.1	Introduction	96
4.2	Materials and methods	102
4.2.1	Clinical samples	102
4.2.2	Quantitative real-time PCR analysis	104
4.2.3	Degenerate PCR	106

4.2.3.1	Design of polyomavirus degenerate PCR primers	106
4.2.3.2	Degenerate PCR methodology	110
4.2.3.3	Assay specificity and sensitivity	111
4.2.3.4	Hodgkin lymphoma samples	111
4.2.3.5	Cloning of degenerate PCR products for sequence analysis	112
4.3	Results	113
4.4	Discussion	116
CHAPTER 5	INVESTIGATION OF GENOME IMBALANCES AND GENE EXPRESSION IN CHL-DERIVED CELL LINES	118
5.1	Introduction	119
5.2	Methods	122
5.2.1	Cell lines	122
5.2.2	RNA and DNA extraction	122
5.2.3	Preparation of samples for array-CGH	122
5.2.4	Labelling of genomic DNA by random priming	123
5.2.5	Array fabrication and processing	124
5.2.6	Array-Comparative Genome Hybridisation	125
5.2.7	Post-hybridisation washes	126
5.2.8	Image acquisition and data analysis	126
5.2.9	Dye-swap hybridisation	131
5.2.10	Gene expression array hybridisation	132
5.2.11	Gene expression array analysis	133
5.2.12	Correlation between array-CGH and gene expression array analysis	133
5.3	Results	134
5.3.1	Array-CGH analyses	134
5.3.2	Gene expression array analysis	161
5.3.3	Correlation of array-CGH and gene expression array analyses	164
5.4	Discussion	167

CHAPTER 6	ANALYSIS OF PRIMARY HRS CELLS BY ARRAY-CGH	177
6.1	Introduction	178
6.2	Optimisation experiments	181
6.2.1	Validation of DOP-PCR products for use in array-CGH	181
6.2.1.1	The GF-D8 cell line	181
6.2.1.2	Array-CGH performed using the GF-D8 cell line	182
6.2.2	Comparison of different fixation and staining methods prior to array-CGH	187
6.2.3	Comparison of array-CGH using different cell numbers	189
6.2.3.1	Array-CGH of cHL-samples using 200 laser microdissected HRS cells	189
6.2.3.2	Validation of 1000 cell-DOP-amplified HRS DNA for array-CGH	195
6.2.3.3	Validation of 6000 cell-DOP-amplified HRS DNA for array-CGH	197
6.3	Array-CGH of a cHL case sample	198
6.3.1	Preparation of DNA sample from case# 6992	198
6.3.2	Results	198
6.4	Discussion	205
CHAPTER 7	FINAL DISCUSSION	209
7.1	The search for potential pathogenic agents for cHL	210
7.2	Recurrent chromosomal imbalances in cHL	212
7.3	Conclusions	215
APPENDICES		216
Appendix A	Combined hybridisation charts of cHL-derived cell lines	217
Appendix B	Chromosome regions containing known functional genes in which gains were identified in three or more cHL-derived cell lines.	223

Appendix C	Chromosome regions containing known functional genes in which losses were identified in three or more cHL-derived cell lines.	225
Appendix D	Gene expression array analysis results for the EBV-positive cHL cell line KMH2	228
Appendix E	Gene expression array analysis results for the EBV-positive cHL cell line L428	230
Appendix F	Gene expression array analysis results for the EBV-positive cHL cell line L591	232
	Reference list	234
	Publications from these studies	275

LIST OF FIGURES

		Page number
Figure 1.1	Cellular origin and B-cell differentiation within secondary lymphoid organs	10
Figure 1.2	The four disease model of HL	26
Figure 1.3	CGH on both metaphase spreads and arrays	38
Figure 1.4	Summary of conventional CGH analysis of HRS cells isolated from cHL biopsies	48
Figure 3.1	Schematic diagram of the measles virus and its RNA genome	73
Figure 3.2	Detection of measles virus (MV) by immunohistochemistry	87
Figure 3.3	Quantitative real-time PCR results for the GAPDH assay.	89
Figure 3.4	Quantitative real-time PCR results for the measles virus (MV) hemagglutinin assay	90
Figure 3.5	Quantitative real-time PCR results for the measles virus (MV) nucleoprotein assay	91
Figure 3.6	Quantitative real-time PCR results for the measles virus (MV) haemagglutinin assay showing amplification curves for replicates of serial 10-fold dilutions of cDNA extracted from MV-infected HOS cells	92
Figure 4.1	Conserved amino acid motifs within the large T antigen of polyomaviruses	108
Figure 4.2	Electropherograms from GeneScan analysis of degenerate PCR products	115
Figure 5.1	Schematic diagram of the array-CGH analysis process	130
Figure 5.2	The combined hybridisation charts from array-CGH of HDLM2 DNA versus IM9 DNA	135
Figure 5.3	Ideogram depicting locations of clones representing gains in chromosomal material within each cHL-derived cell lines	147
Figure 5.4	Ideogram depicting locations of clones representing losses in chromosomal material within each cHL-derived cell lines	151

Figure 5.5	Schematic diagrams depicting smallest regions of overlap across three or more cHL-derived cell lines	155
Figure 6.1	Array-CGH analysis results obtained using non-amplified and DOP-amplified genomic DNA of the GF-D8 cell line	183
Figure 6.2	Scatterplot of the array-CGH data from both the non-amplified and amplified GF-D8 DNA	184
Figure 6.3a	DOP-PCR products from amplification of laser microdissected IM9 cells stained with either CD30 monoclonal antibody or the DiffQuik staining system	188
Figure 6.3b	Combined and ethanol precipitated DOP-PCR products (500 ng) from 200 CD30-stained or 200 DiffQuik-stained laser microdissected cells	188
Figure 6.4	Hybridisation chart from the array-CGH of 200 cells-DOP-amplified case #6992 DNA versus 200 cells-DOP-amplified IM9 DNA	190
Figure 6.5	Four array-CGH analyses of laser microdissected, DOP-amplified IM9 DNA versus laser microdissected, DOP-amplified-IM9 DNA	194
Figure 6.6a	Array-CGH analysis of 1000 cells-DOP-amplified HDLM2 DNA versus 1000 cells-DOP-amplified IM9 DNA	196
Figure 6.6b	Array-CGH analysis of non-amplified HDLM2 DNA versus non-amplified IM9 DNA	196
Figure 6.7	Hybridisation chart of 6000 cells-DOP-amplified HDLM2 DNA versus 6000 cells-DOP-amplified IM9 DNA.	197
Figure 6.8	Array-CGH analysis of 6000 cells-DOP-amplified DNA from HRS cells of the cHL case 6992 versus 6000 cells-DOP-amplified DNA from IM9 cells.	200
Figure 6.9	Array-CGH chart showing sliding averages of 6000 cells-DOP-amplified 6992 DNA versus 6000 cells-DOP-amplified IM9 DNA	200

LIST OF TABLES

		Page number
Table 1.1	The Ann Arbor staging system for HL	3
Table 1.2	The four disease model of cHL	25
Table 2.1	Details of cell lines used in array-CGH and gene expression array analyses	57
Table 3.1	Details of patients in case series 1	78
Table 3.2	Details of patients in case series 2	78
Table 3.3	Conventional PCR primers	83
Table 3.4	Quantitative real-time PCR primers and probes	85
Table 4.1	Patient characteristics	103
Table 4.2	Quantitative real-time PCR (TaqMan®) primers and probes	105
Table 4.3	Degenerate PCR primers for detection of polyomaviruses	109
Table 5.1	Chromosomal regions in each cHL-derived cell line where a gain of DNA has been identified by array-CGH	137
Table 5.2	Chromosomal regions in each cHL-derived cell line where a loss of DNA has been identified by array-CGH	139
Table 5.3	Selected genes of interest in newly identified regions of gain	143
Table 5.4	Selected genes of interest in newly identified regions of loss	144
Table 5.5	Selected genes with known function that are located within gained chromosome regions identified as smallest regions of overlap (SROs) in three or more cells lines	156
Table 5.6	Selected genes with known function that are located within lost chromosome regions identified as smallest regions of overlap (SROs) in three or more cells lines	158
Table 5.7	Genes which are upregulated or downregulated within all three cHL-derived cell lines that were screened by gene expression array analysis	162
Table 5.8	Differentially expressed genes in the EBV-negative cHL-derived cell lines KMH2 and L428	163
Table 5.9	Genes within regions of chromosomal imbalance, identified by array-CGH analysis, which were also differentially	166

	expressed in gene expression array analysis	
Table 6.1	Chromosomal rearrangements present in the GF-D8 cell line, identified by multiplex FISH and convention196a CGH	182
Table 6.2	Comparison of the gains identified by CGH to chromosomes, array CGH of non-amplified DNA and array CGH of DOP amplified DNA	185
Table 6.3	Comparison of the losses identified by CGH to chromosomes, array CGH of non-amplified DNA and array CGH of DOP amplified DNA	186
Table 6.4	The percentage of probes with ratios lying outwith the threshold range <0.7 and >1.3 , and the percentage of clones excluded from analysis due to $SD >0.2$	195
Table 6.5	Gains and losses of chromosomal regions identified within cHL case #6992 DNA	201
Table 6.6	Selected genes with known function in newly identified regions of gain	202
Table 6.7	Selected genes of known function in newly identified regions of loss	204

ABBREVIATIONS

ALL	Acute lymphoblastic leukaemia
BAC	Bacterial artificial chromosome
BCR	B-cell receptor
BLAST	Basic Local Alignment Search Tool
Bp	Base pairs
cDNA	Complementary deoxyribonucleic acid
CGH	Comparative genomic hybridisation
cHL	Classical Hodgkin lymphoma
CI	Confidence interval
CO ₂	Carbon dioxide
Cy3	Cyanine 3
Cy5	Cyanine 5
dATP	2'-Deoxyadenosine 5'-triphosphate
dCTP	2'-Deoxycytidine 5'-triphosphate
dGTP	2'-Deoxyguanosine 5'-triphosphate
dNTP	2'-Deoxynucleoside 5'-triphosphate
DNA	Deoxyribonucleic acid
DOP	Degenerate oligonucleotide primer
EBER	EBV-encoded RNA
EBNA	EBV-determined nuclear antigen
EBV	Epstein-Barr virus
FICTION	Fluorescence immunophenotyping and interphase cytogenetics as a tool for the investigation of neoplasms
FISH	Fluorescence <i>in situ</i> hybridisation
GC	Germinal Centre
H	Haemagglutinin
HL	Hodgkin lymphoma
HOS	Human osteosarcoma
HRS	Hodgkin and Reed-Sternberg
Ig	Immunoglobulin
IHC	Immunohistochemistry
IκB	I kappa B

IKK	I kappa B kinase
IM	Infectious mononucleosis
ISH	<i>In situ</i> hybridisation
Kb	Kilobase
L&H	Lymphocytic and histiocytic
LCL	Lymphoblastoid cell line
LDHL	Lymphocyte-depleted Hodgkin lymphoma
LMD	Laser microdissection
LMP1	Latent membrane protein 1
LPA	Lymphotropic papovavirus
LRCHL	Lymphocyte-rich Hodgkin lymphoma
LRF	Leukemia Research Fund
µl	Microlitres
M	Matrix
MAPH	Multiplex amplification and probe hybridisation
MCHL	Mixed cellularity Hodgkin lymphoma
MDA	Multiple displacement amplification
M-FISH	Multiplex fluorescence <i>in situ</i> hybridisation
mins	Minutes
ml	Millilitres
MLPA	Multiplex ligation-dependent probe amplification
mRNA	Messenger ribonucleic acid
MV	Measles virus
NP	Nucleoprotein
NCBI	National Center for Biotechnology Information
NFκB	Nuclear factor kappa B
NHL	Non-Hodgkin's lymphoma
NLPHL	Nodular lymphocyte-predominant Hodgkin lymphoma
NOS	Not otherwise specified
NSHL	Nodular sclerosis Hodgkin lymphoma
O/N	Overnight
PCNSL	Primary central nervous system lymphomas
PCR	Polymerase chain reaction

PEP-PCR	Primer-extension pre-amplification polymerase chain reaction
PyV	Polyomaviruses
QRT-PCR	Quantitative real-time polymerase chain reaction
RCA	Rolling circle amplification
REAL	Revised European-American Classification of Lymphoid Neoplasms
RMA	Robust multi-chip average
RNA	Ribonucleic acid
RP	Rank products
RS	Reed Sternberg
RT-PCR	Reverse-transcription polymerase chain reaction
SAGE	Serial analysis of gene expression
SD	Standard deviation
SHM	Somatic hypermutation
SNEHD	Scottish and Newcastle Epidemiological Study of Hodgkin's Disease
SNLG	Scotland and Newcastle Lymphoma Group
SRO	Smallest region of overlap
TCR	T-cell receptor
TNFR	Tumour necrosis factor receptor
tRNA	Total ribonucleic acid
U	Units
WGA	Whole genome amplification
WHO	World Health Organization
YAC	Yeast artificial chromosome

CHAPTER 1

INTRODUCTION

1.1 HODGKIN LYMPHOMA

Hodgkin lymphoma (HL) is a malignant disease, mainly affecting lymph nodes, which was first described in 1832 (Hodgkin 1832). The majority of HL patients present with lymphadenopathy, typically in the supraclavicular or lower cervical region. In the absence of treatment, the disease follows a predictable course spreading from one group of lymph nodes to those adjacent in a systematic process. Mediastinal masses are frequent and patients often present with chest discomfort and coughing or breathlessness. Approximately a quarter of HL cases manifest systemic B symptoms including fatigue, weight loss, intermittent fevers and itchy skin associated with night sweats. Diagnosis is usually made by histological examination of an excisional biopsy of an enlarged lymph node. The disease is then staged using the Ann Arbor staging system (see Table 1.1) developed in 1971 (Carbone et al 1971) and modified in 1989 (Lister et al 1989). This system defines the extent of disease progression and helps predict prognosis and direct treatment. Four stages are described followed by the letter A or B, indicating the absence (A) or presence (B) of B symptoms. Treatment is by chemotherapy, radiotherapy or a combination of both. Autologous stem cell transplantation is widely recommended for cases where first-line high-dose chemotherapy has not been successful and there is a high risk of disease progression or relapse (Josting et al 2000; Pavone et al 1997). If left untreated HL is fatal, but with early diagnosis and the use of highly effective treatment strategies it is now curable in most cases (Klimm et al 2005).

Table 1.1. The Ann Arbor staging system for HL (Carbone et al 1971).

STAGE	SYMPTOMS
1	Involvement of one lymph nodes or lymphoid structure
2	Involvement of two or more lymph nodes on the same side of the diaphragm
3	Involvement of lymph nodes on both sides of the diaphragm
4	Involvement of extranodal site(s), with or without associated lymph node involvement

Diagnosis rests on the identification of typical large multinucleated cells, the Reed-Sternberg (RS) cells, surrounded by a heterogeneous cellular infiltrate composed of lymphocytes, histiocytes, eosinophils, plasma cells and polymorphonuclear leukocytes. RS cells measure 20-60µm in diameter and have at least two nuclei with prominent acidophilic or amphophilic nucleoli (Pileri et al 2002). Hodgkin (H) mononuclear cells display similar cytological features to RS cells, and these cells are collectively referred to as HRS cells (Pileri et al 2002). Cells with morphology similar to RS cells have been identified in both infectious mononucleosis (IM) and non-Hodgkin's Lymphoma (NHL), but the presence of the specific heterogeneous cellular background is unique to HL. Unusually for human lymphomas, the neoplastic cells make up a very low proportion (<1%) of the tumour cell population and this, in the past, has restricted a detailed investigation of these cells (Gruss and Kadin 1996; Stein et al 1997; Cossman et al 1998).

Abundant T-lymphocytes are found within the reactive cellular infiltrate surrounding the HRS cells. These are thought to reflect a non-specific response to the release of cytokines by HRS cells. T-lymphocytes express early activation markers and have cytokine production and immunophenotypic properties characteristic of a Th2-type response (Poppema and van den Berg 2000).

1.2 CLASSIFICATION OF HODGKIN LYMPHOMA

The first comprehensive classification of HL, then known as Hodgkin's disease, was the Rye Classification (Lukes and Butler 1966). The proportion of HRS cells in the tumour cell population and the nature of the infiltrate allowed four HL subgroups to be identified: nodular sclerosis (NSHL), mixed cellularity (MCHL), lymphocyte-depleted (LDHL) and lymphocyte-predominant HL.

The International Lymphoma Study Group was founded in Berlin in 1990 and published the Revised European-American Classification of Lymphoid Neoplasms (REAL) in 1994 (Harris et al 1994). This system took into account the morphological, immunological, molecular and genetic components of lymphomas and leukaemias and also recognised entities commonly diagnosed in routine practice. The three major classified groups were HL, B-cell lymphomas/leukaemias and T-cell lymphomas/leukaemias. Diseases were initially classified by their cell of origin and then further subdivided by their histological grade. This classification was expanded upon by the Society for Hematopathology and the European Association of Hematopathologists for the World Health Organisation (WHO) (Harris et al 2000). The WHO classification encompasses haematopoietic and lymphoid neoplasms and is in global use. Two distinct groups of HL are characterised in this classification, classical HL (cHL) and nodular lymphocyte-predominant HL (NLPHL), with the former being further subdivided into NSHL, MCHL, LDHL and lymphocyte-rich classical HL (LRCHL). NLPHL and cHL differ in the origin of their tumour cells, their clinical behaviour and their immunophenotype (Nogova et al 2006).

Immunophenotyping is an important diagnostic tool for differentiating between these two HL groups. In cHL, HRS cells are usually positive for CD15 and CD30, and either positive or negative for CD20 (Schmid et al 1991). In NLPHL cells are usually negative for CD15 and CD30, but positive for CD20 (Anagnostopoulos et al 2000).

1.2.1 NLPHL

NLPHL is regarded as a rare type of B-cell lymphoma histologically distinct from cHL due to the presence of lymphocytic and histiocytic (L&H) cells, also known as ‘popcorn’ cells, in a background cellular infiltrate of predominantly B-lymphocytes. L&H cells are smaller than HRS cells and have less pronounced nucleoli. They display a unique immunophenotype (i.e. CD15-, CD20+, CD30-, CD45+), which is different from that of classical HRS cells (i.e. CD15+, CD20-, CD30+, CD45-). This subgroup accounts for approximately 8% of all HL cases (Jarrett et al 2003). NLPHL will not be discussed further in this thesis since cHL is the focus of this study.

1.2.2 NSHL

NSHL is the most prevalent HL-type accounting for approximately 60% of all HL (Holman et al 1983; Jarrett et al 2003). Most at risk are individuals aged 15-34 years, with neither sex predominating. Diagnosis of this disease is by the identification of nodular areas separated by sclerotic bands, a predominance of T-lymphocytes in the reactive cell population, lacunar cells and a low number of HRS cells. Lacunar cells are RS cell variants observed in NSHL; they are multilobular in shape with large nuclei (Hansmann and Kaiserling 1982). Further categorisation of NSHL cases into nodular sclerosis grade 1 (NS-1) and grade 2 (NS-2) with good and poor prognosis, respectively, is advocated by some workers (Haybittle et al 1985).

1.2.3 MCHL

MCHL accounts for 20% of HL cases, with no age group being at particular risk (Jarrett et al 2003). Histologically there is a heterogeneous cell population of plasma cells, neutrophils, eosinophils and small lymphocytes (predominantly T-cells) clustered around HRS cells (Patsouris et al 1989).

1.2.4 LDHL

The least common (0.8%), but most aggressive, HL subtype is LDHL (Pileri et al 2002). This preferentially affects the older age group (>49 years of age) and has the shortest median survival period. Patients usually present with B symptoms and are often in stage III-IV. Histopathologically, tumour tissue exhibits cellular depletion with disordered fibrosis and a high variability in HRS cell number. Many cases previously classified as LDHL are now thought to be NHLs, and this subtype is seldom diagnosed in current practice.

1.2.5 LRCHL

A fourth cHL subtype was first introduced as a provisional entity in the REAL (Harris et al 1994) then as a distinct category in the WHO classification (Harris et al 2000). This cHL subtype has similar histological characteristics to NLPHL, but an HRS cell phenotype (CD20-, CD30+, CD15+) and morphology identical to that seen in NSHL and MCHL (Anagnostopoulos et al 2000; Pileri et al 2002). B-cells are the predominant lymphocytes within the cellular infiltrate. LRCHL cases account for 2.6% of HL (Jarrett et al 2003). The majority of cases are older adults. LRCHL shares many common features with NLPHL, but a lower frequency of stages I-II and splenic infiltration are common (Pileri et al 2002).

1.3 ORIGIN AND CLONALITY OF HRS CELLS

1.3.1 cHL-derived cell lines

The establishment of permanent cell lines has allowed the biological characterisation of many human neoplasms, but only a few cell lines have been derived from cHL cases: CO, HDLM2, HDMyZ, Ho, KMH2, L1236, L428, L540 and L591. The origins of some are, however, dubious (eg HDMyZ) and some (eg CO) have been reported to have been cross-contaminated with the T-cell acute lymphoblastic leukaemia (ALL) cell line, CCRF-CEM (Drexler 1993; Drexler et al 1999). The remainder have generally been derived from body fluids extracted from patients with end-stage disease. Only the L1236 cell line has been shown to definitely be derived from HRS cells (Kanzler et al 1996a; Wolf et al 1996).

1.3.2 The origin of HRS cells

Analysis of established cHL-derived cell lines has shown that HRS cells do not display specific lineage markers, and often coexpress markers typical for a number of different hematopoietic cell types. Developments in micromanipulation and microdissection procedures, coupled with single cell polymerase chain reaction (PCR) assays for immunoglobulin (Ig) gene rearrangements, have enabled the characterisation of single HRS cells. Ig gene rearrangements involve variable, diversity and joining regions and are unique to B-cells. These rearrangements are therefore distinct markers which can be used to determine the origin of B lineage cells and assess clonality. Several studies have identified Ig gene rearrangements within HRS cells, micromanipulated from cHL cases, which indicates that these cells originate from B-cells (Kanzler et al 1996b; Kuppers et al 1994; Marafioti et al 2000).

Germinal centres (GCs) are specialised microanatomical structures, within secondary lymphoid follicles, which develop from antigen-specific B-cells that have clonally expanded during immune responses (Thorbecke et al 1994). Upon entering the GC, B-cells automatically begin the cell death program and are only able to escape this process if they display key positive selection signals. They undergo several rounds of proliferation, somatic hypermutation (SHM) and selection in order to develop high affinity antigen receptors (see Figure 1.1). The process of SHM is known to take place in secondary lymphoid organs, within the dark zone of the GC, during T-cell-dependent immune responses (see Figure 1.1). SHMs are detectable in the majority of immunoglobulin gene rearrangements. Non-functional gene rearrangements, resulting from SHM, were identified within HRS cells micromanipulated from approximately 25% of cHL cases (Kanzler et al 1996b). Any GC B-cells acquiring non-functional gene rearrangements within the GC undergo apoptosis instead of differentiation, and do not develop into memory B-cells or plasma cells. The presence of SHMs in HRS cells suggested, therefore, that these cells may derive from preapoptotic B-cells that have gained crippling mutations preventing them from undergoing antigenic selection.

The expression of T-cell markers in a small proportion of HL cases suggested that some HRS cells could originate from T-cells (Marafioti et al 2000; Muschen et al 2000a; Seitz et al 2000). In one study HRS cells with a cytotoxic T-cell phenotype were isolated from 3 cHL cases (Muschen et al 2000a). Germline configuration of IgH and T-cell receptor (TCR)- β loci, and both Ig and TCR- β gene rearrangements were investigated. In two of the HL cases, cytotoxic T-cell markers were identified in the HRS cells and the authors suggested that these cells were derived from mature GC B cells that aberrantly express T-cell markers. In the third HL case a typical T-cell

gene rearrangement pattern was observed in the HRS cells indicating these cells were of T-cell origin. TCR α gene rearrangements were detected in 2 of 13 T-cell marker-expressing HL cases in a separate study (Marafioti et al 2000; Seitz et al 2000). The remaining 11 HL cases in this study were of B-cell in origin. This demonstrated that it is possible for HRS cells with a T-cell phenotype to have a B cell genotype, and that in the vast majority of cases HRS cells are derived from B-cells.

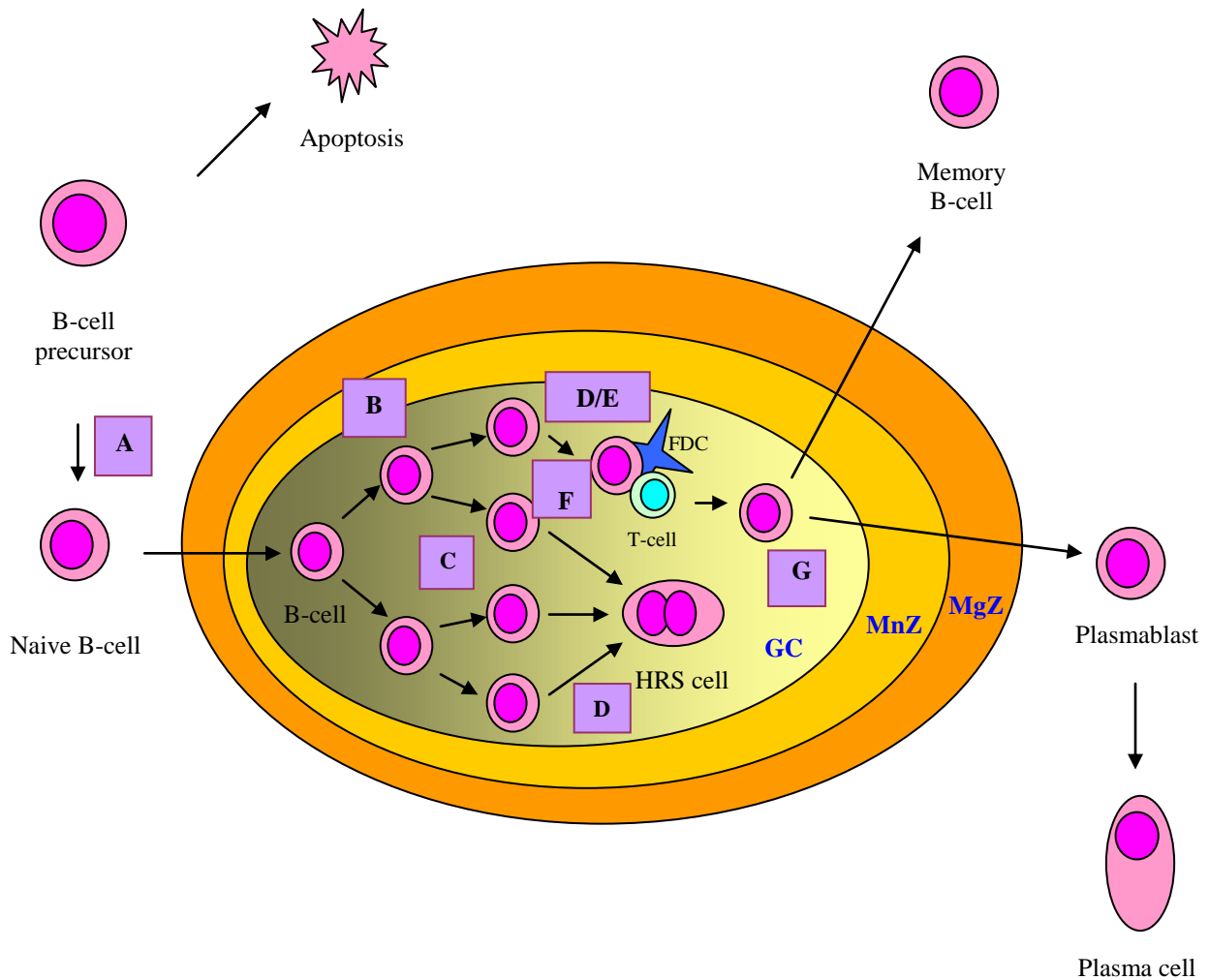


Figure 1.1: Cellular origin and B-cell differentiation within secondary lymphoid organs eg lymph nodes and spleen [adapted from (Kuppers and Hansmann 2005)]. The marginal zone (MgZ) contains post-germinal centre (GC) B-cells and naïve B-cells. The mantle zone (MnZ) is formed by naïve B-cells, which are replaced by proliferating B-cells and displaced to the outside of the primary B-cell follicle. Naive antigen-activated B-cells are transferred into primary B-cell follicles in lymph nodes, known as GC, where they become proliferating GC B-cells within the dark zone. A – V-region gene recombination in the bone marrow; B – clonal expansion; C – somatic hypermutation; D – mutations increasing antigen affinity; E – class switching; F – selection; G – differentiation.

From the unique morphology and the frequent identification of additional chromosomal copies in both the multinucleated RS and the mononucleated H cells, it was proposed that these cells may arise from fusion between a B-lymphocyte and a dendritic cell. A study of 5 cases of HL with two known rearranged IgH alleles sought to investigate this theory (Kuppers et al 2001). The majority of B-cells carry two rearranged IgH alleles whereas IgH alleles in non-B-cells show a germline configuration. The presence of additional IgH alleles in a germline configuration would therefore be consistent with a cell fusion between a B-cell and a non-B-cell. Single HRS cells were micromanipulated from selected HL cases and amplification reactions were performed to identify rearranged alleles in IgH and T-cell receptor β VDJ and DJ genes. None of the cases showed evidence of additional IgH or TCR β alleles to those already identified indicating that HRS cells do not represent fusions of B-cells.

1.3.3 The phenotype of HRS cells

HRS cells have a unique phenotype unrelated to any hematopoietic cell type. They usually express some T-cell markers, dendritic cell markers (eg fascin, thymus and activation-regulated chemokine (TARC)), myeloid cell markers (eg CD15), plasma cell markers (eg CD138) and some B-cell markers (eg Pax-5). Other B-cell markers (eg CD20, Oct-2) and B-cell receptors are rarely identified on HRS cells. Hence, the revelation that HRS cells originated from B-cells prompted a large gene expression study comparing gene expression profiles of HL-derived cell lines and normal B-cells (Schwering et al 2003a). A global downregulation of B-cell specific genes within HRS cells was revealed. It was suggested that the loss of B-cell gene expression could result in these cells not being recognised as B-cells and failing, therefore, to be

identified for apoptosis, the mechanism within the GC by which defective B-cells are normally apoptosed.

1.3.4 Anti-apoptotic mechanisms of the HRS cell

The mechanisms by which HRS cells escape apoptosis are therefore of interest for understanding the pathogenesis of cHL. The CD95 death receptor pathway, the nuclear factor kappa B (NF κ B) pathway, or Epstein-Barr virus (EBV) infection (see Section 1.4) may all protect from apoptosis by the following processes.

1.3.4.1 CD95 death receptor pathway

Death receptors, members of the tumour necrosis factor receptor (TNFR) superfamily, activate intracellular adaptor proteins and thereby start a signalling cascade that can result in cell apoptosis (Ricci-Vitiani et al 2000). CD95 (APO-1, Fas) is the most well studied death receptor which is expressed in the B cell lineage at the GC stage of differentiation and is directly involved in the negative selection of B cells by apoptosis in the GC. Functional mutations in the CD95 gene may therefore result in GC B cells becoming resistant to apoptosis. This has been shown in CD95-deficient *lpr* mice in which autoreactive B cells escape negative selection (Watanabe-Fukunaga et al 1992). Clonal mutations of CD95 have been detected in single micromanipulated HRS cells from two out of ten cHL cases, suggesting that the survival of these cells may be dependent upon CD95 malfunction (Muschen et al 2000b).

1.3.4.2 The NFκB signalling pathway

NFκB transcription factors regulate apoptosis and cytokine production, and are associated with cell proliferation, transformation and tumour development (Graham and Gibson 2005). The NFκB/RelA family consists of 5 members: p50, p52, p65 (RelA), c-Rel and RelB, which form various homodimers or heterodimers (Graham and Gibson 2005). In normal cells NFκB is maintained in the cytoplasm in an inactive form bound to I kappa B (IκB) (Karin 1999). In response to a stimulus, the IκB kinase (IKK) complex is activated and members of the IκB family are phosphorylated promoting their degradation. NFκB dissociates from IκB and translocates to the nucleus where it can activate target genes. Genes activated by NFκB are implicated in cell activation, the immune response and cellular resistance to apoptosis. Inducible NFκB responses are mediated mainly by the NFκB heterodimer p50/RelA.

Abundant constitutive NFκB p50/RelA activity has been identified in HRS cells from 7 cHL-derived cell lines, using electrophoretic mobility-shift assays and an anti-RelA antibody (Bargou et al 1996). Sections from NHL cases were included as negative controls in these assays. No RelA could be detected within these samples. *In situ* immunolabelling of sections from NSHL cases identified a high level of RelA activity in RS cells (Bargou et al 1997). Furthermore, 288 HL biopsies were assessed by tumour microarray analysis and 76% of these cases had nuclear expression of p65/RelA (Garcia et al 2003).

There are several possible mechanisms of NFκB activation in HL. HRS cells consistently express the surface receptor CD40, which regulates the NFκB activation

pathway. Many T-cells in surrounding HRS cells express the CD40 ligand. Signalling from CD40 and related molecules is mediated by TNFR-associated factors (TRAFs), which perform a central role in NF κ B activation. One study reported the detection of TRAFs 1, 2 and 3 at mRNA level within single HRS cells that had been micromanipulated from 6 HL cases (Messineo et al 1998). The EBV latent membrane protein 1 (LMP1) mimics an activated CD40 molecule and, through TRAFs, can initiate NF κ B activation (Devergne et al 1996).

Mutations within the C-terminus of NFKBIA (the I κ B α gene), resulting in truncated proteins, have been identified in two cHL-derived cell lines, KMH2 and L428 (Cabannes et al 1999; Emmerich et al 1999; Wood et al 1998). This region of the gene interacts with the RelA subunit of NF κ B, inhibiting its activity. A deletion of this region would therefore result in a loss of I κ B α activity and allow constitutive NF κ B activity. Emmerich *et al.* (1999) micromanipulated HRS cells from ten lymph node biopsies from HL patients and examined exons 2-6 of I κ B (Emmerich et al 1999). A point mutation, resulting in a stop codon, was located in the HRS cells of one of these cases. A later study also identified clonal deleterious somatic mutations, resulting in truncated I κ B α proteins, within HRS cells micromanipulated from two of three non-EBV-associated HL cases (Jungnickel et al 2000), but not in either of two EBV-associated HL cases. Further investigation suggested that the two mutations detected in one of these cases were located on different alleles implying that no full length I κ B α protein would be synthesised within these HRS cells. Nucleotide sequence analysis demonstrated that the truncated abnormal I κ B α proteins would lack the region of the ankyrin repeat and/or COOH-terminal proline, glutamate, serine and threonine-rich (PEST) domain required for interaction with NF κ B, thus preventing

I κ B association with NF κ B within HRS cells. A more detailed study from our group has shown clonal mutations of NFKBIA in 4/20 cases; however, bi-allelic inactivating mutations were detected in only one case and the mutation would not have affected function (Lake et al., submitted). All four cases were non-EBV-associated, but the majority of non-EBV-associated cases had wild-type NFKBIA genes.

1.4 EPSTEIN-BARR VIRUS

The EBV is a ubiquitous human gamma-herpesvirus, that establishes a persistent infection (Henle and Henle 1966). It is found in all human communities as a predominantly asymptomatic infection. Primary infection usually occurs in early childhood following oral transmission of the virus. Late infection during adolescence is a frequent occurrence in developed countries and in approximately 25-70% of such cases this results in IM (McAulay et al 2007).

The virus was first isolated from a Burkitt's lymphoma specimen (Henle and Henle 1966), and it is estimated that approximately 96% of these tumours contain EBV (Magrath 1990). EBV has also been associated with post-transplant lymphoproliferative disorders (Young et al 1989), some T-cell lymphomas, all nasopharyngeal carcinomas (Klein et al 1974), a small proportion (approximately 10%) of stomach cancers (Leoncini et al 1993) and a subset of HL cases (Levine et al 1971).

The EBV genome is a double-stranded DNA molecule (172kb), which encodes for more than 80 genes (Rickinson and Kieff 2001). In the virion, prior to infection, EBV DNA is an encapsidated linear molecule with cohesive tandem repeat sequence sites at each terminus. Upon infection of a host cell, these termini fuse to form covalently

closed circular episomes within the host cell nucleus. Each circularisation event generates different sized terminal repeat regions which represent a constant clonal marker for the virus and, therefore, for the infected cell (Rickinson and Kieff 2001). It is these terminal repeat fragments upon which the study of clonality in EBV-associated diseases is based.

1.4.1 Lytic and latent infection of EBV

EBV infection can be either lytic or latent. Lytic infection involves the production of viral particles and ultimately results in death of the host cell. In latent infection only a restricted group of latent genes is expressed and there is no production of infectious virus. The switch from latency to lytic infection is tightly controlled by the BZLF1 trans-activator protein (the BamHI fragment Z Epstein-Barr replication activator or ZEBRA) (Countryman et al 1987). This protein initiates the transcription of a set of genes essential for the production of new virus particles. A particular characteristic of latent infection is the expression of two highly abundant, non-polyadenylated small EBV-encoded transcripts (EBER1 and EBER2) present at a level of 10^5 - 10^7 copies per cell.

Three patterns of viral and cellular gene expression have been described in latent EBV infection of B-cells: latency I, II and III (Rowe et al 1992). The set of EBV-encoded proteins determining these patterns include three membrane proteins (LMP1, 2A and 2B) and six nuclear proteins (EBV-determined nuclear antigen (EBNA) 1, 2, 3a, 3b, 3c and LP). Burkitt's lymphomas and some Burkitt's lymphoma cell lines display the latency I pattern where only EBV-encoded EBNA-1 and EBERs are expressed. Latency II is characterised by a larger display of EBV gene expression consisting of

EBNA-1, LMP1, LMP2A, LMP2B and EBERs. This group of genes has been detected in nasopharyngeal carcinoma, some peripheral T-cell lymphomas and HL. The expression of the full set of nuclear (EBNA 1, 2, 3a, 3b, 3c and LP) and membrane (LMP1, 2A and 2B) proteins, along with EBERs, characterises the latency III pattern found in lymphomas of immunocompromised patients and EBV-transformed lymphoblastoid cell lines (LCLs). A consistent characteristic cellular phenotype is also observed for latency III with a high expression of the cell activation markers CD23, CD30, CD39 and CD70. The cellular adhesion molecules leukocyte-function-associated molecule 1 (LFA-1) and intercellular adhesion molecule 1 (ICAM-1) are usually absent or expressed at low levels on resting B cells, but are expressed at high levels during latency III EBV infection.

An understanding of the function of latent proteins is key to understanding the pathogenesis of EBV-associated tumours. The DNA binding protein EBNA1 is required for the maintenance and replication of the episomal EBV genome, and also negatively regulates its own expression (Nonkwelo et al 1996). It has been suggested that EBNA1 may play a direct role in oncogenesis after transgenic mice studies showed that B cell lymphomas develop when EBNA expression is directed to B cells in transgenic mice (Wilson et al 1996). EBNA2 plays an essential role in the transformation of B cells. It activates both cellular and viral genes, including LMP1 and LMP2. Of the EBNA3 proteins, EBNA3A and EBNA3C are required for B cell transformation *in vivo*, but EBNA3B is not essential. EBNA3B has been shown to induce the expression of vimentin and CD40 (Silins and Sculley 1994) and EBNA3C to induce the upregulation of cellular (e.g. CD21) and viral (i.e. LMP1) gene

expression (Allday and Farrell 1994). EBNA-LP is required for the efficient growth of LCLs, but is not essential for B cell transformation (Allan et al 1992).

LMP1 is essential for EBV-dependent B-cell transformation *in vitro* (Kaye et al 1993). When expressed in cells, LMP1 has pleiotropic effects including induction of cell-surface adhesion molecules and B-cell activation antigens (eg CD23), and upregulation of anti-apoptotic proteins (eg BCL2) (Wang et al 1990). LMP1 is implicated in both the NF κ B and JAK/STAT signalling pathways (Gires et al 1999; Huen et al 1995). In addition, LMP1 functionally mimics CD40, and can partially substitute for CD40 *in vivo*, providing growth and differentiation signals to B-cells (Uchida et al 1999).

LMP2A aggregates within the plasma membrane of latently-infected B-cells (Longnecker and Kieff 1990). In transgenic mice with B cell lineage expression of LMP2A, normal B-cell development was blocked, resulting in Ig-negative B-cells lacking in B-cell receptor (BCR) expression colonising the peripheral lymph organs (Caldwell et al 1998). B-cell precursors that are lacking in functional Ig receptors are usually eliminated by apoptosis in the bone marrow (Rajewsky 1996). These results, therefore, suggested that LMP2A can mimic the BCR and activate proliferation and survival of B-cells in the absence of signalling through the BCR (Caldwell et al 1998; Schaadt et al 2005). Immunohistochemical studies have detected LMP2A in 52% of EBV-associated HL cases, but not in non-EBV-associated HL cases (Niedobitek et al 1997). Furthermore, gene expression studies demonstrated that LMP2A-induced alterations in gene expression profiles of LMP2A transgenic mice and LMP2A-expressing B-cell lines are similar to those reported in HRS cells (Portis et al 2003).

The presence of LMP2A in HRS cells has suggested that LMP2A is directly involved in the mechanism by which these cells escape apoptosis, despite their lack of a functional BCR (Portis et al 2004).

Since LMP1 and LMP2A have been shown to mimic CD40 and BCR, respectively, it was proposed that EBV infection could provide a survival mechanism for pro-apoptotic GC B-cells containing a non-functional BCR or lacking BCR expression (Mancao et al 2005). BCR-negative GC B-cells were isolated and successfully infected with EBV and immortalised, indicating that EBV is able to rescue these cells from apoptosis (Mancao et al 2005).

1.4.2 EBV and HL

An association between EBV and HL was first reported from seroepidemiological studies conducted in the early 1970s (Levine et al 1971) although the direct involvement of an infectious agent in HL had been proposed earlier (MacMahon 1966). Elevated antibody titres to EBV early antigens, viral capsid antigens and nuclear antigens were observed in HL cases compared with control cases (Levine et al 1971). An increased risk of HL was documented in patients with a past history of IM, known to be a result of late primary EBV infection (Munoz et al 1978). An interesting case was subsequently reported where EBNA-positive B immunoblasts were detected in a patient initially diagnosed with infectious mononucleosis (Poppema et al 1985). After 6 months, the patient developed MCHL with EBNA-positive HRS cells. This was the first publication to show positive EBNA-staining within the nuclei of HRS cells.

Early molecular assays failed to detect EBV genomes in HL due to the low levels of HRS cell within the total tumour population and the insensitivity of the assays at this time (Lindahl et al 1974). It wasn't until the late 1980s that EBV genomes were shown to be present within HL biopsy samples. In a number of small case studies EBV genomes were detected in 17-41% of HL biopsies (Boiocchi et al 1989; Gledhill et al 1991; Staal et al 1989; Weiss and Movahed 1989). In many of these studies EBV infection was shown to be clonal, which indicated that the infected cell population had been derived from a single EBV-infected cell.

At the time these results invoked some scepticism and it was suggested that these assays were detecting latent EBV within B cells of the reactive component, and not within HRS cells. It was important therefore to determine the cellular localisation of the EBV. This was initially achieved using immunohistochemistry (IHC) with both acetone-fixed cryostat sections and paraffin sections, and monoclonal antibodies directed against LMP1 and EBNA2 (Pallesen et al 1991). In 40 out of 84 HL cases all HRS cells positively stained for LMP1, but were negative for EBNA2. In this study, LMP1 expression in HRS cells was found to correlate strongly with the HL histological subtype with 96% of MCHL cases, 32% of NSHL cases and 10% of LPHL cases harbouring positively stained HRS cells. These results indicated that HL cases have a different latent infection protein phenotype from other EBV-associated lymphomas and LMP expression is HL subtype specific. As mentioned earlier (see Section 1.4.1), EBERs are expressed at high levels (10^5 - 10^7 copies per viral genome) in all cells latently infected with EBV. Probes hybridising with these RNAs have been developed for use with paraffin-embedded tissue (Wu et al 1990) and EBV EBER *in situ* hybridisation is a highly sensitive tool for detecting EBV infection in

HL. Using EBER *in situ* hybridisation, the presence of EBV genomes has been demonstrated within HRS cells in 33% of cHL cases (Jarrett 2002). PCR can also be used to screen for the presence of EBV genomes, but does not permit the cellular localisation of the genomes, unless coupled with either flow cytometry or laser microdissection, and therefore is less useful.

In order to determine which EBV latency type is associated with HRS cells, reverse transcriptase PCR (RT-PCR) was conducted on HL biopsies and subsequently RNA expression of LMP1, LMP2A, LMP2B and EBNA1 was observed (Deacon et al 1993). This latency II pattern of expression of EBV genes is a consistent feature of HL. The expression of the transactivator protein BZLF1, which controls the switch from latent to lytic infection, was reported within some HL biopsies examined using *in situ* hybridisation and IHC (Brousset et al 1993; Pallesen et al 1991). In these two series the BZLF1 protein was expressed in 6% (Pallesen et al 1991) and 16.7% (Brousset et al 1993) of the EBV-associated HL cases, and was detected in only some of the HRS cells in these cases. This suggests that lytic infection of HRS cells is a rare event.

1.4.3 Epidemiology of HL

HL accounts for less than 1% of cancers in the U.K. (Cancer Research UK: Hodgkin Lymphoma incidence statistics 2007). The incidence of HL in the U.K. population is 2.4 cases per 100,000 and 3 cases per 100,000 in the U.S.A (Glaser 1987; McKinney et al 1989). HL is one of the most common forms of malignancy amongst young people and has an unusual age distribution. A bimodal age incidence curve has been reported by the majority of studies, but the shape of the curve varies across

geographical locations (MacMahon 1966). This led to the identification of three epidemiological patterns of HL: type I is found in developing countries, type III is specific to developed countries, and type II represents a transition from type I to III seen in rural areas of developed countries and associated with an improvement in living conditions (Merk et al 1990). In type I the first peak occurs in childhood, with low incidence in those aged 30-39, and the second peak is in older individuals. Type III is defined by low childhood rates, a peak in young adults and a second peak in older adults.

Epidemiological studies have consistently provided evidence suggesting that the development of HL is dependent upon a combination of environmental and host factors. A high socioeconomic status during childhood is related to the risk of developing HL in young adulthood (Alexander et al 1991; Glaser 1987; Gutensohn and Cole 1981). The incidence of young adult HL cases (aged between 15 and 39 years old) in the USA was reported to be on the increase in 1990 (Glaser and Swartz 1990). An epidemiological study in the USA found a significant association of the risk of developing HL with pre-school attendance (Chang et al 2004). Young adults who had attended nursery school were found to have a decreased risk of developing HL, and it was suggested that childhood exposure to common infections aided the maturation of cellular immunity in these individuals. Another USA study of 325 HL cases was unable to find a link between social status and the onset of older adult HL (Gutensohn 1982). The results of this epidemiological study suggested that other factors are involved in the aetiology of older adult cases.

Within young adult HL there is no sex bias, but male cases predominate in childhood and the older adults age group (Glaser and Swartz 1990; Jarrett et al 2003; McKinney et al 1989).

1.4.4 Epidemiology of EBV and HL

In situ hybridisation and immunohistochemical studies in Western Europe and North America provide evidence for EBV infection of HRS cells in 26-50% of HL cases (Herbst et al 1992; Jarrett et al 1996; Poppema and Visser 1994). These cases display latency II pattern of EBV gene expression. The presence of EBV infection in HL cases is associated with a number of factors i.e. histological subtype, sex, age, geographical location and ethnicity. In the UK, over 60% of MCHL cases are EBV-associated compared to approximately 25% of NSHL cases (Jarrett et al 2003). Only 2.4% of NLPHL and 1.8% of LDHL cases are EBV-associated. From a large epidemiological study of 622 HL cases in Scotland and northern England, researchers were able to examine both the age- and sex-specific incidence of EBV-associated and non-EBV-associated HL cases analysed separately (Jarrett et al 2003). Among cHL cases, one third were identified as EBV-associated. EBV-associated and non-EBV-associated cases showed distinct age-specific incidence curves. The majority (66%) of EBV-associated HL cases in this study were male. The incidence of early age of infection is higher in developing countries, which is most likely to be due to poor socioeconomic conditions resulting in malnutrition-induced immunological impairment (Weinreb et al 1996). In two studies EBV latent gene products were detected in the HRS cells of 40-46% of Hispanic and Asian (predominantly Chinese) HL biopsies using LMP1 IHC and/or EBERS *in situ* hybridisation (Glaser et al 1997; Gulley et al 1994). In both studies more MCHL than NSHL cases were EBV-

associated and age was reported to be a confounding factor with older HL patients more likely to be EBV-associated.

Combining the results of epidemiological studies examining both the incidence of HL and risk factors for HL development, a new model of HL status has been proposed – the 4 disease model (Jarrett 2002) (see Figure 1.2; Table 1.2). This model outlines a single group of non-EBV-associated cases and three groups of EBV-associated HL that are characterised by their age at diagnosis: childhood (below the age of 10); young adults (aged 15-34) and older adults (>50 years). The majority of those cases diagnosed within childhood and older adults are male. In developed countries only, the largest group in the four disease model accounts for non-EBV-associated HL cases in young adults. The majority of this group are NSHL and both sexes are equally affected.

Table 1.2: The four disease model of cHL (Jarrett 2002)

Disease	Age range	Histological subtype	Male:female ratio	Epidemiological features
EBV-associated cHL of childhood	<10 years	MCHL=NSHL	Males > females	More common in developed countries Most probably related to young age of infection, high infectious dose, decreased immunity Associated with material deprivation and independently with Asian ethnicity in UK (Flavell et al 1999)
Young adult EBV-associated cHL	15-24 years	Predominantly MCHL	Equal	Occurs following IM More common in developed countries
Older adult EBV-associated cHL	≥50 years	MCHL=NSHL	Males > females	Includes all adult cases of cHL occurring in context of immunosuppression Probably related to reactivation of EBV Poorer clinical outcome than non-EBV-associated age-matched cases Often associated with other malignancies
Non-EBV-associated cHL	15-24 years	Predominantly NSHL	Equal	Characteristic of developed countries Associated decreased pre-school attendance Associated decreased exposure to childhood pathogens

cHL, classical Hodgkin lymphoma; EBV, Epstein-Barr virus; IM, infectious mononucleosis; MCHL, mixed cellularity Hodgkin lymphoma; NSHL, nodular sclerosis Hodgkin lymphoma

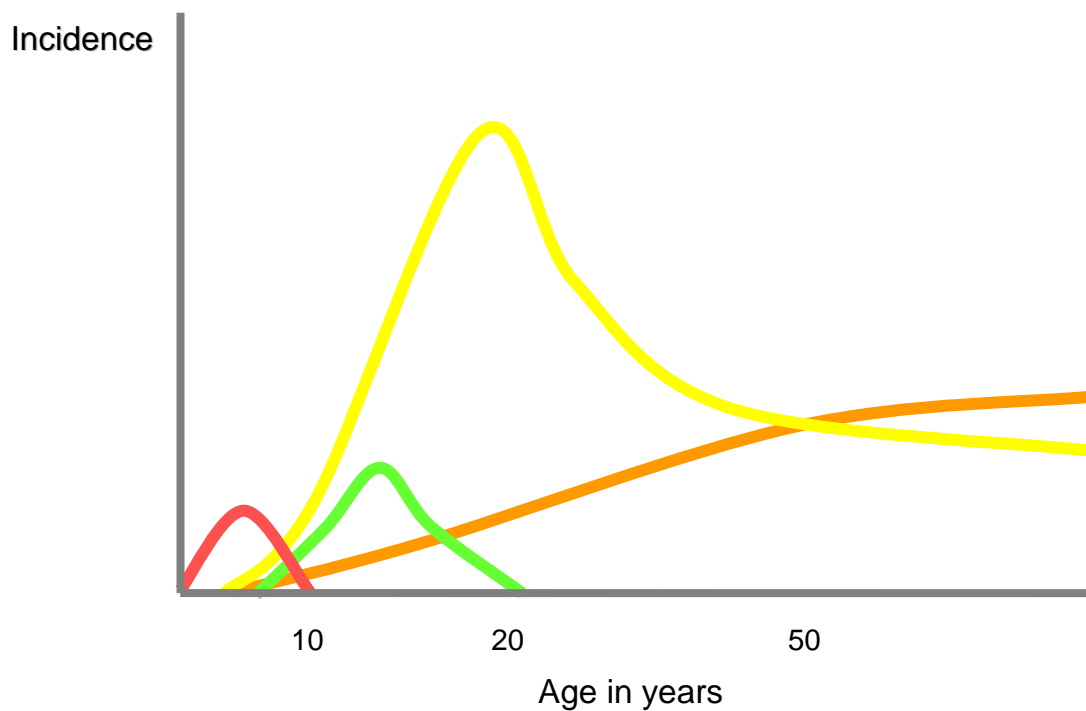


Figure 1.2. The four disease model of HL (Jarrett 2002). The red, green and orange lines represent the three groups of EBV-associated HL cases and non-EBV-associated HL cases are indicated by the yellow line. The height magnitudes of the various curves will vary in different geographical locales, and be influenced by genetic and environmental factors.

Two independent studies investigated the association between EBV-associated IM and risk of developing HL (Alexander et al 2003; Hjalgrim et al 2003). An epidemiological study of 408 cHL cases from Scotland and Newcastle (Alexander et al 2003) noted a significant increase of EBV-associated HL in young adults who had either IM or who have a blood relative with a history of IM. This was also reported by a Scandinavian study in which patients with previous IM were found to be at a significantly increased risk of developing EBV-associated HL (Hjalgrim et al 2003). Although these studies provide compelling evidence for an association between IM

and development of EBV-associated HL, two American groups (Glaser et al 2005; Sleckman et al 1998) have failed to confirm these findings.

1.4.5 Non-EBV-associated HL cases

Approximately 82% of young adult cHL cases in European countries are non-EBV-associated (Alexander et al 2001). The risk of developing young adult cHL is associated with a high social class background, small family size, high standard of education and early birth order position in childhood (Gutensohn 1982). These factors may diminish an individual's exposure to infectious agents and thereby increase their susceptibility to developing a virus-induced pathogenesis later in life. It has been suggested that such an infection later in life could account for the development of HL in non-EBV-associated cases. The identity of such an agent remains unknown, but a candidate virus is likely to be a common virus that can infect most people.

The inability to detect EBV in some HL cases could be explained by a failure to detect low copy number viral genomes, but this is unlikely given the high sensitivity of the standard screening techniques. It is possible that EBV never infected HRS cells in non-EBV-associated HL cases; or alternatively these cells may have been infected with EBV, but viral genomes were lost after the initial infection, the so-called 'hit and run' mechanism (Ambinder 2000). It is also possible that some fragments of the EBV genome remain integrated into the host cellular DNA. This has been demonstrated in EBV-associated Burkitt's lymphoma (Razzouk et al. 1996). In non-EBV-associated HL cases, however, fluorescence *in situ* hybridisation (FISH) using cosmid clones spanning the genome failed to detect deleted viral genomes integrated into host cell

DNA (Staratschek-Jox et al 2000). The results of a combined serological and molecular investigation of biopsies from 30 young adult cHL cases with confirmed non-EBV-association provided further evidence to disprove the hit and run theory (Gallagher et al. 2003). These cases were screened with 7 highly sensitive real-time (QRT) PCR assays specific for the EBV genome. Viral fragments were detected in equimolar amounts in the cHL cases, but there was no evidence of defective EBV genomes. Rearranged EBV genomes have been detected in 31% of 32 EBV-associated and 33% of 24 non-EBV-associated paediatric HL tumours (Gan et al. 2002). Such defective EBV genomes may disrupt gene regulation and, therefore, account for the loss of EBV from individual HRS cells. However, Gallagher *et al.* (2003) did not detect EBV genome rearrangements in adult cHL samples using either conventional or quantitative real-time PCR (QRT-PCR) (Gallagher et al 2003).

A number of serological and molecular studies have investigated the possible association of HL with variella zoster virus, herpes simplex virus, parainfluenza virus, human herpesvirus (HHV-8), JCV, BKV, cytomegalovirus (CMV), simian virus 40 (SV40), lymphotropic papovavirus (LPV), human T-cell leukaemia virus types 1 and 2 (HTLV-1 and 2) and adenoviruses type 5 and type 12 (Armstrong et al 1998; Berneman et al 1998; Evans and Gutensohn 1984; Gallagher et al 2002; MacKenzie et al 2003). Other than the association between non-EBV-association and high human herpesvirus 6 antibody titres, none of these viruses has been associated with HL.

A recent publication suggested a possible association of measles virus (MV) with cHL in Israel (Benharroch et al. 2003). MV genomes were identified in 60.3% of 68 cHL cases tested by IHC and RT-PCR. This study was later extended to include 143 HL

patients and MV antigens were identified in 73.4% of samples (Benharroch et al. 2004). This prompted us to test a group of UK cHL cases for any association with MV. IHC was used to screen 97 cHL cases for the MV antigen, and both IHC and RT-PCR were used to test a second series of 20 cHL cases. This study is discussed in chapter 3 of this thesis.

We also investigated the possibility of an association of cHL with polyomaviruses using QRT-PCR and a set of degenerate PCR assays with the potential to detect the large T antigen of novel polyomaviruses. Chapter 4 contains details of the assays performed and the results we obtained.

1.5 CLASSICAL CYTOGENETICS

Cytogenetics is defined as the study of structure, function and evolution of chromosomes. Heinrich von Waldeyer-Hartz first used the term 'chromosome' in 1888 (Waldeyer 1890; Waldheyer 1888), but the concept of the human chromosome had been proposed earlier in 1882 by Walther Flemming (Flemming 1882).

Due to technical limitations, cytogenetics did not advance much further until 1952 when the discovery of 'hypotonic shock', caused by submerging cells in a hypotonic salt solution before fixation, enabled the production of a good chromosome spread on slides (Hsu 1952). Four years later it was discovered that adding colchicines to cell cultures destroys the mitotic spindle and halts the cell growth cycle in metaphase (Ford and Hamerton 1956a; Ford and Hamerton 1956b). This enabled the production of the perfect metaphase chromosome spread on slides and it was therefore possible to determine that the number of chromosomes in a human cell is 46 (Tijo and Levan 1956). These chromosomes can be arranged into 8 different groups (A-G plus the sex chromosomes) according to their size and the location of the primary constriction, or centromere.

1.5.1 Chromosome banding techniques

A more precise identification of the unique structure and sub-regions of each chromosome was achieved using a number of chromosome banding techniques developed in the 1970s. Several banding techniques were introduced including staining with quinacrine (Q-banding) (Caspersson et al 1968; Caspersson et al 1970), or following various pre-treatments with Giemsa stain (G-banding) (Seabright, 1972) or acridine orange (Reverse or R-banding) (Caspersson et al 1968; Caspersson et al

1970; Verma and Lubs 1975). The development of these banding techniques resulted in the detection of acquired and inherited chromosomal changes (i.e. translocations, insertions, inversions, deletions and duplications) within a number of diseases.

The resolution of chromosome banding was limited at approximately 500 bands per haploid genome until the development of high-resolution banding in 1975, which increased resolution to >1000 bands per haploid genome (Yunis and Sanchez 1975). Yunis and Sanchez (1975) synchronized lymphocyte cultures, which resulted in an increased number of cells arresting their cycle at the pro-metaphase or prophase stages instead of at metaphase. The chromosomes were much longer and consequently the bands and sub-bands appeared separated and were easier to identify.

Classical cytogenetic methods have played a significant role in the identification of distinct subsets and specific molecular pathways involved in human lymphomas. Their application to the study of solid tumours, and HL in particular, has been limited however by the scarcity of biopsy material and the low number of high quality metaphase spreads available. These problems have been addressed during the development of molecular cytogenetic techniques.

1.5.2 Classical cytogenetics and HL

As just mentioned, karyotype analysis of HL using classical cytogenetics has been limited. However recurrent breakpoints and translocations have been identified in HL cases using classical cytogenetic techniques (Dohner et al 1992; Tilly et al 1991; Schlegelberger et al 1994; Falzetti et al 1999). Imbalances were identified within all chromosomes in 59% of HL patients analysed in one study, although losses in chromosomes 13 and Y occurred more frequently (Tilly et al 1991). A later study

analysed metaphase cells from 25 HL patients identified gains in chromosomes 2, 9, 11, 19 and 20, losses in chromosomes 10, 13, 15, 16, 21 and Y, and translocations involving 1p11-1p13, 1p36, 4q35, 14q11 and 15p11 (Dohner et al 1992). In addition, Dohner et al. (1992) observed recurrent losses on 1q, 4q, 6q and 17p and proposed that these losses of chromosomal material may be involved in the pathogenesis of HL.

Classical cytogenetic analysis of HL cases, therefore, introduced the hypothesis that recurrent chromosomal imbalances are present within these tumours and may play an important role in the pathogenesis of this disease.

1.6 MOLECULAR CYTOGENETICS

1.6.1 *In situ* hybridisation

The resolution of chromosomes was improved by the development of *in situ* hybridisation (ISH). This molecular technique is based upon the same principle as Southern blot analysis. In place of a membrane, the target DNA of metaphase chromosomes, interphase cells or tissue sections is bound to a glass microscope slide and either radioactive-labelled DNA probes (radioactive *in situ* hybridisation) (Gall and Pardue 1969) or non-isotopic DNA probes (i.e. immunofluorescent, biotin or digoxigenin) are hybridised to this target DNA. Biotin- or digoxigenin-labelled DNA can be detected by immunocytochemical methods using peroxidase or alkaline phosphatase enzymes (Garson et al 1987), and visualised under a brightfield or reflection-contrast microscope. ISH provides a resolution of 50kb-2Mb.

1.6.2 Fluorescence *in situ* hybridisation

The application of ISH for routine screening came about with the development of fluorescence ISH (FISH). This molecular cytogenetic technique uses the conjugation of different fluorochromes (i.e. fluorescein-isothiocyanate, rhodamine or Texas Red) to a DNA probe. This is referred to as 'direct labelling'. Alternatively, 'indirect labelling' uses either immunological (i.e. anti-digoxigenin antibodies) or enzymatic (i.e. avidin to detect biotin-labelled sequence) detection of target DNA which have been incorporated into the DNA probe (Langer-Safer et al 1982). Human Cot-1 DNA is introduced to the denatured probe prior to hybridisation in order to bind repetitive DNA sequences and thereby prevent non-specific binding. The minimum size limit of a probe for reliable detection on metaphase chromosomes is approximately 3-5kb. Thousands of different probes are now available across the genome so it is possible to specifically stain particular parts of a chromosome or the whole chromosome in a resolution range of 5kb-500kb.

Probes can also be used in combination in a single hybridisation, allowing the simultaneous visualisation of all 23 human chromosome pairs with each fluorescing a different colour. This approach is used in multiplex-FISH (M-FISH) (Speicher et al 1996), spectral karyotyping (SKY) (Schrock et al 1997) and combined binary ratio labelling (COBRA) (Tanke et al 1999). Increasing the number of fluorochrome-labelled probes used improves the otherwise relatively low resolution (3Mb) of these multicolour techniques.

In addition to the advances that have been made in cytogenetic technology, considerable progress has been made in the development of both the hardware and software with which FISH images are analysed.

1.6.3 FICTION analysis

In immunocytochemical studies of cases with a low percentage of tumour cells, such as HL cases, the limited number and banding quality of analysable mitoses is a problem. In order to overcome this, a method has been developed which allows FISH and IHC to be performed on the same preparation. This has been referred to as ‘fluorescence immunophenotyping and interphase cytogenetics as a tool for the investigation of neoplasms’ (FICTION) (Weber-Matthiesen et al. 1992). The genotypic and phenotypic features of a tumour cell are correlated whilst attempting to retain cell morphology. This technique has successfully been used on cytopsin preparations, cryostat sections and bone marrow smears. The results of FICTION analysis of 30 cytogenetically analysed cHL cases have been published (Weber-Matthiesen et al. 1995). CD30+ HRS cells were isolated from cytopsin preparations and a variety of numerical chromosomal aberrations were observed in the majority of these cells. In particular, gains of chromosomes X, Y, 1, 8, 12, 15 and 17 were observed. More recently, FICTION analysis of 12 cHL cases detected a gain of the chromosomal region 2p13-16, which includes the c-Rel gene (Barth et al. 2003). FICTION has also been used to demonstrate the presence of both mantle cell lymphoma (MCL) and HL in the same patient (Martinez-Ramirez et al. 2004).

The methodology has been further developed with the introduction of multicolour FICTION (M-FICTION), which allows the simultaneous analysis of multiple

chromosomal aberrations in a single experiment (Martin-Subero et al. 2002). Two assays, using multiple differentially-labelled probes, were established to demonstrate the use of M-FICTION in B-cell NHL and in anaplastic large-cell lymphomas. For each assay, antigens were investigated using a combination of up to five FISH probes, to detect what were considered the most important diagnostic chromosomal aberrations within these tumours.

In order to analyse a sample using FISH or FICTION, details of the target sequence must be known in order to select a suitable probe. An alternative method which requires no prior knowledge of likely genetic aberrations has now been established: comparative genomic hybridisation (CGH).

1.6.4 Comparative Genomic Hybridisation

CGH was developed as a method of screening the whole genome for loss or gain of chromosomal material in a single hybridisation, without the need for the sample to be mitotically active, and without knowing anything about the genetic makeup of the sample (Kallioniemi et al 1992). The chromosomal origin of these gains and losses of genetic material can be identified and mapped to specific chromosome bands. Conventional CGH was introduced in 1992 as a method of chromosomal analysis obviating the need for obtaining metaphase spreads from tumour samples, a limiting factor for solid tumours as mentioned earlier (Kallioniemi et al. 1992). This molecular cytogenetics technique is based upon quantitative two-colour FISH and can detect and map the relative DNA copy number between genomes with a resolution in the range of 2-10 Mb. Test (tumour) and reference genomic DNA are differentially labelled using, respectively, biotin and digoxigenin conjugated to dUTP (see Figure

1.3). The samples are combined and hybridised to normal human reference metaphase chromosomes. Two different fluorochromes, red-fluorescing rhodamine antidigoxigenin and green-fluorescing fluorescein isothiocyanate (FITC)-avidin, are used to detect the test and reference DNA respectively and the relative colour intensities of these fluorochromes indicate DNA copy number alterations within the tumour genome. Direct labelling, using nick translation, of test and reference genomic DNA was introduced by the same research group several years later and is now the recognised method of fluorescence labelling for CGH (Kallioniemi et al. 1994).

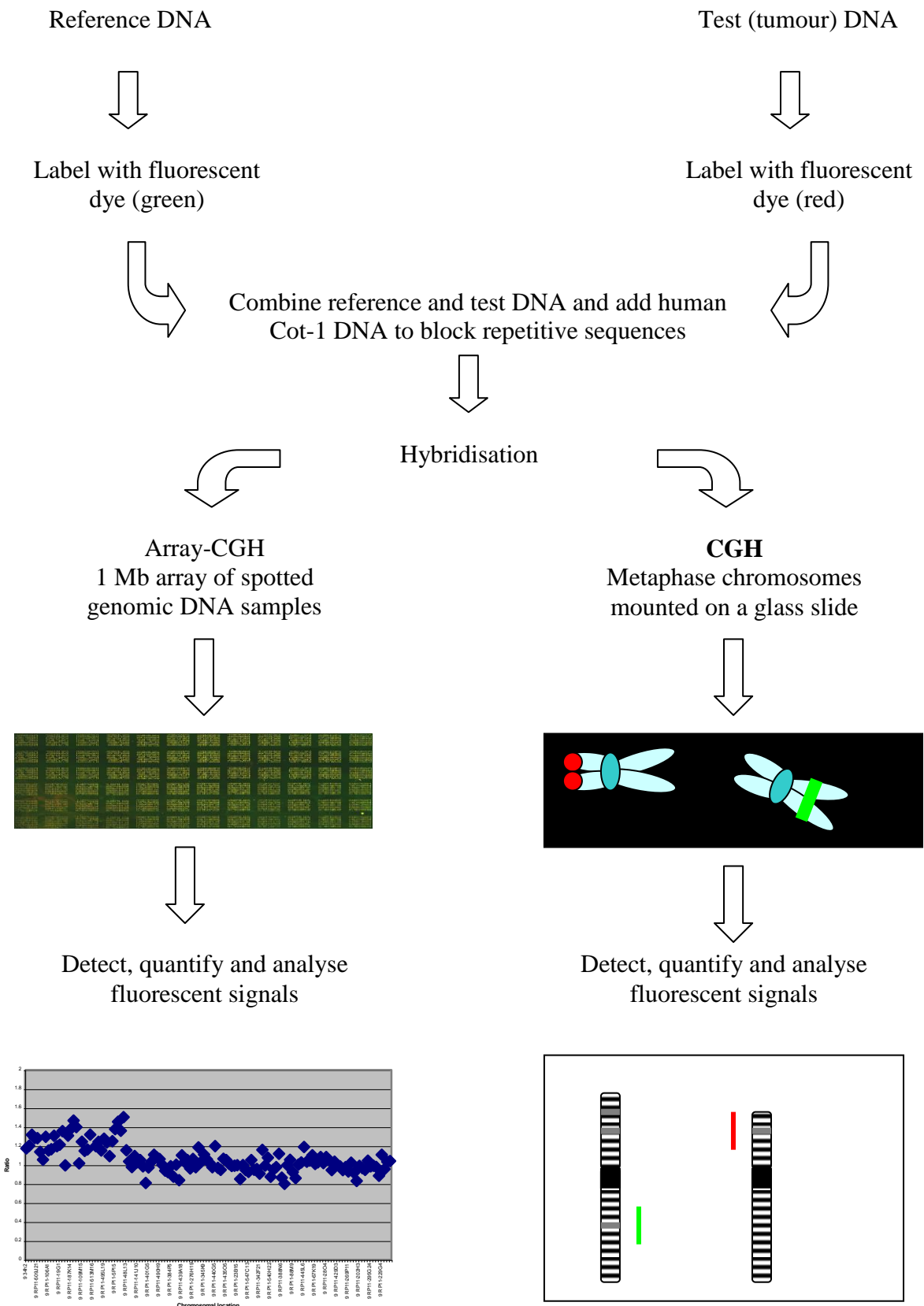


Figure 1.3. Schematic outline of CGH using arrays and metaphase spreads (adapted from Mantripragada et al. 2004). Reference and test DNA are labelled with a fluorescent dye, then hybridised to either metaphase chromosomes on a glass slide or an array of genomic DNA samples spotted onto a glass slide. The fluorescence of the two dyes can either be visualised under the microscope, as in conventional CGH, or is detected and analysed using specialised software packages, as in array-CGH. For conventional CGH, results are depicted schematically, with gains (red) and losses (green) indicated adjacent to the chromosomal region in which they are located. For array-CGH, the fluorescence intensity of each dye for each genomic DNA spot is combined as a ratio and plotted in a chart against chromosome location. Ratio thresholds are selected so that gains and losses can be identified. For example, a gain of chromosomal material is indicated when a point on the chart has a ratio >1.15 and a loss is indicated by a ratio of <0.85 .

In the first CGH paper (Kallioniemi et al. 1992) the authors investigated 11 cancer cell lines using CGH and identified 16 previously undetected gains of chromosomal material. They suggested that CGH could be used to detect chromosomal imbalances within DNA extracted from solid tumours and that this may result in the identification of recessive mutant tumour suppressor genes. Following this several different studies were published where CGH was used to analyse breast, bladder and ovarian cancer cell lines (Gay et al. 1994; Iwabuchi et al. 1995; Kallioniemi et al. 1995) and this has now become an established technique.

1.6.4.1 Investigation of lymphomas using CGH

The first publication to report the use of CGH to identify chromosomal aberrations in lymphomas investigated DNA extracted from 24 primary mediastinal B-cell lymphoma patients (Joos et al. 1996). A subset of these cases was also examined using Southern blot analysis and FISH. A common pattern of chromosomal gains on 2p, 9p and Xq, and losses on 12q was observed in several of these cases. The authors proposed *REL* as a candidate gene involved in the tumourigenesis of primary mediastinal B-cell lymphoma due to its location on chromosome 2, within the region of chromosomal gain. These results also confirmed the gain on chromosome 9 that had been reported earlier in a cytogenetic study of NHL cases (Offit et al. 1989). In a later study, 29 T-cell NHL cases were screened with CGH to identify chromosomal changes (Renedo et al. 2001). Chromosome gains of Xq were identified once more, along with gains of chromosomal material on 9q34 and on chromosomes 17, 19 and 20.

CGH has been used to distinguish between different orbital NHL cases (Matteucci et al. 2003). These lymphomas constitute approximately 8% of all extranodal lymphomas, and the majority are histologically derived from mucosa-associated lymphoid tissue (MALT). FISH had been used in previous studies, but limited amounts of biopsy material and limited knowledge of suitable probes prevented analysis of these cases by this technique. These limitations were resolved by the use of conventional CGH, which enabled the detection of chromosomal duplications in 3q24-qter and 6p21.1-21.3; these are typical of marginal zone lymphomas and an orbital location respectively. Chromosomal loss was detected in 1q, 6q, 9q, 11q and 13q.

1.6.4.2 Limitations of CGH

Conventional CGH using metaphase spreads has limited resolution. In the detection and mapping of DNA sequence copy number, gains and losses larger than 10-20 Mb were identified within the tumour genome (Isola et al. 1994). A resolution of 40Mb was achieved when DNA amplified from a single cell was hybridised to metaphase chromosomes (Voullaire et al. 1999). CGH is also limited to the detection of gains or losses of chromosomal material and point mutations, small intragenic rearrangements, balanced translocations and inversions are all undetectable using this method. Furthermore, imbalances must be present within all cells to ensure detection. It has also been noted that there is a decrease in the red and green fluorescence intensity at the chromosome telomeres, which can result in difficulties with interpretation (Mantripragada et al. 2004).

Recurrent copy number variations or inversions have been identified within regions of the genome in healthy humans (Iafate et al 2004). The details of known structural variants can be found within the Database of Genomic Variants (<http://projects.tcag.ca/variation/>), which is constantly updated (Zhang et al 2006). It is important that any chromosomal region of imbalance detected in a tumour sample is checked against this database representing the normal human genome.

1.6.5 Whole genome amplification

Obtaining sufficient quantity of DNA from small solid tumours can be very difficult and will limit the choice of subsequent methodologies. However, whole genome amplification (WGA) techniques have been developed to produce large quantities of genomic DNA from small amounts of template material. The success of WGA for use in CGH is determined by both the amount of product that is generated and how representative the final product is of the original DNA template. Three PCR-based WGA methods and a cascading, strand displacement methodology have been developed.

1.6.5.1 Linker-adaptor PCR

Linker-adaptor mediated (LA) PCR was the first PCR-based genome amplification technique to be reported, but was developed for the detection of DNA regions involved in DNA-protein interactions rather than for WGA (Ludecke et al 1989). The DNA template is digested with a restriction enzyme and then adaptor sequences are ligated on to the ends of the DNA molecules. The adaptor sequence is then used as a primer in a subsequent PCR. Ten years after the first publication, LA-PCR was adapted for WGA from a single cell for use in CGH; this technique was termed single

cell comparative genomic hybridisation (SCOMP). Technical problems, related to the ligation reaction, have prevented the widespread use of this methodology (Klein et al. 1999).

1.6.5.2 Primer-extension pre-amplification PCR

Primer-extension pre-amplification (PEP) PCR was initially designed for multiple genotyping from a single sperm nuclei (Zhang et al. 1992). It uses multiple extension rounds with *Taq* polymerase and a random mix of completely degenerate 15-mer primers. It has been estimated that this method is able to amplify 78% of the genome from a single cell (Zhang et al. 1992). An improved PEP-PCR protocol has been now been developed using a lysis buffer containing proteinase K, then an enzyme mix of *Taq* DNA polymerase and proofreading Pwo polymerase, and an additional elongation step (Dietmaier et al. 1999). These changes result in a more efficient WGA reaction.

1.6.5.3 Degenerate oligonucleotide-primed-PCR

Degenerate oligonucleotide-primed (DOP) PCR was developed in 1992 for genome mapping studies (Telenius et al. 1992). Since then the technique has been adapted for use with lower starting amounts of DNA template, improved genomic representation and increased yield, fragment length and fidelity. Each DOP-primer is designed to contain a CG-rich 5' end, followed by 6 random degenerate nucleotides, and 6 specific nucleotides at the 3' end. The primer mix, therefore, contains 4^6 partially degenerate primers. The first PCR uses a low stringency annealing temperature (25°C) to enable primer binding. The annealing temperature is increased to 55°C in the second part of the PCR allowing exponential amplification of sequences.

DOP-PCR efficiently produces large quantities of highly representative genomic DNA from very small amounts of starting material. When the reproducibility of DOP-PCR was compared with PEP-PCR, results were comparable with 89% and 91% of loci successfully amplified, respectively (Wells et al 1999). However, DOP-PCR can amplify a greater quantity of DNA product than PEP-PCR allowing visualisation of the product on an agarose gel.

1.6.5.4 Multiple displacement amplification

The multiple displacement amplification (MDA) reaction is based upon the rolling circle amplification used by circular DNA genomes for replication (Kornberg and Baker 1992). MDA was initially developed to amplify large circular DNA templates (Dean et al. 2001), but has been adapted for genomic DNA amplification (Dean et al. 2002). This non-PCR-based method uses phi29 DNA polymerase with random exonuclease-resistant primers in a single reaction. The DNA template is denatured before a single extension incubation enables the cascading, strand displacement reaction to take place. Initially, the random primers anneal to and extend from the denatured template DNA, then the 5' end of any extending product is displaced by an upstream fragment which is extending in the same direction. A hyperbranching mechanism is generated which is only stopped when the enzyme is inactivated by heating at the end of the reaction. Large amounts of DNA can be produced with this method and products are larger than is possible with PCR-based WGA. A more complete coverage of the genome occurs with very low amplification bias (Dean et al 2002). A number of commercial kits have become available over the last year: GenomiPhi and TempliPhi (Amersham Biosciences), GenomePlex (Sigma-Genosys).

Currently, however, MDA has not been successfully developed for WGA from single cells.

To summarise, PEP-PCR, DOP-PCR and MDA are the most efficient methods of WGA. Whilst PEP-PCR and MDA reliably amplify good representative DNA, DOP-PCR is the preferred method at present when using small amounts of template. This methodology reliably produces high quantities of DNA with a reasonably good representation of the genome.

1.6.6 Whole genome amplification, CGH and lymphomas

WGA has been used to produce DNA for CGH analysis of NHL biopsies and to identify chromosomal imbalances (Weber et al 2000). Primary central nervous system lymphomas (PCNSL) form in the lymph tissue of the brain and/or spinal cord and are morphologically recognised as high-grade NHLs of the diffuse large B-cell type (DLBCL), but their origin is poorly understood. These tumours are commonly removed by stereotactic surgery so only a minute amount of material is available for analysis. In one study DOP-PCR was used to amplify DNA from 19 PCNSL cases, which was then used in both conventional CGH and array-CGH (see Section 1.6.8) where the target sequences were PCR products derived from yeast artificial chromosome (YACs) (Weber et al. 2000). A set of characteristic chromosomal imbalances was observed within 18 of the cases with the most frequent, a gain on 12q, being detectable in 63% of cases. Other abnormal regions were 1q, 9q, 11q, 12p, 16p, 17q, 18q and 22q.

1.6.7 Laser microdissection and whole genome amplification

Since many tumours contain large numbers of non-malignant cells, often accounting for over 50% of the total DNA content of the tumour, the fluorescence ratio calculated after CGH using whole tumour DNA will not be representative of the tumour cells (Kallioniemi et al., 1994). The introduction of laser microdissection (LMD) has made possible the selection of a pure tumour cell population from biopsy material. Cells can be picked from cytopsin slides, frozen tissue sections, or paraffin-embedded tissue sections. A laser is used to cut around the cells, which either drop or are catapulted into a tube lid. The cells then undergo either proteinase K digestion or alkaline lysis to extract the genomic DNA, which can be used as a DNA template for WGA.

Combining LMD and WGA has provided a very powerful tool for the detection and identification of unknown chromosomal aberrations in tumours. This was first successfully demonstrated using DNA extracted from microdissected peripheral blood lymphocytes and the breast cancer cell line MCF-7 (Kuukasjarvi et al. 1997). DOP-PCR was performed with only 50 pg of cell line DNA as template and the products were successfully hybridised to normal metaphase preparations. Many studies have now been published where LMD was used to collect pure cell populations from a tumour sample for CGH (Pyakurel et al 2006; Morandi et al 2006; Huang et al 2005b; Yan et al 2005; Chang et al 2005; Morohara et al 2005).

1.6.8 CGH analysis of classical HL

Three groups have analysed cHL using CGH. Ohshima *et al.* (1999) selected HRS cells from 9 fresh cHL biopsies using a Fluorescent Activated Cell Sorter (FACS),

and the DNA was subsequently amplified using DOP-PCR (Ohshima et al. 1999). The products were hybridised to normal metaphase preparations. Gains and losses were observed in the HRS cells from all nine cHL cases with the most common being a loss of 16q11-21 and a gain of 1p13 and 7q35-36. Five of the HL cases were associated with EBV, but the authors reported no significant relationship between EBV and the chromosomal changes observed. CGH was also performed using DNA from B and T lymphocytes to investigate the chromosome imbalances in the multicellular infiltrate surrounding the HRS cells. No chromosomal abnormalities were detected in the latter cells.

Joos *et al.* (2000) selected HRS cells from 12 cHL biopsies for cytological analysis (Joos et al 2000). For each case, DNA was extracted from 30 HRS cells and amplified using DOP-PCR before analysis by conventional CGH. A number of recurrent chromosomal imbalances were detected; including gains in 2p, 9p and 12q and losses in 17p (see Figure 1.4). This study was expanded to 41 cHL cases (Joos et al 2002) and frequent gains in chromosomal material were identified on chromosomes 2p, 9p, 12q, 16p, 17p, 17q and 20q (see Figure 1.4). The most frequent losses affected chromosome 13q. Further analysis by FISH demonstrated that the REL oncogene was amplified within chromosome 2p15-p16, especially in HRS cells isolated from NSHL cases (Joos et al 2000; Joos et al 2002). Recurrent gains on chromosomes 2p and 9p were also detected in the cHL-derived cell lines HDLM2, KMH2, L1236 and L428 using DOP-PCR, CGH and M-FISH (Joos et al 2003). FISH analysis identified amplification of the REL locus on chromosome 2p15-p16, in all four cHL-derived cell lines, and the JAK2 locus on chromosome 9p24, in the HDLM2, KMH2 and L428 cell lines.

In our laboratory, HRS cells were laser-microdissected from 20 cHL cases and 4 HL-derived cell lines, amplified using DOP-PCR, and analysed by conventional CGH (see Figure 1.4) (Chui et al. 2003). The most frequently occurring chromosomal gains were located on 2p, 9p, 12q, 14q, 16p, 17 and 22q. The most frequently observed losses were on 4q, 6q, 11q and 13q. There were significantly more gains in 2p and 14q in older adult cHL cases, and a loss on 13q was associated with a poor outcome. These results are remarkably similar to those of the studies by Joos *et al.* (Joos et al 2000; Joos et al 2002) and with the CGH analysis of four HL cell lines (L1236, L428, KMH2 and HDLM2) (Joos et al., 2003). This suggests that recurrent genomic imbalances are a feature of cHL.

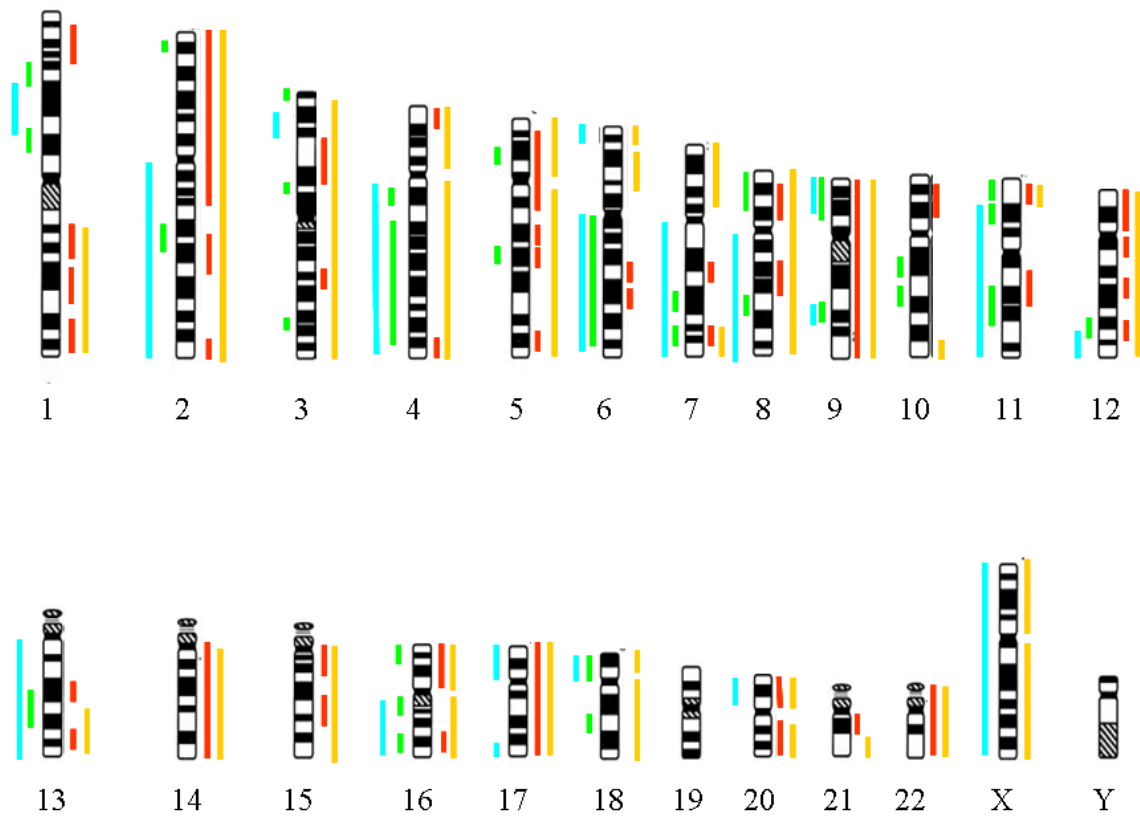


Figure 1.4. Summary of conventional CGH analysis of HRS cells isolated from cHL biopsies. Chromosomal gains are indicated by red (Chui et al 2003) and orange (Joos et al 2000; Joos et al 2002) vertical lines to the right of the chromosome ideograms, and losses by green (Chui et al 2003) and blue (Joos et al 2000; Joos et al 2002) vertical lines to the left.

1.6.9 Array-CGH

In 1997 the replacement of the target metaphase chromosome spread in CGH with an array of bacterial artificial chromosome (BAC), P1-derived artificial chromosome (PAC) or yeast artificial chromosome (YAC) DNA was introduced (Solinas-Toldo et al. 1997) (see Figure 1.3). This allows DNA copy number aberrations to be detected at higher resolution. These CGH arrays can be created by spotting BAC DNA (Solinas-Toldo et al. 1997), DOP-PCR derivatives of BAC DNA (Telenius et al. 1992), or amplified fragment pools (AFP) of BAC DNA generated by linker mediated PCR (Pfeifer et al. 1989), onto a glass slide. The resultant array can be used for high-resolution detection of copy number changes and is limited only by the size and spacing of large insert clones included in the array.

In array-CGH, reference and test DNA samples are differentially labelled with fluorescent dCTPs (cyanine-3 (Cy3) and cyanine-5 (Cy5)) (see figure 1.3). The samples are then combined to form the probe DNA and, prior to hybridisation, Cot-1 DNA is added to block repetitive sequences and prevent non-specific binding. Following hybridisation, the fluorescent ratios of each spot on the array are analysed in order to determine the copy number differences between the two DNA samples. Initially confocal microscopy was used for manual evaluation, but now analysis is automated with specialised software packages similar to those used in the analysis of cDNA microarrays. A second 'dye-swap' hybridisation is usually performed where the initial labelling of both DNA samples is reversed. This prevents scoring of any spurious results, which are not confirmed in the reciprocal hybridisation.

The construction of a genomic array spanning the whole genome was reported by two studies which described the synthesis of an array using 2460 and 3500 BAC-derived DNAs respectively (Fiegler et al. 2003; Snijders et al. 2001). Each DNA clone sequence represented, on average, 1Mb of the genome. Recently, a submegabase resolution array-CGH (SMRT array) has been published comprising 32,433 overlapping BAC clones covering the entire human genome (Ishkanian et al. 2004). This array has the potential to identify minute recurrent genomic imbalances and allow the detailed characterisation of critical genomic regions and genes of known or anticipated pathogenic relevance. The technique can be used to aid the identification of prognostic markers, to which a specific anti-tumour/cancer therapy can be assigned, and thereby contribute to both a greater understanding of cancer biology and improved patient management.

1.7 AIMS OF THESIS

In order to identify potential pathogenic agents for cHL, we screened a number of cHL cases for MV (Chapter 3) and polyomaviruses (Chapter 4) using IHC, conventional PCR and QRT-PCR. In addition, we designed several degenerate PCR assays, against highly conserved regions of the virus genome, which would detect known and unknown members of the polyomavirus family.

Recurrent chromosomal imbalances have previously been reported in cHL cell lines and cases using classical cytogenetic techniques and, more recently, conventional CGH, which has a limited resolution of 40 Mb. To examine these chromosomal imbalances at a higher resolution (1 Mb) and to identify smaller chromosomal changes previously undetected, we analysed six well-established cHL cell lines using array-CGH analysis (Chapter 5).

When this project began, there were no publications of studies using LMD and WGA to prepare genomic DNA samples for array-CGH analysis. We, therefore, optimised the analysis of DOP-PCR amplified laser microdissected single cells, from a cHL-derived cell line for array-CGH (Chapter 6). Once optimised, these methodologies were performed to analyse chromosomal imbalances within single HRS cells from a cHL case sample (Chapter 6).

CHAPTER 2

MATERIALS AND METHODS

The general materials and methods used in this project will be described in this chapter. A more detailed account of the methodology related to array-CGH is detailed in chapter 5.

2.1 MATERIALS

All chemicals used were of Analar or Molecular Biology grade and were obtained from either the Sigma-Aldrich Company Ltd. (Poole, Dorset, UK) or VWR International Ltd. (Lutterworth, Leicestershire, UK), unless otherwise stated. De-ionised water, from a Seradest S600 ion-exchange system, was used in the preparation of buffers. Molecular biology grade water, supplied in aliquots of 1 ml by Microzone Limited (Haywards Heath, West Sussex, UK), was used in all enzymatic reactions.

2.2 METHODS

2.2.1 Tissue collection

Freshly removed tissue biopsies were delivered in travel medium (see Appendix C) to the laboratory directly from collaborating hospitals in the West of Scotland on either the day of excision or the following day. A patient information form with relevant clinical details was completed by the hospital pathologist and diagnostic information was obtained. All relevant information was entered on a bespoke database in our laboratory, and a unique patient number was assigned. All studies were approved by a Multicentre Research Ethics Committee and informed consent was obtained from all patients. Samples were coded before use in research.

2.2.2 Tissue biopsy processing

Specimens were processed as quickly as possible in order to maintain cell viability. Since samples were used in several different projects, sample processing was performed by several different group members in a containment level II laboratory within a Class II Microbiological Safety Cabinet (MSC), according to the local Code of Practice.

2.2.3 Preparation of viable cell suspensions

Following removal from travel medium, biopsy samples were transferred to a sterile Petri dish and washed in 70% ethanol to remove any surface contaminants. The samples were then bisected and two touch imprints were made on polylysine slides (VWR International Ltd.); these were allowed to air dry before being stained with eosin G and thiazine using the DiffQuik staining system (Dade Behring Inc., Illinois, USA).

The tissue was then cut into smaller pieces and forced through a cell strainer with Cell Suspension buffer (containing 10% 10x phosphate buffer solution (PBS), 2% heat-inactivated fetal bovine serum (Invitrogen), 1 M ethylene diamine triacetic acid (EDTA; Sigma-Aldrich Company Ltd.) and 2.5 mg bovine serum albumin (BSA; Sigma-Aldrich Company Ltd.)) using the plunger of a 2 ml Plastipak sterile syringe (Becton Dickinson, New Jersey, USA). The resultant suspension was centrifuged at 1200 g for 5 minutes (mins) and the cells were resuspended in 10 ml of Cell Suspension buffer.

2.2.4 Cell counting

A 20 µl aliquot of the cell suspension was mixed with 20 µl of 0.4% trypan blue solution (Sigma-Aldrich Company Ltd.), and approximately 20 µl of this was pipetted beneath a coverslip on an improved Neubauer haemocytometer chamber (Fisons Scientific Equipment, Loughborough, UK). The total live cell count was made across 16 large grid squares, and this number was multiplied by the dilution factor to give the concentration $\times 10^4$ per ml.

2.2.5 Enrichment of mononuclear cells from lymph nodes

Mononuclear cells were enriched and debris removed by gradient density centrifugation. The cell suspension was slowly layered over Lymphoprep (Axis Shield, Norway) and then centrifuged at 1500 g for 20 mins in a bench top centrifuge (Allegra GR, Beckman Coulter, High Wycombe, UK) with the brake off. The mononuclear cells accumulated at the interface between the two phases and were removed carefully using a pipette. Following washing in Cell Suspension buffer, a repeat cell count was performed. The cells were then washed again and centrifuged at 1000 g for 5 mins with the brake on.

2.2.6 Storage of viable mononuclear cell suspensions

A proportion of the cells was used for cytospin preparation (see Section 2.2.8). The remainder were resuspended in an appropriate volume of foetal calf serum (92%) and dimethyl sulphoxide (8%), and divided into aliquots of 1×10^7 or 5×10^6 cells/ml in 1.5 ml Nunc tubes (Nalgene, Herefordshire, UK). These viable cell suspensions were initially stored overnight (O/N) at -80°C in a Cryo 1° freezing container (Nalgene) before being transferred the following day into liquid nitrogen for long term storage.

2.2.7 Cell lines

Cell lines were handled in a class II MSC microbiological safety cabinet, and non-EBV-infected, or EBV-negative, cell lines were handled prior to those which were EBV-infected, or EBV-positive. Details of the cell lines used in array-CGH and gene expression array analyses are given in Table 2.1.

2.2.7.1 Recovery and maintenance of cell lines

All cell lines were cultured from viable stocks of 5×10^5 cells that had been stored long term in liquid nitrogen, as described in section 2.2.2. The cells were defrosted slowly at 37°C , washed once in the appropriate medium to remove DMSO, and then resuspended in 10 ml (5×10^4 cells/ml) of the appropriate medium in a vented tissue culture flask. The cultures were incubated at 37°C in 5% CO_2 and passaged twice a week with fresh medium. Cell growth curves were compiled in order to calculate the optimal time for harvesting to use in RNA experiments. Harvesting took place when cells were in log phase growth and at least 1×10^8 cells were available. Four flasks of 50 ml of culture at the pre-determined optimal density (see Table 2.1) were harvested at the appropriate time point and the resultant cell pellet was used for both DNA and RNA extraction.

Table 2.1. Details of cell lines used in array-CGH and gene expression array analyses.

Cell Line	Sex	Details	EBV status
IM-9	Female	ATCC CCL-159 Bone marrow cells from a multiple myeloma patient RPMI 1640 + 10% FCS Doubling time 48 hours Harvest at maximal density of 0.5-1.0x10 ⁶ cells/ml	Positive
HDLM2	Male	DSMZ# ACC 17 Pleural effusion from a NSHL (stage IV) patient RPMI 1640 + 10% FCS Doubling time 72 hours Harvest at maximal density of 2.0-2.5x10 ⁶ cells/ml	Negative
KM-H2	Male	DSMZ# ACC 8 Peripheral blood of MCHL (stage IV) patient RPMI 1640 + 10% FCS Doubling time 48 hours Harvest at maximal density of 1.0x10 ⁶ cells/ml	Negative
L1236	Male	DSMZ# ACC 530 Peripheral blood of MCHL (stage IV) patient RPMI 1640 + 10% FCS Doubling time 48 hours Harvest at maximal density of 0.6x10 ⁶ cells/ml	Negative
L428	Female	DSMZ# ACC 197 Peripheral blood of NSHL (stage IVB) patient RPMI 1640 + 10% FCS Doubling time 48 hours Harvest at maximal density of 0.5-1.0x10 ⁶ cells/ml	Negative
L540	Female	DSMZ# ACC 72 Bone marrow of NSHL (stage IVB) patient RPMI 1640 + 20% FCS Doubling time 48 hours Harvest at maximal density of 1.5x10 ⁶ cells/ml	Negative
L591	Female	Kindly provided by Dr. David Jones, Southampton University RPMI 1640 + 10% FCS Doubling time 72 hours Harvest at maximal density of 0.5x10 ⁶ cells/ml	Positive

ATCC, American Type Culture Collection; DSMZ, Deutsche Sammlung von Mikroorganismen und Zellkulturen GmbH (German cell culture collection); FCS, foetal calf serum; MCHL, mixed-cellularity Hodgkin Lymphoma; NSHL, nodular sclerosis Hodgkin lymphoma; RPMI, Roswell Park Memorial Institute.

2.2.8 Preparation of cytopsin slides

Cytopsin slides for LMD were prepared in-house by attaching a piece (50 x 22 mm) of PENfoil membrane (PALM Microlaser Technologies, Bernried, Germany), with Fixogum rubber cement (Marabu, Tamm, Germany) along two opposing sides, to the surface of plain glass slides (BDH, Poole, UK). The slides were left to dry for 2-3 days in clean slide box and any with wrinkled PENfoil were discarded.

Cytopsins were prepared from cell line cultures or viable cells that were either fresh or had been stored in liquid nitrogen. PENfoil slides and double or single chamber cytopsin funnels (ThermoShandon, Cheshire, UK) were fastened together with a cytopsin clip and loaded into the cytopsin holder. Following a viable cell count, 100 µl of 2.5×10^5 cells in suspension were pipetted into each chamber and the cells were spun at 450 rpm for 10 mins in a cytocentrifuge (Cytopsin 2; ThermoShandon, Cheshire, UK). The slides were immediately removed from the holders and air-dried. When completely dry, an Immunopen (Dakocytomation, Cambridgeshire, UK) was used to circle each cell spot and once these circles had dried the slides were either used immediately or wrapped in aluminium foil and stored at -80°C until required.

2.2.9 CD30-staining using the ABCComplex method

The cytopsins were CD30-stained by IHC, using the ABCComplex method and Fast Red substrate, in order to facilitate the identification of HRS cells. CD30-positive lymphocytes may also be present in cell suspensions from cHL biopsies, but these are usually smaller than HRS cells, have less prominent nucleoli and are less likely to rosette lymphocytes.

Cytospins were equilibrated to room temperature and then rehydrated in 1x Tris buffered saline (TBS) with 0.1% Tween 20 (TBST) (Serotec, Oxford, UK) for 5 mins. The whole staining procedure was performed at room temperature and the slides were washed twice in 1x TBST for 3-5 mins between each step. Heat inactivated rabbit serum (20%) (Vector Labs) was added to the cell spots for twenty mins to inhibit non-specific binding. An anti-CD30 primary monoclonal antibody (clone HRS4, Immunotech, France) was then diluted 1:100 and pipetted onto each cell spot. The cytospins were incubated for 30 mins at room temperature. A third incubation, for 30 mins at room temperature, was set up with a 1 in 300 dilution of biotinylated rabbit anti-mouse secondary antibody (DAKO). An aliquot of ABCComplex/AP (DAKO) was then added to each cell spot and incubated for thirty mins, followed by the addition of two drops of Fast Red substrate (DAKO). After 15-17 mins, the slides were washed twice in distilled water, before being counterstained in 0.1% toluidine blue and air-dried O/N.

2.2.10 Laser microdissection from cytospin slides

LMD was performed using a Leica AS Laser Microdissection system (Leica, Milton-Keynes, UK) in a room set up specifically for this use. This instrument uses a UV laser to cut around the cells enabling them to drop into the cap of an open 0.2 ml PCR tube. The 0.2 ml tubes, equipment and the cutting room were UV-irradiated approximately one hour prior to cutting to decrease static and reduce the possibility of contamination.

Ten single cells were laser microdissected into each tube lid, directly into 6 μ l of DOP-lysis buffer (1x Thermosequenase buffer [260 mM Tris-HCl pH 9.5, 65 mM

MgCl₂], 0.25 mg/ml proteinase K, 0.45% Tween 20, 0.45% NP40). An LMD cutting blank control was included after every 10 tubes of laser microdissected cells. These control tubes contained only DOP-lysis buffer and were kept open in the microscope rack throughout a set of cutting experiments, but no cells were cut into these tubes.

Once a cutting session was completed, the samples were incubated for an hour at 55°C to enable proteinase K digestion. This lysis method was selected over alkaline lysis since Dietmaier et al. (1999) suggested that protease degrades the nuclear proteins involved in packaging of chromosomes and thereby enables more efficient extraction of DNA from cells (Dietmaier et al 1999). The lysis reaction was stopped by heating the sample to 96°C for 10 mins in order to denature the enzyme. The tubes were stored at 4°C O/N and DOP-PCR was performed the following day (see Section 2.2.15).

2.2.11 Total RNA extraction

The RNAqueous[®] kit (Ambion[®]; Applied Biosystems, Warrington, UK) was used, according to the manufacturer's protocol, for small scale extraction of RNA from $\leq 5 \times 10^6$ cells. The RNA pellet was resuspended in 10-60 μ l of elution buffer, supplied in the RNAqueous[®] kit.

Large scale extraction of RNA, from $\geq 6 \times 10^7$ cells, was performed from larger volumes of fresh cultured cells using 1 ml of TRIZOL reagent (Invitrogen Ltd., Paisley, UK) per aliquot of 1×10^7 cells, according to the manufacturer's protocol. Following the addition of TRIZOL, the cells were lysed by repetitive pipetting, then

incubated in a 30°C waterbath for 5 mins. For every 1 ml of TRIZOL, 200 µl of chloroform was added to the lysate and mixed by shaking vigorously for 15 seconds. The lysate was incubated again for 5 mins in a 30°C waterbath, before centrifugation at 12000 g for 15 mins at 4°C. The colourless upper aqueous layer containing the RNA was removed using a Pasteur pipette and transferred into a fresh Falcon tube. Isopropyl alcohol (500 µl per 1 ml of TRIZOL initially used) was added to precipitate the RNA and the sample was incubated in a 30°C waterbath for 10 mins before centrifugation at 12000 g for 10 mins at 4°C. The resultant RNA pellet was then washed once in 75% ice cold ethanol (1 ml per 1 ml of TRIZOL initially used), mixed by vortexing and then centrifuged at 7500 g for 5 mins at 4°C. The supernatant was removed and the pellet air-dried for 5-10 mins. The resultant RNA pellet was then resuspended by adding 30 µl of RNase-free water (Qiagen), for every 1×10^7 cells processed, and incubated at 55°C for 15 mins. All RNA samples were pooled stored at -80°C until required.

2.2.12 DNA extraction from tumour samples or cell lines

The cell pellet was washed twice in 1x PBS (137 mM NaCl, 2.7 mM KCl, 10 mM Na₂HPO₄, 2 mM NaH₂PO₄, pH 7.2) then resuspended in 1x TNE buffer (100 mM Tris Base, 10 mM EDTA, 2 M NaCl, adjusted to pH7.4), 0.5% sodium dodecyl sulphate (SDS) and 50 µg/ml proteinase K. Following incubation at 56°C for 1.5-2 hours, an equal volume of phenol was added to the lysate and the solution was thoroughly mixed by gentle inversion for 10 mins. The phases were separated by centrifugation at 1700 g for 10 mins. The top layer of solution was pipetted off into a fresh tube to which an equal volume of phenol was added. The phases were thoroughly mixed together again and separated by centrifugation. This mixing and separation of phases

was repeated twice with phenol: chloroform: isoamyl alcohol (25:24:1; Sigma-Aldrich Company Ltd.) and once with chloroform: isoamyl alcohol (24:1; Sigma-Aldrich Company Ltd.). Two volumes of ice cold 100% ethanol were then added to the solution and the DNA was spooled on the end of a pipette tip and transferred to a 1.5 ml microfuge tube. The pellet of DNA was washed in ice cold 70% ethanol, air-dried, and resuspended in 1x TE buffer (10 mM Tris pH 8.0, 1 mM EDTA, pH 8.0) (500 µl was required to resuspend DNA extracted from 1×10^7 cells). Overnight incubation at 37°C enabled the DNA to completely resuspend.

2.2.13 Ethanol precipitation of DNA

Nucleic acids were cleaned up and concentrated using ethanol precipitation. One tenth volume of 3 M sodium acetate was added to the DNA solution, followed by 2 volumes of ice-cold 100% ethanol. The solution was mixed well, then placed at -20°C O/N to allow precipitation to take place. The following day the mixture was centrifuged at 13000 g in a microfuge (Minispin Plus, Eppendorf UK Ltd., Cambridge, UK) for 30 mins at 4°C. The supernatant was discarded and 250 µl of 70% ethanol was added to the pelleted nucleic acid. The mixture was briefly vortexed, then centrifuged for 30 mins at 4°C. The supernatant was discarded and Parafilm[®] (VWR International Ltd.) was placed tightly over the top of the open microfuge tube and pierced twice with a sterile needle. The microfuge tube was left on the bench until all traces of supernatant had evaporated away. The pellet was then resuspended in a suitable volume of TE buffer or water.

2.2.14 Quantification of Nucleic Acids

The quantity and quality of DNA and RNA were assessed using a Nanodrop ND-1000 Spectrophotometer (Nanodrop Technologies Ltd., Delaware, USA) to measure optical density (OD) at wavelengths of 230 nm, 260 nm and 280 nm. The concentration of DNA was calculated by assuming that 50 µg/ml of double stranded DNA has an OD_{260nm} of 1.0, and 40 µg/ml of RNA has an OD_{260nm} of 1.0. The purity of a sample was indicated by an OD_{260nm}/ OD_{280nm} ratio reading of approximately 1.8 for DNA and approximately 2.0 for RNA. For DNA a secondary measurement of nucleic acid purity is provided by the OD_{260nm}/ OD_{230nm} ratio; a value lower than 1.8-2.2 suggests the presence of contaminants.

2.2.15 Polymerase chain reaction

Several different PCR techniques were used in this project. The protocols for reverse transcription (RT)-PCR, conventional PCR and QRT-PCR are outlined in Chapter 3 and degenerate PCR is described in Chapter 4. The methodology for DOP-PCR is discussed below.

2.2.15.1 DOP-PCR

DOP-PCR was performed using a protocol devised by Huang et al. (2000), which had then been adapted and optimised by Dr Daniel Chui in this laboratory (Huang et al 2000; Chui et al 2003). The initial template for the two-step WGA was 6 µl of either genomic DNA or DNA extracted from LMD cells by proteinase K digestion. Each tube containing 10 microdissected cells was treated as a separate amplification reaction, and 40 tubes were DOP-amplified at the same time. The universal UN1

DOP-primer, also called 6MW (Telenius et al 1992), was used in both rounds of PCR, unless otherwise stated.

The first amplification involved a 10 µl reaction containing 1x Thermosequenase reaction buffer (Amersham Biosciences), 200 µM of each dNTP (Amersham BioScience, Buckinghamshire, UK), 1 µM DOP-primer (NAP-purified; Sigma-Genosys) and 4 U of Thermosequenase polymerase (Amersham Biosciences). Thermal cycling conditions were 3 mins at 95°C, followed by 4 cycles of 1 minute at 94°C, 1 minute at 25°C, and then 3 mins ramping up to an extension step of 72°C for 2 mins. This was followed by a final extension step at 72°C for 10 mins. The total reaction volume from the first amplification was used as template for the second amplification reaction, which was set up in the same tubes as the first reaction. The second reaction contained 1x custom-made buffer (WMegaMix, Microzone Limited, West Sussex, UK). A master mix was then added to give a final reaction volume of 50 µl containing 200 µM dNTPs, the UN1 DOP-primer at 1 µM and 5 units of AmpliTaq[®] DNA polymerase (Applied Biosystems). Thermal cycling conditions were as follows: an initial denaturation at 95°C for 3 mins, followed by 35 cycles of 94°C for 1 minute, 56°C for 1 minute and 72°C for 2 mins, with a final extension step at 72°C for 10 mins. All amplifications were performed using the GeneAmp PCR System 2400 or 9700 (Applied Biosystems).

A positive control of 60 pg of normal human genomic DNA (either male or female; Promega) was amplified in every DOP-PCR assay. Negative controls were also included (one per ten reaction tubes), by substituting the DNA for molecular biology

grade water (Microzone Limited), in order to check for the introduction of DNA contamination during PCR set up.

Initially, DNA contamination was consistently observed within negative water controls in the DOP-PCR assays. When these contaminated controls were investigated using QRT-PCR assays specific for the human housekeeping genes adenosine monophosphate deaminase (AMPD), β -globin and heat shock protein 90 (HSP90), results were negative confirming that the contamination was not of human origin. Since PCR reagents can sometimes be the source of bacterial DNA contamination, several sources of each reagent were tested by DOP-PCR with the UN1 primer, and both a positive (normal human genomic DNA) and negative (water) control. We found that replacing the second round DOP-amplification buffer GeneAmp 10x PCR Buffer (Applied Biosystems) with a custom-made buffer, WMegaMix (Microzone Limited, West Sussex, UK) removed the smear of contaminating DNA. The GeneAmp 10x PCR Buffer is composed of 500 mM KCl, 100 mM Tris-Hcl (pH8.3), 15 mM MgCl₂ and 0.01% (weight/volume) gelatine. WMegaMix contains an alternative synthetic stabiliser to gelatine and so we concluded that the DNA contamination previously seen in our DOP-products was probably bovine DNA from gelatine in the GeneAmp 10x PCR Buffer.

Following amplification, 4 μ l of DOP-product from each tube was subjected to electrophoresis on 1% agarose gels in order to assess the size range and amount of amplified products. The DNA size marker *Hae*III-digested ϕ X174 RF DNA (Invitrogen Ltd.) was always electrophoresed (0.5-1 μ g) alongside the DOP-products.

Successfully amplified DOP-products were then combined and subjected to ethanol precipitation, in order to remove free nucleotides that could interfere with subsequent labelling reactions and to concentrate the products. The resultant DNA pellet was resuspended in dH₂O. Following quantification using the Nanodrop ND-1000 Spectrophotometer, 500 ng of the resultant DNA was electrophoresed on a 1% agarose gel (see below) to assess the size range of the DOP-products.

2.2.16 Analysis of PCR products

2.2.16.1 Agarose gel electrophoresis

Agarose gel electrophoresis was used to analyse PCR products. Agarose powder (Invitrogen) was dissolved (0.8% weight/volume) in 1x TBE buffer by heating to >90°C. Once the gel solution had cooled to approximately 65°C, 2 µl of 0.5 µg/ml ethidium bromide was added per 100 ml of gel mix. The gel solution was poured into the Sub-Cell GT cell (Bio-Rad Laboratories, Hertfordshire, UK), with a well-forming comb in place, and left at room temperature to set. Once set, the gel was submerged in 1x TBE buffer and the comb was removed. One-tenth volume of gel-loading buffer (0.42% bromophenol blue, 0.42% xylene cyanol, 50% glycerol) was mixed with the DNA samples before loading into the wells. A DNA size marker (0.5-1 µg) was always included: either *Hind*III-digested bacteriophage lambda DNA (Invitrogen Ltd.) or *Hae*III-digested φX174 RF DNA (Invitrogen Ltd.). Electrophoresis was performed at 4-8 V/cm for approximately 90 mins, depending on gel size and the size of the fragments to be separated. DNA was visualised using a UV emitting Spectroline Transilluminator (Model TC-254A) and the results were recorded with a UVIsave Gel Documentation System (Jencons-PLS, East Sussex, UK).

2.2.16.2 Polyacrylamide gel electrophoresis

For the separation of PCR products of less than 1kb in length, polyacrylamide gel electrophoresis was used. The gel was made from 5% acrylamide (Sigma Aldrich Company Ltd.), 3% bisacrylamide (Sigma Aldrich Company Ltd.), and 1x TBE buffer, and was polymerised by the addition of 0.06% (w/v) ammonium persulphate (APS) and 0.03% TEMED (N, N, N, N – tetramethylethyldiamine). Gels were poured between glass plates, a well-forming comb was put in place and the apparatus (Mini-Protean System, Bio-Rad Laboratories, Hertfordshire, UK) was left at room temperature, for approximately 45 mins, for the gel to solidify. The gel was then submerged in 1x TBE buffer and the comb removed. Gel-loading buffer was added to each DNA sample, and these were loaded into the wells alongside a DNA size marker (*Hae*III digested ϕ X174 RF DNA; Invitrogen Ltd.). Electrophoresis was performed at 120 V for approximately 45 mins. The gel was then carefully removed from the glass plates and stained in 0.5 μ g/ml ethidium bromide. The separated DNA was visualised using a UV light source (Spectroline Transilluminator, Model TC-254A) and images captured using the UVIsave Gel Documentation System (Jencons-PLS).

2.2.17 Cloning and plasmid preparations

Following purification using the Quickstep 2 PCR Purification kit (EDGE Biosystems), amplification products were cloned using the TOPOTM TA Cloning[®] kit (Invitrogen Ltd.) according to the manufacturer's protocol. Cloning was achieved using the PCR[®]2.1-TOPO[®] vector and One Shot[®] TOP10 chemically competent *E. Coli* cells. In order to identify a clone containing the sequence of interest following transformation, single colonies were picked with a sterile rod. The rod was then dropped into 3 ml of L-broth containing 50 mg/ml ampicillin or the appropriate

antibiotic. The cultures were placed in a 37°C shaking incubator O/N. The following day the High Pure Plasmid Isolation Kit (Roche, Lewes, East Sussex, UK) was used to extract plasmid DNA from the bacterial culture. At the end of the protocol, purified plasmid DNA was eluted from the High Pure filter columns by the addition of 100 µl of elution buffer and 60 seconds of centrifugation at 13000 g.

One microgram of plasmid DNA was digested in a total reaction volume of 20 µl containing 10 U of restriction enzyme (Invitrogen) and 2 µl of the appropriate 10x restriction buffer (Invitrogen). Reactions were incubated at 37°C O/N and then the digests were analysed by agarose (0.8%) gel electrophoresis.

2.2.18 Nucleotide sequence analysis

Cycle sequencing was performed directly on plasmid DNA using the Big Dye[®] Terminator v3.1 Cycle Sequencing Kit (Applied Biosystems), forward or reverse M13 primers (Forward: 5'-GTAAAACGACGGCCAGTG-3'; Reverse: 5'-GGAAACAGCTATGACCATG-3') and a GeneAmp PCR System 2400 or 9600 (Perkin-Elmer). Products were purified through Performa DTR Gel Filtration Cartridges (EDGE Biocolumns), and then dried in a dessicator. The resultant pellet was resuspended in 21 µl of High Dye Formamide (Applied Biosystems) and then analysed on an ABI PRISM[®] 3100 Genetic Analyzer (Applied Biosystems). Nucleotide sequences were entered into the Basic Local Alignment Search Tool for nucleotides (blastn) program (<http://www.ncbi.nlm.nih.gov/BLAST>) for identification.

CHAPTER 3

NO EVIDENCE FOR A DIRECT ASSOCIATION BETWEEN MEASLES VIRUS AND HODGKIN LYMPHOMA

The material presented in this chapter has been published as a scientific paper:

Measles virus and classical Hodgkin lymphoma: No evidence for a direct association.

Wilson KS, Freeland JM, Gallagher A, Cosby SL, Earle JA, Alexander FE, Taylor

GM, Jarrett RF. *Int J Cancer*. 2007. Jul 15;121(2):442-7.

3.1 INTRODUCTION

In the four disease model, described in Section 1.4.3, the largest group of HL cases within the developed world are young adults aged 15-34 years old (Jarrett 2002). The risk of developing young adult HL has been associated with high social class, a high level of maternal education, small family size, early birth order (Gutensohn 1982) and lack of preschool attendance (Chang et al 2004). It has been proposed that such factors diminish an individual's exposure to infectious agents in early childhood and thereby increase their susceptibility to a virus-induced pathogenesis later in life – this is the so-called late host response model.

Paradoxically, since <25% of young adult cases are EBV-associated (Jarrett et al 2003), EBV is not the elusive agent implicated in this group of cases. A potential candidate virus should be common and infect most, or many, individuals in childhood. Serological and molecular studies have explored possible associations with other members of the herpesvirus family, the polyomaviruses (JCV, BKV, SV40 and lymphotropic papovavirus (LPV)), parainfluenza virus, human T-cell leukaemia virus types 1 and 2, and adenovirus types 5 and 12 (Armstrong et al 1998; Berneman et al 1998; Evans and Gutensohn 1984; Gallagher et al 2002; MacKenzie et al 2003). With the exception of an association between non-EBV-associated HL and high antibody titres to human herpesvirus 6, no positive associations have emerged (Clark et al 1990) (D. Clark and R. Jarrett, unpublished data).

Recently an association between measles virus (MV) and HL in Israel was reported (Benharroch et al 2003). Prompted by epidemiological findings, biopsies from 68 HL patients were analysed for the presence of MV proteins using IHC. Using an anti-

MV-nucleoprotein (NP)-specific antibody H14 cytoplasmic MV NP was detected within the HRS cells of 41 (60.3%) of their original cohort of 68 HL patients, the majority of which were classified as NSHL (Benharroch et al 2003). This cohort was later expanded to 143 cHL cases and IHC was performed using a larger panel of anti-MV antibodies (anti-NP [H14, L39/22, L39/61] and anti-hemagglutinin [K83, L77, NS32]) (Benharroch et al 2004). Expression of MV antigens was demonstrated within the HRS cells of 105 (73.4%) cHL cases,^a but there was not complete concordance between the results from different antibodies. EBV was detected in 44 (30.8%) of cases but there was no evidence of an inverse relationship between EBV and MV positivity. MV RT-PCR was subsequently performed on biopsy samples from 19 of the cHL cases, of which only 2 (10.5%) were positive.

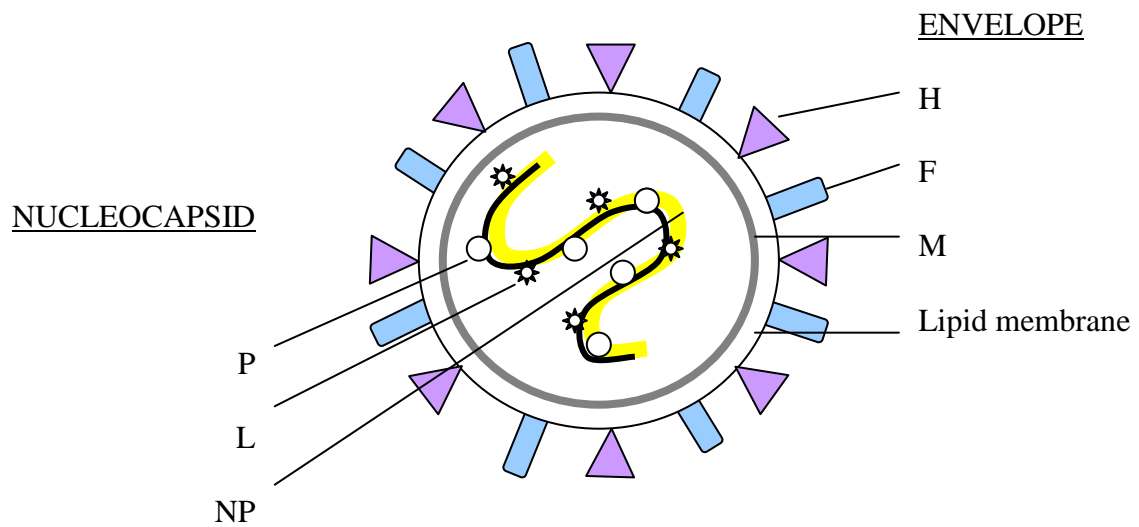
The MV is a member of the genus *Morbillivirus* within the Paramyxoviridae family (Griffin 2001). The virions are spherical (see Figure 3.1a) with a helical nucleocapsid (NP) and are enclosed by an envelope containing two different surface projections (called peplomers) with distinct morphologies: the hemagglutinin (H) proteins appear conical in shape and the fusion (F) proteins are dumbbell-shaped. The matrix (M) protein lines the inside of the envelope and interacts with the peplomers and the nucleocapsid. The large (L) and phosphoprotein (P) proteins are internal virion components present in limited quantities and may represent part of the transcription complex. The MV genome (see Figure 3.1b) is a linear, negative-sense, single-strand RNA and has been completely sequenced. It is approximately 15.9kb in length, although this differs slightly between virus strains or passage histories of the same strain. Eight proteins are encoded from six genes which are arranged in the order 3'-NP-P-M-F-H-L-5'. Several proteins are encoded by the P gene: the P protein and

^aDNA sequences homologous to measles virus RNA have been identified in tissues affected with systemic lupus erythematosus, providing evidence for the integration of these viruses into the cellular genome (Zhdanov, 1975).

three non-structural proteins (C, V and R), which are translated from alternative reading frames.

MV establishes a systemic infection beginning in the respiratory tract and spreading initially to the lymphatic tissues, then to organs and tissues. Monocytes and macrophages have been identified in mice as early targets of MV infection, with both B- and T-lymphocytes infected at lower levels (Roscic-Mrkic et al 2001). An efficient MV-specific immune response is usually initiated which eliminates the infection and incurs life-long immunity against the virus (Griffin 2001). Secondary infections can occur in immunosuppressed individuals.

a)



b)

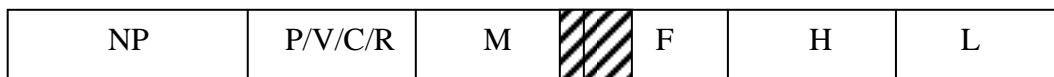


Figure 3.1. Schematic diagram of a) the measles virus and b) its RNA genome (based on a figure from (Griffin 2001)). P/V/C/R region encodes the phosphoprotein (P) and the V, C and R non-structural proteins. The shaded region indicates untranslated RNA. F, fusion protein; H, hemagglutinin; L, large protein; M, matrix, NP, nucleoprotein; P, phosphoprotein

There is a body of literature linking MV and HL. In a study primarily designed to investigate the association between mumps virus and HL, Truant and Hallum (1976) detected measles-specific antigens in six out of seven HL lymph nodes using an anti-measles antiserum (Truant and Hallum 1976). The cellular localisation of the MV was not reported and MV antigens were also detected in 9 out of 18 control tissues in this study. Despite these positive findings, a large serological study of HL in young adults found no significant difference between the distributions of measles antibody titres in cases and controls (Rocchi et al 1975). A later case-control study of HL in young adults aged 15-24 years reported that the risk of developing HL was decreased in individuals with a past history of measles (Alexander et al 2000). Case-control differences were significant for measles infection at all ages, measles infection at 5-10 years of age, and for non-EBV-associated cases compared to controls. These data suggest a specific protective effect of measles in school age children and are consistent with the late host response model described earlier.

Overall, previous publications do not provide evidence for a consistent association between MV infection and the development of HL. In addition to studies investigating an aetiological association between MV and HL, there are several case reports describing the regression of HL following measles infection (Mota 1973; Taqi et al 1981; Zygiert 1971). It has been suggested that this regression may be related to interferon production or other immunomodulatory effects of MV (Gopas et al 1992; Schattner 1984).

The live attenuated Edmonston B strain of MV is known to have a specific oncolytic effect in a number of human tumours, including B-cell lymphoma xenografts in

severe combined immune deficient (SCID) mice (Grote et al 2001). Infection has been shown to cause immediate cytopathic effect with extensive syncytial formation in some tumours, with minimal damage to normal cells (Peng et al 2001). The mechanism by which this occurs is not well understood.

MV is normally associated with lytic infection and cell fusion. Occasionally the virus is able to establish a persistent infection, best described in subacute sclerosing panencephalitis. Persistent infection of lymphoid cell lines has also been reported (Fernandez-Munoz and Celma 1992; Minagawa and Sakuma 1977) and the virus has been detected in peripheral blood mononuclear cells and lymphoid subsets (Jacobson and McFarland 1982; Joseph et al 1975; Kawashima et al 1996). These data, coupled with the case reports mentioned above, suggest that MV may be able to infect and persist in HRS cells. Mechanisms involved in the establishment of persistent infection are not well understood but both virus and host cell variation have been implicated (Boriskin et al 1986; Hummel et al 1994; Rima et al 1977; Rustigian 1966; Young et al 1985).

This chapter will describe how, in response in the publication by Benharroch and colleagues (2003), we expanded previous observations on reported history of measles infection and subsequent risk of HL, and screened HL samples from the UK for evidence of MV infection.

Aims

- To investigate HL biopsies from UK patients for evidence of MV infection.

3.2 MATERIALS & METHODS

3.2.1 Case selection

A population-based, case-control study called the Scotland and Newcastle Epidemiological Study of Hodgkin's Disease (SNEHD) has been undertaken by our group and described previously (Alexander et al 2003; Jarrett et al 2003). HL cases were identified from the Scotland and Newcastle Lymphoma Group (SNLG) Registry, the Scottish Cancer Registry and Northern Region Cancer Registry. Five hundred and eighty-four confirmed cases of HL aged between 16 and 74 years old were eligible for inclusion. A similar number of controls were matched by age, sex and residential region. Ethical permission was obtained and interviews were conducted with a structured questionnaire being completed by consenting cases and controls. Any childhood infections were recorded, including measles, mumps, chicken pox, rubella and pertussis. The age of infection was noted and results were analysed with respect to the age of infection in three age groups: 0-4 years; 5-10 years; and over 10 years. Following the collection of data, four comparisons were performed systematically: all cases versus controls; non-EBV-associated HL cases versus controls; EBV-associated cases versus controls; and non-EBV-associated versus EBV-associated cases. All statistical analyses were performed by Professor Freda Alexander (University of Edinburgh, UK).

Biopsy material was retrieved from the SNEHD cases and subjected to histological review, which was approved by the pathology working party of the SNLG. The EBV status of the tumours was determined by EBER ISH on paraffin-embedded sections (performed by Mrs. June Freeland). In cases where the results were difficult to interpret or where there were large numbers of EBV-positive cells, LMP1 IHC was

also performed. A case was identified as EBV-associated if HRS cells were positive in either assay.

A subset of 97 HL cases (see Table 3.1), from which surplus paraffin-embedded tissue was available, was investigated for the presence of MV antigen using IHC. Viably stored biopsy material was available from a second group of 20 cHL cases (see Table 3.2) and these samples were investigated for evidence of MV infection using RT-PCR. Thirteen lymph node biopsies, which demonstrated only reactive changes, were included as controls in these latter experiments.

Table 3.1. Details of patients in case series 1.

Age group	n	Histological subtype				EBV status	
		MCHL	NSHL	LDHL	LRCHL	Non-EBV-associated	EBV-associated
15-34 years	51	7	43	-	1	38	13
35-49 years	17	7	9	-	1	10	7
50-74 years	29	11	17	1	-	17	12
All	97	25	69	1	2	65	32

MCHL, mixed cellularity Hodgkin lymphoma; NSHL, nodular sclerosis Hodgkin lymphoma; LDHL, lymphocyte depleted Hodgkin lymphoma; LRCHL, lymphocyte rich classical Hodgkin lymphoma; n, number of patients.

Table 3.2. Details of patients in case series 2.

LYMPH NODE HISTOLOGY					
Age group	n	MCHL	NSHL	LRCHL	Reactive node
<35 years	24	-	11	-	13
35-49 years	5	1	3	1	-
50+ years	4	1	3	-	-
All	33	2	17	1	13

MCHL, mixed cellularity Hodgkin lymphoma; NSHL, nodular sclerosis Hodgkin lymphoma; LRCHL, lymphocyte rich classical Hodgkin lymphoma; n, number of patients.

3.2.2 Immunohistochemistry

Sections of formalin-fixed, paraffin-embedded lymph node biopsy material from 97 HL cases and 13 controls were examined by IHC (performed by Mrs. June Freeland and myself) using a mouse monoclonal antibody (IgG1- κ clone 49-21; Immunologicals Direct, Oxford, UK) known to be reactive with the MV NP.

Sections on slides were dewaxed and rehydrated by the following series of immersive steps: CitrocLEAR (HD Supplies, Aylesbury, UK) for 20 mins, 90% ethanol for 2 mins, 70% ethanol for 2 mins, and water. Antigen retrieval was performed by heating EDTA buffer (pH8.0) in a pressure cooker until boiling, then transferring the dewaxed slides into the pressure cooker and placing the lid on top securely. The pressure cooker was allowed to reach full pressure for 3 mins, then the slides were removed and cooled to room temperature. The remainder of the procedure was performed at room temperature and the sections were not allowed to dry out. Initially the sections were washed twice in 1x Tris buffered saline (TBS; 50 mM Tris-HCl pH8.0, 150 mM NaCl, adjust to pH7.6) for 5 mins. The slides were then immersed in 1.5 % hydrogen peroxide/methanol for 10 mins to inhibit endogenous peroxidase, which may otherwise contribute to background staining. Two washes in water for 5 mins each, followed by a further two 5 minute washes in 1x TBS were performed before 100 μ l of 20% normal horse serum (from the Vectastain® kit; Vector Laboratories, Peterborough, UK) was pipetted over each section and incubated for 10 mins. The primary MV NP antibody (Immunologicals Direct, Oxford, UK), diluted 1:80, was pipetted over the sections, which were incubated for 1 hour. The slides were washed twice in 1x TBS, as before, then 100 μ l of the secondary antibody (biotinylated anti-mouse IgG from the Vectastain® kit; Vector Laboratories), was pipetted onto each

section and allowed to incubate for 30 mins. The slides were washed twice in 1x TBS then a few drops of the avidin-biotin peroxidase complex [ABC] (from the Vectastain® kit; Vector Laboratories) were added to each section, to detect bound antibody, and allowed to incubate for 30 mins. The slides were immersed twice in 1x TBS prior to incubation in the chromogenic substrate, tetrahydrochloride 3,3'-diaminobenzidine [DAB] (Sigma-Aldrich Company Ltd., Dorset, UK), for approximately 10 mins, until staining of the positive control could be visualised. The slides were washed twice in 1x TBS before counterstaining with haematoxylin and dehydration by a series of immersions in methanol, 100% ethanol and citrate buffer (10mM Citric Acid, 0.05% Tween 20, adjust to pH 6.0). Once dry, the sections were mounted, using the resinous mounting medium depex polystyrene (DPX), and left to dry O/N on a heat block.

MV (Zagreb strain)-infected Vero cells were obtained from Dr. S.L. Cosby (Queen's University, Belfast). Cells were harvested at 72 hours after infection, pelleted, fixed in formalin and paraffin-embedded. Sections were subsequently used in the IHC assay as positive controls. In order to avoid contamination of case DNA with MV within the laboratory, the cells were handled within a Class II MSC hood, which was sterilised with formalin following the harvesting of infected cells.

3.2.3 Reverse Transcription (RT)-PCR

Single cell suspensions were prepared from lymph node biopsies and total RNA was extracted using the RNeasy® kit (Qiagen Ltd., Crawley, UK). One microgram of RNA was used as the template for cDNA synthesis with the Superscript™ II RNase H⁻ reverse transcriptase (Invitrogen Ltd.) and 2.5 μM random

oligonucleotide primers (Invitrogen Ltd.), according to the manufacturer's instructions. The resultant cDNA was used as template in both conventional and QRT-PCR (100 ng and 50 ng used per reaction respectively).

cDNA prepared from MV (Zagreb-strain) infected Vero cells and MV (Edmonston-strain) infected human osteosarcoma (HOS) cells were included as positive controls. Total RNA was extracted from both cell types using the QIAamp Viral RNA Mini kit (QIAGEN Ltd, Crawley, West Sussex, UK). cDNA was synthesised as above for use as positive control templates in both conventional and QRT-PCR studies.

3.2.4 Conventional PCR

Previously published oligonucleotides (see Table 3.3) for the amplification of the MV H and NP genes were synthesised and used for nested PCR (Chadwick et al 1998).

First round PCR involved the use of 200 μ M of nucleotides (Amersham Pharmacia Biotech, Buckingham, UK), ReddyMixTM PCR Master Mix (containing 5 U/ μ l of Thermoprime Plus DNA polymerase; Abgene®, Surrey, UK), primers at the stated concentrations (see Table 3.3) and 1 μ g of cDNA template in a total reaction volume of 50 μ l. The following thermal cycling conditions were used on a GeneAmp PCR System 9700 (Applied Biosystems): 94°C for 2 mins followed by 35 cycles (H assay) or 40 cycles (NP assay) of 94°C for 30 seconds; 46°C (H assay) or 55°C (NP assay) for 1 minute; 72°C for 30 seconds; and a final extension at 72°C for 5 mins. The nested PCRs were performed in a total reaction volume of 25 μ l and included 1 μ l of the first round product, the oligonucleotides shown in Table 3.3, and ReddyMixTM PCR Master Mix and nucleotides as described above. Thermal cycling conditions

were as detailed above, but for 25 and 40 cycles in the H and NP assays respectively. One hundred nanograms of positive control cDNA template, synthesised from both MV-infected Vero and MV-infected HOS cells, was included in each assay in order to confirm specificity. All PCR products were analysed by electrophoresis on 8% polyacrylamide gels (see Section 2.2.16). The outer primers and nested PCR assays were expected to result in amplicons of 595bp and 335bp respectively for the H assay, and 528bp and 459bp respectively for the NP assay.

Confirmation that all samples contained sufficient amplifiable cDNA was provided by amplification of the GAPDH gene using the forward and reverse primers designed in-house (see Table 3.3). Reaction conditions were identical to those described for the initial NP outer primer set and an amplicon of 603bp was generated from each sample.

Table 3.3. Conventional PCR primers.

Conventional PCR primer	Gene	Position (bp)	Sequence	Final concentration in PCR (μ M)
H1 5' outer	H	8106-8125	CAG TCA GTA ATG ATC TCA GC	0.25
H2 3' outer	H	8677-8701	CTT GAA TCT CGG TAT CCA CTC CAA T	0.25
H3 5' inner	H	8147-8171	GAG CTC AAA CTC GCA GCC CTT TGT C	1
H4 3' inner	H	8458-8482	ATC CTT CAA TGG TGC CCA CTC GGG A	1
N1 5' outer	NP	97-126	GGG ATA TCC GAG ATG GCC ACA CTT TTA AGG	1
N2 3' outer	NP	597-625	GGG CTA GGA TGG TAC CCA GAA TCA TGT TG	1
N3 5' inner	NP	106-128	GAG ATG GCC ACA CTT TTA AGG AG	0.25
N4 3' inner	NP	564-587	GGG TCT TGC ACT TCA ATA TCT GAG	0.25
GAPDH 5'	GAPDH	210-228	TTC CAC CCA TGG CAA ATT C	1
GAPDH 3'	GAPDH	791-811	TTT CTA GAC GGC AGG TCA GGT	1

H – hemagglutinin primers; NP – nucleoprotein primers; H1, H3, N1 and N3 – forward primers; H2, H4, N2 and N4 – reverse primers

3.2.5 Quantitative real-time PCR

The Primer Express™ version 1.0 software (Applied Biosystems) was used to design TaqMan® assays based upon regions of highly conserved sequence in the MV H and NP coding sequences (see Table 3.4). Amplification reactions were performed in a final volume of 25 µl (see Section 2.2.7) with 100 ng of cDNA template, and primers and probes used at the concentrations shown in table 3.4. Thermal cycling and analysis were performed on an ABI PRISM® 7700 Sequence Detection System (Applied Biosystems). Samples were initially incubated at 50°C for 2 mins, then 95°C for 10 mins followed by 40 cycles of 95°C for 15 seconds and 60°C for 60 seconds. cDNA was extracted from MV-infected HOS cells and included as a positive control. ‘No template controls’, containing molecular biology grade water in place of cDNA, were included after every second cDNA sample. A TaqMan® Pre-Developed Assay for GAPDH (Applied Biosystems) was utilised to confirm that each sample contained amplifiable cDNA. cDNA (50 ng per reaction) from seven HL-derived cell lines (L1236, L428, L540, L591, KMH2, HDLM2 and HO) was also investigated using both MV TaqMan® PCR assays.

Table 3.4. Quantitative real-time PCR primers and probes.

Primers & Probes	Gene	Position (bp)	Sequence	Final concentration in PCR (μ M)
MVH5'	H	7651-7677	GGA TAG GGA GTA CGA CTT CAG AGA TCT	0.05
MVH3'	H	7708-7734	GCA CAG TAT TGA TCA TAA TCC AAT TTG	0.05
MVH probe	H	7679-7706	FAM-ACT TGG TGT ATC AAC CCG CCA GAG AGA A	0.2
MVN5'	NP	301-319	AGC GGG CCC AAA CTA ACA G	0.3
MVN3'	NP	371-391	GGT CAT CGG TGA TCC TCT GAA	0.3
MVN probe	NP	330-369	FAM-AGG TAT ATT ATC CTT ATT TGT GGA GTC TCC AGG TCA ATT G	0.2

3.3 RESULTS

3.3.1 Epidemiology

A self-reported history of previous measles was available for 463 controls and 344 cHL cases included in the SNEHD study. There was no significant difference in the proportion of cases reporting measles (237/463, 69%) compared to controls (343/463, 74%) [odds ratio (OR) 0.82, 95% confidence interval (CI) 0.60-1.13]. Consistent with the introduction of the measles vaccine in the UK in the 1960s, a smaller proportion of young adults reported previous measles, but there was no significant difference between cHL cases and controls. No significant differences emerged when EBV status of cHL tumours was included in the case/control analyses, or when EBV-associated cHL cases were compared with non-EBV-associated cHL cases. When the analysis was restricted to young adults and age at infection with MV was taken into consideration, all cases and the non-EBV-associated cases showed considerable heterogeneity. Similar, though weaker, associations are evident for the EBV-associated cases. Few infections occurred in subjects over the age of 10 years; among young adults only 6 controls and 4 cases reported measles after this age.

3.2.2 Immunohistochemistry

Sections from 97 HL biopsies and 13 reactive nodes were screened for the presence of MV nucleoprotein using IHC. No positive staining was observed in any of these samples, although a strong reactivity was displayed by the positive controls (see Figure 3.2). Case histories were available for 78 of these patients, 52 of whom had reported prior measles infection.

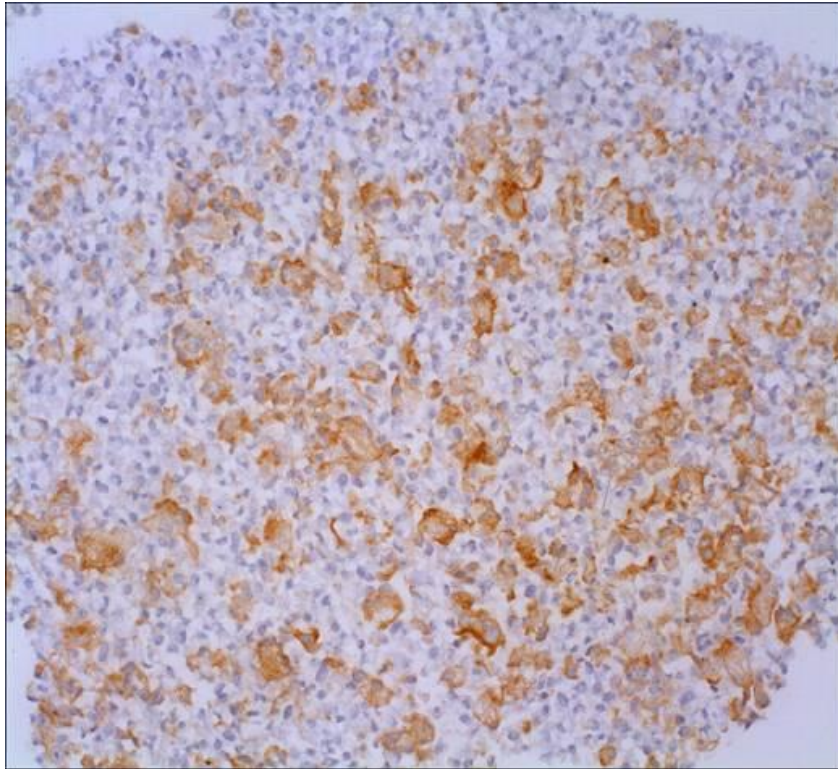


Figure 3.2. Detection of measles virus (MV) by immunohistochemistry. MV-infected Vero cells stained with a mouse monoclonal antibody reactive with the MV NP protein (x200).

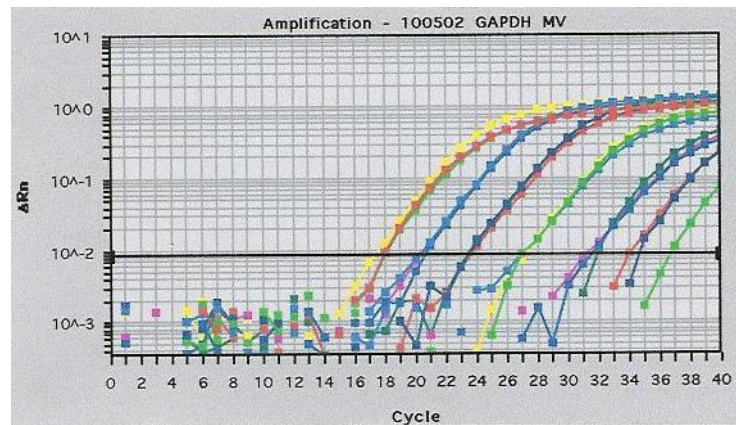
3.3.3 Reverse Transcriptase (RT)-PCR

RT-PCR was performed using RNA extracted from biopsy samples from cases in series 2 and seven HL-derived cell lines. All resultant cDNA samples were shown to be amplifiable by the generation of positive results in both conventional and quantitative real-time GAPDH PCR assays (see Figure 3.3). Products were not detected following PCR of the cHL and reactive node cDNA samples using the H and NP assays (see Figures 3.4 and 3.5).

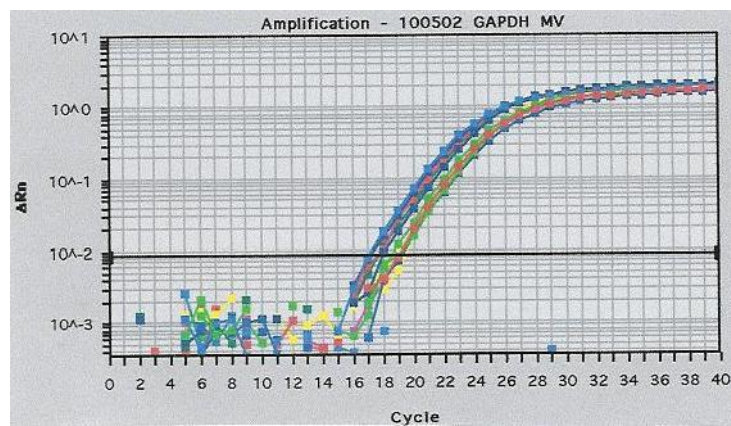
In the H and NP QRT-PCR assays, MV+HOS cDNA was included to indicate the validity of each assay and to set up a standard curve which could be used to compare

positive results. Replicates of 10-fold serial dilutions of the positive control MV+HOS cDNA were used for sensitivity analysis. In the H assay, 2/2 replicates corresponding to 1×10^{-3} ng amplified MV+HOS DNA, and 1/2 replicates corresponding to 1×10^{-4} ng amplified MV+HOS DNA were positive (see Figure 3.6). In the final publication, serial dilutions of MV+HOS cDNA were amplified using the NP assay and products down to 1×10^{-3} ng amplified MV+HOS DNA were detectable (performed by Dr Alice Gallagher).

(a) Serial dilutions of MV + HOS cDNA



(b) cDNA extracted from reactive nodes



(c) cDNA extracted from cHL samples

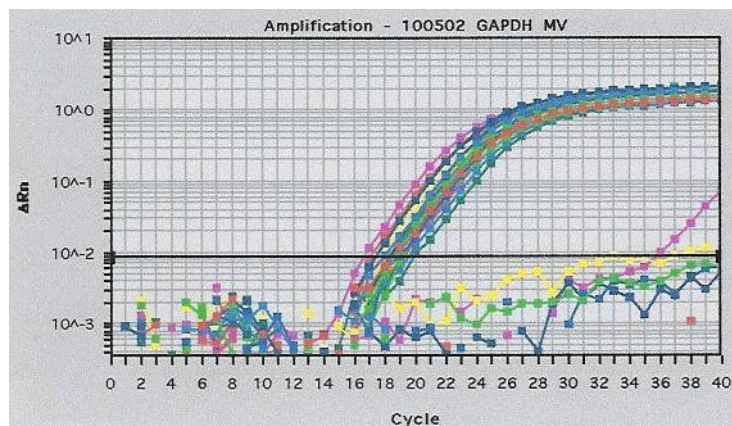
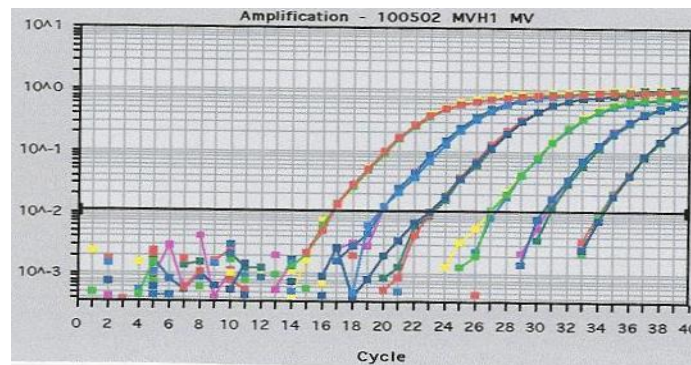
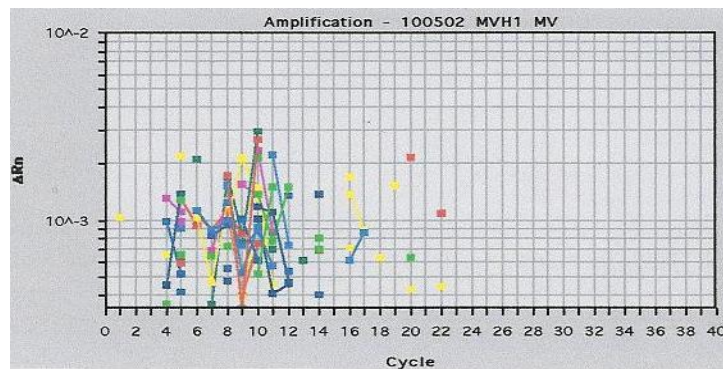


Figure 3.3. Quantitative real-time PCR results for the GAPDH assay. Amplification curves are shown for (a) serial dilutions of cDNA extracted from MV-infected HOS cells; (b) cDNA extracted from reactive nodes; and (c) cDNA extracted from cHL samples.

(a) Serial dilutions of MV + HOS cDNA



(b) cDNA extracted from reactive nodes



(c) cDNA extracted from cHL samples

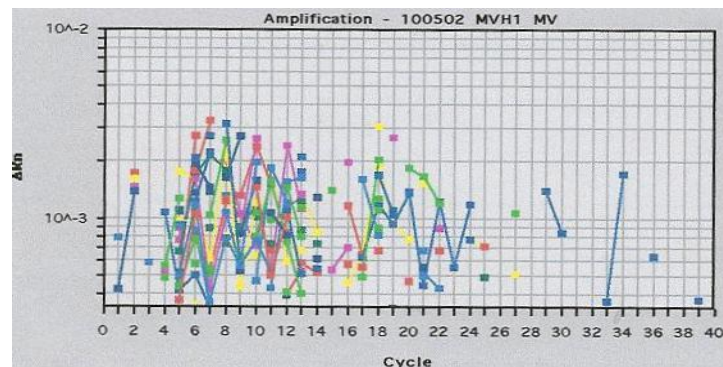
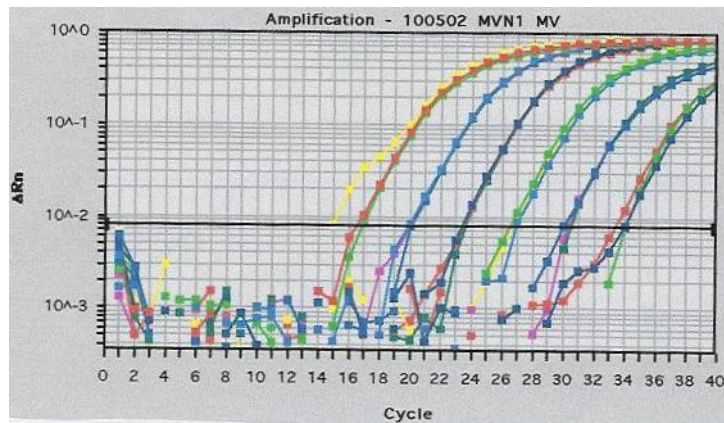
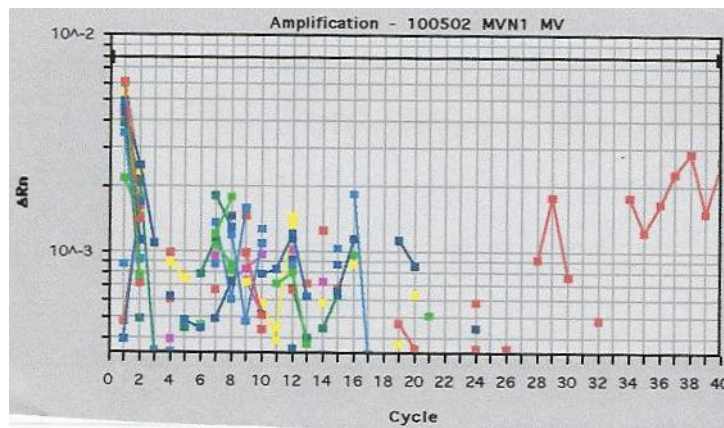


Figure 3.4. Quantitative real-time PCR results for the measles virus (MV) hemagglutinin assay. Amplification curves are shown for (a) serial dilutions of cDNA extracted from MV-infected HOS cells; (b) cDNA extracted from reactive nodes; and (c) cDNA extracted from cHL samples. No amplification products were present in (b) and (c) so the amplification plots do not cross the threshold.

(a) Serial dilutions of MV + HOS cDNA



(b) cDNA extracted from reactive nodes



(c) cDNA extracted from cHL samples

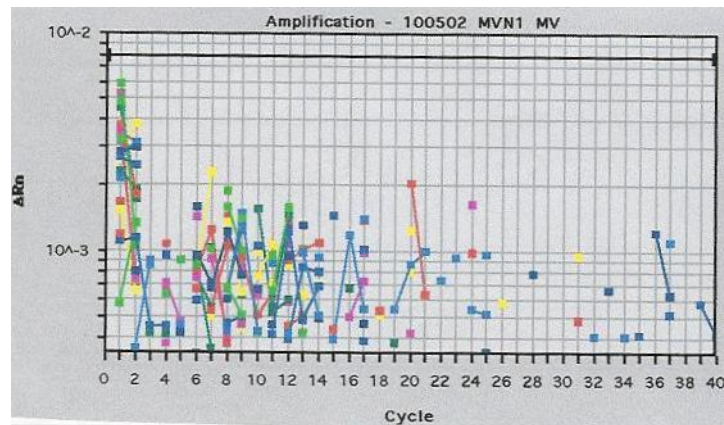


Figure 3.5. Quantitative real-time PCR results for the measles virus (MV) nucleoprotein assay. Amplification curves are shown for (a) serial dilutions of cDNA extracted from MV-infected HOS cells; (b) cDNA extracted from reactive nodes; and (c) cDNA extracted from cHL samples.

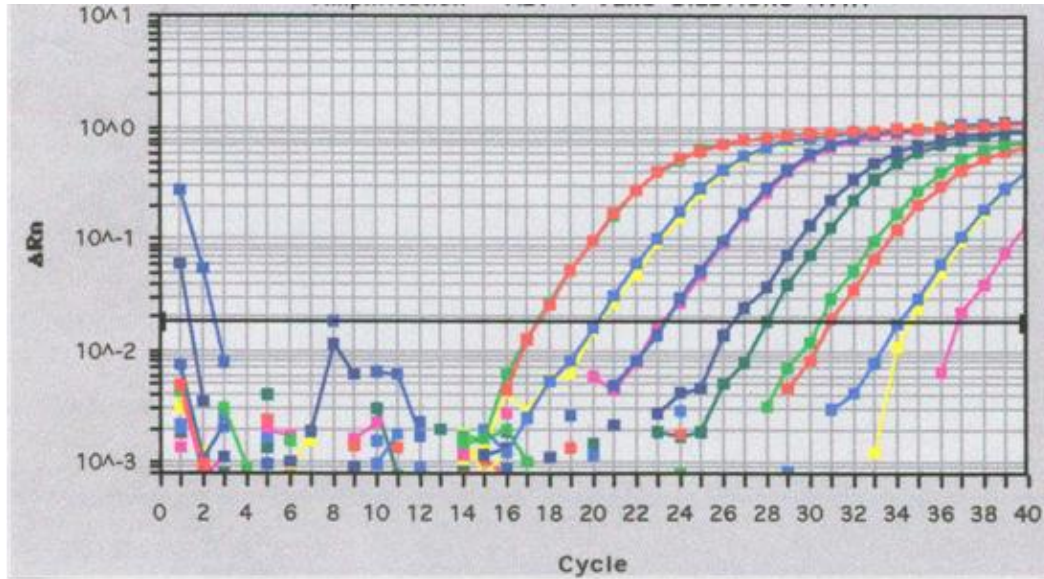


Figure 3.6. Quantitative real-time PCR results for the measles virus (MV) haemagglutinin assay showing amplification curves for replicates of serial 10-fold dilutions of cDNA extracted from MV-infected HOS cells. Replicates corresponding to 1×10^{-3} ng of MV-infected HOS DNA were detected by this assay.

3.4 DISCUSSION

Benharroch *et al.* (2003, 2004) previously reported an association between MV and HL. Although cautious about attributing any causal role to the virus, they proposed an international effort to verify (or refute) their preliminary findings. We therefore examined this association using both epidemiological and laboratory-based methods. In a population-based, case-control study we found no significant differences between the proportion of cases and controls reporting a previous history of MV infection, either in all cases or when only young adults were included in the analysis. Few individuals reported measles over the age of 10 years. These results do not, therefore, support the hypothesis that late exposure to MV, which can occur in unvaccinated patients and in vaccinated young adults with waning immunity, is associated with an increased risk of developing young adult cHL. When age at MV infection was considered, all cases and non-EBV-associated cHL cases in the young adult age group were significantly more likely to report measles below the age of 5 years, compared with those who reported measles at an older age. A previous study of young adult (15-24 years) HL showed similar data, which suggests that this association could be true (Alexander *et al.* 2000). It is not clear if measles occurring in school age children has a protective effect or may be proxy for another infection, which is aetiologically associated with cHL, and specifically non-EBV-associated cHL.

IHC was used to examine 97 HL biopsies for the presence of MV antigens in HRS cells. A monoclonal antibody reactive with the nucleoprotein was selected as this protein is expressed at high levels in infected cells and was the antigen detected most frequently by Benharroch *et al.* (2003). In addition the antibody used is robust, works well on paraffin sections and shows little non-specificity (McQuaid and Cosby 2002).

We did not detect any positive reactivity in our samples suggesting that MV was not present in any of these biopsies. Furthermore we were unable to detect evidence of MV RNA in lymph nodes affected by HL using RT-PCR, despite using previously described conventional PCR assays and a highly sensitive TaqMan® assay.

Recently, a German-based research group has also reported no evidence of MV in cHL (Maggio *et al.* 2007). Four cHL-derived cell lines (HDLM2, KMH2, L1236 and L428) and HRS cells microdissected from 25 cHL cases (from Germany and Israel) were analysed using nested RT-PCR assays, for the MV nucleoprotein, matrix and haemagglutinin genes, followed by Southern blot hybridisation. IHC was performed on 12 cHL paraffin-embedded biopsies using an anti-nucleoprotein and an anti-haemagglutinin MV antibody. MV proteins had previously been reported in these Israeli cases by Benharroch *et al.* (2004). However, Maggio *et al.* did not detect MV genomes or gene products in any of the samples or cell lines using these three highly sensitive detection techniques. Our results are completely concordant with these findings.

Technical differences between the methodologies used and the possibility of non-specific immunohistochemical staining may account for the different findings reported by Benharroch *et al.* (2003, 2004) with those from Maggio *et al.* (2007) and our study. Additional studies including international collaborations should resolve these issues. However, the combined results of our study and that of Maggio *et al.* (2007) make it highly unlikely that MV is a significant pathogen in cHL.

CHAPTER 4

NO EVIDENCE OF POLYOMAVIRUS GENOMES IN HODGKIN LYMPHOMA

The material presented in this chapter has been published in two scientific papers:

Viruses and Hodgkin lymphoma: no evidence of polyomavirus genomes in tumor biopsies.

Wilson KS, Gallagher A, Freeland JM, Shield LA, Jarrett RF.

Leuk Lymphoma. 2006 Jul;47(7):1315-21.

Molecular methods for virus discovery.

Jarrett RF, Johnson D, **Wilson KS**, Gallagher A.

Dev Biol (Basel). 2006;123:77-88;119-32.

4.1 INTRODUCTION

Polyomaviruses (PyV) are widely distributed in nature, infect most individuals at a young age and are known to be oncogenic in experimental systems (Cole 2001). They can therefore be considered as etiological candidates in HL.

Papillomaviruses and PyVs are non-enveloped, circular, double-stranded DNA viruses belonging to the Papovaviridae family. PyV are 45 nm in diameter, with a genome in the range of 4.7-5.3kb (Cole 2001). These viruses have been isolated from humans (BKV, JCV), primates (SV40, lymphotropic papovavirus), bovines (BPyV), rodents (mouse and rabbit PyV) and birds (budgerigar fledgling PyV, goose PyV). Each PyV has a specific host range.

BKV, JCV and SV40 are very similar to each other in size (approximately 5.2kb), genome organisation and DNA sequence. The genome of these viruses is organised into two regions of approximately the same size containing the early and late transcription units. Early transcription proceeds in a counterclockwise direction from the origin of DNA replication (ori) and late transcription occurs in a clockwise direction from ori. The early region encodes two alternatively spliced transforming proteins: large T antigen and small t antigen. The large T antigen directs production of early mRNA, initiation of viral DNA replication and activation of late gene transcription (Lee and Langhoff 2006). The function of the small t antigen in human PyVs has not yet been confirmed, but it has been suggested that this protein supports the activity and cell transformation of the large T antigen (Lee and Langhoff 2006). The mouse and hamster PyVs encode three T antigens: large T, middle T and small t.

The late region of the PyV genome encodes a small regulatory protein called the agnoprotein as well as the capsid structural proteins VP1, VP2 and VP3, which are derived by alternative splicing from the same late transcript.

A target cell may be either permissive or nonpermissive towards infection with PyV. A permissive cell is able to support DNA viral replication and lytic infection, whereas a non-permissive cell will not support viral replication and hence abortive infection or oncogenesis will result from viral entry into this cell (White and Khalili 2004).

The two human PyVs were discovered in 1971. BKV was isolated from the urine of a renal transplant recipient (with the initials BK) (Gardner et al 1971). JCV was first identified in the brain of a progressive multifocal leucoencephalopathy (PML) patient (with the initials JC) (Padgett et al 1971). Serological studies have detected JCV antibodies in 70-90% of normal healthy adults (Padgett and Walker 1973; Taguchi et al 1982), and BKV antibodies in approximately 80% of individuals (Chatterjee et al 2000). Both PyVs are known to establish asymptomatic persistent infections in childhood, and are thought to be transported by peripheral blood leucocytes from primary infection sites (i.e. tonsil) to secondary sites of infection (i.e. kidney) where persistent latent infection continues throughout life (Atwood et al 1992; Dorries et al 1994). The genomes of JCV and BKV have been identified in peripheral blood leucocytes by Southern blot analysis and immunofluorescence (Smith et al 1998; Houff et al 1988; Dorries et al 1994). In immunocompromised patients, however, JCV infection can become lytic and will induce the destruction of oligodendrocytes producing myelin, and result in PML (Major and Vacante 1989). BKV infection of severely immunocompromised patients can induce acute urinary tract infections (e.g.,

BKV-associated nephropathy), which often leads to allograft rejection in renal transplant patients (Nickeleit et al 1999).

The oncogenic potential of these human polyomaviruses has been demonstrated by the development of ependymomas, pancreatic insulinomas and osteocarcinomas in BKV-inoculated newborn hamsters (Corallini et al 1978). There have been recent reports of the detection of the BKV large T antigen in osteosarcomas, Ewing's sarcoma, and brain tumours (De Mattei et al 1995). JCV has been associated with brain cancer (Rencic et al 1996), paediatric medulloblastomas (Krynska et al 1999) and colon cancers (Enam et al 2002).

It has been difficult to evaluate the exact role of JCV and BKV in human tumours due to the high level of seropositive individuals and the presence of latent BKV in normal human tissues. One study has offered strong evidence against a causative role of these viruses in tumour development (Knoll et al 2003). QRT-PCR was performed using DNA extracted from microdissected cells of human urogenital carcinomas and normal surrounding tissue. JCV and BKV DNA sequences were present to the same levels in both normal and tumour DNA.

SV40 is a related primate virus which does not naturally infect humans but may have been introduced into human populations as a result of contamination of polio vaccines in the 1950s and early 1960s (Sangar et al. 1999; Shah & Nathanson 1976). SV40 has been shown to be highly oncogenic in experimental animals and transforms rodent cells in culture (Diamandopoulos and Enders 1965). Hamsters inoculated with SV40

develop lymphomas, brain tumours, osteosarcomas and mesotheliomas (Carbone et al 1998).

Two studies have reported the presence of the SV40 genome in a large proportion of NHLs in the USA using specific primers and probes designed against the large T antigen sequence of the viral genome (Shivapurkar et al. 2002; Vilchez et al. 2002). Shivapurkar *et al.* (2002) used conventional PCR to screen DNA samples extracted from 68 NHL tumours and identified SV40 sequences in 43% of cases. The large number of amplification cycles (45 cycles) they required for reproducible detection led the authors to suggest that the virus was present at only low copy number within NHLs. In a second study, by Vilchez *et al.* (2002), DNA samples extracted from the tumours of 154 NHL patients were screened for the polyomavirus large T antigen, using conventional PCR and consensus primers derived from a region of the antigen that is highly conserved across the human polyomaviruses. Amplification of this region of the large T antigen was achieved in 64/154 (42%) of the samples. The authors also performed Southern blot hybridisation using virus-specific probes to determine that the amplified sequences were derived from SV40 (Vilchez et al 2002). We were unable to confirm these findings following investigation of a series of 152 NHL samples from the UK (MacKenzie et al 2003). NHL samples were screened with a highly sensitive QRT-PCR assay for SV40, and also with the same polyomavirus consensus PCR assay that had been used by Vilchez *et al.* (2002). All products from the consensus PCR assay underwent Southern blot analysis and were hybridised with an SV40-specific oligonucleotide probe (MacKenzie et al 2003). No evidence of SV40 genomes was observed within this series of NHL cases. A serological study in the USA screened 520 lymphoma cases with an enzyme

immunoassay for SV40 antibodies and also failed to find any evidence for an association of SV40 with lymphomas (de Sanjose et al. 2003). They noted that HL cases in their study were associated with a non-statistically significant two-fold increased risk of being SV40 seropositive. Since then a number of studies in the USA, Germany and Tasmania have also reported a lack of evidence for the association of SV40 with NHL (Schuler et al 2006; Sui et al 2005; Rollison et al 2005; Engels et al 2005). It has been suggested that a possible source of the false positives reported in previous molecular studies was contamination with laboratory plasmids, and that positive serological results may result from cross-reactivity with BKV and JCV (Shah 2007) and perhaps other polyomaviruses.

Volter *et al.* (1997) previously used degenerate PCR to screen a series of cases, including five cases of HL, for the presence of polyomaviruses (Volter et al. 1997). Degenerate PCR differs from conventional PCR by its use of a pool of degenerate primers. These degenerate primers are designed by back-translating a highly conserved peptide motif into the corresponding nucleotide sequence. Degenerate assays have been used extensively to identify genes and proteins related to known proteins and are particularly useful when highly conserved regions or motifs of amino acids are present within proteins, including viral proteins. Some amino acids are encoded by a number of different codons so in these positions a nucleotide variation is inserted within the oligonucleotide primer sequence during synthesis. For example a Y in the primer sequence indicates that either a cytosine or thymine-containing nucleotide may be present at this position. The degeneracy level of a primer is defined by the number of nucleotide variations present within its sequence. The higher the degeneracy level of a primer, the greater the number of nucleotide

variations it contains, and the lower the predicted sensitivity of subsequent amplification reactions. Previously we determined that a primer degeneracy of 128-fold or less is required to achieve an acceptable level of sensitivity for investigation of cHL biopsies (Jarrett et al 2006).

The assays designed by Volter *et al.* were based on well conserved amino acid motifs within the structural protein VP1 and were reported to have the ability to detect single copy genomes (Volter et al. 1997). Polyomavirus genomes were not detected in this study but, given the heterogeneous nature of HL, examination of a larger series of cases, with more sensitive assays based on the large T gene, appeared warranted. A series of cHL cases was therefore investigated using specific QRT-PCR assays for the two human polyomaviruses and SV40, as well as degenerate PCR assays with the potential to detect novel polyomaviruses. Our study was limited to cases of cHL; NLPHL was excluded since this histological subtype is thought to represent a distinct entity with a different cell of origin (Stein 2001).

Aim

- To screen biopsies from cHL patients for evidence of polyomavirus genomes.

4.2 MATERIALS AND METHODS

4.2.1 Clinical Samples

Lymph node biopsy samples from 35 non-selected cases of cHL were investigated (see Table 4.1); 17 cases were part of a previous study in which I had examined the association between SV40 and lymphoma (MacKenzie et al. 2003). DNA was extracted from fresh or frozen lymph nodes using either proteinase K digestion followed by extraction with organic solvents, or the QIAamp DNA Blood Mini kit (Qiagen, Crawley, UK). The EBV status of tumours was determined using EBV EBER *in situ* hybridisation (performed by Mrs. June Freeland). Briefly, sections of paraffin-embedded lymph node biopsies were hybridised with a commercially available probe (Vector Laboratories, Peterborough, UK) and reactivity was detected using a hybridisation kit (Dako, Cambridgeshire, UK). Cases in which the HRS cells were positive are designated EBV-associated.

Table 4.1. Patient characteristics.

Patient characteristics	Number of patients
Sex	
Male	19
Female	16
Age at diagnosis:	
≤ 14	1
15-54	32
≥ 55	2
Histological subtype:	
NSHL	29
MCHL	5
cHL NOS	1
EBV status:	
EBV-associated	12
Non-EBV-associated	23

NSHL - nodular sclerosis Hodgkin lymphoma; MCHL - mixed cellularity HL; cHL NOS – classical Hodgkin lymphoma not otherwise specified as further subtyping not possible.

4.2.2 Quantitative Real-Time PCR analysis

DNA samples (500 ng) were screened using QRT-PCR assays for JCV, BKV and SV40 (MacKenzie et al. 2003) (see Table 4.2). A QRT-PCR assay for β -globin was also performed to confirm that all samples contained sufficient amplifiable DNA (Gallagher et al. 1999) (see Table 4.2). Thermal cycling and analysis were performed on an ABI PRISM® 7700 Sequence Detection System. Samples were initially incubated at 50°C for 2 mins, then 95°C for 10 mins followed by 40 cycles of 95°C for 15 seconds and 60°C for 60 seconds.

Table 4.2. Quantitative real-time PCR (TaqMan®) primers and probes.

Primer/Probe	Sequence (bp)	Final concentration in PCR (μ M)
BKV (MM) 5'	TTG CTT CTT CAT CAC TGG CAA	0.3
BKV (MM) Probe	FAM-CAT ATC TTC ATG GCA AAA TAA ATC TTC ATC CCA TTT	0.2
BKV (MM) 3'	AGT CCT GGT GGA GTT CCT TTA ATG	0.3
BKV (AS strain) 5'	TTG CTT CTT CAT CAC TGG CAA	0.3
BKV (AS strain) Probe	FAM- CAT ATC CTC ATG GCA GAA TAA ATC TTC ATC CCA TTT	0.2
BKV (AS strain) 3'	AGT CCT GGT GGA GCT CCT TTA ATG	0.3
JCV5'	TTC TCC CAG CAA TGA AGA GCT T	0.9
JCV Probe	FAM - CAC ACC CAA ACC ATT G	0.2
JCV3'	TGC TAT TGC TTT GAT TGC TTC AG	0.9
SV40 5'	TTT GGG CAA CAA ACA GTG TAG C	0.5
SV40 Probe	FAM- AAG CAA CTC CAG CCA TCC ATT CTT CTA T	0.2
SV403'	TGT TTG GTT CTA CAG GCT CTG C	0.5
β -globin5'	GGC AAC CCT AAG GTG AAG GC	0.5 μ M
β -globin Probe	FAM- CAT GGC AAG AAA GTG CTC GGT GCC T	0.2 μ M
β -globin3'	GGT GAG CCA GGC CAT CAC TA	0.5 μ M

4.2.3 Degenerate PCR

4.2.3.1 Design of polyomavirus degenerate PCR assays

Polyomavirus degenerate PCR primers were designed based on large T antigen sequences since defective, integrated genomes lacking the large T antigen coding sequences are unlikely to be associated with transformation (Cole & Conzen 2001). Sequences in the 5' end of the large T gene were avoided since SV40 sequences from this region are present in many cloning vectors and are known to be a source of PCR contamination (Lopez-Rios et al. 2004b). Since HRS cells generally constitute 1% or less of the total cellular mass, we aimed to develop assays with the ability to detect a single copy genome present in <1% of the cells in any sample.

Amino acid sequences from all available large T antigen sequences were aligned using ClustalW, courtesy of the BCM search launcher (<http://dot.imgen.bcm.tmc.edu/multi-align/multi-align.html>), and conserved blocks of amino acids were identified (see Figure 4.2). Three peptide motifs were selected for design of degenerate primers. The single forward primer was derived from the sequence E/DDVKG, which is conserved in all polyomaviruses except the Kilham strain of murine polyomavirus. Since codons for E (glutamic acid) and D (aspartic acid) have the same nucleotides in positions 1 and 2, both amino acids are covered by this primer (see Table 4.3).

The conserved sequence VNLE was selected for design of the reverse primer; two primers were synthesised with one including all nucleotide sequences encoding KVNLE and the other including all those encoding PVNLE (see Table 4.3). A third reverse primer, based on the sequence TMNEY, was also synthesised (see Table 4.3);

although this sequence is not perfectly conserved across all polyomaviruses, the resultant primer has low degeneracy (16-fold) and therefore use of this primer was predicted to result in an assay with superior sensitivity. Clamp sequences of 15-16 nucleotides were added to the 5' end of each primer. These sequences were based on the consensus nucleotide sequence at the relevant position of the viral genomes, with some modifications to ensure a reasonably high melting temperature (T_m). The presence of clamp sequences within the primers stabilises the primer binding. Primers including clamp sequences plus two nucleotides of non-degenerate polyomavirus sequence were also synthesised separately for use in second round PCRs (see Table 4.3). The EDVKG and CLAMP-EDVKG primers were labelled with FAM and the CLAMP-VNLE was labelled with HEX; all primers were synthesised by TAG Newcastle Ltd. (Gateshead, UK).

	EDVKG	KVNLE	TMNEY
BKV	-----	-----	-----
JCV	-----	-----	-----
LPV	D-----	-----	-----
SV40	-----	-----	----F
HaPV	-----	-----	-A----
Py (Crawford)	-----	-----	-----
Py (strain A2)	-----	-----	-----
Py (strain A3)	-----	-----	-----
Py (Kilham)	-VLAE	-----	-S----
BPyV	-----	P-----	-C----
BFDV	-----	P-----	---N-
GHPV	-----	P-----	---H-

Figure 4.1. Conserved amino acid motifs within the large T antigen of polyomaviruses. BKV - BK virus; JCV - JC virus; LPV -lymphotropic papovavirus; SV40 - simian virus 40; HaPV - hamster polyomavirus; Py - murine polyomavirus; BPyV - bovine polyomavirus; BFDV - budgerigar fledgling disease virus; GHPV - goose haemorrhagic polyomavirus.

- denotes amino acid identity.

Table 4.3. Degenerate PCR primers for detection of polyomaviruses. Clamp sequences are shown in italics.

Primers	Fold Degeneracy
Forward Primer EDVKG <i>*GTTTATGGTTGTCTTTGANGAYGTNAARGG</i>	64
Reverse Primer KVNLE <i>GTTTCGGTGTTTCTTTTCNARRTTNACYTT</i>	128
Reverse Primer PVNLE <i>GTTTCGGTGTTTCTTTTCNARRTTNACNGG</i>	256
Reverse Primer TMNEY <i>GTTTGAGGCACAGAATAYTCRTTCATNGT</i>	16
Forward CLAMP-EDVKG <i>*GTTTATGGTTGTCTTTGA</i>	0
Reverse CLAMP-VNLE <i>#GTTTCGGTGTTTCTTTTC</i>	0

N = A + G + C + T; Y = C + T; and R = A + G.

* FAM-labelled oligonucleotides

HEX-labelled oligonucleotide.

4.2.3.2 Degenerate PCR methodology

PCR reaction mixtures contained 1 µg DNA template, 4 µM of each primer, 200 µM dNTPs (Amersham Pharmacia Biotech, Buckinghamshire, UK), 10x PCR buffer containing 1.5 mM MgCl₂, 5x Q-solution and 1.25 units of HotStarTaq DNA polymerase (all from Qiagen). Thermal cycling was performed on a GeneAmp PCR System 2400 (Applied Biosystems) using the following parameters: 95°C for 15 mins, followed by five cycles of 94°C for 60 s; 44°C for 2 mins; 72°C for 3 mins, followed by 35 cycles of 94°C for 60 s; 55°C for 2 mins; 72°C for 3 mins followed by a final extension step at 72°C for 7 mins. The lower annealing temperature (44°C) used in the initial five amplification cycles enables the primer to anneal to the template via its degenerate sequence. The annealing temperature is then raised to 55°C for the rest of the reaction to allow more specific amplification. Following amplification with primer pair EDVKG/KVNLE or EDVKG/PVNLE, 1 µl of first round products was subjected to a further 20 cycles of amplification using primers CLAMP-EDVKG and CLAMP-VNLE and an annealing temperature of 45°C.

Amplification products were purified through EDGE Biocolumns in the Quickstep™ PCR purification kit (VHBio). One microlitre of purified product was mixed with 12 µl HiDi Formamide, 0.25 µl of water and 0.25 µl of a 1:4 dilution of the GeneScan™ size standard GeneScan®-350 [ROX]™. Analysis was performed using the ABI PRISM® 310 Genetic Analyzer and GeneScan® analysis software (Applied Biosystems) to give greater sensitivity and fragment size resolution than could be obtained by conventional electrophoresis.

4.2.3.3 Assay specificity and sensitivity

The following templates were used to validate the specificity of the assay: SV40 viral DNA (Form 1; Invitrogen, Paisley, UK); DNA from the COS-7 cell line, which contains integrated SV40 large T antigen (Gluzman 1981); DNA extracted from cell culture supernatants containing BPyV; and plasmids containing the complete JCV, BKV, LPV and hamster polyomavirus (HaPV) genomes. All samples were assayed in a background of 1 µg of DNA extracted from the T-lymphoblastoid J-JHAN cell line. In addition, DNA from the rabbit papovavirus (strain 443; LGC Promochem, London UK), a known but uncharacterised polyomavirus, was tested. DNA was extracted from tissue culture supernatants using the QIAamp UltraSens Virus Kit (Qiagen).

Replicates of serial 10-fold dilutions, predicted to contain from 10^6 to 10 viral genomes, of SV40 and BPyV were assayed in a background of high molecular weight DNA to determine assay sensitivity. Semi-log dilutions of viral templates were used to determine sensitivities in the range 10^2 - 10^4 viral genomes per 1 µg DNA.

4.2.3.4 Hodgkin lymphoma samples

Following optimisation and validation of the degenerate assays, DNA from the HL biopsies was assayed using each primer set. In addition, a second round PCR was performed using the CLAMP primers (see Table 4.3). Negative controls, with water replacing the DNA template, were included after each sample in order to control for PCR contamination, and J-JHAN DNA (1 µg) was used to control for non-specific amplification. A conventional PCR assay for β-globin, which amplifies a 110 base pair product, was performed on all samples to verify the presence of amplifiable DNA (Saiki et al. 1988).

4.2.3.5 Cloning of degenerate PCR products for sequence analysis

Degenerate PCR products were cloned, using the TOPOTM TA Cloning[®] kit (Invitrogen Ltd.) and transformed into competent cells (see Section 2.2.17). Plasmid DNA was extracted from the subsequent bacterial culture using the High Pure Plasmid Isolation Kit (Roche) (see Section 2.2.17). Sequence analysis was performed on an ABI PRISM[®] 3100 Genetic Analyzer (Applied Biosystem), as described in Section 2.2.18, to further characterise degenerate PCR products in the anticipated size range for amplicons of polyomavirus genomes. Nucleotide sequences were entered into blastn searches (<http://www.ncbi.nlm.nih.gov/BLAST>) for identification.

4.3 RESULTS

In order to determine whether polyomaviruses are involved in the pathogenesis of HL, biopsy samples were first screened using sensitive PCR assays for the known human polyomaviruses JCV and BKV, and the primate virus SV40. All samples were negative in these assays despite the presence of amplifiable DNA.

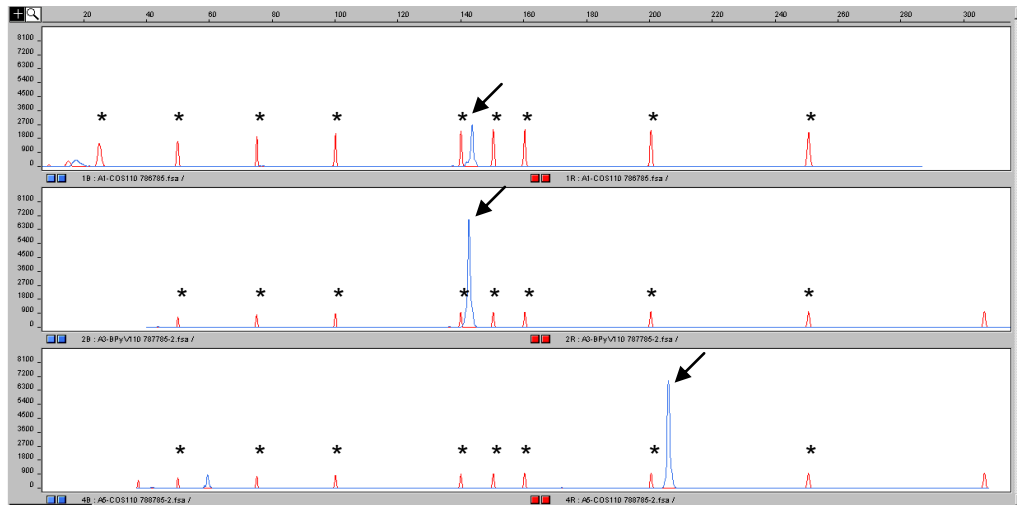
Degenerate PCR assays with the potential to identify novel polyomaviruses were then designed and validated. Primers were derived from the 3' region of the large T gene and therefore do not amplify the SV40 sequences that are most frequently present in cloning vectors (Lopez-Rios et al. 2004). Three assays, utilising a common forward primer, were developed. Primer pairs had the expected specificities: JCV, BKV, SV40, LPV and HaPV templates were amplified using the reverse primer KVNLE, whereas BPyV was amplified more efficiently using the PVNLE reverse primer. JCV, BKV and LPV genomes were also successfully amplified using the reverse primer TMNEY; despite an imperfect sequence match, SV40 was also efficiently amplified using this primer. All amplification products were of the expected size – 146 bp for the EDVKG/KVNLE or EDVKG/PVNLE assays and 208 bp for the EDVKG/TMNEY assay (see Figure 4.3a). When DNA from the rabbit papovavirus (RabPyV) was used as template, negative results were obtained using the PVNLE and TMNEY reverse primers but a 146 bp product was generated using the EDVKG/KVNLE primer set (see Figure 4.3b). The nucleotide sequence of this amplification product, and the predicted translation, were found to have homology with known polyomavirus genomes and large T antigens, respectively. This nucleotide sequence has been deposited as GenBank accession number AY911513.

The ability to amplify sequences from a previously uncharacterised member of the polyomavirus family confirms the usefulness of these assays.

Analysis of serial dilutions of template DNA, in a background of 1 µg of high molecular weight DNA, was performed in order to determine assay sensitivity. To have the ability to detect a single copy viral genome present in 1% of the cells, the assay should be able to detect 1.5×10^3 genomes in a 1 µg DNA sample. Using the EDVKG and KVNLE or PVNLE primers we were able to detect $10^{3.5}$ genome copies of SV40, JCV, BKV and BPyV, but could not consistently detect 10^3 copies. Using the CLAMP primers in a second round reaction, we were able to detect $10^{2.5}$ SV40 genomes and 10^3 BPyV genomes. As predicted, the assay incorporating the TMNEY primers was most sensitive having the ability to detect $<10^2$ SV40 genomes.

DNA samples from 35 cases of cHL were assayed using the above degenerate PCR assays for polyomaviruses, on multiple occasions. No PCR products in the anticipated size range were detected on GeneScan analysis. Given the sensitivity of these assays and their ability to detect a wide range of polyomavirus genomes, it is therefore highly unlikely that any of the HRS cells in our HL cases are infected by polyomaviruses. In addition, since the assays are based on large T antigen, it is unlikely that these cells harbour defective, integrated genomes.

a)



b)

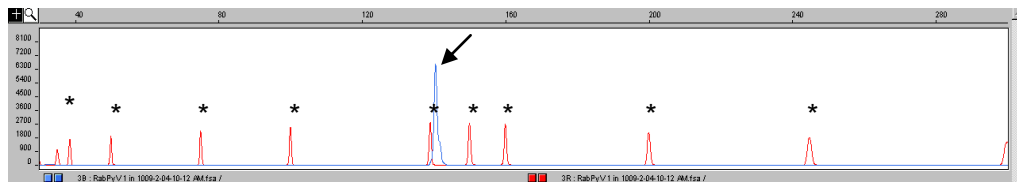


Figure 4.2. Electropherograms from GeneScan analysis of degenerate PCR products: a) upper panel: amplification of SV40 sequences using primer pair EDKVG and KVNLE; middle panel: amplification of bovine polyomavirus sequences using primer pair EDKVG and PVNLE; lower panel: amplification of SV40 sequences using primer pair EDKVG and TMNEY. b) Amplification of partial genomic sequence from rabbit papovavirus. Arrows indicate specific polyomavirus PCR products; * indicates ROX350 size marker (Applied Biosystems).

4.4 DISCUSSION

The epidemiological features of young adult non-EBV-associated HL suggest that an infectious agent is involved in disease pathogenesis (Gutensohn & Cole 1980). Previous studies from our laboratory indicate that herpesviruses are unlikely to be involved and the available data do not support the idea that EBV is using a 'hit and run' mechanism in non-EBV-associated HL cases (Gallagher et al 2002; Gallagher et al 2003).

In our search for a potential viral etiological agent of young adult cHL, we designed a number of highly sensitive degenerate PCR assays capable of detecting the presence of both novel and known polyomaviruses down to $10^{2.5}$ genome copies. The specificity of these assays was demonstrated using DNA from BKV, JCV, BPyV, LPV, HaPV and COS-7 cells (known to contain integrated SV40). A partial sequence from a previously uncharacterised rabbit polyomavirus was successfully amplified using this method demonstrating the validity of these assays. The rabbit polyomavirus amplified PCR product was sequenced and entered into the GenBank database (accession number AY911513).

We used these polyomavirus-specific degenerate PCR assays and QRT-PCR assays, specific for SV40, JCV and BKV, to screen DNA samples from a group of 35 cHL patients. No novel or known polyomavirus genomes were detected in any of these cHL cases providing strong evidence that polyomaviruses are not directly involved in HL pathogenesis.

Two new human PyVs, the KI and WU viruses, have recently been identified (Allander et al 2007; Gaynor et al 2007). In Sweden, the KI virus was detected within 1% (6/637) of nasopharyngeal aspirates using PCR (Allander et al 2007). Sequence analysis indicated low homology (<30% amino acid identity) with known PyV, but phylogenetic analysis suggested a close relation with known primate PyVs. The KI virus would have been detected by our EDVKG/KVNLE degenerate PCR assay if present in any of our samples. In Australia, the WU virus was initially detected in the nasopharyngeal aspirate of a child with pneumonia (Gaynor et al 2007). Sequence analysis indicated that the small T antigen, large T antigen, and the VP1, VP2 and VP3 capsid proteins were encoded, and phylogenetic analysis showed divergence with all known PyV. A screening programme in both Australia and the USA, using WU-specific conventional PCR primers, revealed that 2% (43/2135) of patients with acute respiratory tract infections had the WU virus. If present within any of our samples, this virus would have been detected by the EDVKG/TMNEY degenerate PCR assay.^b

The putative virus for young adult cHL remains elusive but complementary techniques for virus discovery, such as Virochip analysis (Wang et al 2003) or representational difference analysis (MacKenzie et al 2006) which do not require *a priori* knowledge of the likely agent, need to be explored before a direct role for viruses in this disease can be excluded.

^bSince completion of this thesis, a new human PyV, the Merkel cell PyV, has been identified in 8 out of 10 patients with Merkel cell carcinoma (GenBank accession number NC010277; Feng et al. 2008). Although the large T antigen has been identified within this virus, it would not be detected with any of our three degenerate PCR assays.

CHAPTER 5

INVESTIGATION OF GENOME IMBALANCES AND GENE EXPRESSION IN cHL-DERIVED CELL LINES

5.1 INTRODUCTION

Previous studies using conventional CGH have detected recurrent chromosomal imbalances in HRS cells and cHL-derived cell lines (Chui et al 2003; Joos et al 2000; Joos et al 2002; Joos et al 2003). Array-CGH should help to refine the location of these imbalances.

Joos and colleagues (2003) analysed cells from four EBV-negative cHL-derived cell lines, HDLM2, KMH2, L1236 and L428, using M-FISH, FISH and conventional CGH. Recurrent gains were detected in 9p24 (in all four cell lines), 2p16-p13 (KMH2, L1236 and L428), 5p15 (HDLM2, KMH2 and L428) and 12p13 (HDLM2, L1236 and L428). Both arms of chromosome 18 displayed losses of chromosomal material in HDLM2, KMH2 and L428. Some gains were detected in just two of these EBV-negative cell lines: 1q31-q44, 2q23-q31, 3q26.1-q29, 5q34-q35, 6p25-p22, 7q21, 7q31, 7q34-q35, 8p23-p22, 8q24.1-q24.3, 9q34, 11q24-q25, 16q23-q24 and 17q11.2-q22. Likewise, losses in 13q21-q31 were found in only KMH2 and L428.

Chui *et al.* also used conventional CGH to examine chromosomal imbalances in four cHL-derived cell lines (Chui et al 2003): EBV-negative KMH2, L1236, L428 and EBV-positive L591. A gain of chromosomal material in 9p24-p23 was detected in all four cell lines. Recurrent gains in 2p16-p13 and losses in chromosome 13, 15p11.1, 21p13 and 22p13 were identified within the 3 EBV-negative cell lines. A large number of imbalances were common to only two of the EBV-negative cell lines. The EBV-positive L591 cell line had a different pattern of chromosome changes with a lower number of gains and losses.

Despite the different protocols and analysis methods used, the results of this latter study are largely similar to those reported by Joos *et al.* (2003). When the results for the KMH2, L1236 and L428 cell lines are compared between the two studies, the imbalances reported in L428 show the most similarity. Recurrent gains of 2p13-p16 and 9p24, and recurrent losses in 13q were reported by both groups, suggesting that cHL is associated in some way with chromosomal imbalances within these regions.

Conventional CGH is limited in its mapping resolution of 20 Mb (Kallioniemi *et al* 1994). However, array-CGH provides a more sensitive and quantitative approach to assess DNA copy number aberrations within tissue samples (Pinkel *et al* 1998; Snijders *et al* 2001; Solinas-Toldo *et al* 1997).

This chapter will describe the detailed analysis of chromosomal imbalances in cHL-derived cell lines using array-CGH. As previously discussed (see Section 1.3), some of the cHL-derived cell lines have an uncertain association with the HRS cells in the tumours from which they originated (Wolf *et al* 1996), but conventional CGH analysis of these cell lines in our laboratory has confirmed that they contain chromosome abnormalities similar to those identified in single HRS cells (Chui *et al* 2003).

Gene expression microarray studies of breast and prostate cancer cells have indicated that chromosomal imbalances have a significant impact on global gene expression patterns (Phillips *et al* 2001; Pollack *et al* 1999). Given the recent identification of chromosome imbalances by conventional CGH analysis, it seemed possible that a similar process may occur in cHL. Gene expression profiling was therefore

performed on 3 cHL-derived cell lines, using commercially available oligonucleotide microarrays (Affymetrix, UK Ltd., High Wycombe, UK), and the results were correlated with specific chromosome imbalances identified by array-CGH analysis.

Aims

- To refine the location of recurrent chromosomal imbalances in cHL-derived cell lines using array-CGH analysis.
- To identify recurrent chromosomal imbalances common to the cHL-derived cell lines.
- To investigate whether these chromosomal imbalances are reflected in the gene expression profile.

5.2 METHODS

5.2.1 Cell lines

Six stable cell lines derived from cHL tissue or body fluids were used in this study. Five of these were EBV-negative: L1236, L428, L540, HDLM2 and KMH2. The sixth, L591, is the only stable cHL-derived cell line known to be infected with EBV and is described as EBV positive. The reference cell line used in both array-CGH and expression array hybridisation was the B-lymphoblastoid cell line IM9, which is derived from a female patient with multiple myeloma and is considered to have a stable diploid karyotype (Fahey et al 1971). The source, tissue culture conditions, doubling time and harvesting details for each cell line are described in Chapter 2 (Section 2.2.7).

5.2.2 RNA and DNA extraction

RNA was extracted using TRIZOL reagent following the manufacturer's instructions (Section 2.2.8). DNA was obtained by phenol-chloroform extraction, as described in Section 2.2.9.

5.2.3 Preparation of samples for array-CGH

DNA (25 µg) from each cell line was fragmented by sonication, using the Bandelin Sonopuls HD2070 (GM 2070 generator with a UW 2070 ultrasonic converter) with a 3mm titanium probe, then purified using DNA Clean and ConcentratorTM-25 spin columns (Zymo Research) in accordance with the manufacturer's protocol.

5.2.4 Labelling of genomic DNA by random priming

Following sonication, equal quantities of the reference (IM9) and test (cHL cell line) DNA samples were labelled with either of the fluorescent dyes cyanine 5- or cyanine 3-dCTP (Perkin Elmer Life Sciences, Bucks, UK) by random priming using the BioPrime DNA Labelling System (Invitrogen Ltd.) as follows. Forty microlitres of 2.5x random primers were added to 2 µg of both test and reference DNA in black Treff microfuge tubes (Anachem Ltd., Bedfordshire, UK) and the volume made up to 82 µl with dH₂O. Following denaturation, by placing at 95°C for 7 mins, the tubes were placed on ice. To each of the samples, 10 µl of 10x low-dCTP dNTPs, 5 µl of either Cy5- or Cy3-dCTP (Perkin Elmer Life Sciences, Bucks, UK) and 80 units of high concentration Klenow fragment (BioPrime labelling kit, Gibco/BRL) were added. The tubes were vortexed briefly then incubated at 37°C O/N. Cy5 and Cy3 are light-sensitive reagents so care was taken to work quickly in order to keep any light exposure to a minimum during the labelling, hybridisation, and post-hybridisation stages of the experiment.

The following day, 400 µl of TE buffer (pH 7.4) was added to each labelled sample and then the entire reaction was purified through a Microcon 30 filter (Millipore (UK) Limited, Watford, UK). The Cy5- and Cy3-labelled probes were combined and a master mix, which contained 1 mg/ml human Cot-1 DNA (Roche Diagnostics GmbH, Germany), 10 mg/ml yeast tRNA and 253 µl TE buffer (pH 7.4), was added. Addition of human Cot-1 DNA is essential in order to block repetitive sequences present in the human genome. Yeast tRNA was included to aid precipitation. The combined labelled target was then concentrated by purification through a Microcon 30 filter. The reaction volume was made up to 46 µl with dH₂O, to allow for a potential

loss of 2 μ l by evaporation during pre-hybridisation boiling,^c and then 9.35 μ l of 20x SSC (3 M NaCl, 300 mM sodium citrate, adjusted to pH 7.0) plus 1.65 μ l of 10% SDS were added. The target was stored for up to an hour at 4°C or several hours at -20°C until required.

5.2.5 Array fabrication and processing

Array probes were prepared at The Wellcome Trust Centre for Human Genetics (Oxford, UK) by Dr. Samantha Knight and colleagues, as described below. The 1 Mb resolution arrays were then synthesised, as described below, by the Genomics Facility at the Wellcome Trust Centre for Human Genetics, Oxford, UK.

DNA was extracted from 5 ml cultures of BAC clones using the standard alkaline-lysis protocol (Sambrook 1989). The BAC DNA was amplified in two PCR reactions using a WGA protocol modified from a previously published method (Fiegler et al 2003). Each DOP-PCR was performed with 100 ng of BAC DNA template and either the SANGER-DOP-2 primer (5'-CCGACTCGAGNNNNNTAGGAG-3'; MWG Biotech, London, UK) or the SANGER-DOP-3 primer (5'-CCGACTCGAGNNNNNTTCTAG-3'; MWG Biotech, London, UK). For each clone, the DOP products from both PCR reactions were checked using agarose gel electrophoresis, then combined and ethanol precipitated for >48 hours at -70°C in 1/10th volume of 3 M sodium acetate and twice the volume of 100% ethanol. Precipitated DNA was pelleted, washed in 70% ethanol and resuspended O/N at 4°C in 21 μ l of dH₂O. After a further agarose gel electrophoresis, the products were mixed with DMSO, to give a final arraying solution of 50% dH₂O: 50% DMSO, prior to transfer to a 384 well plate (product code X5001; Genetix Ltd., New Milton, UK).

^cPrior to hybridisation, the level of Cy5- and Cy3-dCTP incorporation in the labelled combined sample was measured on a Nanodrop ND-100 Spectrophotometer. Samples were only considered suitable for hybridisation if >7 pmol/ μ l of each dye was detected.

The DOP-products were then spotted in triplicate onto aminosilane coated slides (CMT-GAP slides; Sigma-Aldrich Company Ltd., Dorset, UK) using a Gen III Microarray spotter (Amersham Pharmacia Biotech). The spots were arranged in 72 blocks (12 x 6) on the array; each block contained 160 spots (16 x 10). The arrays were allowed to dry, then UV irradiated in a Stratalinker (Stratagene Europe, Amsterdam, The Netherlands) and baked for 2 hours at 80°C. The arrays were then sealed inside foil envelopes and stored at room temperature until required.

Prior to hybridisation, the DNA on the arrays was denatured by immersing the array in boiling water for 2 mins, then washing in dH₂O. To improve the hybridisation signal, non-specific binding to the array was reduced by incubation in a blocking solution of 3.5x SSC, 0.1% SDS, 1% BSA at 50°C for 45 mins. The arrays were then washed briefly in dH₂O and dehydrated by passing through a series of 70%, 95% and 100% ethanol washes followed by centrifugal drying. Arrays were stored in plastic containers at room temperature until use.

5.2.6 Array-CGH

In preparation for hybridisation, the labelled genomic DNA samples were denatured at 95°C for 5 mins, and immediately transferred to a 37°C heatblock for 55 mins, to enable the blocking step to proceed. Coverslips were stored in 100% ethanol prior to use to prevent smearing or dust sticking to the surface. During incubation of the probe, the coverslips were placed into 50 ml Falcon tubes (Becton Dickinson, Cowley, UK) and dried in a microwave at full power for 30 seconds. When only 5 mins of sample incubation remained, the hybridisation chambers (Fisher Scientific UK, Loughborough, UK) were prepared by adding a few drops of 3.4x SSC to the

wells at each end of the chamber. Both the coverslip and array slide were checked to make sure they were dust and smear-free before the labelled target was pipetted onto the centre of the coverslip, and the array slide carefully lowered onto the coverslip. The slide was then turned the correct way up and placed inside the hybridisation chamber. The closed and sealed chambers were immersed in a gently shaking waterbath at 65°C for over 36 hours.

5.2.7 Post-hybridisation washes

During the post-hybridisation washes the array slides were kept in the dark. On removal from the hybridisation chamber, the slide was placed in a Coplin jar containing 2x SSC, 0.03% SDS for 5 mins at room temperature. The coverslip was then gently removed and discarded before transfer of the array slide to a glass slide holder with no base. The holder was submerged in 2x SSC, 0.03% SDS preheated to 65°C, and shaken vigorously in the dark for 5 mins. The slide and holder were then briefly rinsed in 0.2x SSC at room temperature and then submerged in 0.2x SSC and vigorously shaken for 15 mins in the dark at room temperature. This latter wash step was repeated a further five times before the slide was removed and dried by centrifugation. Hybridised slides were placed in a light-proof plastic box and scanned immediately, as described below.

5.2.8 Image acquisition and data analysis

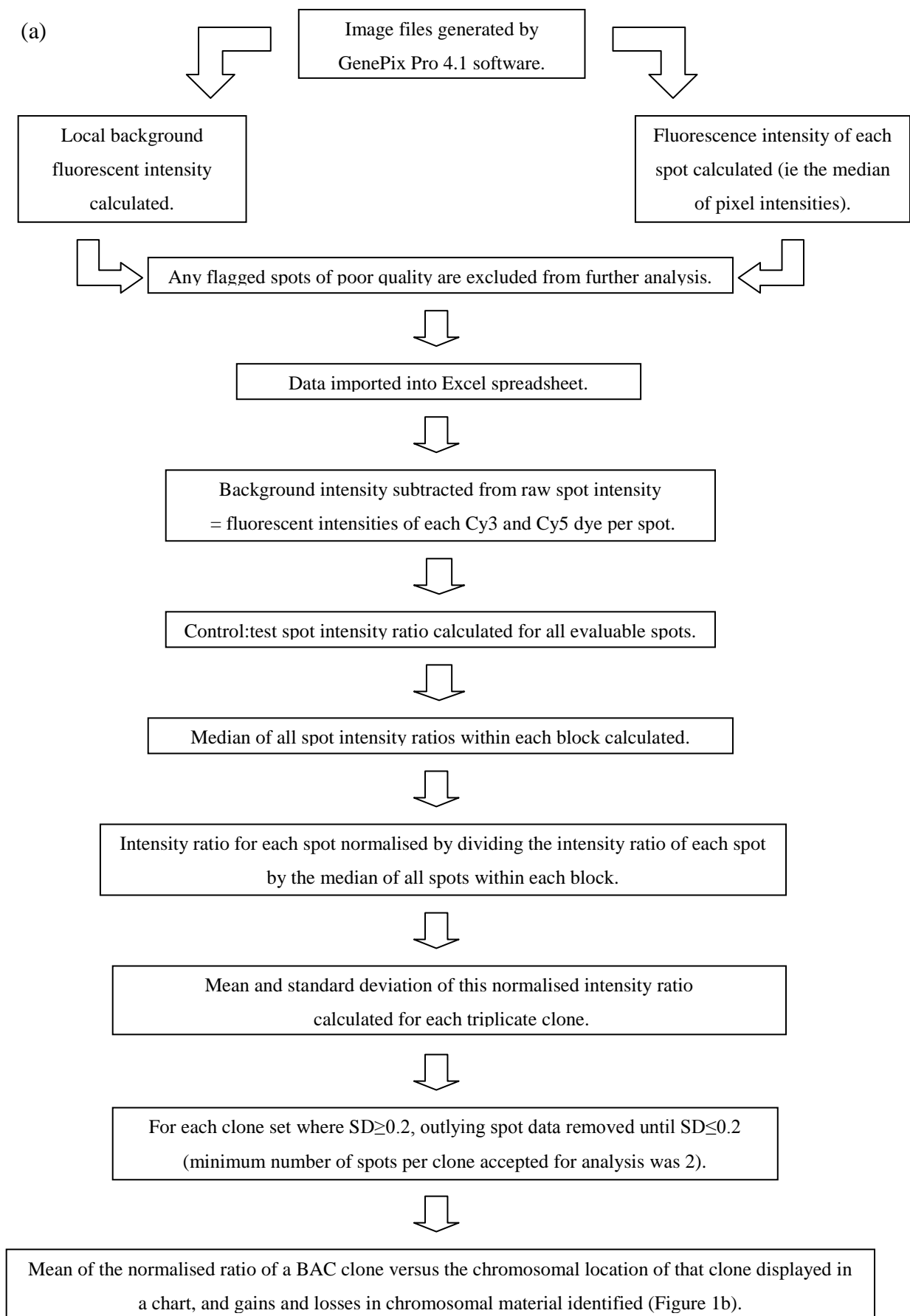
The fluorescent intensity data were collected from hybridised array slides by scanning in a GenePix 4000B machine (GRI/Axon Instruments Ltd., Essex, UK) using GenePix Pro 4.1 software. The scanning process involves first exciting the fluorochromes, Cy5 and Cy3, with a laser, then capturing the fluorescence emission through a

photomultiplier tube (PMT). The ideal scanned image is obtained when the same amount of red and green signal is acquired in each channel, resulting in a pixel ratio, or count ratio, of approximately 1.0. The PMT gains were, therefore, adjusted for each image to give a count ratio as close to 1 as possible without spot saturation. The Cy5 and Cy3 images of a slide were then aligned and target DNA location and identification details were imported into the software in a GenePix Array List (GAL) file. Absent or poor quality spots were identified on the screen array image and flagged. Abnormal spots occur either when flecks of dust interfere with the fluorescence intensity, or when there has been a problem with the Gen III Microarray spotter machine during array synthesis and the BAC DNA spots have unacceptable morphology. All abnormal spots were excluded from the data analysis.

The data were stored in a GenePix Results file (GPR) and imported into Microsoft Excel. Clones representing regions within the X and Y chromosomes were not analysed since our samples were not sex matched. A number of previous publications have excluded chromosome Y from analysis after variable hybridisation results were observed in normal versus normal hybridisations (Lage et al. 2003; Snijders et al. 2001).

A series of customised Macro files were used in Excel to complete the analysis, as outlined in Figure 5.1. Briefly, the fluorescent intensity of the local background was subtracted from the raw intensity of each spot. The reference versus test DNA spot intensity ratio was calculated (ie Cy5/Cy3), and then the median of all spot ratios within each block was calculated. Normalisation of each spot intensity ratio was achieved by dividing the intensity ratio by the median of all spot ratios within each

block. For each clone, the mean and standard deviation (SD) across the identical triplicate spots were calculated. Any spot with a $SD > 0.2$ was discarded from analysis. If 2 of the triplicate spots representing a clone had a $SD > 0.2$, the clone was discarded from further analysis. The mean normalised fluorescent intensity ratios were depicted in a chart, from which clones representing gains and losses of chromosomal material were identified.



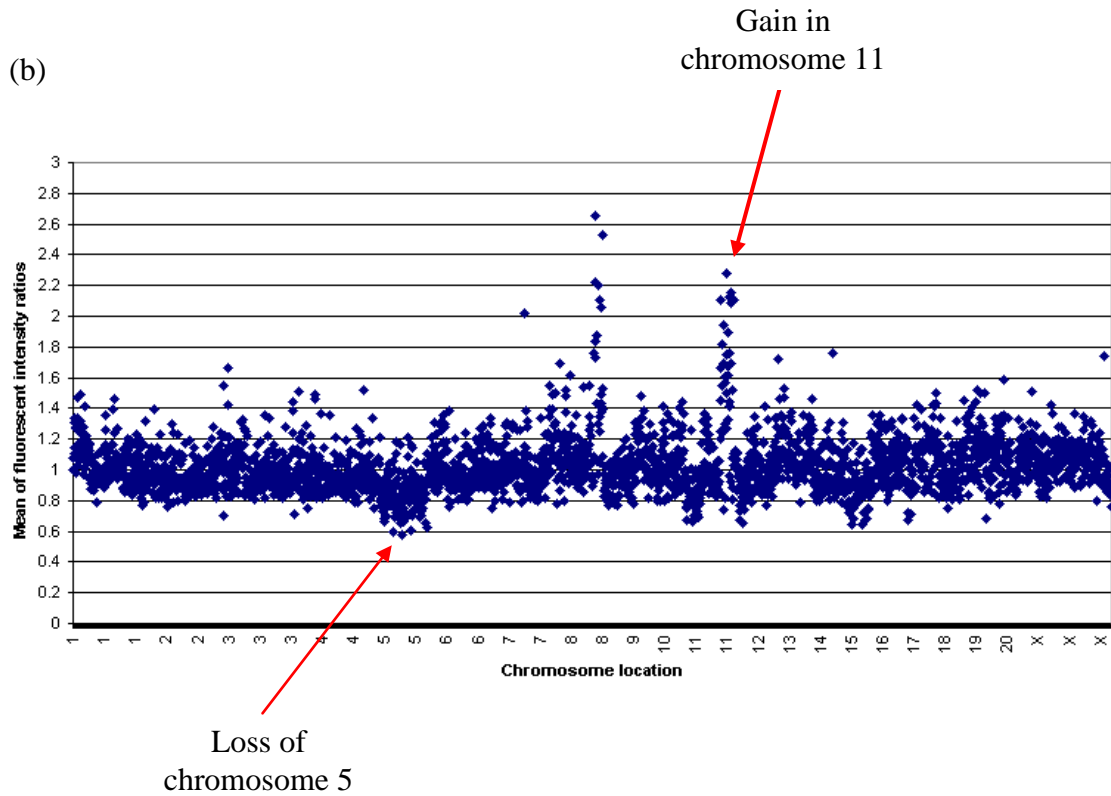


Figure 5.1. Schematic diagram of the array-CGH analysis process. (a) The flow chart outlines each stage in the analysis of array-CGH data collected from the image file produced by GenePix Pro 4.1 software. (b) The results of analysis are displayed in chart form, generated by Excel, as shown here. Clones representing a gain or loss of chromosome material can be identified on this chart as spots with a mean fluorescent intensity ratio >1.15 or <0.85 . Examples of gains and losses are indicated by red arrows.

Locus information for clones, associated with a gain or loss of chromosomal material, was obtained from the Ensembl database website (www.ensembl.org). Each of these clones was checked against the Database of Genomic Variants (compiled by the Centre for Applied Genomics, Ontario, Canada; <http://projects.tcag.ca/variation/>) for the presence of known copy number variations observed in normal individuals (Iafraite et al 2004; Zhang et al 2006). This database provides details of structural variations in the human genome, involving segments of DNA >1 kb from healthy control samples, and is continually updated from peer-reviewed research studies. Clones mapping to known regions of variation in normal control samples were recorded but discarded from further analysis for this study. Some clones displayed recurrent characteristic deviations from the ratio 1.0 in normal DNA versus normal DNA hybridisations, performed routinely by Dr Samantha Knight and Dr Regina Regan at the WTCHG in Oxford. These clones were also discarded from further analysis.

Genes of known function located within regions of gain or loss were identified using the Ensembl database website. Accurate positions for these regions and genes were defined in terms of base pairs from the p-telomere, or megabase (Mb) position.

5.2.9 Dye-swap hybridisation

For each pair of test and reference genomic DNA samples, a second ‘dye-swap’ hybridisation was performed where the samples were labelled with the different fluorescent dye (Cy5- or Cy3-dCTP) from that which was used in the first hybridisation. The dye-swap aids interpretation of a sample since a genuine gain, indicated by a high intensity ratio in the first hybridisation, will be represented as a low intensity ratio in the dye-swap experiment. Also, the Cy3 and Cy5 dyes are

known to be incorporated slightly differently within certain regions of DNA, such as GC-rich DNA, and this can generate false positives during hybridisation. Dye-swapping will highlight any such artefact introduced by dye-labelling.

5.2.10 Gene expression array hybridisation

Total RNA from IM9, KMH2, L428 and L591 cultured cells was sent to the Sir Henry Wellcome Functional Genomics Facility for Human Genomics (Glasgow University) where RNA amplification, fragmentation of cRNA and labelling were performed according to the protocol outlined by Affymetrix. IM9 total RNA was used as the reference sample. The labelled samples were hybridised with the GeneChip[®] Human Genome U133 Plus 2.0 array (Affymetrix), as laid out in the manufacturer's protocol. This array contains >22,000 probe sets. For each expression measurement, 11 pairs of probes (each 25 bp in length) are routinely present on the array. Each pair consists of a perfect match probe, which is perfectly complementary to a subsequence of the target mRNA, and a mismatch probe, which is identical to the corresponding perfect match probe except that the middle (13th) base has been changed to its Watson–Crick complement. The probe sequences are derived from sequences published on the following databases: GenBank[®] (<http://www.ncbi.nlm.nih.gov/Genbank/index.html>), dbEST (<http://www.ncbi.nlm.nih.gov/dbEST/>) and RefSeq (<http://www.ncbi.nlm.nih.gov/RefSeq/>).

5.2.11 Gene expression array analysis

A routine set of statistical analysis methods were applied to all samples, analysed using gene expression arrays, by Dr Pawel Herzyk (Sir Henry Wellcome Functional Genomics Facility of Human Genomics, Glasgow University) including robust multi-chip average [RMA] (Irizarry et al. 2003) and rank products [RP] (Breitling et al. 2004b). Dr Lesley Nicolson provided help with interpretation of the analyses that are specific to this project.

In order to correct for background noise, which is caused by non-specific binding, low-level normalisation is performed using a statistical tool called the RMA. This combines all perfect match probe distributions across the chip, and the end product is a summary of the log-normalised probe level data.

RP analysis was subsequently used to identify genes, represented by the probe sets, which were differentially expressed between the cHL-derived cell line sample and the IM9 reference sample. RP produces highly reliable results from hybridisations with high background (Breitling et al 2004). Probe sets which do not represent genes of known function were discarded leaving 3058 probe sets for analysis. The top 100 up- and downregulated genes, in each cell line, were identified.

5.2.12 Correlation between array-CGH and gene expression array analyses

Genes located within regions of chromosomal gain or loss in three or more cHL-derived cell lines were compared to the top 100 differentially expressed genes identified from our gene expression array analysis of 3 cHL-derived cell lines:

KMH2, L428 and L591. Our array-CGH results were also compared to the gene expression profile of HRS cells proposed by Schwering *et al.* (2003) from Affymetrix gene expression analysis of the HDLM2, KMH2, L428 and L1236 cHL-derived cell lines (Schwering et al 2003b).

5.3 RESULTS

5.3.1 Array-CGH analyses

Following array-CGH, analysis was performed as described in Section 5.2.8. For each cHL-derived cell line, the dye-swap hybridisation results were plotted onto the same chart as the first hybridisation results. In Figure 5.2, the combined charts from array-CGH analyses of HDLM2 versus IM9 DNA and the corresponding dye-swap hybridisation are shown. Each clone is represented by a single spot on the chart: blue for the test versus reference DNA hybridisation and pink for the dye-swap hybridisation. A large number of gains and losses of chromosomal material can be seen to occur in this cell line, ranging from single clones to contiguous clones representing large regions of the genome. Combined hybridisation charts for KMH2, L1236, L428, L540 and L591 are shown in Appendix A.

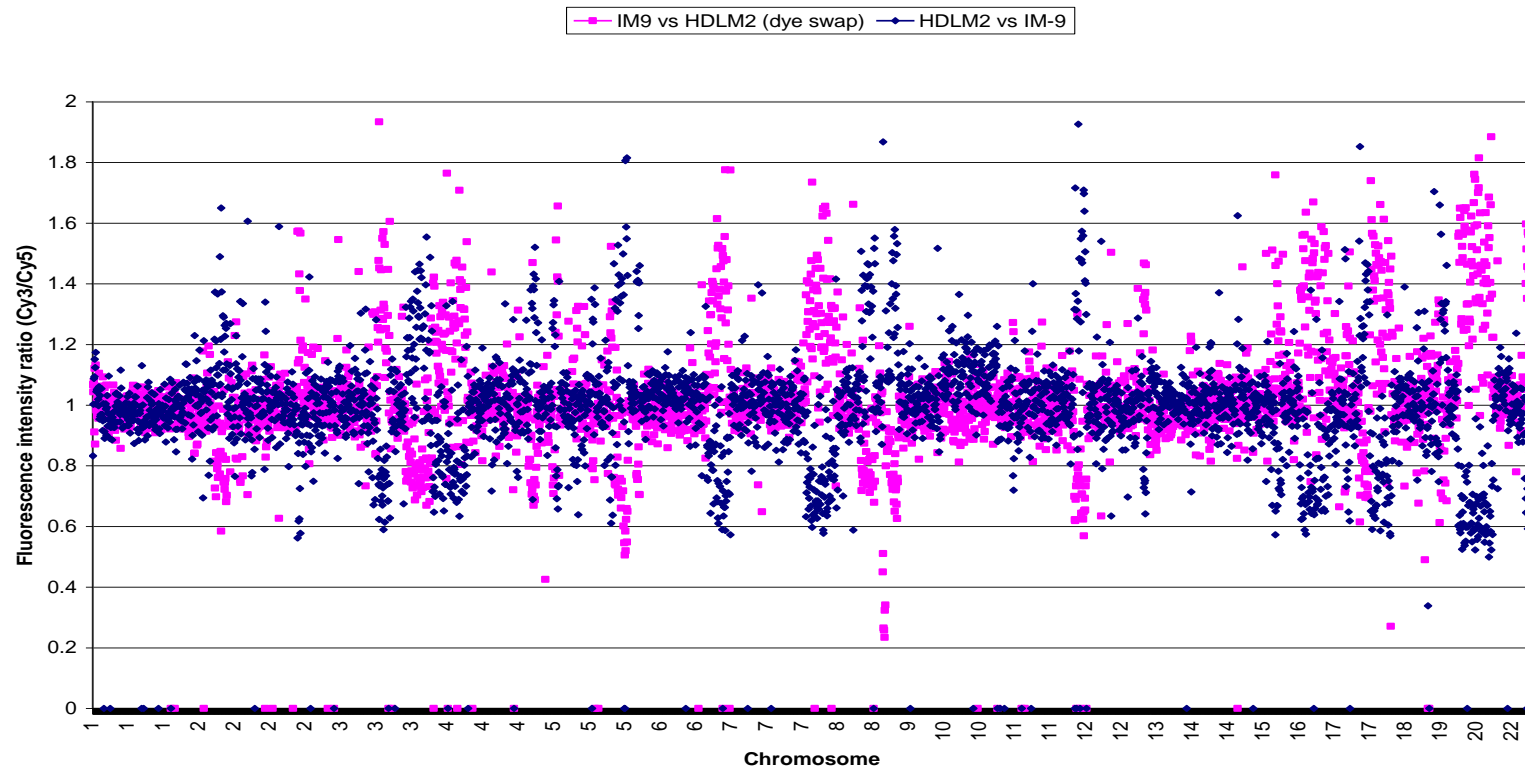


Figure 5.2. The combined hybridisation charts from array-CGH of HDLM2 DNA versus IM9 DNA. Each blue spot on the chart represents the mean intensity fluorescent ratio of a single clone, represented by triplicate spots on the array. The mean intensity fluorescent ratio of each clone in the dye-swap hybridisation is represented by a pink spot on the chart.

Hybridisations with a high level of background noise display a high level of scattering in their analysis chart and have a high percentage of spots discarded from the analysis, for example the hybridisations of KMH2 and L428 shown in Appendix A. Samples of low quality display a high level of scattered clones, but since the quality of all DNA samples was checked by measurement on a Nanodrop ND-1000 Spectrophotometer (Nanodrop Technologies Ltd., Delaware, USA) before and after labelling it is more likely that the high level of scattering observed on some of the hybridisation charts is due to smears or dust on the array resulting in high background fluorescence.

Tables of gains and losses in chromosomal regions from each cHL-derived cell line were compiled (see Tables 5.1 and 5.2) and compared with published conventional CGH analyses (Chui et al 2003) of the HDLM2, KMH2, L1236, L428 and L591 cell lines (shown in red in Tables 5.1 and 5.2). HDLM2, KMH2 and L1236 display the greatest number of additional affected chromosome regions, whilst L591 displays the lowest. Recurrent gains in 2p and 9p, previously identified by conventional CGH, were identified in all six cHL-derived cell lines using array-CGH. A previously reported recurrent gain in 7p was observed in all except the HDLM2 cell line. Similarly, a recurrent loss of chromosome material in 14q was observed in all except HDLM2.

Table 5.1. Chromosomal regions in each cHL-derived cell line where a gain of DNA has been identified by array-CGH. Chromosome regions in red had previously been identified using conventional CGH (Chui et al 2003; Joos et al 2003).

Cell Line	Chromosome regions gained
HDLM2	2p25.3, 2p22.2-p16.1, 2p11.2, 2q11.2, 2q24.3, 2q36.3, 3q12.3, 3q25.3, 3q25.32-q29, 4p15.31, 4q22.3, 5p15.33-p15.2, 5p14.2, 5p13.2-p12, 5q11.2, 5q23.1-q23.2, 5q34-q35.3, 6p22.3, 6q27, 7q21.13, 7q21.3, 8q11.22-q11.23, 8q22.3-q23.1, 8q23.3-q24.22, 9p24.3-p21.1, 9q31.1, 9q34.3, 10q11.22, 11q12.3, 12p13.33-p12.3, 12q13.12, 14q12, 14q23.1, 14q32.33, 15q25.1, 16p12.1, 16q21-q22.1, 17p12, 17q11.2, 17q21.31-q22, 17q23.2, 18p11.21, 18q22.1, 18q23, 19p12, 19q12-19q13.12, 22q12.1
KMH2	1p36.31-p36.23, 1p36.21, 1q23.3, 1q25.1, 1q31.3-q32.2, 1q41-q42.11, 1q42.13-q42.2, 1q43, 2p25.3-p25.1, 2p21-p16.1, 2p13.1-p12, 2q14.2, 2q24.2-q24.3, 2q36.3, 3p14, 3q25.1, 3q26.1-q26.32, 3q27.3, 3q28, 4q25, 5p14.3, 5p12, 5q13.3, 5q23.1, 5q35.2, 6p25.3-p25.2, 6p24.3, 6p24.1, 6p22.3, 7p11.2, 7q34, 7q36.1-q36.3, 8p23.3, 9p21.2, 10q23.31, 10q23.33, 10q26.13-q26.2, 10q36.13, 11p15.4-p15.3, 11p15.1, 11p14.1, 11q12.2-q12.3, 12q13.13, 12q13.3, 12q21.31, 12q23.1, 12q24.21-q24.31, 14q21.3, 14q24.3, 14q32.2-q32.31, 15q22.2, 15q22.31, 15q22.33-q23, 16p13.2, 16p13.13, 16q13.2-q13.13, 16q22.1-q22.2, 16q23.1-q23.3, 17p12, 17q21.2-q21.31, 18q12.1, 21q22.12
L1236	1p31.1, 1q23.2, 1q24.2, 1q25.3-q31.3, 1q32.2, 1q41-q42.11, 1q42.2-q43, 2p25.3-p22.3, 2p22.1-p13.3, 2q24.2, 2q31.1, 2q36.3, 3p26.3-p26.1, 3p24.3, 3p14.2, 3q12.3, 3q13.13, 3q13.32, 3q21.1, 3q21.3-q25.1, 3q25.31-q26.31, 3q26.33, 4p15.31, 4p13, 4q13.1, 4q21.1, 4q24-q27, 5p15.33-p15.32, 5p14.2, 5p13.1, 5q11.2, 5q22.2, 5q23.1-q23.2, 5q31.1, 5q31.3, 6p22.3, 6p21.32, 6p11.2, 6q14.3, 7p22.2, 7p21.1-p14.3, 7p14.1, 7p11.2, 7q11.23-q21.11, 7q21.13-q22.2, 8p12, 8q24.21-q24.3, 9p24.3-p21.1, 10p15.1-p13, 10p12.31, 10p12.1, 10p11.23-cent, 10q11.21, 10q21.3, 10q23.31, 11p14.1, 11q13.1, 11q22.3-q23.1, 11q23.3-q25, 12p13.32-p12.3, 12p21.1-cent, 12q12-q13.13, 12q13.3, 14q22.3-q23.1, 15q11.2, 15q23, 15q24.3-q25.2, 16q22.1, 16q23.2, 17p12, 17q21.31, 17q22, 18p11.21, 18q21.1, 18q23, 20p13-p12.1, 20p11.21, 20q11.23-q12, 20q13.12

Cell Line	Chromosome regions gained
L428	2p22.1-p16.1, 2p14-p12, 3p26.3, 3q26.31, 5q11.2, 6p22.33, 6p21.1, 6p12.1, 6q21, 6q23.3-q24.2, 7p11.2, 7q32.1, 7q32.3-q33, 8p11.21, 8q24.21-q24.3, 9p24.3-p24.2, 9q33.2-q33.3, 11q24.3-q25, 12p12.1, 12q13.13, 15q14, 15q25.1, 16p11.2, 16q23.1, 17p11.2, 17q12, 17q25.3, 20q13.13
L540	1p36.22-36.21, 1p31.1, 2p25.3-p23.3, 2p23.1-p22.3, 2p16.3, 2p12-p11.2, 2q11.2-q22.3, 2q23.2-q33.3, 2q34, 2q36.3, 3p26.3, 3p12.3, 3q26.1, 4p15.31, 4q22.3, 4q31.21, 4q35.1-q35.2, 5p15.33, 5q23.2, 5q34-q35.2, 6p25.3, 6p25.1-p24.3, 6p24.1-p22.1, 7p14.2-p14.1, 7q11.23-q21.13, 7q22.1, 7q22.3-q31.31, 7q31.33-q32.1, 7q32.3-q34, 7q36.2-q36.3, 8q11.23, 8q21.3, 9p24.3-p21.1, 9q31.1, 11q13.5, 11q22.3-q23.3, 11q24.2-q25, 12p13.2, 12p12.3-p12.1, 12p11.22, 12q21.31, 13q34, 14q23.3-q31.3, 14q32.13-q32.31, 14q32.33, 15q11.2, 15q21.1, 15q26.1-q26.3, 16q12.2, 16q21-q22.1, 17p22, 17p12, 17q11.2-q12, 17q21.2-q21.32, 17q22-q23.3, 18p11.21-q11.2, 18q22.1, 19p12, 19q13.32, 19p13.2, 20p13-p11.21, 20q11.21-q12, 20q13.13-q13.33, 22q12.3
L591	6p22.3, 7p21.3-p21.2, 7q21.13, 9p24.1-p22.3, 9p21.3-p21.1, 10q11.22, 11q24.2, 11q25, 18p11.21

Table 5.2. Chromosomal regions in each cHL-derived cell line where a loss of DNA has been identified by array-CGH. Chromosome regions in red had previously been identified using conventional CGH (Chui et al 2003; Joos et al 2003).

Cell lines	Chromosome regions lost
HDLM2	2p24.3, 2p23.3, 2q22.1, 2q33.1, 2q33.3-q35 , 2q37 , 3p14.1, 3p12.1, 3q11.2, 3q12.2, 3q13.11-q21.2, 3q25.1, 3q29, 4p16.3, 4p16.1-p12, 4cent-4q13.1, 4q25, 4q33, 4q34.1, 5p15.32, 5p14.1, 5cent-q11.2, 5q13.2-q15, 5q21.3, 5q33.1-q34, 6q26, 7p22.3-p14.3, 7p14.1, 7q21.11, 8p23.3-q11.23 , 8q12.3, 11p14.1, 12q12, 12q13.13, 12q23.1, 12q24.32-q24.33, 15q15.1, 15q24.3, 15q25.3-q26.3, 16q12.1-q12.2, 16p13.13, 16q21-q23.3, 16q24.3, 17p13.1, 17q11.2-q12, 17q23.2-q23.3, 17q24.2-q25.3, 18p11.32-p11.21 , 18q12, 18q22.1, 19p12, 20p13-p11.23 , 20q11.23-q13.33 , 21q21.1, 22q13.2-q13.33
KMH2	2q33.3-q34, 3p25.2, 3q13.2-q13.31, 3q21.1-q21.2, 4q13.3, 4q28.2, 4q35.1-q35.2 , 5q14.1, 5q32-q33.3, 6p21.31, 6q14.1 , 6q21-q22.1 , 6q22.32 , 6q24.2-q24.3 , 7p22.3, 7p15.1, 7q32.1, 8p21.2, 8p11.21, 8q12.2 , 8q13.3 , 8q22.3, 9p22.3, 9q21.11, 9q21.13, 9q21.31, 9q22.11, 10q22.3, 10q25.1-q25.2, 11q23.1, 11q23.3, 11q24.3-q25, 12q14.3, 12q21.31, 13q12.11 , 13q12.12 , 13q12.3 , 13q13.3 , 13q14.11, 13q14.2-q14.3, 13q21.2-q21.33 , 13q22.2-q22.3 , 13q31.1 , 13q31.3-q32.1 , 13q32.3-q33.2, 14q13.2, 14q32.33 , 15q11.2, 15q13.3, 15q15.1, 15q22.31, 16q12.1-q12.2, 18p11.31 , 18q12.1, 18q12.3 , 18q12.3-q21.1 , 18q21.22 , 18q23 , 20p13-p12.2 , 20p11.23 , 20q13.13 , 22q11.22, 22q12.1-q13.31
L1236	1p36.22, 1p36.12-p36.11, 1p34.3, 1q31.1, 1q32.1, 2q11.2, 2q13, 2q27, 3p14.3, 3q13.31, 3q26.2, 3q27.2-q29, 4p16.3, 4p16.1, 4p15.1-p14 , 4q13.1, 4q28.2-q28.3, 4q31.21-q31.22, 4q31.3-q32.1, 4q34.1-34.2 , 4q35.1 , 5q11.2, 5q13.1-q14.3, 5q22.2, 5q32, 6p21.31-6p21.1, 6p12.3-p12.1, 6q14.1, 6q15-q22.31 , 6q22.33-q23.3 , 6q24.2, 7p21.3-p21.2, 7p15.2, 7q31.1, 7q32.1, 7q32.3-q34, 7q36.1-q36.3, 8p23.3-p23.1 , 8q12.2, 9q21.13, 9q21.32-q21.33, 9q22.2-q34.3 , 10q22.1 , 10q22.3 , 10q26.13 , 11p15.5-p15.2, 11p14.3-p14.2 , 11p13, 11q12.2-q13.4, 11q14.1, 12q14.1, 12q21.1-q21.2 , 12q22-q23.3 , 12q24.13-q24.21, 12q24.23-q24.31, 12q24.33, 13q12.11-q14.3 , 13q21.33-q31.1 , 13q31.3-q33.2 , 13q34, 14q11.2-q12 , 14q21.2-q22.1, 14q23.3-q24.1, 14q24.3, 14q32.13, 14q32.33, 15q21.3, 15q22.31, 15q25.2-q25.3, 16p13.3, 16p13.13-p11.2 , 16q12.1, 16q21.1, 16q23.1-q23.2, 17p13.3-p11.2, 17q12, 17q21.2-q21.31, 17q23.2-q23.3, 17q24.2-q25.3 , 18p11.31, 18q22.1, 18q23, 19p13.3-p13.2, 19p13.11, 19q12-q13.12, 19q13.31-q13.32, 20q13.33, 21q22.11, 21q22.13, 21q22.3, 22q11.21-q13.33

Cell lines	Chromosome regions lost
L428	4p15.31, 4p15.1, 4q34.1, 5q11.2, 5q12.3, 5q13.3, 5q14.3, 5q21.2, 6p22.1, 6p12.3, 7p21.3, 9q21.2-q21.31, 9q21.33, 9q22.2-q33.1, 9q34.13, 9q34.3, 11q11.1-q23.3, 12p11.21, 12q21.31, 12q21.33-q22, 12q24.21, 12q24.31, 12q23.2-q23.3, 13q12.11-q34, 14q32.33, 15q21.3, 15q22.31, 15q25.2, 18q11.2-q12.1, 18q12.3, 18q21.1, 18q21.32-q23, 20p11.23
L540	1p31.1-p21.3, 1p13.3-p12, 2q11.2, 3p25.1, 3p24.2, 3p14.2-p14.1, 3q13.13, 4q33, 5q31.2, 5q32, 6p22.2, 6p21.2-p12.3, 6p12.1, 6q12-q22.1, 6q22.31-q27, 7p15.1, 7p14.1, 7q21.11, 7q21.13, 8p23.3-p12, 8q11.23, 8q12.2-q12.3, 8q13.2, 8q23.3-q24.3, 9p21.13-q22.3, 9q22.32-q34.3, 10p15.3, 10p15.1-p12.33, 10p21.31-p11.21, 10q11.21-q26.3, 11p11.2, 11q12.1, 11q25, 12q13.3-q14.1, 12q24.11-q24.13, 13q12.11-q33.3, 14p15.5, 14p15.33, 14p15.1, 14q11.2-q13.2, 14q21.1, 14q21.3-q22.3, 15q22.31, 15q24.1, 15q24.3-q25.1, 16p13.3, 16p11.2, 16q21-q23.3, 16q24.1, 17p13.2-p13.1, 17p11.2, 17q25.2-q25.3, 18q12.2-q23, 19q12, 19q13.12, 22q11.21, 22q13.1-q13.2
L591	2q34, 3p21.31, 5q14.1, 7q31.2-q31.32, 7q32.3-q34, 7q36.1-q36.3, 8p23.3-p21.2, 8p12, 11q23.1, 12q21.31, 13q32.2, 14q32.2-q32.33, 16q12.1, 22q11.22

Array-CGH results from all 6 cHL-derived cell lines were combined in order to identify regions that were commonly gained or lost within three or more cell lines. The results are displayed in ideograms (see Figures 5.3 and 5.4) showing the location of each clone that was gained or lost within three or more cell lines. The coloured circles each represent the presence of a gain, or loss, of this clone within a different cell line. Genes with known functions, that are located in these regions, are shown in Appendices B and C. The regions containing the largest number of chromosomal gains in the cell lines were: 2p21-p16.1, 6p22.3 and 9p24.2-p21.2 (see Figure 5.3).

Gains in 2p21-p16.1 were identified only within the EBV-negative cell lines but not in the EBV-positive L591 cell line. Known functional genes located within this region are FSHR (49.04-49.23 Mb), PRKCE (45.73-46.26 Mb), REL (60.96-61.00 Mb) and BCL11A (60.53-60.63 Mb) (see Appendix B). Gains in 6p22.3 were observed in the six cHL-derived cell lines within regions containing the MYLIP (16.23-16.25 Mb), FAM8A1 (17.70-17.71 Mb), NUP153 (17.72-17.81 Mb), ID4 (19.945-19.948 Mb) and CDKAL1 (20.64-21.34 Mb) genes (see Appendix B). However, only one region (22.57-22.66Mb), represented by the RP11-33I5 clone, was gained within all the cell lines. There are no genes with known function in this clone, or directly adjacent to this region.

From the 19 clones gained within 9p24.2-p21.2, only five clones include genes of known function: SMARCA2 (20.05-21.83 Mb), VLDLR (25.25-26.44 Mb), ATL1 (50.09-50.16 Mb), MLLT3 (20.33-20.61 Mb), MOBKL2B (27.31-27.51 Mb) and IFNK (27.514-27.516 Mb).

A large number of clones corresponding to a loss of chromosome material, within three or more cell lines, were located within 8p23.2-p12, 9q21.13-q34.3, 13q and 22q13.1-q13.31 (see Figure 5.4), with the latter three regions affected only within EBV-negative cell lines. Many functional genes are located within these regions (see Appendix C). Gains in 9q22 and 9q33-q34 have been previously identified by conventional CGH analysis of the L428 and L1236 cHL-derived cell lines (Joos et al 2003). In our results from hybridisation of L1236, one gain in 9q21.2 was identified, although chromosomal imbalances were not identified in adjacent clones or clones near to this region. Two gains in 9q33.2-q33.3, 1.6 Mb apart, were identified in our L428 hybridisations. This region, therefore, warrants further analysis. The region of loss on chromosome 13 is the largest area of imbalance identified in our analysis with regions across the whole of the q-arm affected. This anomaly was also reported from conventional CGH analysis of cHL-derived cell lines and case samples (Chui et al 2003; Joos et al 2000; Joos et al 2002; Joos et al 2003).

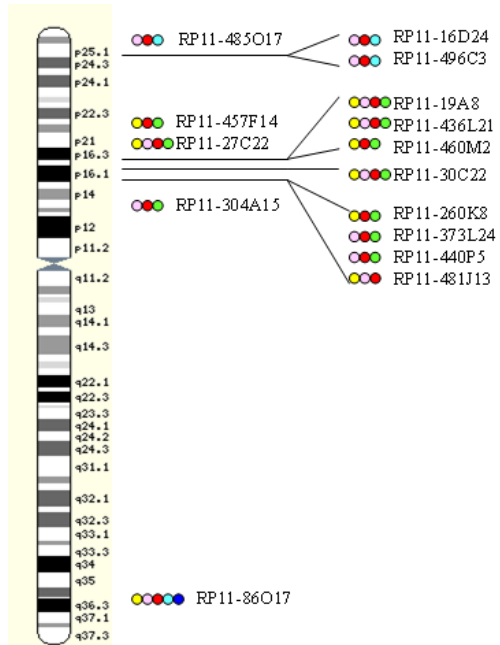
Several novel chromosome imbalances were also identified, and the Ensembl and Genecard databases were used to locate the genes with known function located within these regions (see Appendices B and C). Selected genes and their known functions are listed in Tables 5.3 and 5.4.

Table 5.3. Selected genes of interest in newly identified regions of gain (details from www.ensembl.org and www.genecards.org).

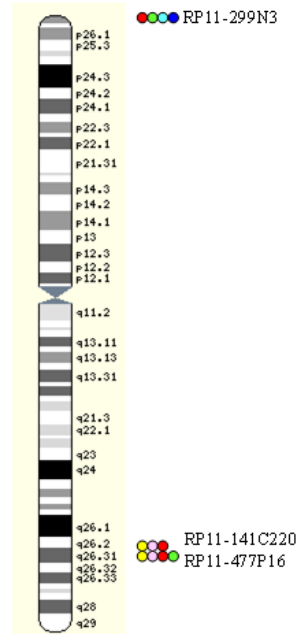
Chromosome Location	Gene	Mb position	Function
5q22.2	APC (Adenomatous polyposis coli protein)	112.10-112.20 Mb	Tumour suppressor that promotes rapid degradation of CTNNB1 and participates in Wnt signalling
8q24.12	TAF2 (TAF2 RNA polymerase II, TATA box binding protein (TBP)-associated factor)	120.81-120.91 Mb	Stabilizes transcription factor (TFIID) binding to core promoter (Transcription factor TFIID is one of the general factors required for accurate and regulated initiation by RNA polymerase II)
11q23.3	IGSF4 (Immunoglobulin superfamily member 4)	114.55-114.88 Mb	Acts as a tumour suppressor in non-small-cell lung cancer (NSCLC) cells; interaction with CRTAM promotes natural killer (NK) cell cytotoxicity and IFN-gamma secretion by CD8+ cells in vitro as well as NK cell-mediated rejection of tumours expressing CADM3 <i>in vivo</i>
17q22	HLF (hepatic leukaemia factor)	50.69-50.75 Mb	Rearranged in acute B-cell leukaemia, with translocation t(17;19); transcription from RNA polymerase II promoter

Table 5.4. Selected genes of interest in newly identified regions of loss (details from www.ensembl.org and www.genecards.org).

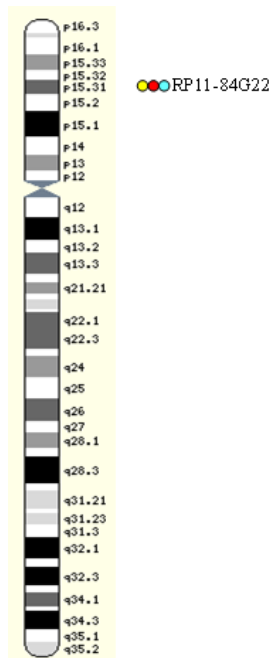
Chromosome Location	Gene	Mb position	Function
6q21	WISP3 (Wnt inducible signalling pathway protein 3)	112.48-112.49 Mb	Overexpressed in colon tumours; involved in cell growth and differentiation
6q24.3	SHPRH (SNF2 histone linker PHD RING helicase)	146.22-146.32 Mb	Involved in DNA repair
15q22.31	RAB11A (RAB 11A oncogene)	63.94-63.96 Mb	RAS related GTP-binding protein
16q12.1	ZNF423 (zinc finger protein)	48.04-48.42 Mb	An early B-cell factor associated zinc finger protein
17q25.3	TIMP2 (tissue inhibitor of metalloproteinase 2)	76.36-76.43 Mb	Involved in the invasive phenotype of acute myelogenous leukaemia
17q25.3	RAB40B	78.20-78.24 Mb	A member of RAS oncogene family; involved in small GTPase mediated signal transduction
18q21.33	BCL2 (B-cell CLL/lymphoma 2)	58.94-59.13 Mb	Suppresses apoptosis in a variety of cell systems including factor-dependent lymphohaematopoietic and neural cells; regulates cell death by controlling mitochondrial membrane permeability; appears to function in a feedback loop system with caspases; inhibits caspase activity either by preventing the release of cytochrome c from the mitochondria and/or by binding to the apoptosis-activating factor (APAF-1)
18q21.33	FVT (Follicular lymphoma variant translocation protein 1)	59.14-59.18 Mb	Involved in t(2;18)(p11;q21) in follicular lymphoma



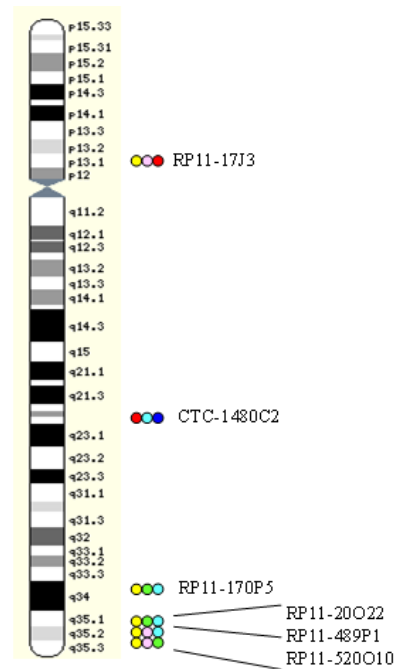
2



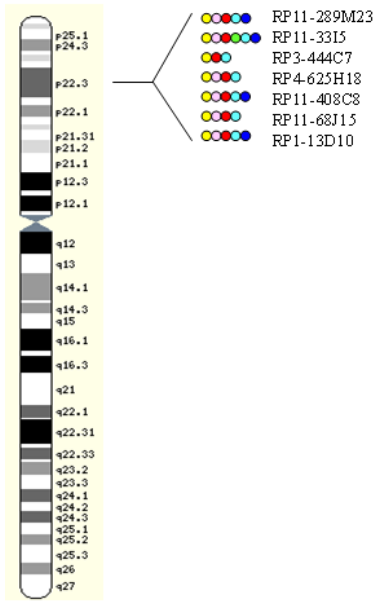
3



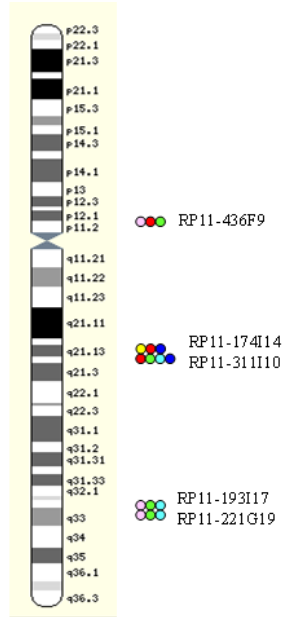
4



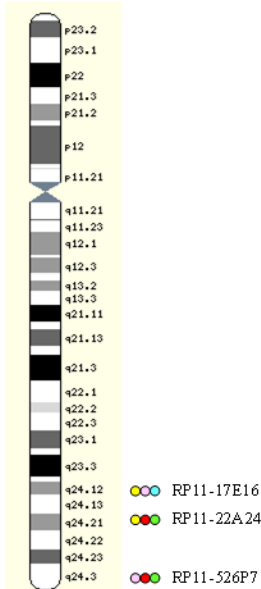
5



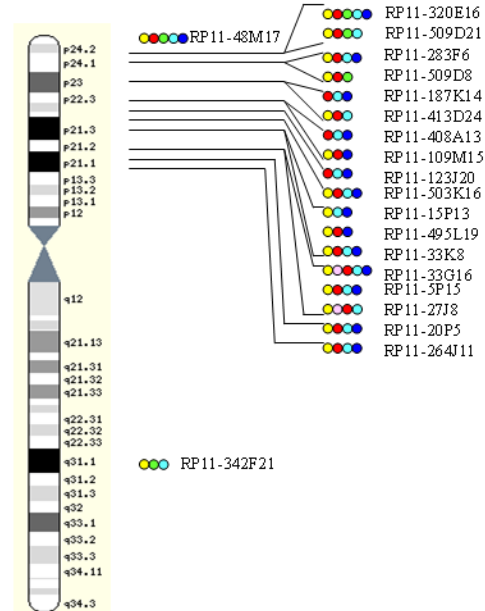
6



7



8



9

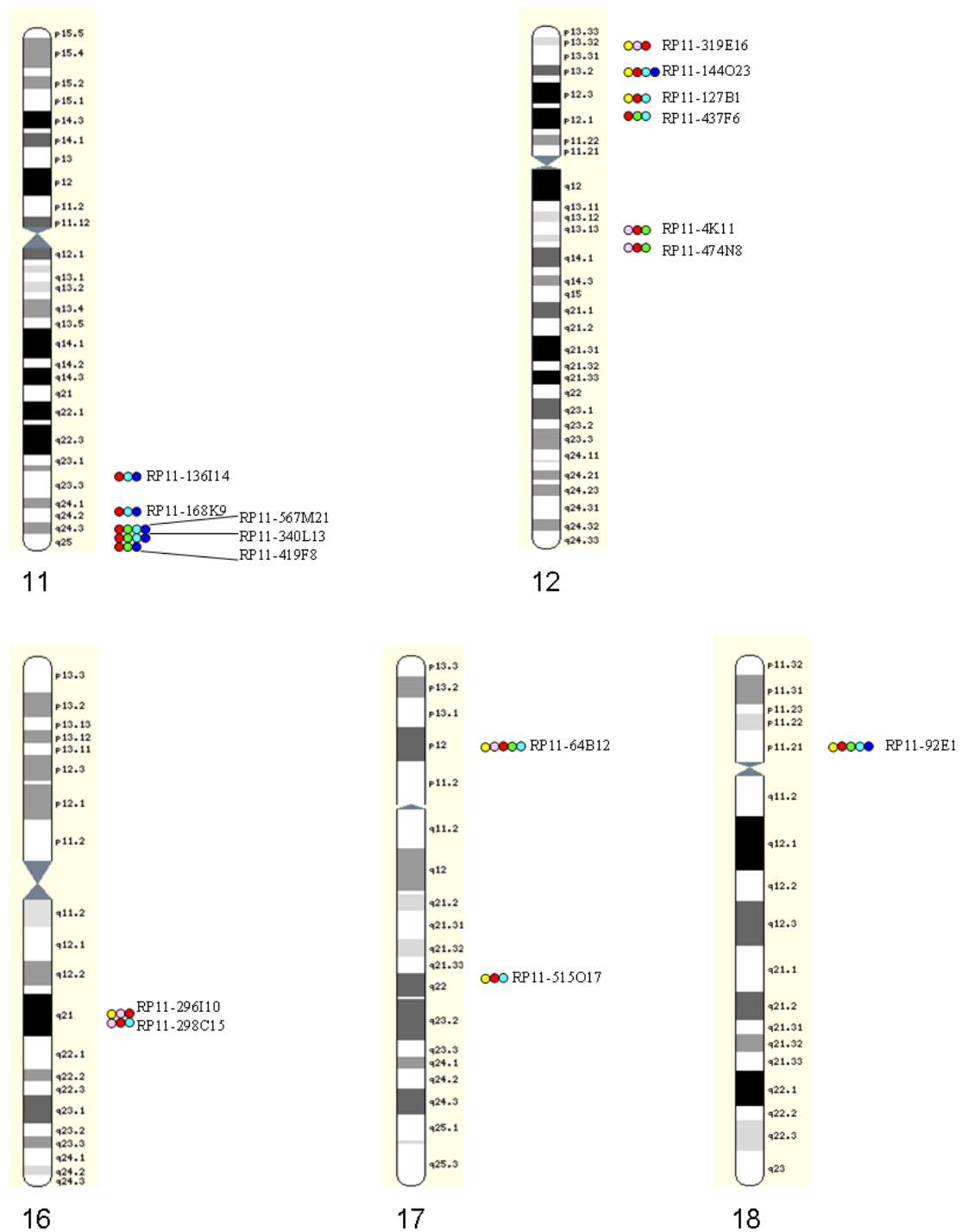
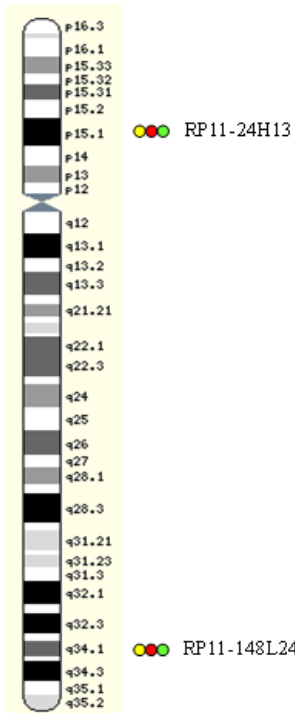
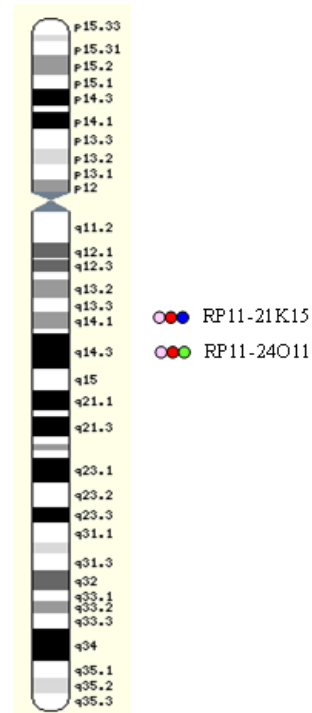


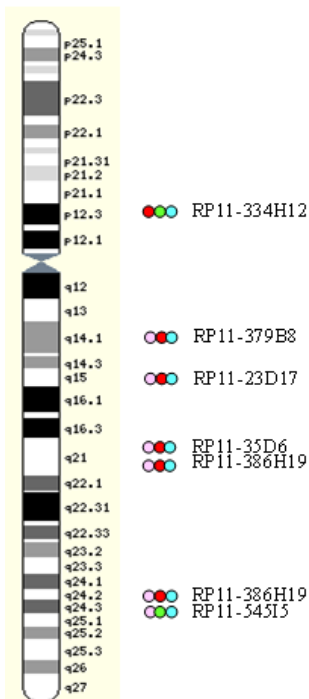
Figure 5.3. Ideogram depicting locations of clones representing gains in chromosomal material within each cHL-derived cell lines. Yellow circles - HDLM2; pink circles - KMH2; red circles - L1236; green circles - L428; pale blue circles - L540; dark blue circles - L591.



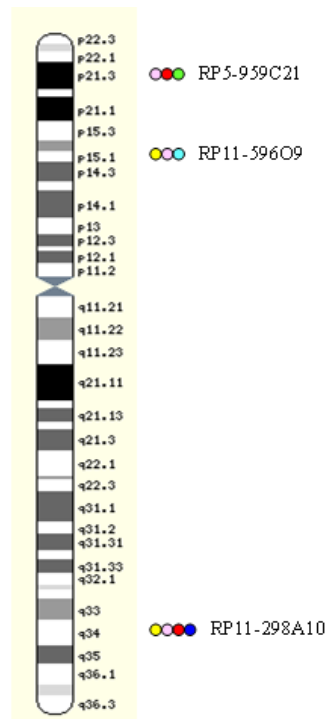
4



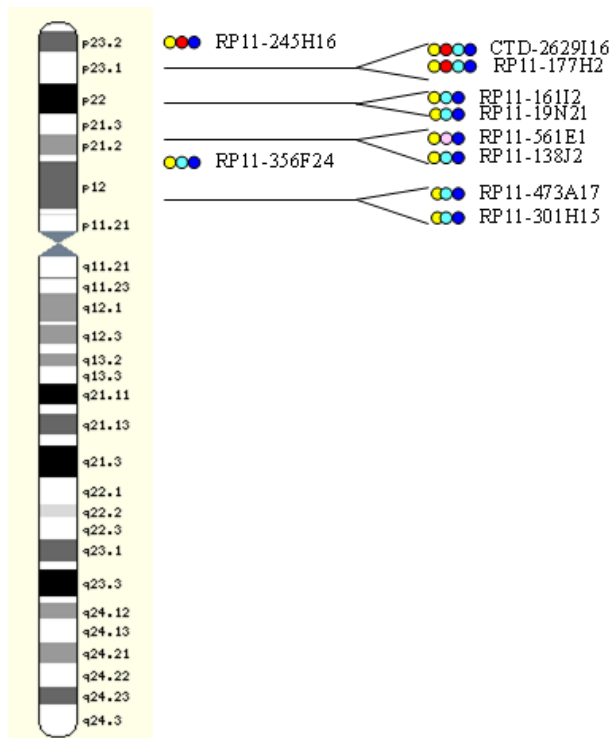
5



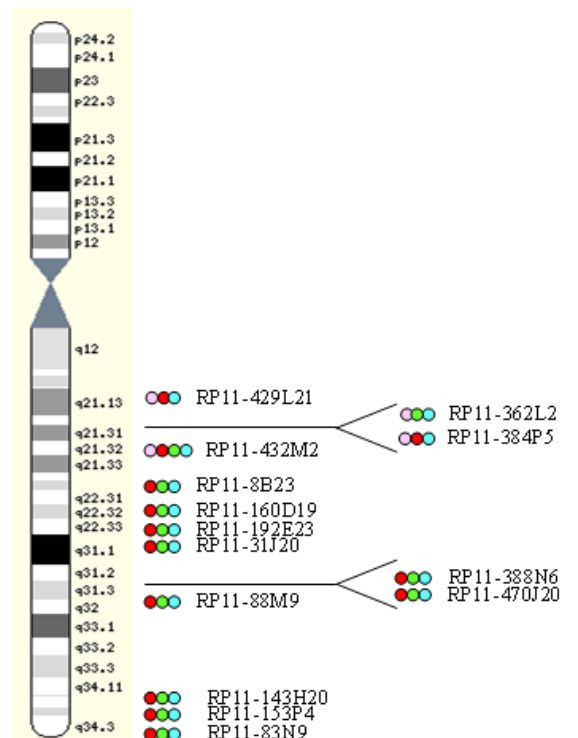
6



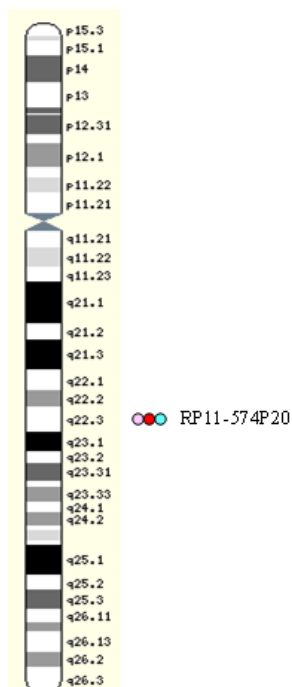
7



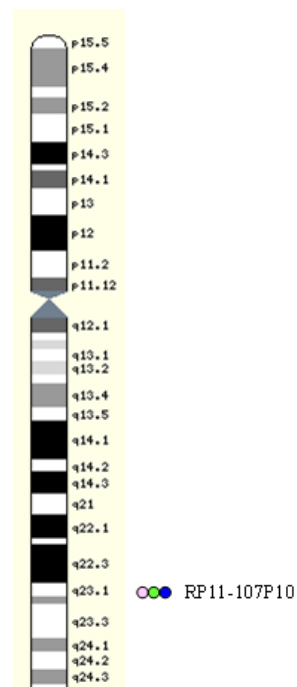
8



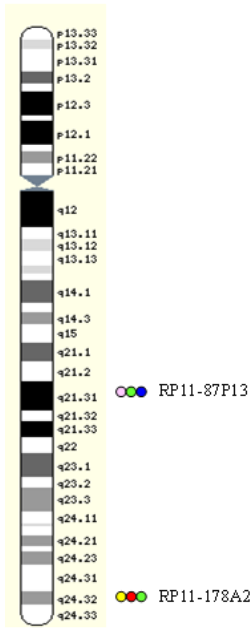
9



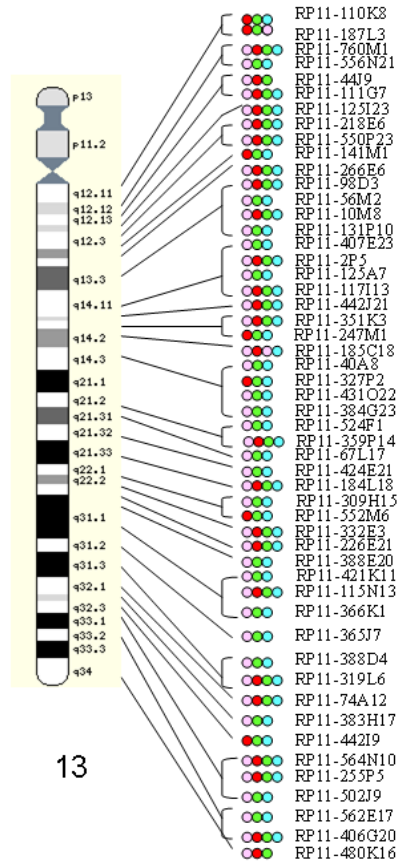
10



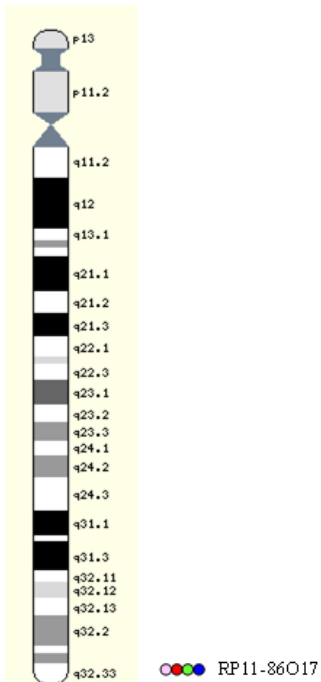
11



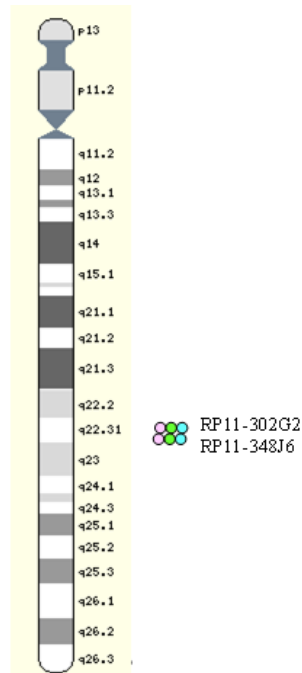
12



13



14



15

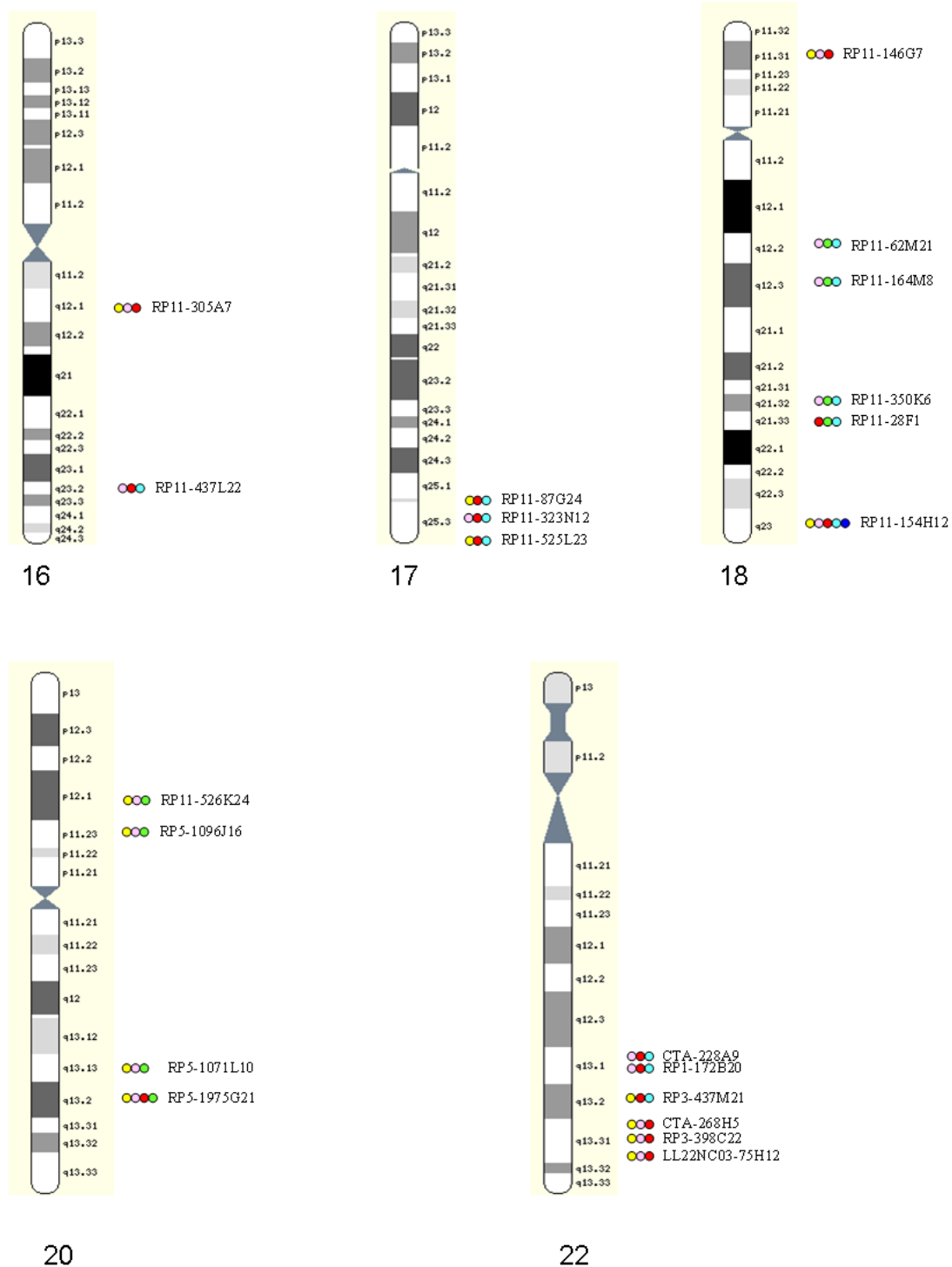
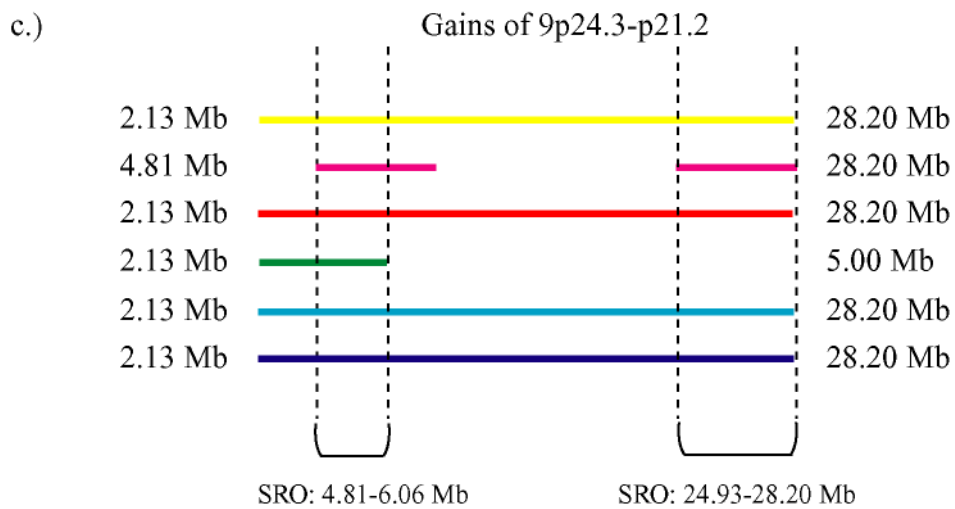
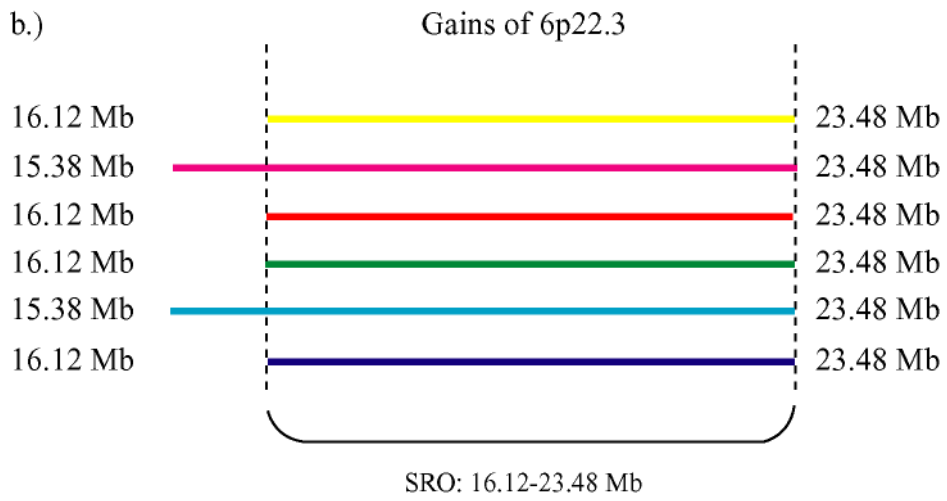
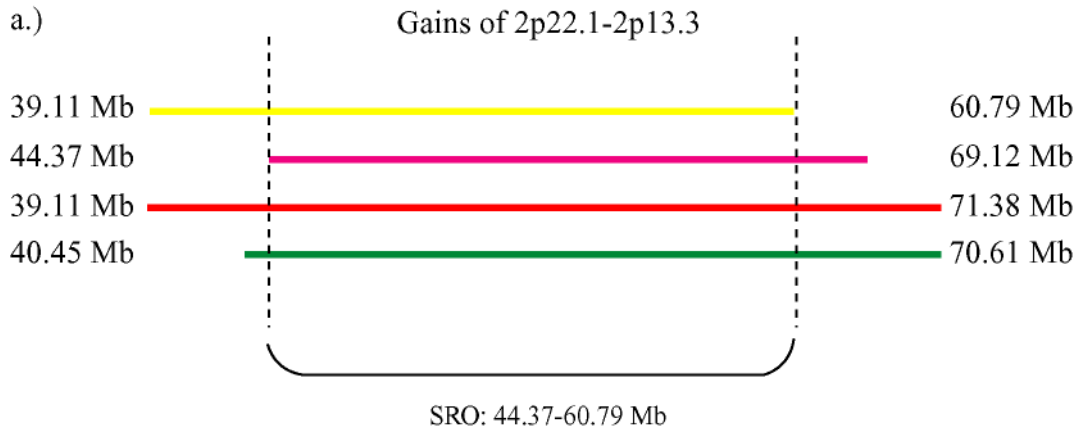
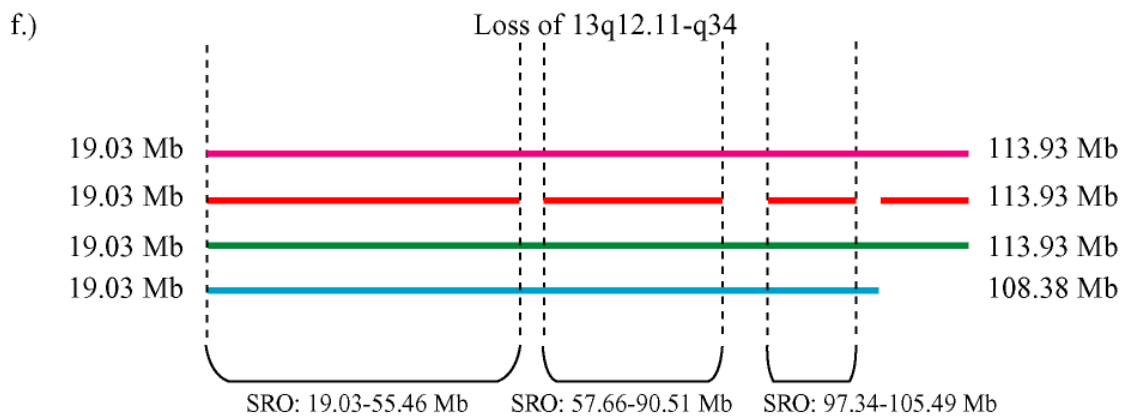
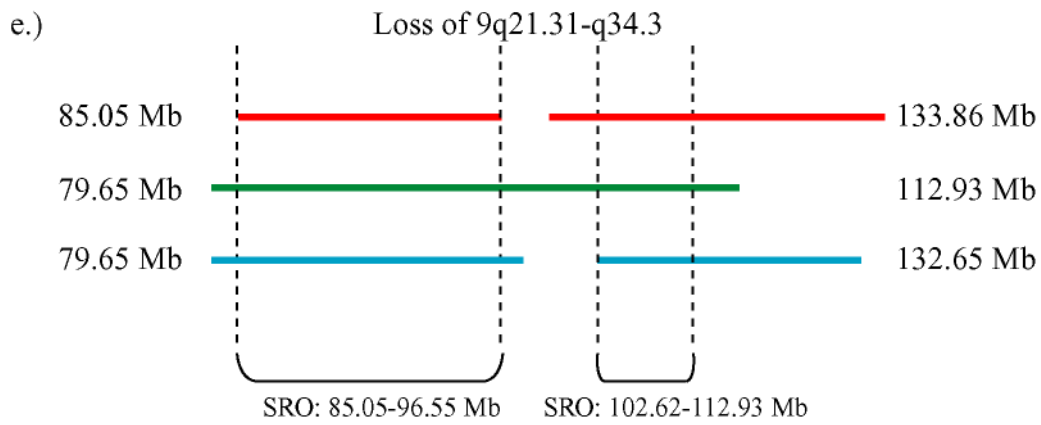
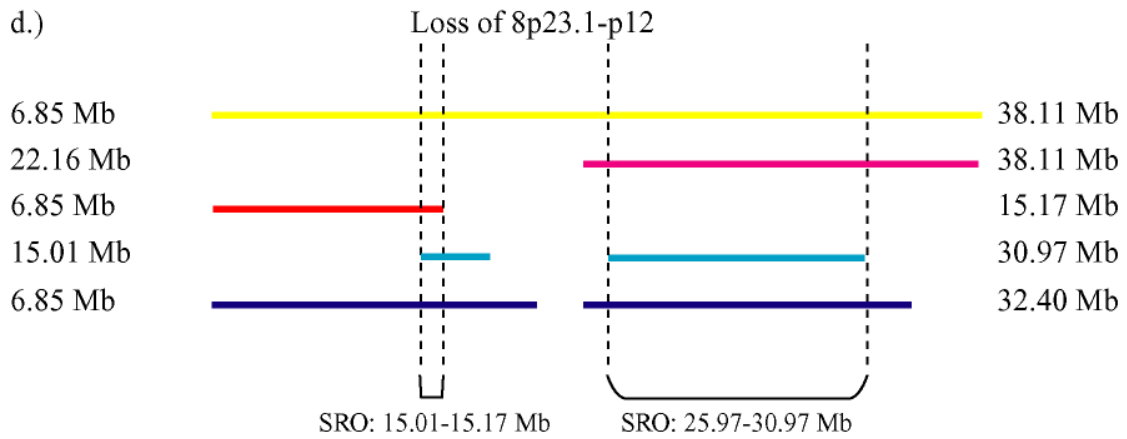


Figure 5.4. Ideogram depicting locations of clones representing losses in chromosomal material within each cHL-derived cell lines. Yellow circle - HDLM2; pink circle - KMH2; red circle - L1236; green circle - L428; pale blue circle - L540; dark blue circle - L591.

In the initial analysis, only clones with intensity ratios within the defined threshold, in both initial and dye swap experiments, were scored as regions of gain (intensity ratios >1.15) or loss (intensity ratios <0.85); however, when the intensity ratios of all clones in these regions with multiple imbalances (e.g., 2p22.1-p13.3) were examined, many had intensity ratios close to the threshold or one of the replicates was above or below the threshold. This suggests that these clones may also be regions of gain or loss. By checking the intensity ratios within the most commonly gained (2p22.1-p13.3, 6p22.3, 9p24.3-p21.2) or lost (8p23.1-p12, 9q21.31-q34.3, 13q12.11-q34, 22q13.1-q13.31) regions across all 6 cell lines, it was possible to identify the smallest region of overlap (SRO) (Figure 5.2). The Ensembl database was used to identify functional genes within the SROs (see Tables 5.5 and 5.6), which may play a role in the pathogenesis of cHL, although further array-CGHs of these cell lines would be required to confirm that these regions are indeed gained or lost. Some of these genes have been reported to be associated with cHL, and these will be discussed in depth at the end of this chapter (Section 5.4).





g.)

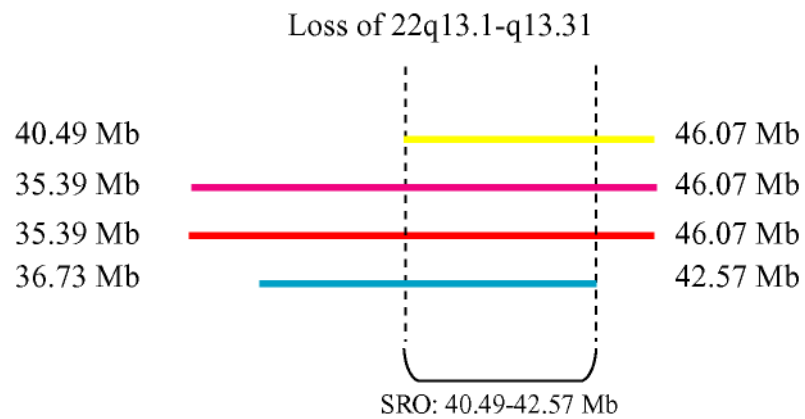


Figure 5.5. Schematic diagrams depicting smallest regions of overlap across three or more cHL-derived cell lines. Diagrams a), b) and c) show regions of gain, and diagrams d), e), f) and g) show regions of loss. The megabase (Mb) position within the chromosome is indicated for each region. HDLM2 (yellow), KMH2 (pink), L1236 (red), L428 (green), L540 (pale blue) and L591 (dark blue).

Table 5.5. Selected genes with known function that are located within gained chromosome regions identified as smallest regions of overlap (SROs) in three or more cells lines (details from www.ensembl.org and www.genecards.org).

REGIONS OF GAIN			
SRO (Mb position)	Gene	Location (Mb)	Known function
2p21-2p16.1 (44.37-60.79 Mb)	PRKCE (Protein kinase C epsilon type)	45.73-46.26 Mb	Receptor for phorbol esters, a class of tumour promoters; involved in apoptosis and in the NFκB pathway
	MSH2 (mutS homolog 6 (E. coli))	47.48-47.56 Mb	Encodes a DNA mismatch repair protein; part of the BRCA1- associated genome surveillance complex (BASC)
	MSH6 (mutS homolog 6 (E. coli))	47.86-47.88 Mb	Encodes a DNA mismatch repair protein; part of the BRCA1- associated genome surveillance complex (BASC); involved in apoptosis
	RTN4 (reticulon 4)	55.05-55.13 Mb	Interacts with BCL-XL and BCL-2 reducing their anti-apoptotic activity; regulation of apoptosis
	BCL11A (B-cell CLL/lymphoma 11A)	60.53-60.63 Mb	Functions as a myeloid and B-cell proto-oncogene; may play important roles in leukemogenesis and haematopoiesis; essential for lymphopoiesis; involved in B- and T-cell differentiation
6p22.3 (16.12-23.48 Mb)	DEK (oncogene)	18.33-18.37 Mb	Interacts with histones; binds DNA; involved in viral genome replication; involved in regulation of transcription from RNA polymerase II promoter; a chromosomal translocation involving DEK is found in a subset of acute myeloid leukaemia (AML)
	ID 4 (Inhibitor of DNA binding 4)	19.94-19.98 Mb	An oncogene candidate in bladder cancer

REGIONS OF GAIN (continued)			
SRO (Mb position)	Gene	Location (Mb)	Known function
6p22.3 (16.12-23.48 Mb)	E2F3 (transcription factor)	20.51-20.60 Mb	Regulation of progression through cell cycle; transcription initiation from RNA polymerase II promoter
9p24.1 (4.81-6.06 Mb)	JAK2 (Janus kinase 2)	4.97-5.11 Mb	Mediates the activation of STAT proteins; also activated in leukaemia or constitutively expressed in acute lymphoblastic leukaemia (ALL)
	CD274	5.44-5.46 Mb	Interacts with the co-inhibitory molecule Programmed Death Receptor-1 (CD279) on T-cells reducing TCR-mediated proliferation and cytokine production; essential for T lymphocyte proliferation and production of IL10 and IFNG; upregulated in B- and T-cells
	PDCD11G2 (CD273 antigen)	5.5-5.56 Mb	Involved in the co-stimulatory signal; essential for T lymphocyte proliferation and IFN γ production
9p21.3-p21.2 (24.93-28.20 Mb)	IFNK (interferon, kappa)	27.514-27.516 Mb	May play a role in the regulation of immune cell function; Provides cellular protection against viral infection in a species-specific manner; involved in JAK-STAT signalling pathway

Table 5.6. Selected genes with known function that are located within lost chromosome regions identified as smallest regions of overlap (SROs) in three or more cells lines (details from www.ensembl.org and www.genecards.org).

REGIONS OF LOSS			
SRO (Mb position)	Gene	Location (Mb)	Known function
8p23.1-p12 (25.97-30.97 Mb)	BNIP3L (BCL2/adenovirus E1B 19 kDa protein-interacting protein 3-like)	26.29-26.32 Mb	Induces apoptosis; interacts with viral and cellular anti-apoptosis proteins; can overcome the suppressors BCL-2 and BCL-XL, although high levels of BCL-XL expression will inhibit apoptosis; may function as a tumour suppressor.
	TRIM35 (Tripartite motif-containing protein 35)	27.19-27.22 Mb	Haemopoietic lineage switch protein; induces apoptosis
	CLU (clusterin)	27.51-27.52 Mb	Involved in DNA double-strand break repair by end joining (non homologous recombination) and V(D)J recombination; involved in apoptosis
	ESCO2 (Establishment of cohesion 1 homolog 2)	27.68-27.71 Mb	Involved in the cell cycle: required for the establishment of sister chromatid cohesion and couple the processes of cohesion and DNA replication to ensure that only sister chromatids become paired together.
	PBK (PDZ binding kinase)	27.72-27.75 Mb	Expression is regulated by E2F; seems to be active only in mitosis; may also play a role in the activation of lymphoid cells
	ELP3 (Elongator complex protein 3)	28.00-28.10 Mb	May play a role in chromatin remodelling and is involved in acetylation of histones H3 and probably H4; regulation of transcription from RNA polymerase II promoter

REGIONS OF LOSS (continued)			
SRO (Mb position)	Gene	Location (Mb)	Known function
9q21.32-q22.32 (85.05-96.55 Mb)	DAPK1 (death-associated protein kinase 1)	89.30-89.51 Mb	Involved in apoptosis; Triggered by IFN γ
	CKS2 (CDC28 protein kinase 2)	91.11-91.12 Mb	Involved in the G1/S transition of the cell cycle; involved in spindle organisation
9p31.1-q31.3 (102.62-112.93 Mb)	RNF20 (ring finger protein 20)	103.33-103.36 Mb	Interacts with p53; transcriptional activator; chromatin modification
	PPP3R2 (Protein phosphatase 2B regulatory subunit 2)	103.393-103.397 Mb	T cell receptor signalling pathway; involved in apoptosis; Wnt signalling pathway
	TAL1 (T-cell acute lymphocytic leukaemia 1)	47.45-47.46 Mb	Implicated in the genesis of haemopoietic malignancies; may play an important role in haemopoietic differentiation
	IKBKAP (I κ B kinase complex-associated protein)	110.66-110.73 Mb	Interacts preferentially with MAP3K14/NIK followed by IKK-alpha and IKK-beta; regulation of transcription
13q12.11-q21.1 (19.03-55.46 Mb)	TNFRSF19 (tumour necrosis factor receptor superfamily, member 19)	23.04-23.14 Mb	Can mediate activation of JNK and NF κ B; may promote caspase-independent cell death
	CENPJ (centromere protein J)	24.35-24.39 Mb	May play an important role in cell division and centrosome function.
	BRCA2 (Breast cancer type 2 susceptibility protein)	31.78-31.87 Mb	Regulation of progression through cell cycle; DNA repair; chromatin remodelling

REGIONS OF LOSS (continued)			
SRO (Mb position)	Gene	Location (Mb)	Known function
13q12.11-q21.1 (19.03-55.46 Mb)	TNFSF11 (tumour necrosis factor receptor superfamily, member 11)	42.03-42.08 Mb	May be an important regulator of interactions between T-cells and dendritic cells and may play a role in the regulation of the T-cell-dependent immune response; cell differentiation
	RB1 (retinoblastoma 1)	47.77-47.95 Mb	A key regulator of entry into cell division that acts as a tumour suppressor; directly involved in heterochromatin formation by maintaining overall chromatin structure and, in particular, that of constitutive heterochromatin by stabilising histone methylation; acts as a transcription repressor of E2F target genes by recruiting chromatin-modifying enzymes to promoters
13q21.2-q31.3 (57.66-90.51 Mb)	MYCBP2 (MYC binding protein 2)	76.51-76.79 Mb	May function as a facilitator or regulator of transcriptional activation by MYC
	NDFIP2 (Nedd4 family interacting protein 2)	78.95-79.02 Mb	May be involved in endocytosis; may be involved in NFκB and MAPK signalling pathways; induced by T-cell activation
13q32.2-q33.2 (97.34-105.49 Mb)	EBI2 (EBV-induced G protein-coupled receptor 2)	98.74-98.75 Mb	Membrane protein which is a probable mediator of EBV effects on B lymphocytes or of normal lymphocyte functions
22q13.2 (40.49-42.57 Mb)	BIK (BCL2-interacting killer (apoptosis-inducing))	41.83-41.85 Mb	Accelerates programmed cell death; binds to the apoptosis repressors BCL-XL, BHRF1 and BCL-2.

5.3.2 Gene expression analysis

Following gene expression array analysis, RP analysis (as described in Section 5.2.11) was used to identify the top 100 up- and downregulated genes in the KMH2, L428 and L591 cHL-derived cell lines. The top 20 differentially expressed genes for each cell line are listed in Appendix B, along with corresponding chromosomal locations. Those genes which are differentially expressed within all three cell lines are listed in Table 5.7.

In addition, some differentially expressed genes were common to the two EBV-negative cHL-derived cell lines only (see Table 5.8).

Table 5.7. Genes which are upregulated or downregulated within all three cHL-derived cell lines that were screened by gene expression array analysis.

	Gene	Chromosome region
Upregulated	SORT1	1p13.3
	ID2	2p25.1
	IL1R2	2q12-q22
	CD200	3q13.2
	FAM8A1	6p22.3
	NQO2	6p25.2
	PSD3	8p22
	ACO1	9p21.1
	PHYH	10p13
	SCGB1A1	11q12.3
	APLP2	11q24.3
Downregulated	VANGL1	1p13.1
	ID3	1p36.12
	MIG-6	1q36.23
	DNASE1L3	3p14.3
	GPR15	3q12.1
	EDNRA	4q31.22
	GUCY1A3	4q32.1
	GUCY1B3	4q32.1
	SH3MD2	4q32.3
	GABRG2	5q34
	GFOD1	6p24.1
	PKHD1L1	8q23.1
	PTS	11q23.1
	TEAD4	12p13.33
	TNFRSF19	13q12.12
	KCTD12	13q22.3
	PRKCH	14q23.1
	CCL3///CCL3L1///CCL3L3	17q12
	HYK	20q11.21
	CYSLTR1	Xq21.1
	NAP1L3	Xq21.32
	RPA4	Xq21.33
	BTK	Xq22.1
CD99	Yp22.3	

Table 5.8. Differentially expressed genes in the EBV-negative cHL-derived cell lines KMH2 and L428.

	Gene	Chromosome region
Upregulated	AKT3	1q44
	ZNF238	1q44
	MEIS1	2p14
	ENO3	17p13.2
	PRKCA	17q24.2
	KLHL15	Xp11.22
	BCOR	Xp11.4
Downregulated	VMD2L2	1p34.1
	SLAMF6	1q23.3
	SLAMF7	1q23.3
	CBLB	3q13.11
	PDCD6	5p15.33
	ARL4	7p21.3
	ASB15	7q31.32
	MRPL15	8q11.23
	PFKFB3	10p15.1
	CSTF2T	10q21.1
	PDLIM1	10q24.1
	MGST1	12p12.3
	GREM1	15q13.3
	SEC14L1	17q25.2
	GMIP	19p13.11
	CD37	19q13.33
	ADA	20q13.12
	ZD77D08	22q11.1
	SEPT6 /// N-PAC	Xq24

5.3.3. Correlation of array-CGH and gene expression array analyses

The genes identified in regions of chromosomal imbalance were compared with those which were differentially expressed in our gene expression array analyses. Those within the up- or downregulated regions on the X and Y chromosomes could not be included in this comparison since the sex chromosomes had not been analysed by array-CGH as previously explained (Section 5.2.7). Only three genes located within regions of chromosomal imbalance, and present in more than two cHL-derived cell lines in our array-CGH analysis, also appeared within the top 100 differentially expressed genes (see Table 5.9). FAM8A1 and APLP2 were both upregulated in all three assayed cell lines and are located on regions of chromosomal gain.

A member of the tumour necrosis factor receptor superfamily, TNFRSF19, was downregulated in all three assayed cell lines, and its corresponding clone was within a region of loss in the KMH2, L1236, L428 and L540 cell lines.

Previously, Schwering et al. (2003) had assessed the gene expression profiles of the HDLM2, KMH2, L428 and L1236 cHL-derived cell lines, compared to normal B-cells, using Affymetrix gene expression arrays and the L1236 cell line by serial analysis of gene expression (SAGE) (Schwering et al 2003a; Schwering et al 2003b). When our array-CGH results for L1236 were compared to the SAGE analysis of the same cell line, 31.4% (11/35) of the downregulated B-cell specific, lymphoid-specific and haematopoietic-specific genes were located close to regions of loss identified by array-CGH of the L1236 cell line, but none was represented by clones on our CGH-array. Recurrent abnormalities identified by array-CGH in three or more cHL-derived cell lines were then compared to the up- and downregulated genes that were most

specific to cHL cell lines in the study by Schwering *et al.* (2003). Two of these genes (Syk and GPR18) were located within chromosome bands (8p23.1 and 13q32.3, respectively) in which a loss had been detected in our array-CGH analysis. One clone on (RP11-297N6 (11.40-11.57 Mb)) our CGH-array is located on the same region as the BLK gene (11.38-11.45 Mb). Although this clone is unchanged in our HDLM2 array-CGH results, adjacent clones are lost. The SYK gene is located at 92.60-92.70 Mb on 9q22.31. In our L540 array-CGH results, clone RP11-240L7 (92.43-92.60 Mb), which slightly overlaps this region, is lost, although adjacent clones are unchanged. Our results confirm that the regions containing the BLK and SYK genes are lost in cHL-derived cell lines, although only in the HDLM2 and L540 cell lines.

Table 5.9. Genes within regions of chromosomal imbalance, identified by array-CGH analysis, which were also differentially expressed in gene expression array analysis. Each gene was represented on the CGH array by a single clone, listed in the table, and the gain or loss of this clone was identified in more than two cell lines.

Clone	Gene	Location	Gain	Upregulated
RP11-68J15	FAM8A1	6p22.3	HDLM2	-
			KMH2	KMH2
			L1236	L428
			L540	L591
RP11-567M21	APLP2	11q24.3	-	KMH2
			L1236	-
			L428	L428
			L540	-
			L591	L591
Clone	Gene	Location	Loss	Downregulated
RP11-760M1	TNFRSF19	13q12.12	KMH2	KMH2
			L1236	-
			L428	L428
			L540	L591

5.4 DISCUSSION

We have successfully shown that array-CGH can be used to analyse and identify chromosomal imbalances within six cHL-derived cell lines. Comparison of chromosomal gains and losses across all six cell lines allowed the identification of previously reported recurrent imbalances in cHL and, in addition, the detection of several new imbalances. Any genes of known function located within these regions of interest were identified.

Our results correlated well with conventional CGH analysis of cHL-derived cell lines previously performed within our laboratory (Chui et al 2003), although some small differences were seen in comparison to those chromosomal imbalances reported by Joos *et al.* (2003). By combining the results from all six cHL-derived cell line hybridisations, we identified several regions of recurrent chromosomal imbalance, present in three or more cell lines: gains on 2p22.1-p13.3, 6p22.3 and 9p24.3-p21.2, and a loss on 13q12.11-q34. These have also been detected in previous conventional CGH analysis; however, the increased resolution of array-CGH and the identification of SROs across these regions has enabled us to ‘fine-tune’ the location of these recurrent regions of gain and loss from that previously described as: 2p16-p13, 6p25-p22 and 9p24-p23, and 13q21-q31 respectively. For example, a gain of 2p16-p13 was detected by Chui *et al.* following conventional CGH analysis of the KMH2, L1236, and L428 cell lines (Chui et al 2003). We observed a gain in 2p22.1-p13.3 within all five EBV-negative cHL-derived cell lines assayed. By identifying the exact megabase position of the region of gain on this chromosome within each cell line, the SRO common to all five cell lines was defined as 44.37-60.79 Mb (2p21-p16.1).

Several new regions of recurrent imbalance were identified from our array-CGH analysis: a gain of 16q22.1, and losses of 5q, 7p, 7q, 8p, 8p, 9q, 10q, 15q, 17q, 20p, 20q and 22q. The T-cell acute lymphocytic leukaemia 1 (TAL1) gene is located within the recurrent region of loss identified on 9q31.1-q31.3 and a translocation involving this gene, t(9;17)(q34;q23), has recently been identified in four paediatric NHL patients (Lones et al 2007). It was suggested that this translocation had contributed to poor prognosis, although further studies are required to confirm this.

A recent study by Feys *et al.* (2007) aimed to identify new chromosomal imbalances in the HDLM2, KMH2, L1236 and L540 cell lines (Feys et al 2007a). Thirty-five new imbalances were detected and the study focused on a gain on 12q13.3 (L1236) and losses on 15q26.1 (HDLM2) and 16q12.1 (KMH2). The RGMA gene (91.38-91.43 Mb) is located immediately adjacent to a clone (RP11-266O8; 91.55-91.71 Mb) on our CGH-array which showed evidence of a deletion in the HDLM2 cHL-derived cell line. The next clone (RP11-41P8) at 92.11-92.27 Mb is also deleted in this cell line. FISH studies are warranted to confirm this deletion.

Six clones on our CGH-array lie within 16q12.1 and 5 of these are deleted in our KMH2 results. The RP11-147B17 clone (49.09-49.26 Mb) is located before the CYLD gene (49.33-49.40 Mb), identified as deleted by Feys *et al.* (2007), but is not gained or lost within our results. However, clone RP11-424K7 (49.62-49.80 Mb) lying beyond the CYLD gene is deleted in our KMH2 results. Our results are consistent, therefore, with Feys *et al.* (2007) and warrant further investigation by FISH.

As mentioned, Feys et al. (2007) reported an amplification of clone RP11-474N8 (12q13.3; 55.58-55.75 Mb), which was also gained in our L1236 cell lines. The STAT6 gene is located nearby at 55.77-55.79 Mb, but no clone on our array is located on this region. However we did detect amplification of the next clone, RP11-181L23 (12q13.3-q14.1; 56.52-56.29 Mb), within the L1236 cell line. Our results, therefore, strongly suggest that the region inbetween these clones is amplified, and that STAT6 would be affected in this cell line. STAT6 is a signal transducer and transcription activator that is known to be induced by IL13, a cytokine frequently expressed by HRS cells. Immunoblotting and IHC assays have demonstrated the constitutive phosphorylation of STAT6 in the HDLM2, KMH2, L428 and L540 cHL-derived cell lines and HRS cells from 78% of cHL cases assayed (Skinnider et al 2002). In the presence of a neutralising anti-IL13 antibody, cellular proliferation was significantly decreased in cHL-derived cell lines and STAT6 phosphorylation was inhibited (Skinnider et al 2002).

Some changes were unique to the EBV-positive cHL-derived cell line L591. A gain of chromosomal material at 7p21.3-p21.2 was identified. The only known functional gene within this region encodes a presynaptic cytomatrix protein, Piccolo (PCLO), which may act as a scaffolding protein and is thought to be involved in both the organization of synaptic active zones and in synaptic vesicle trafficking. The deletion of region 7q31.2-q36.3 could result in a downregulation or dysfunction of the suppression of tumorigenicity 7 (ST7) gene.

These results suggest that the pattern of chromosomal abnormalities may be different in EBV-associated and non-EBV-associated cases of cHL, with fewer changes in

EBV-negative cells. However, some degree of caution must be exercised in extrapolating results from the L591 cell line (Niedobitek 2006). Although derived from a cHL patient, there is no definitive proof that it is derived from HRS cells and the pattern of EBV expression in L591 cells is reminiscent of B-lymphoblastoid cell lines rather than primary EBV-associated cHL (Schaadt et al 1989). However, L591 cells do display typical features of HRS cells, such as expression of the CD15 antigen (Drexler 1993; Vockerodt et al 2002) and the EBV gene expression pattern may simply reflect drift *in vitro* as seen in Burkitt's lymphoma cell lines.

Using gene expression array analysis, we identified differentially expressed genes in three cHL-defined cell lines and compared these results with those from our array-CGH analysis in order to see if changes in chromosomal material will affect expression profile. When our array-CGH analyses of the cHL-derived cell lines was compared to results from gene expression array analysis of the KMH2, L428 and L591 cell lines, three highly differentially expressed genes (i.e., within the top 100 upregulated or downregulated genes following RP analysis of each cell line) were located within regions of chromosomal imbalance identified by our array-CGH analyses: FAM8A1 (6p22.3), APLP2 (11q24.3) and TNFRSF19 (13q12.12). When overexpressed, the TNFRSF19 gene is known to activate the JNK pathway and it can induce apoptosis by the caspase-independent pathway (Eby et al 2000). The downregulation of this gene in cHL-derived cell lines may prevent apoptosis by this pathway, and may help explain how HRS cells escape apoptosis in the GC. Further analysis of these genes by RT-PCR using RNA extracted from other cHL-derived cell lines will confirm if these genes are downregulated in all cHL-derived cell lines.

Kluiver *et al.* (2007) performed array-CGH analyses of four cHL-derived cell lines and compared the results with those from serial analysis of gene expression (SAGE) for the L1236 and L428 cell lines (Kluiver *et al.* 2007). It was found that only 17.8% and 18.4% of differentially expressed genes in L428 and L1236, respectively, mapped to regions of gain or loss, indicating that differential gene expression is not a direct result of copy number changes. Kluiver *et al.* (2007) suggested that noncoding regions, such as interspersed repeat elements like Alu repeats or LINEs, may significantly contribute to differential gene expression (Wang *et al.* 2006). However, probe sets not relating to a gene of known function, but which may contain such repeat elements, were removed from our gene expression array analyses. It must be considered, therefore, that non-translated genes or as yet unidentified coding sequences may be of importance in cHL, but have been undetected by our study. Further understanding of the genome is required to answer these questions.

As previously mentioned, our results confirmed the presence of recurrent chromosomal imbalances within cHL-derived cell lines: gains on 2p22.1-p13.3, 6p22.3 and 9p24.3-p21.2, and a loss on 13q12.11-q34.

The BCL11A proto-oncogene is located within 2p16.1 and is known to be expressed at high levels within germinal centre B-cells (Liu *et al.* 2006). Since HRS cells are derived from pre-apoptotic germinal centre B-cells, the functional implications of this gene should be considered. Translocations involving the immunoglobulin heavy chain (IgH) locus, on 14q32.3, and BCL11A, on 2p16.1, were reported within 3 B-cell chronic lymphocytic leukaemia (CLL) cases (Satterwhite *et al.* 2001) and BCL11A

was proposed as a candidate oncogene for cHL following detection of a gain within 2p by conventional CGH analysis of 44 cHL cases (Martin-Subero et al 2002). Further investigation by FICTION identified breakpoints within the REL locus adjacent to BCL11A, not within BCL11A, which suggested that REL may be the gene affected in cHL instead.

We detected amplification of the REL oncogene (2p16.1; 60.96-61.00 Mb) within the KMH2, L1236 and L428 cell lines. REL is a member of the NFκB family and has been a focus of interest in previous cHL studies (Barth et al 2003; Joos et al 1996; Joos et al 2003; Rodig et al 2005; Xiao et al 2004). Two IHC studies showed nuclear staining for REL in HRS cells from 23/25 and 51/59 cHL cases (Rodig et al 2005; Xiao et al 2004). Like BCL11A, REL was also involved in chromosomal translocations with the immunoglobulin loci in HRS cells from cHL cases (Martin-Subero et al 2006). When the regions of gain on 2p across all six cHL-derived cell lines were aligned and an SRO identified at 2p21-p16.1, REL lay just outside this region. However, it should still be considered in this study since it is located in a region of gain on three cHL-derived cell lines. REL was not within our top 100 list of upregulated genes from gene expression array analysis of the KMH2, L428 and L591 cell lines, so we have no evidence that gains of REL are associated with increased expression. A recent publication by Kluiver *et al.* presented SAGE and array-CGH analysis of the KMH2, L1236, L428 and L591 cell lines (Kluiver et al 2007). From array-CGH analysis, a SRO on 2p16.1-p13.3 (59-71 Mb) was identified, but SAGE analyses of the L1236 and L428 cell lines failed to detect tags corresponding to the REL gene. Furthermore, no increased expression of the REL mRNA was detected by QRT-PCR. These results suggested that REL is not a candidate in the pathogenesis of

cHL. When the location of our identified SRO on 2p (44.37-60.79 Mb) was correlated with the SRO (59-71 Mb) by Kluiver *et al.* (2007), a region of 2p16.1 (59-60.79 Mb) was scored as a gain in both array-CGH studies. This region includes the proto-oncogene BCL11A, suggesting that the functional association of this gene with cHL should be further investigated.

Amplifications within the 6p21-p23 region have previously been reported within several types of neoplasia, including NHL, large B cell lymphoma and follicular lymphoma (Stokke *et al* 2001; Monni *et al* 1996; Kuchiki *et al* 2000), and it has been suggested that this region may contain a number of potential oncogenes (Santos *et al* 2007). A number of functional genes are located within the 6p22.3 region commonly gained within the cHL-derived cell lines assayed in our investigation: NUP153; FAM8A1; ID4 (inhibitor of DNA binding 4) which has been suggested as a oncogene candidate in bladder cancer (Wu *et al* 2005); and CDKAL1 (CDK5 regulatory subunit associated protein 1-like 1), previously proposed as an oncogene (Hurst *et al* 2004). The CDKAL1 gene lies downstream from E2F3 (6p22.3), which is located within the SRO we identified on 6p22.3. Overexpression of this transcription factor is associated with aggressive tumours in human bladder cancer, prostate cancer and retinoblastoma (Olsson *et al* 2007; Orlic *et al* 2006). It has been suggested that E2F3 may mediate HLX9 activation via the phosphatidylinositol 3 kinase (PI3K) pathway which will in turn stimulate the expression of the cytokine interleukin 6 (IL6) (Nagel *et al* 2005). IL6 has been shown to be expressed by HRS cells (Herbst *et al* 1997) and has been suggested to stimulate 'B' symptoms in HL patients (Reynolds *et al* 2002).

The presence of a recurrent chromosomal gain on 9p24.3-p21.2 was also confirmed by this study. This region includes the following genes of known function: SMARCA2 (SWI/SNF related, matrix associated, actin dependent regulator of chromatin, subfamily a, member 2) involved in transcriptional activation; ATL1 (GTP-binding protein 3); MLLT3 (meloid/lymphoid or mixed-lineage leukaemia *Drosophila* homolog) which is involved in a chromosome translocation, t(9;11)(p22;q23), associated with acute leukaemias; MOBKL2B (Mps one binder kinase activator-like 2B) which is a member of the MOB1/phocein family (mitotic checkpoint genes); VLDLR (very low density lipoprotein receptor); and IFNK (interferon kappa) which is known to regulate immune cell function and is known to aid cellular protection against viral infection and genes. The JAK2 gene is located within 9p24 and is a tyrosine kinase involved in the JAK-STAT signalling pathway. It has been proposed by several groups as a potential oncogene in cHL (Chui et al 2003; Kluiver et al 2007; Joos et al 2000; Joos et al 2002; Joos et al 2003; Weber-Matthiesen et al 1995). A clone including the JAK2 gene (9p24) was not present on our CGH-arrays but the SRO (4.81-6.06 Mb) includes the JAK2 gene (4.97-5.11 Mb). JAK2 was not included in the 100 most upregulated genes in this study and similarly Kluiver *et al.* (2007) reported no increase in JAK2 expression in both SAGE analysis and QRT-PCR analysis (Kluiver et al 2007). Conversely, a translocation involving JAK2, t(4;9)(q21;p24), has been recently reported in one NSHL case using FISH analysis, providing support for the idea that dysregulation of this gene may be crucial (Van Roosbroeck et al 2007).

Losses within 13q have previously been reported within cHL and other haematological malignancies (Wada et al 1999; Struski et al 2007; Schraders et al

2005; Joos et al 2003; Chui et al 2003). A number of functional genes have been identified within this region and require further investigation to determine if they have a role in the pathogenesis of cHL: TNFRSF19 (tumor necrosis factor receptor superfamily, member 19) which can mediate activation of JNK and NF κ B and may promote caspase-independent cell death; GTF3A (general transcription factor IIIA); POSTN (periostin) which is overexpressed in breast cancer; ELF1 (E74-like factor 1 (ets domain transcription factor)) known to be expressed in lymphoid and myeloid cells; RCBTB1 (regulator of chromosome condensation (RCC1) and BTB (POZ) domain containing protein 1), also known as the chronic lymphocytic leukaemia deletion region gene 7 (Mabuchi et al 2001; Solomou et al 2003); LECT1 (leukocyte cell derived chemotaxin 1) which is known to suppress tumour angiogenesis (Hayami et al 1999); and MYCBP2 (MYC binding protein 2) which regulates transcription activation by MYC. Three SROs were identified on chromosome 13q, but the possibility of the loss of the whole of the q-arm should be considered. Further investigation of this region using FISH or FICTION is required to answer this question. Chui *et al.* (2003) analysed 20 cHL cases by conventional CGH and observed that the loss of 13q was associated with poorer outcome (Chui et al 2003).

Since all the EBV-negative cHL-derived cell lines contained recurrent imbalances on 2p, 6p, 9p and 13q, and these cell lines are known to originate from cHL patients with poor prognosis, it may be that accumulation of all of these recurrent imbalances is associated with a poor prognosis.

Following the success of our in-house arrays in this investigation, we moved on to use array-CGH to examine chromosomal imbalances within laser microdissected HRS cells from a cHL biopsy. This process will be discussed in Chapter 6.

CHAPTER 6

ANALYSIS OF PRIMARY HRS CELLS BY ARRAY-CGH

Section 6.2.1 of this chapter was presented in a poster at the 5th European Cytogenetics Conference in Madrid in 2005:

K.S. Wilson, E. Ballabio, R. Regan, A. Hedman, R. Jarrett, S. Knight and S. Tosi
DOP-PCR products amplified from genomic DNA can be used reliably in whole genome array CGH studies for the detection of deletions and duplications in leukaemia.

6.1 INTRODUCTION

In the previous chapter I described the use of array-CGH in the successful identification of chromosomal gains and losses in genomic DNA extracted from HL-derived cell lines. The next step was to use these arrays to investigate genomic imbalances in primary HRS cells, isolated from cHL biopsies, to determine if there were changes common to these tumour cells.

HRS cells were isolated using LMD, a method by which a laser cuts single or groups of whole cells from a tissue section, leaving the DNA undamaged. This method has been successfully used in our laboratory to isolate HRS cell for conventional CGH (Chui et al 2003), and for the investigation of NFKBIA mutations (Lake *et al.*, manuscript submitted).

In Chapter 1 (see Section 1.6.4), WGA was presented as an effective method of amplifying DNA from very small quantities of starting material, and the different WGA methods were discussed. In a previous study in our laboratory, recurrent chromosomal gains and losses were identified following investigation of 20 cHL cases using DOP-PCR as the method of WGA following laser microdissection of HRS cells (Chui et al 2003). Briefly, cytopins were prepared using aliquots of 1-5 x 10⁵ viable cells from cHL biopsies and IHC was performed using a CD30 monoclonal antibody (Chui et al 2003). HRS cells were identified by positive staining for the CD30 antigen in addition to morphological criteria. Following a series of optimisation experiments, it was found that microdissecting 10 single HRS cells into the lids of 5 PCR tubes (i.e., 10 cells per lid), instead of 50 cells into one single lid,

resulted in a higher yield and better size range of DOP-products. Lysis buffer, containing a non-ionic detergent and proteinase K, was pipetted into each lid prior to microdissection, thereby allowing DNA lysis to be performed immediately after microdissection. The DOP-PCR reagents were added directly to the lysate. Following amplification, the five DOP-products from each cHL case were pooled, ethanol-precipitated and approximately 1.5 µg of each sample was labelled. A reference sample was prepared with exactly the same methodology. Conventional CGH was performed with approximately 0.8-1 µg of labelled test and reference DOP-products, and normal male metaphase target slides (Vysis).

Following on from the success of this study, it was proposed that the same methodology should be used to prepare DNA samples from HRS cells for array-CGH. This would enable the investigation of chromosome abnormalities and imbalances in cHL at a higher resolution than had been possible with conventional CGH. As resolution increases, however, the representativeness of the test DNA samples becomes more critical and it is important, therefore, to have a good quality starting sample and to use a WGA technique which maintains a good representation of the starting DNA.

It was recognised that validation and/or optimisation of the methods would be required before proceeding to the analysis of cHL biopsy samples. This chapter describes the optimisation experiments which were performed, culminating in the successful analysis of a primary cHL case using array-CGH.

Aims

- To establish methods for analysing HRS cells, obtained by LMD, by array-CGH
- To optimise DOP-PCR for amplification of good quality, highly representative genomic DNA from small numbers of isolated HRS cells
- To identify stable chromosomal gains and losses within HRS cells and to speculate on their possible involvement in the pathology of cHL.

6.2 OPTIMISATION EXPERIMENTS

A series of optimisations and modifications were made to the original protocol and are described below. All materials, methods and analysis procedures have been described in detail within chapters 2 and 5. The cell lines discussed in this chapter were cultured by Sabrina Tosi, June Freeland and I. Cytospins were prepared and laser microdissected, performed by Lesley Shield and myself.

6.2.1 Validation of DOP-PCR products for use in array-CGH

In order to investigate if the product of our DOP-PCR protocol is a good genomic representation which can be used successfully for array-CGH, we used DOP-PCR to amplify a cell line with known chromosomal imbalances and compared the subsequent array-CGH data with that produced from non-amplified DNA from the same cell line. Previous publications have advocated that amplification bias is reduced and efficient hybridisation of a DOP-amplified sample DNA is achieved if the reference DNA is also DOP-amplified (Daigo et al 2001; Tsubosa et al 2005). Therefore, in these optimisation experiments DOP-amplified normal human genomic DNA was used as the reference sample in the hybridisations.

6.2.1.1 The GF-D8 cell line

GF-D8 is a human myeloid leukaemia cell line that was established from the peripheral blood of a patient suffering from acute myeloid leukaemia FAB subtype M1 (Rambaldi et al 1993; Tosi et al 1999). This cell line has been fully characterised by a number of molecular cytogenetic techniques (Tosi et al 1999), including M-FISH and CGH to metaphase chromosomes. A number of gains (in chromosome 7, 8q, 11q and 13), losses (in chromosome 5q, 11p, 12p, 15q, 17p and Yq), unbalanced translocations and structural abnormalities were identified (see Table 6.4). The

multiple, complex chromosome imbalances present within this leukaemia cell line make it an ideal model to use for testing the validity of our DOP-PCR protocol.

Table 6.1. Chromosomal rearrangements present in the GF-D8 cell line, identified by M-FISH and conventional CGH (modified from Tosi *et al.* (1999)).

47,X,der(Y)t(Y;12)del(Y),der(5;15)t(5;7)t(7;15), inv(7)x2, der(7)t(7;15)del(7)del(15), dup(8), +der(8)trp(8)ins(8;11)dup(11), der(11)dup(11)t(8;11)trp(8), der(11)t(11;17), der(12)t(7;12)del(12), +13, -15, -17

del, deletion; der, derivative chromosome; dup, duplication; ins, insertion; inv, inversion; t, translocation; trp, triplication

6.2.1.2 Array-CGH performed using the GF-D8 cell line

Five hybridisations were performed using DOP-amplified and non-amplified GF-D8 DNA (see Figure 6.1). Normal genomic male DNA was simultaneously prepared alongside the cell line DNA and used as reference DNA in the hybridisations. The non-amplified DNA samples were prepared, labelled and hybridised by Miss Erica Ballabio. With the exception of a very small number of outlying clones, the results obtained using the non-amplified genomic DNA and the DOP-amplified products were concordant (see Figure 6.2). The DOP-amplified array-CGH results confirmed the gains of 7q, 8, 11q and the entire chromosome 13, which were detected in the original CGH, performed using metaphase chromosomes by Dr Sabrina Tosi (Tosi *et al.* 1999) (see Table 6.2). The losses of 5q, 11p, 12p, 15, 17p and 20q could also be identified. However, some smaller chromosomal regions of imbalance identified in the non-amplified GF-D8 array-CGH results were not detected in the DOP-amplified DNA (see Tables 6.2 and 6.3). It was concluded, therefore, that although array-CGH

using DOP-PCR products can be successfully used to identify the chromosomal gains and losses, it is possible that very small changes, for example gains or losses in single clones, may be missed.

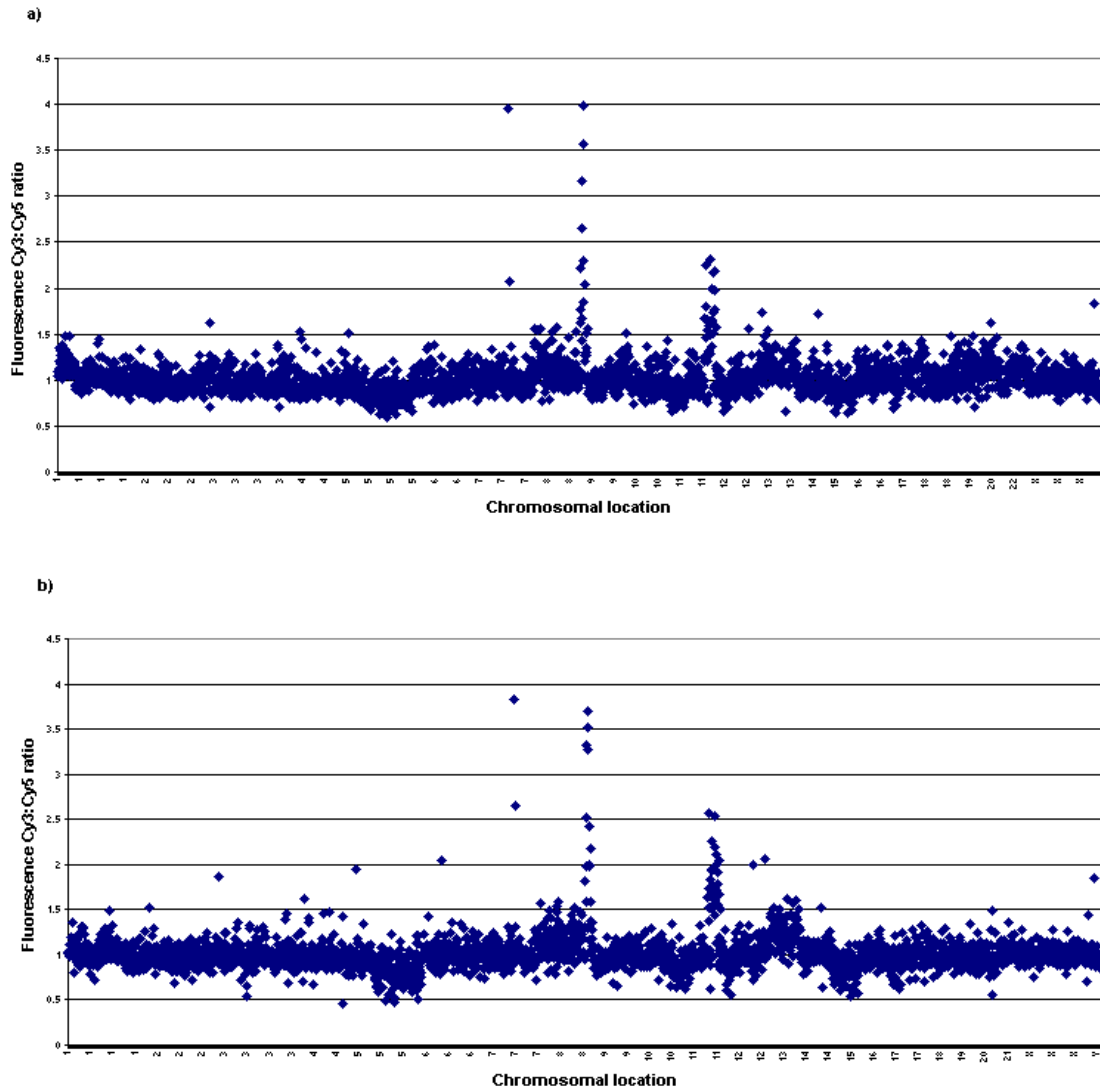


Figure 6.1. Array-CGH analysis results obtained using a) non-amplified and b) DOP-amplified genomic DNA of the GF-D8 cell line.

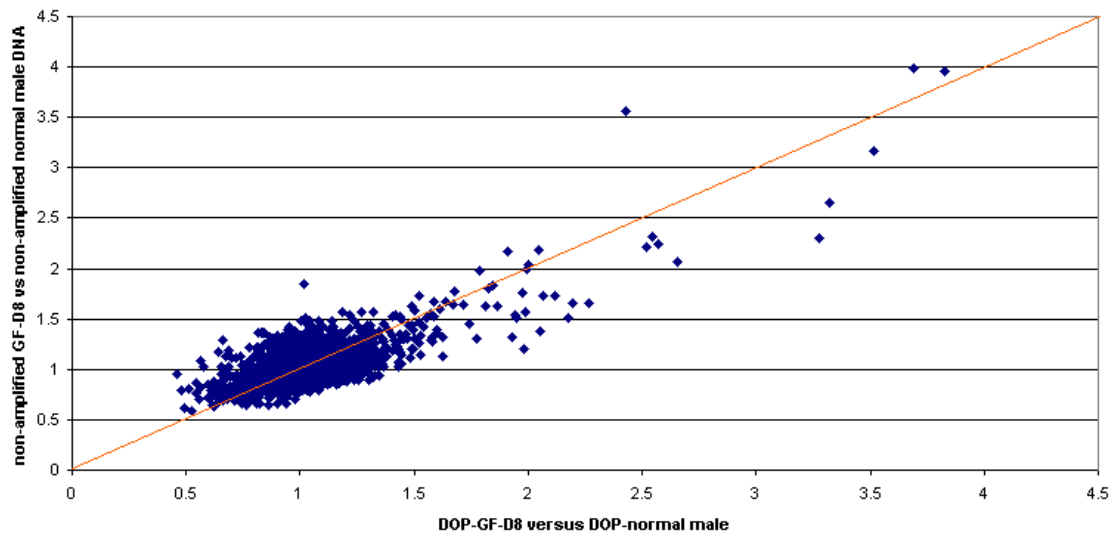


Figure 6.2. Scatterplot of the array-CGH data from both the non-amplified and amplified GF-D8 DNA demonstrating a good correlation between these sets of data, with the exception of a few clones.

Table 6.2. Comparison of the gains identified by CGH to chromosomes (Tosi et al 1999), array CGH of non-amplified DNA and array CGH of DOP amplified DNA.

GAINS IN GF-D8 CELL LINE		
CGH to Chromosome	Array CGH with non-amplified DNA	Array CGH with DOP-amplified DNA
	1p36.31-p32.3	
7pter->q22.1	7pter	
	7q21.3-q22.3	
7q33-qter	7q33-qter	7q34-qter
8q22.3-qter	Whole chr 8	Whole chr 8
	9q33.3-qter	
11q21-qter	11q22.2-qter	11q22.2-qter
	12q13.12-q14.1	
	12q24.11-qter	
Whole chr 13	Whole chr 13	Whole chr 13

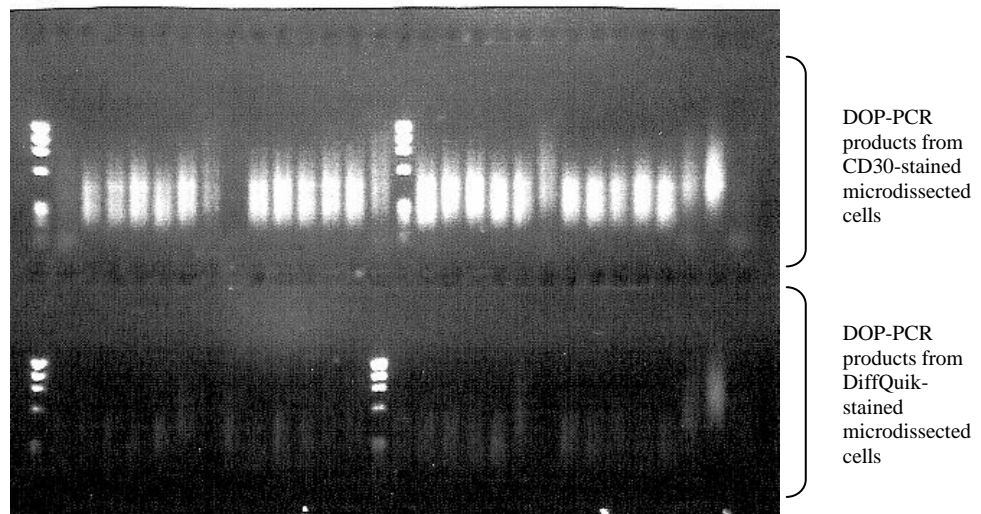
Table 6.3. Comparison of the losses identified by CGH to chromosomes (Tosi et al 1999), array CGH of non-amplified DNA and array CGH of DOP amplified DNA.

LOSSES IN GF-D8 CELL LINE		
CGH to Chromosome	Array CGH with non-amplified DNA	Array CGH with DOP-amplified DNA
5q11-qter	5q11.2-qter	5q11.2-qter
11p11-pter	11p11-pter	11p11.2-pter
12p11.2-p13.3	12p11.23-p13.2	12p11.23-p13.2
15q14-q24	15q14-q21.3 15q25-q26.2	Whole chr 15
17p11-pter	17p12->q12	17p13.3->q12 20q13.13-q13.3
Yq12-qter	Yq11-q11.23	

6.2.2 Comparison of different fixation and staining methods prior to array-CGH

It has been reported that staining using some chromogenic reagents can affect the integrity and downstream use of DNA, particularly in PCR (Gjerdrum and Hamilton-Dutoit 2005). An experiment was performed to investigate the possible downstream effects of fixation and staining in our assays. Two cytopins of IM9 cells were stained with either a CD30 monoclonal antibody, using the ABCComplex method (Dako), or with eosin G and thiazine using the DiffQuik staining system (Dade Behring Inc., IL, U.S.A.). From each slide, 10 single IM9 cells were microdissected into each of 20 0.2 ml tubes and digested with proteinase K. DOP-PCR was then performed using the UN1 DOP-primer. The positive genomic DNA control consisted of 60 pg of normal female genomic DNA (Promega). When the DOP-products were examined under UV light following electrophoresis on a 1% agarose gel and ethidium bromide staining, those derived from DiffQuik-stained cells were considerably fainter in intensity than those from CD30-stained cells (see Figure 6.3a). Each set of DOP-products were combined, purified, quantified using the Nanodrop ND-1000 Spectrophotometer and 500 ng was examined again by electrophoresis (see Figure 6.3b). The DOP-products amplified from DiffQuik-stained laser microdissected cells were smaller in size than those derived from CD30-stained cells. Therefore, the DiffQuik fixation and staining protocol either inhibits amplification of larger products or degrades genomic DNA. Poor CGH hybridisation using DOP-DNA from DiffQuik-stained cells has been reported (Hirose et al 2001), and more recently it was suggested that components in the DiffQuik process may in some way reduce DOP-product size (Huang et al 2005a). There was no evidence that CD30 staining using the described protocol inhibited the downstream reactions.

(a)



(b)

ϕ x174/ HaeIII	normal female DNA	CD30- stained IM9	DiffQuik- stained IM9
------------------------	-------------------------	-------------------------	-----------------------------

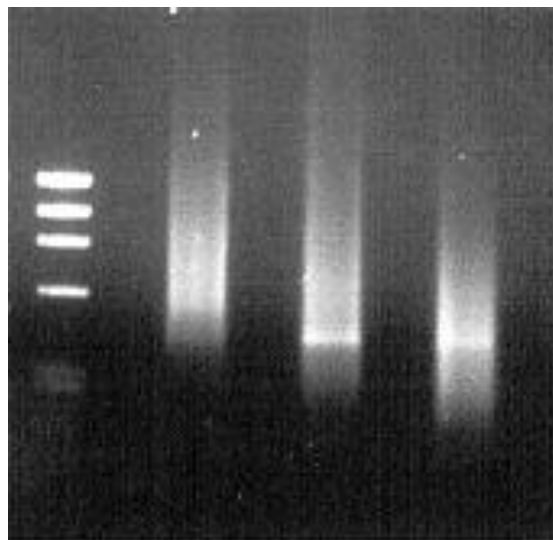


Figure 6.3. (a) DOP-PCR products from amplification of laser microdissected IM9 cells stained with either CD30 monoclonal antibody or the DiffQuik staining system. (b) Combined and ethanol precipitated DOP-PCR products (500 ng) from 200 CD30-stained or 200 DiffQuik-stained laser microdissected cells.

6.2.3 Comparison of array-CGH using different cell numbers

6.2.3.1 Array-CGH of cHL samples using 200 laser microdissected HRS cells

Authors of current publications describing the use of laser microdissected cells as templates for DOP-PCR have used large numbers of cells (100-5000) as starting material for their amplification reactions (Daigo et al 2001; Hughes et al 2004; Peng et al 2003; Peng et al 2004). Due to the difficulty of obtaining large numbers of HRS cells from a cHL case sample, and following discussions with Dr Stefan Joos, we initially microdissected 200 HRS cells from 4 cHL cases (#5440, 6625, 6666 and 6992) and performed DOP-PCR. The cases were selected on the basis of having large numbers of strongly CD30-staining HRS cells with good morphology on the cytopsin preparations. A reference DNA sample was prepared by the same methodology: microdissection of 200 IM9 cells and DOP-PCR. The combined DOP-products from each sample were then labelled and hybridised to our CGH-array. A representative hybridisation chart (case #6992, male diagnosed with NSHL) is shown in Figure 6.4. For each of the 4 cHL cases, background levels were high and large numbers of clones had an intensity ratio outside the threshold level.

It was concluded that DOP-amplification products from 200 cells did not produce a good representation of the genome. The question was whether the template DNA quality was too poor for amplification of highly representative DNA products, or whether increasing the number of laser microdissected cells would improve the quality of the hybridisation.

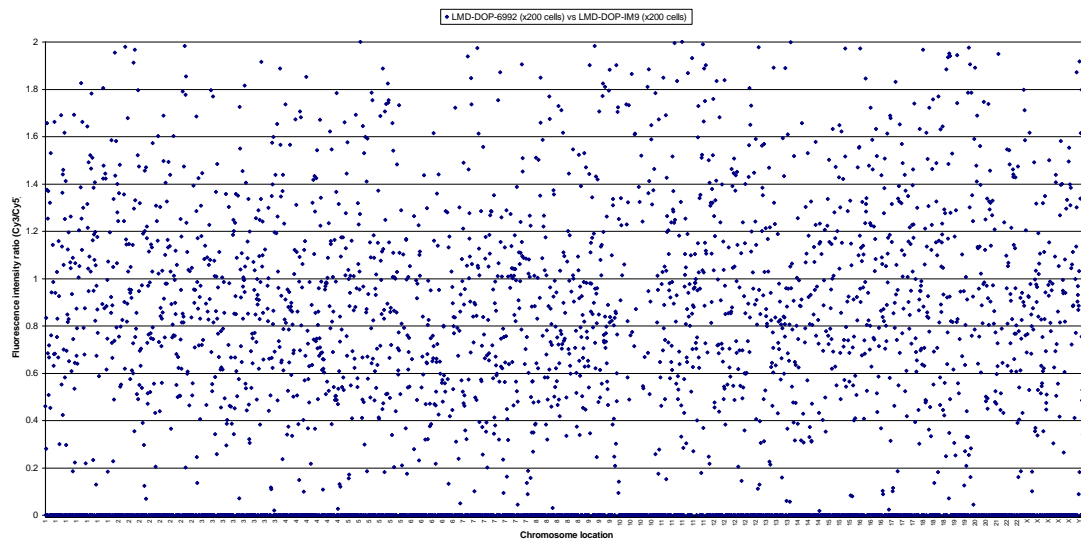


Figure 6.4. Hybridisation chart from the array-CGH of 200 cells-DOP-amplified case 6992 DNA versus 200 cells-DOP-amplified IM9 DNA.

In order to investigate whether increasing the number of microdissected cells, used for DOP-amplification, would improve the analysis of array-CGH, a number of optimisation experiments were performed initially using IM9 cells and the cHL-derived cell lines HDLM2 and L428.

Cytospins of IM9 cells were stained with the CD30 monoclonal antibody, as described earlier (see Section 2.2.8), and 10 cells were microdissected into each of 120 tubes. Following proteinase K digestion and DOP-PCR, each DOP-product was electrophoresed to check quality. Equal amounts of DNA (5 μ l) from 20, 40, 60, 80 and 100 tubes were then combined to represent DOP-products from 200, 400, 600, 800 and 1000 IM9 cells, respectively. These products were ethanol precipitated and were used as the sample DNA for array-CGH.

As was mentioned in Section 6.2.3, reference DNA should also be amplified by DOP-PCR if it is to be hybridised with DOP-amplified sample DNA, in order to decrease any sequence amplification bias. Therefore 120 DOP-PCR reaction tubes were set up, each containing the equivalent of 10 cells (60 pg) of IM9 DNA. The DNA had been extracted, using phenol/chloroform, from the same batch of IM9 cells from which the cytopins had been prepared. Successful DOP amplification was confirmed by electrophoresis and equal quantities from each of 20, 40, 60, 80 and 100 tubes were combined to represent starting templates of 200, 400, 600, 800 and 1000 cells, respectively. The combined DNA products were ethanol precipitated and used as reference DNA in array-CGH.

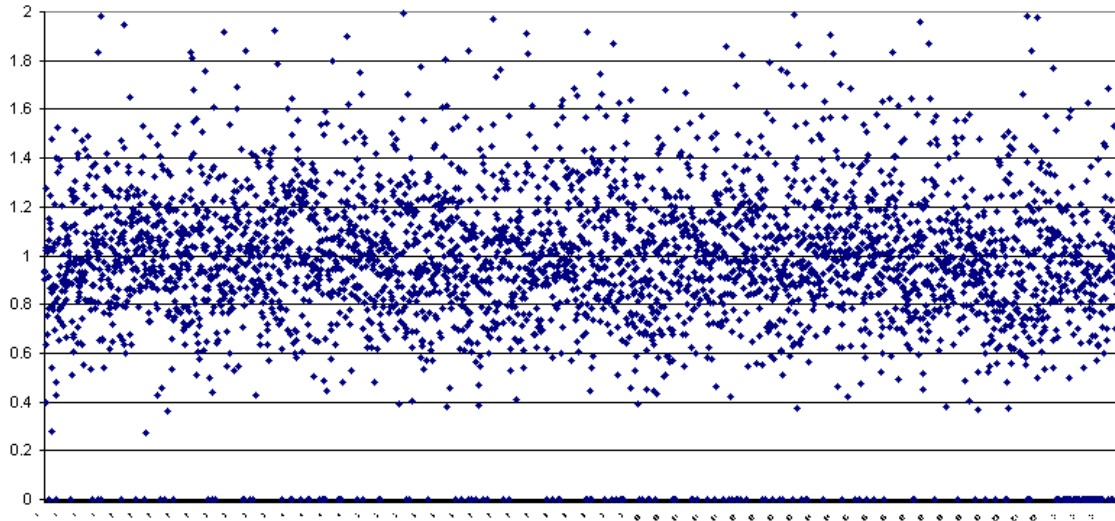
Equal amounts (2 μ g) of each of the sample and reference amplified DNA, corresponding to 200, 400, 600, 800 and 1000 template cells, were labelled and hybridised to the 1Mb resolution arrays.

Analysis of each of the five hybridisations showed that each successive increase in the number of microdissected cells, used as template for DOP-PCR, improved the quality of hybridisation (see Figure 6.5), as judged by the mean intensity ratios on the hybridisation charts (i.e., the mean of the normalised ratios is <0.7 or >1.3) (see Table 6.4). For example, 9.3% and 12.4% of clones displayed mean intensity ratios of below 0.7, or above 1.3 in the hybridisation of DOP DNA from 200 IM9 cells, whereas in the hybridisation of 1000 IM9 cell-derived DNA, only 0.7% and 3.2% of clones lay outside these threshold limits respectively. Also the number of spots excluded from analysis, due to abnormal hybridisation, decreased as more microdissected cells were used to generate the DOP-amplified sample DNA. Only

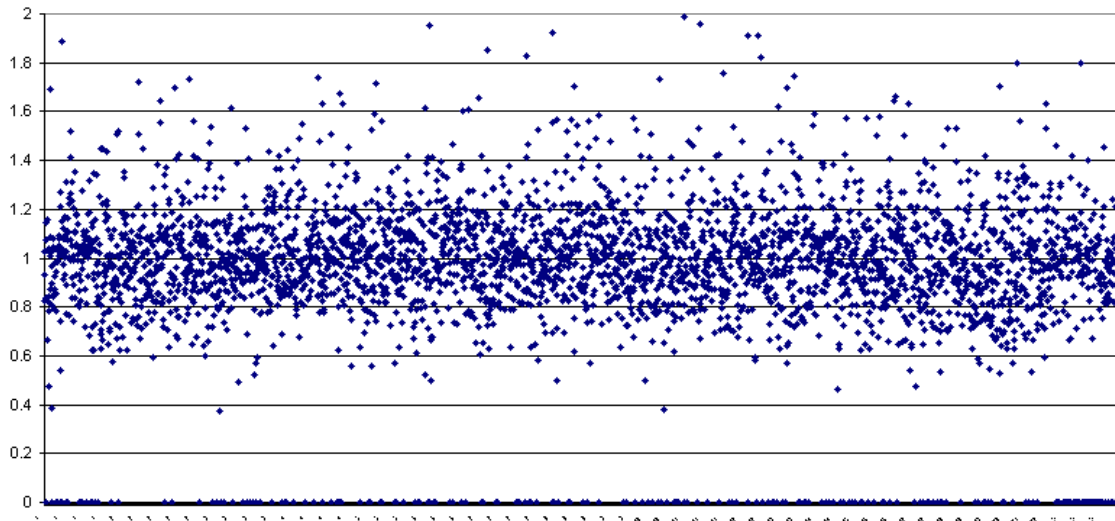
2.6% of clones were excluded from analysis of the 1000 cell-DOP-amplified product, compared with 4.7% of clones on the 200 cell-DOP-amplified product. The analysis of the 600 cell-DOP-amplified product was unsatisfactory, due to smearing of the array, so this was excluded from analysis. The thresholds, of the mean of the normalised ratios, differ to those used in the cell line array-CGH analyses in the previous chapter because a higher level of scattering of spots was seen in the DOP-amplified laser microdissected DNA hybridisations. Widening the thresholds allowed more spots to be included in the analysis.

It was concluded from this set of experiments that the greater the number of microdissected cells from which DOP-PCR products could be pooled, the greater the representation of the template genome and the more accurate the array-CGH results.

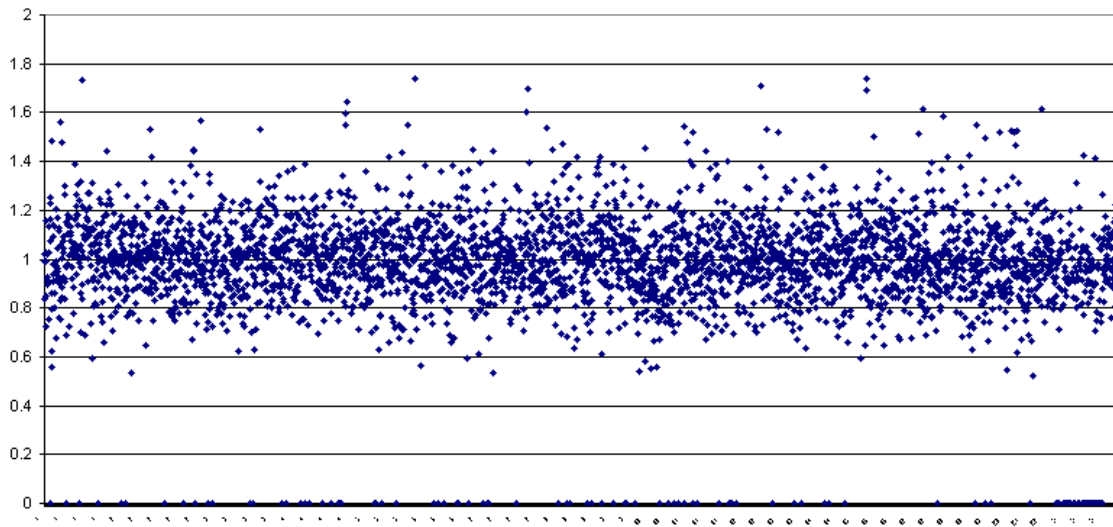
(a)



(b)



(c)



(d)

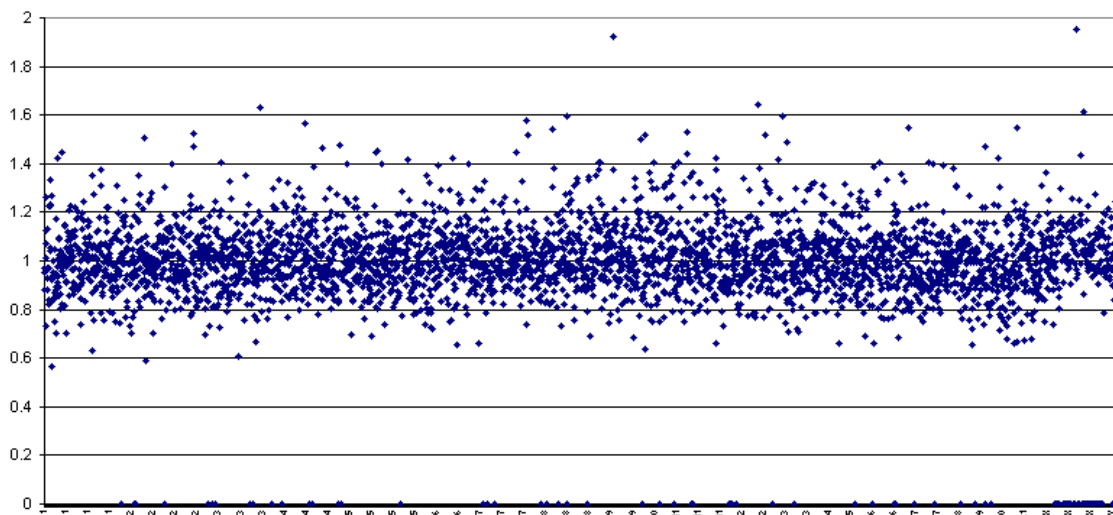


Figure 6.5. Four array-CGH analyses of laser microdissected, DOP-amplified IM9 DNA versus laser microdissected, DOP-amplified-IM9 DNA: a) 200 cells-DOP-amplified; b) 400 cells-DOP-amplified; c) 800 cells-DOP-amplified; d) 1000 cells-DOP-amplified.

Table 6.4. The percentage of probes with ratios lying outwith the threshold range <0.7 and >1.3, and the percentage of clones excluded from analysis due to SD >0.2.

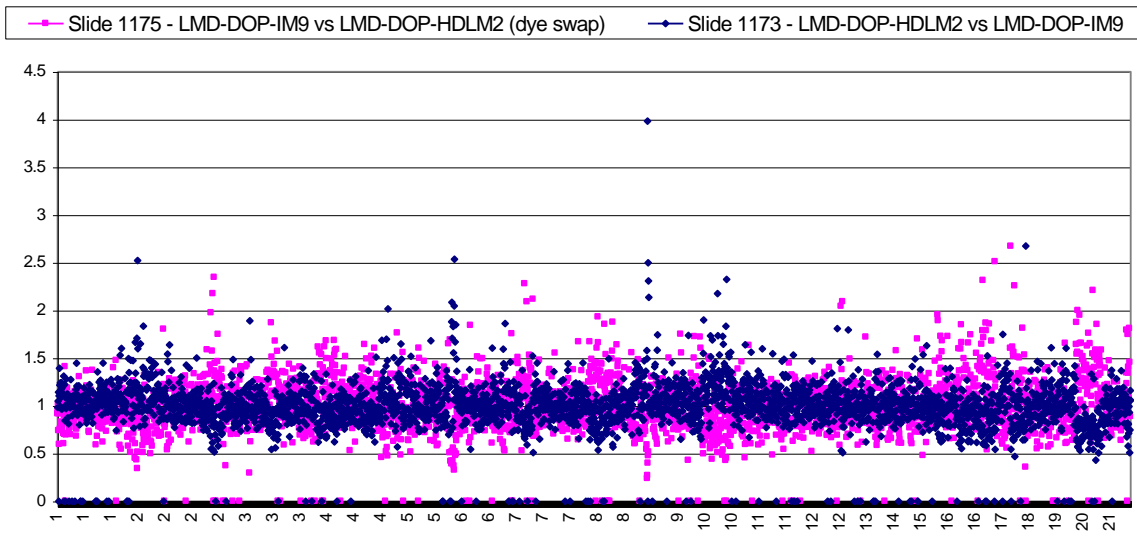
	% of probes with mean intensity ratio >1.3	% of probes with mean intensity ratio <0.7	% of probes excluded from analysis
200 cells-DOP-amplified	12.4	9.3	4.7
400 cells-DOP-amplified	7.5	3.9	6.6
800 cells-DOP-amplified	3.6	1.8	3.3
1000 cells-DOP-amplified	3.2	0.7	2.6

6.2.2.2 Validation of 1000 cell-DOP-amplified HRS cell DNA for array-CGH

In order to validate the use of DOP-amplified PCR products from 1000 microdissected cells for array-CGH, the previous experiment was repeated using 1000 microdissected HRS cells, which had been isolated from HDLM2 cell cultures. The reference sample was DOP-amplified IM9 DNA, as described in the previous section.

A second dye-switch hybridisation was performed using an array from the same batch. The combined charts (see Figure 6.6) were compared with the array-CGH analysis of the non-amplified cell line DNA (see Figure 5.2 in Chapter 5). Although spots on the hybridisations chart from the experiment using laser microdissected cells and DOP-amplified DNA were not as close to the intensity ratio of 1 as the original experiment, the main changes were detected.

(a)



(b)

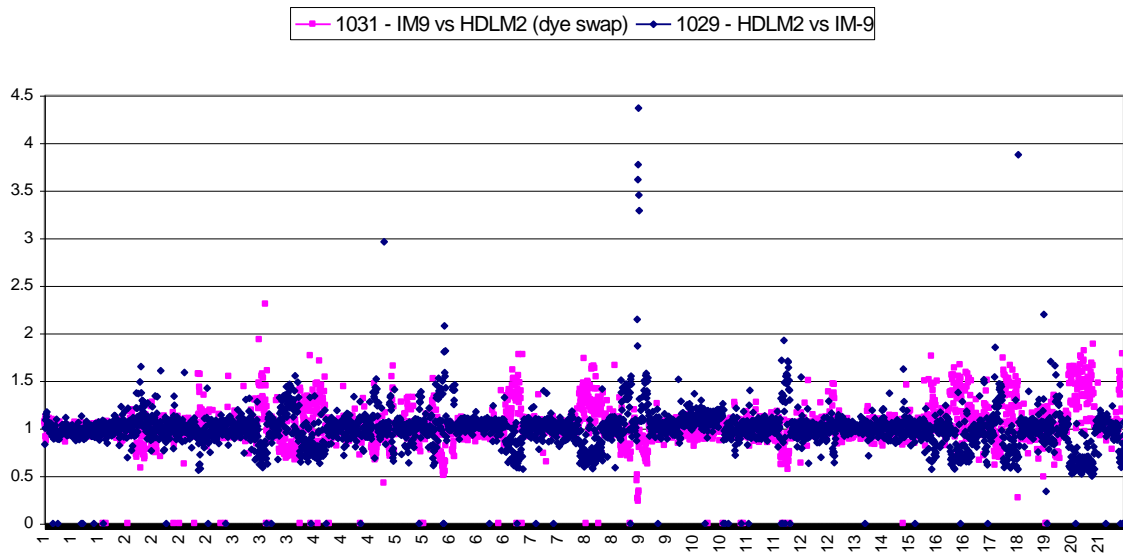


Figure 6.6. Array-CGH analysis of (a) 1000 cells-DOP-amplified HDLM2 DNA versus 1000 cells-DOP-amplified IM9 DNA and (b) non-amplified HDLM2 DNA versus non-amplified IM9 DNA.

6.2.2.3 Validation of 6000 cells-DOP-amplified HRS cell DNA for array-CGH

Before examining a cHL case, a final optimisation experiment designed to investigate the quality of hybridisation with DOP-amplified DNA derived from 6000 laser microdissected cells was performed. Cytospins prepared from fresh HDLM2 cell culture were used, as in the previous experiment. Reference sample DOP-amplified DNA was derived from 6000 laser microdissected IM9 cells. A dye-switch hybridisation was also performed, using an array from the same batch.

As expected, the resulting hybridisations had a reduced background noise from that seen in the hybridisations using 1000 cells-DOP-amplified DNA, with markedly less scattering (see Figure 6.7).

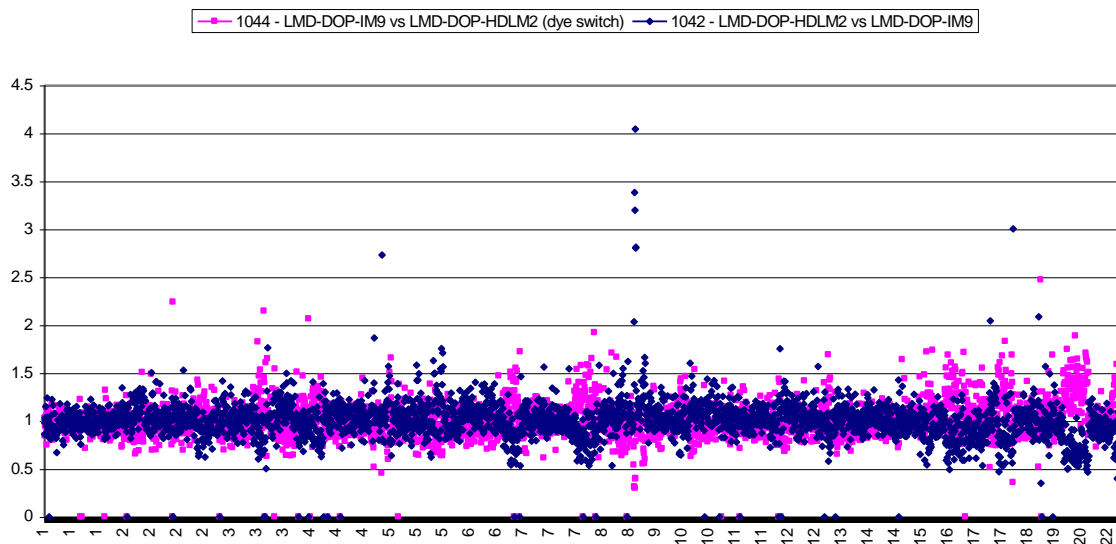


Figure 6.7. Hybridisation chart of 6000 cells-DOP-amplified HDLM2 DNA versus 6000 cells-DOP-amplified IM9 DNA.

6.3 ARRAY-CGH OF A cHL CASE SAMPLE

From the preceding experiments, it was clear that increased cell numbers markedly improved the quality of the array-CGH analysis and a primary cHL tumour, from which large numbers of HRS cells were available, was subsequently analysed.

6.3.1 Preparation of DNA sample from case #6992

Cytospins were made from cell suspensions that had been frozen in liquid nitrogen when the fresh biopsy sample was processed (protocol described in Sections 2.2.2 and 2.2.17 of Chapter 2). DNA was prepared from 6000 laser microdissected HRS cells as described in Section 6.2.4. The reference DNA was the 6000 cell-DOP-amplified IM9 DNA that was used in Section 6.2.4. Array-CGHs and analysis were performed as described in Chapter 5.

6.3.2 Results

The dye-swap hybridisation charts were combined (see Figure 6.8). ‘Sliding averages’ were calculated for every 5 contiguous clones in the two hybridisations, to produce a ‘moving window’ (see Figure 6.9). For example, in each chromosome, the intensity ratios for clones 1-5 were averaged, then the intensity ratios for clones 2-6, then clones 3-6, etc. The resultant average intensity fluorescent ratios were plotted on a hybridisation chart (see Figure 6.9). This had the effect of smoothing out the scattering of outlying spots, so that chromosomal imbalances could be identified by eye prior to detailed analysis.

Regions identified with a gain or loss of chromosomal material are detailed in Table 6.5. Chromosomal imbalances which had been identified in three or more cHL-

derived cell lines were detected within this case: gains in 2p, 3q, 4p, 5q, 7q, 8q, 9p and 12p, and losses in 6q, 8p, 9q, 10q, 13q, 15q, 16q, 17q, 18p, 18q, 20q and 22q. A large number of novel chromosome imbalances were also identified. Functional genes located within all chromosomal regions of imbalance within this case were identified using the Ensembl database (www.ensembl.org) and selected genes are shown in Tables 6.6 (gains) and 6.7 (losses).

To our knowledge, this is the first time that chromosomal imbalances within the HRS cells of a cHL case have been analysed using array-CGH.

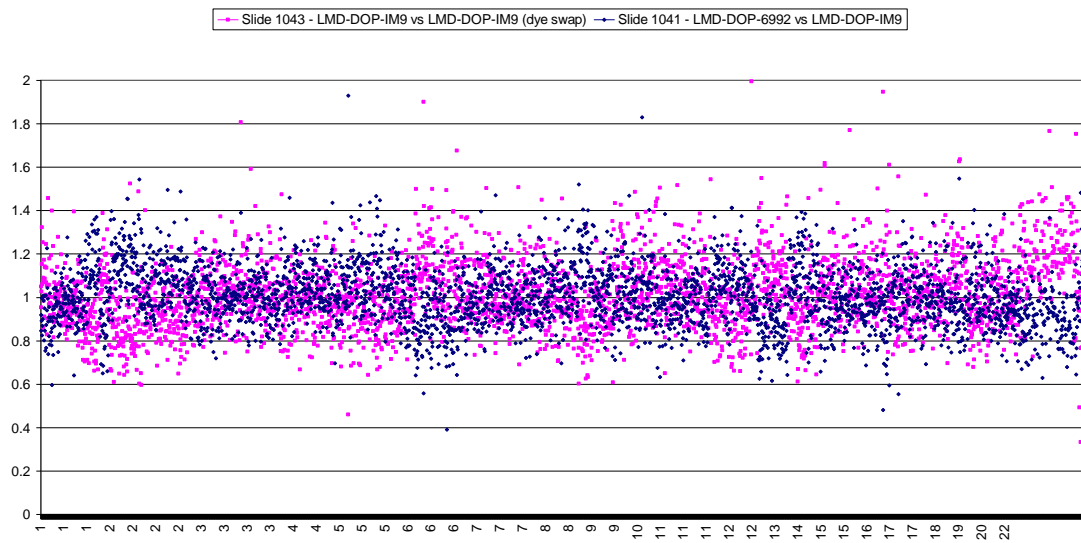


Figure 6.8. Array-CGH analysis of 6000 cells-DOP-amplified DNA from HRS cells of the cHL case 6992 versus 6000 cells-DOP-amplified DNA from IM9 cells.

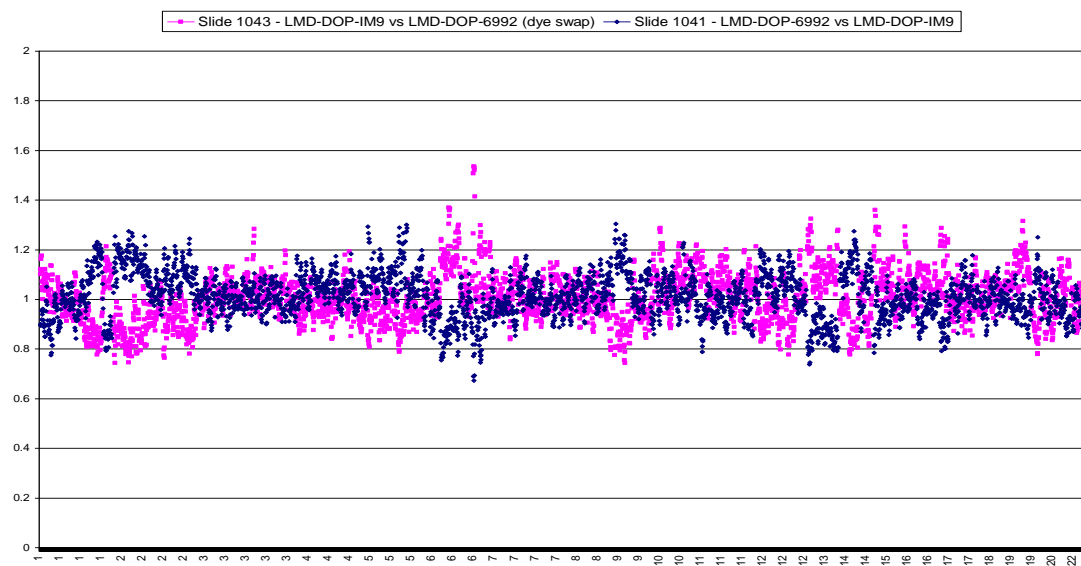


Figure 6.9. Array-CGH chart showing sliding averages of 6000 cells-DOP-amplified 6992 DNA versus 6000 cells-DOP-amplified IM9 DNA.

Table 6.5. Gains and losses of chromosomal regions identified within cHL case 6992

DNA.

Chromosomal regions of imbalance in case #6992	
Gains	1p36.12, 1p31.1, 1p22.3, 1q21.3, 1q24.1, 1q24.2, 1q25.2, 1q25.3, 1q31.2, 1q31.3, 1q32.1, 1q32.2, 1q32.3, 2p25.2, 2p25.1, 2p24.3, 2p24.1, 2p23.3, 2p23.1, 2p22.3, 2p22.2, 2p22.1-p21, 2p21-p16.3, 2p16.2-16.1, 2p15, 2p14, 2p13.3, 2p13.2, 2p12, cent-2q11.2, 2q12.1, 2q21.3, 2q22.1, 2q22.3, 2q24.3, 2q31.1, 2q32.1, 2q32.2, 2q33.1, 2q33.2, 2q33.3, 2q36.1, 3q13.33, 3q22.3, 3q26.31, 4p15.31, 4p15.1, 4p14, 4p13, 4q13.1, 4q13.2, 4q25, 4q26, 4q27, 4q28.3, 4q31.21, 4q35.1, 5p15.32, 5p15.31, 5p13.3, 5p13.2, 5p13.1, 5q12.1, 5q12.3, 5q14.3, 5q15, 5q21.3, 5q22.2, 5q22.3, 5q23.1, 5q23.3, 5q31.3, 5q34, 7p21.3, 7p13, 7p11.2, 7q21.2, 7q21.3, 7q31.31, 7q31.33, 7q32.3-q33, 7q35, 8q11.21, 8q11.22-11.23, 8q21.12, 8q21.3, 8q23.1, 8q24.12, 8q24.22-24.23, 9p24.2, 9p24.1, 9p23, 9p22.3, 9p22.2, 9p21.3, 9p21.2, 9p21.1, 9q21.13, 9q21.2, 9q21.31, 9q21.32, 9q33.1, 10p11.23, 10q11.22, 10q21.1, 11q14.3, 12p13.32-13.31, 12p13.2-13.1, 12p12.3, 12p12.1, 12p11.22, 12q12, 12q13.11, 12q13.13, 12q13.3, 12q14.1, 12q15, 12q21.2, 12q21.31, 12q21.32, 12q21.33, 12q22, 12q24.23, 14q12, 14q21.1, 14q22.1, 14q22.2, 14q22.3, 14q23.1-23.2, 14q23.3, 14q24.1, 14q24.2, 14q31.1, 14q31.3, 14q32.12, 14q32.2-32.31, 16q12.2, 17p13.2, 17p12, 17q12-21.1, 17q21.32, 17q21.33, 17q23.2, 17q24.2, 18p11.21, 18q12.3, 18q22.3, 19q13.42-13.43, 20p12.3, 20p12.1, 20q11.22, 20q11.23, 20q13.2-13.31, 20q13.32, 22q13.2
Losses	1p36.32, 1p36.22, 1p36.13, 1p36.11, 1p35.2, 1p34.3, 1p34.2, 1p32.3, 1p13.3, 1q12, 1q42.11, 1q42.12, 1q42.2, 1q42.3, 1q43, 1q44, 2q21.2, 3p25.3, 3p22.1, 3p21.31, 3p21.1, 3q12.1, 3q23, 3q25.31, 3q26.2, 3q27.2, 3q28, 4p15.31, 4q28.1, 4q35.1, 4q35.2, 5p13.2, 5q32, 6p21.32, 6p24.1, 6p21.32, 6p21.31-21.2, 6p21.1, 6p12.3, 6p12.1, cent, 6q12, 6q14.1, 6q15, 6q16.1, 6q21, 6q22.33-23.1, 6q23.2, 6q23.3, 6q24.1, 6q25.2, 6q25.3, 6q27, 7p21.2-21.1, 7p12.3, 7q11.22, 7q11.23, 7q32.1, 7q36.1, 8p23.1, 8p21.2, 8p12, 8q21.13, 8q21.3, 8q22.1, 9p21.3, 9q31.3, 9q34.11, 9q34.3, 10p13, 10q22.3, 10q24.2, 10q25.3, 10q26.12, 10q26.3, 11p15.1, 11p15.5, 11p15.4, 11p15.2, 11p14.3, 11q13.2, 11q13.4, 11q13.5, 11q23.1, 11q24.2, 11q23.3, 12p13.32, 12q13.13, 12q24.23, 13q12.11, 13q12.12, 13q12.13, 13q12.2, 13q12.3, 13q13.1-13.2, 13q13.3, 13q14.12, 13q14.3, 13q21.31, 13q31.2, 13q31.3, 13q32.2, 13q32.3, 13q34, 14q24.3, 15q11.2, 15q13.3, 15q14, 15q15.1, 15q15.3, 15q21.1, 15q21.3, 15q22.31, 15q24.3, 15q26.1, 15q26.3, 16p13.13, 16q12.1, 16q21, 16q22.1, 16q24.1, 16q23.2, 17p13.2, 17p13.1, 17p12, 17p11.2, 17q21.2, 17q25.3, 18p11.31, 18q11.2, 18q22.3, 18q23, 19p13.2, 19p13.11, 19q12, 19q13.12, 19q13.32, 20q13.13, 21q11.2, 21q21.1, 21q22.2, 21q22.3, 22q11.23, 22q13.2

Table 6.6. Selected genes with known function in newly identified regions of gain (details from www.ensembl.org and www.genecards.org).

Chromosome Location	Gene	Position (Mb)	Function
1q31.2	RGS18 (Regulator of G-protein signalling 18)	190.39-190.42	Negative regulation of signal transduction
1q32.1	PIK3C2B (Phosphatidylinositol-4-phosphate 3-kinase C2 domain-containing beta polypeptide)	202.65-202.72	Involved in apoptosis, Toll-like receptor signalling pathway, JAK-STAT signalling pathway and T cell receptor signalling pathway
1q32.1	IKBKE (I kappa-B kinase epsilon)	204.71-204.73	Phosphorylates inhibitors of NFκB; may play a special role in the immune response
1q32.2	IL20 (interleukin 20)	205.105-205.109	Acts through STAT3, Cytokine-cytokine receptor interaction, JAK-STAT signalling pathway;
1q32.2	IL24 (interleukin 24)	205.13-205.14	Selectively induces apoptosis in human breast cancer cells; involved in cytokine-cytokine receptor interaction and the JAK-STAT signalling pathway
2p23.3	NCOA1 (Nuclear receptor coactivator 1)	24.66-24.84	Involved in co-activation mediated by STAT3, STAT5A, STAT5B and STAT6 transcription factors; displays histone acetyltransferase activity toward H3 and H4
2p22.2	BIRC6 (Baculoviral IAP repeat-containing protein 6)	32.43-32.69	May protect cells from undergoing apoptosis
2p14	MEIS1 (myeloid ecotropic viral integration site 1 homolog (mouse))	66.51-66.65	Acts as a transcriptional regulator of PAX6; required for haematopoiesis, and megakaryocyte lineage development
2q11.2	ZAP70 (70 kDa zeta-associated protein)	97.69-97.72	Associates with the T-cell antigen receptor zeta chain (CD3Z); plays a role in lymphocyte activation
4q35.1	MLF1IP (Myeloid leukaemia factor 1 interacting protein)	185.85-185.90	Component of the CENPA-NAC (nucleosome-associated) complex, a complex that plays a central role in assembly of kinetochore proteins, mitotic progression and chromosome segregation; interacts with the N-terminal domain of Kaposi's sarcoma-associated herpesvirus latent nuclear antigen (LNA); interacts with myeloid leukaemia factor 1

Chromosome Location	Gene	Position (Mb)	Function
5p13.1	FYB (FYN (an oncogene) binding protein)	39.14-39.25	Acts as an adapter protein of the FYN and SH2-domain-containing leukocyte protein-76 (SLP76) signalling cascades in T cells; modulates the expression of IL2
5q22.2	APC (adenomatosis polyposis coli)	112.10-112.20	Tumour suppressor; promotes rapid degradation of CTNNB1 and participates in Wnt signalling
5q22.2	MCC (mutated in colorectal cancers)	112.38-112.85	Candidate for the putative colorectal tumour suppressor gene located at 5q21; involved signal transduction and negative regulation of cell cycle progression
8q24.12	TAF2 (TAF2 RNA polymerase II, TATA box binding protein (TBP)-associated factor)	120.81-120.91	Stabilizes transcription factor (TFIID) binding to core promoter (Transcription factor TFIID is one of the general factors required for accurate and regulated initiation by RNA polymerase II)
9p21.3	IFNB1 (interferon, beta 1, fibroblast)	21.0671-21.0679	Involved in cytokine-cytokine receptor interaction, Toll-like receptor signalling pathway, Jak-STAT signalling pathway, natural killer cell-mediated cytotoxicity; induction of apoptosis
9p21.2	IFNK (interferon, kappa)	27.514-27.516	May play a role in the regulation of immune cell function; provides cellular protection against viral infection in a species-specific manner; involved in JAK-STAT signalling pathway
12p12.3	PIK3C2G (Phosphatidylinositol 3-kinase, class 2, gamma polypeptide)	18.30-18.69	Involved in apoptosis, Toll-like receptor signalling pathway, JAK-STAT signalling pathway and T cell receptor signalling pathway
20q13.2	NFATC2 (nuclear factor of activated T-cells, cytoplasmic 2)	49.44-49.59	Plays a role in the inducible expression of cytokine genes in T cells, especially in the induction of IL-2, IL-3, IL-4, TNF-alpha or GM-CS; related to the NFκB/REL proteins

Table 6.7. Selected genes of known function in newly identified regions of loss(details from www.ensembl.org and www.genecards.org).

Chromosome Location	Gene	Position (Mb)	Function
6p21.31-21.2	CDKN1A (cyclin-dependent kinase inhibitor 1A (p21, Cip1))	36.75-36.76	May be the important intermediate by which p53 mediates its role as an inhibitor of cellular proliferation in response to DNA damage; regulator of cell cycle, cyclin dependent kinases 2 and 4 (CDK2/CDK4) inhibitor protein; involved in cell cycle exit of megakaryocytes; inhibits cycle progression
6q15	MAP3K7 (transforming growth factor beta-activated kinase 1)	91.28-91.35	A component of a protein kinase signal transduction cascade; mediator of TGF-beta signal transduction; stimulates NFκB activation and the p38 MAPK pathway
9p21.3	MTAP (methylthioadenosine phosphorylase)	21.79-22.00	Often co-deleted with CDKN2A in adult acute T cell type leukaemia; plays a major role in polyamine metabolism and is important for the salvage of both adenine and methionine
10q26.3	BNIP3 (BCL2/adenovirus E1B 19kDa interacting protein 3)	133.63-133.64	An apoptosis-inducing protein that binds to the adenovirus E1B 19 kDa protein or to BCL-2, and which can overcome BCL-2 suppression; can also interact with BHRF1 of EBV
13q12.12	TNFRSF19 (tumour necrosis factor receptor superfamily, member 19)	23.04-23.14	Can mediate activation of JNK and NFκB; may promote caspase-independent cell death.apoptosis and induction of apoptosis

6.4 DISCUSSION

Prior to this project, LMD and DOP-PCR had been used successfully within our laboratory to isolate HRS cells and prepare the extracted DNA for conventional CGH (Chui et al 2003), but the methodology required optimisation for array-CGH. This chapter has discussed the optimisation experiments performed to determine the conditions required to perform array-CGH using laser microdissected HRS cells.

The validity of DOP-PCR was demonstrated by comparison of the hybridisation of amplified and non-amplified DNA extracted from the fully characterised human myeloid leukaemia cell line, GF-D8. Good reproducibility of known chromosomal changes was demonstrated using amplified DNA, but some subtle changes were missed. These findings are consistent with other studies showing that DOP-PCR occasionally produces false positives and false negatives in hybridisation (Hughes et al 2004).

Previous experiments in our laboratory compared the use of PEP-PCR and DOP-PCR for conventional CGH analysis. Although PEP-PCR products were highly representative of the sample template, DOP-PCR was the method of choice since it consistently generated much larger amounts of DNA and the products were sufficiently representative for use in conventional CGH (Dr Daniel Chui, unpublished data). It was decided to continue with DOP-PCR to prepare our laser microdissected samples for array-CGH since DOP-PCR was universally recognised as the preferred method of WGA for CGH and array-CGH. However, the results of the above experiments suggest that laser microdissection of primary HRS cells coupled with DOP-PCR may not result in optimal products for use in array-CGH. Towards the end

of the project commercial MDA kits became available (i.e., GenomiPhi and TempliPhi, Amersham Biosciences), but pilot experiments (data not shown) suggested that the DNA in our laser microdissected samples was not of sufficient quality to capitalise on this methodology. However, GenomePlex, a proprietary technology from Sigma-Genosys has produced promising initial results (Feys et al 2007b).

From a series of optimisation experiments, it was found that increasing the number of laser microdissected cells, lowers the sequence bias and background noise of the downstream array-CGH. To put this finding into practice, a cHL case (#6992) was selected, on the basis of the large amounts of good viable cells available from biopsy material, and 6000 HRS cells were laser microdissected. DOP-PCR was performed, followed by array-CGH analysis. Chromosomal gains and losses were identified within this cHL case, many of which had been identified previously. As discussed in Chapter 5, conventional CGH analysis of cHL-derived cell lines and biopsy material identified recurrent chromosomal imbalances (Chui et al 2003; Joos et al 2003). Within the 6992 cHL case, gains in 2p, 7q, 9p, 12q, 14q, and 17p, and losses in 4q, 6q, 11q, 13q and 14q were identified.

All genes with known function located within all regions of gain and loss within this case were identified, and particular attention was paid to any genes with known involvement in apoptosis, the cell cycle, the NF κ B or Wnt signalling pathways, the pathogenesis of other tumours, and T-cell/B-cell growth, differentiation or function. Many of the gained chromosomal regions encode proteins which play an active role in signalling pathways implicated in the aetiology of cHL: the Jak/STAT signalling pathway (IL20, IL24, IFNB1, IFNK and PIK3C2G), the NF κ B pathway (IKBKE and

NFATC2), the Wnt signalling pathway (APC) and the cell cycle pathway (MCC). The MAP3K7 and TNFRSF19 genes are located within regions of chromosomal loss identified in this case. These genes are known to be involved in the NFκB pathway.

In Chapter 5, several SROs were identified by comparing regions of gain and loss across the six cHL-derived cell lines. When the fluorescence intensity ratio of clones representing these regions were examined in the hybridisation results from case #6992, some ratios were found to be close to the threshold, or above or below the threshold in one replicate only. Although further hybridisations would be required to verify these results, these results suggest that these are regions of imbalance. In this way, three of the previously identified gained SROs were detected in the results from case #6992: 2p21-p16.1 (44.37-60.79 Mb), 9p24.1 (4.81-6.06 Mb) and 9p21.3-p21.2 (24.93-28.20 Mb). These regions of the genome are known to contain the BCL11A (60.53-60.83 Mb) and Rel (60.96-61.00 Mb), JAK2 (4.97-5.11 Mb) and IFNK (27.514-27.516 Mb) genes, respectively. The SROs for three regions of loss on chromosome 13q were also identified from the hybridisation results for case #6992.

These results lend further support to the idea that there is a recurrent pattern of gains and losses of chromosomal material in cHL. Further work is required to be performed to delineate the precise areas affected and the key genes (or RNAs) involved. Further experiments are therefore warranted. In order to improve the quality of the hybridisations and reduce the number of HRS cells required for analysis, it is necessary to try and improve the quality of the starting sample material. In addition, newer methods of WGA, such as the technology used in the GenomePlex kit, may

improve the representativeness of the amplified product and this, in turn, should improve the quality of the hybridisation.

To conclude, we have demonstrated that sufficient DNA can be extracted from laser microdissected HRS cells, from a cHL biopsy sample, to perform DOP-PCR and array-CGH. We have successfully used this methodology to detect previously reported recurrent regions of chromosomal imbalance within a cHL case, in addition to identifying several novel chromosomal imbalances which warrant further investigation.

CHAPTER 7

FINAL DISCUSSION

This thesis presents different approaches used to investigate the pathogenesis of cHL. In the search for a potential viral agent involved in the aetiology of non-EBV-associated cHL cases, cases were screened for the MV and PyV using molecular biological techniques (Chapters 3 and 4). Array-CGH has been successfully used in Chapter 5 to detect recurrent chromosomal gains and losses within six cHL-derived cell lines and results were compared to gene expression array data from three cHL-derived cell lines to assess whether or not these chromosomal imbalances had any influence on gene expression. In Chapter 6, HRS cells were laser microdissected from a cHL biopsy and analysed by array-CGH, resulting in the identification of recurrent chromosomal gains and losses, in addition to some previously unreported imbalances.

7.1 THE SEARCH FOR POTENTIAL PATHOGENIC AGENTS FOR cHL

The aetiology of non-EBV-associated cHL is unknown, but epidemiological studies have suggested that delayed exposure to a common infectious agent may play a key role. Viruses are the most likely candidates since they are widespread and infect individuals at an early age. As a result of previous molecular biology studies within this laboratory, the involvement of known herpesviruses (Armstrong et al 1998; Gallagher et al 2002) and SV40 (MacKenzie et al. 2003) can be ruled out. Using IHC, QRT-PCR, conventional PCR and degenerate PCR assays MV and PyV genomes were not detected within cHL biopsies (Chapters 3 and 4).

Prior knowledge of the putative viral agent or virus family is a prerequisite for these molecular biology techniques, but several virus discovery methods are now available for which this is not required. Representational difference analysis (RDA) has been

used within our laboratory to investigate childhood ALL (MacKenzie et al. 2006). However, this technique is very labour intensive and requires very good quality high molecular weight DNA. An alternative method of virus discovery, which uses gene expression profiling for rapid detailed analysis of cDNA libraries, is serial analysis of gene expression (SAGE) (Velculescu et al. 1995). SAGE is currently being used in our laboratory by Dr Alice Gallagher as a method to detect viral transcripts present in HRS cells from biopsy. Transcripts corresponding to unknown tags in SAGE libraries will be identified and used to search public databases.

Rolling circle amplification (RCA) has been used to amplify circular DNA genomes, including the genome of a novel papillomavirus in a sample from a Florida manatee (Rector et al. 2004). RCA is a well-established WGA technique that uses random hexamers to preferentially amplify small circular molecules and requires no prior knowledge of the viral genomic sequence. Using a commercially available RCA kit (TempliPhi 100, Applied Biosystems), complete viral genomes have successfully been amplified within our laboratory (Miss Debbie Johnson, unpublished), including the uncharacterised rabbit papovavirus which was analysed using our polyomavirus degenerate PCR assays, described in chapter 4.

The ViroChip is another method of viral detection for which prior knowledge of the virus is not required. This DNA microarray contains 70 mer sequences of highly conserved regions within every fully sequenced viral genome listed in GenBank (Wang et al 2003). This method has been successfully used to characterise known viruses within patients with respiratory tract infections, in addition to identifying novel variants present (Kistler et al 2007; Kistler et al 2007). Results correlated well

with those from pathogen-specific PCR assays, both in terms of sensitivity and specificity.

7.2 RECURRENT CHROMOSOME IMBALANCES IN cHL

Molecular studies of cHL have been significantly hampered by the scarcity of HRS cells within the lymphomas. Advances in molecular biology and cytogenetic techniques have now made it possible to identify recurrent regions of chromosomal imbalance in HRS cells from cHL-derived cell lines and biopsies (Chui et al. 2003; Joos et al. 2000; Joos et al. 2002; Joos et al. 2003). Using array-CGH analysis, the presence of several recurrent changes within six cHL-derived cell lines was confirmed and the location of these chromosomal regions was refined down to the megabase level. HRS cells were isolated from a cHL case using laser microdissection, and the DNA from these cells was amplified for array-CGH analysis using DOP-PCR as a method of WGA. This allowed us to identify a number of previously identified recurrent chromosome gains and losses within this cHL case.

As discussed in Chapter 1, HRS cells originate from germinal centre B-cells, but do not express BCRs and have no surface immunoglobulins. Non-functional B-cells would normally be destroyed by apoptosis, but HRS cells have survived by some, as yet, unknown mechanism. Any chromosomal change which may affect a gene that is known to play a role in an apoptotic pathway (i.e., NF κ B signalling pathway, the CD95 death receptor pathway, the JAK-STAT signalling pathway or Wnt signalling pathway) must, therefore, be considered in the search for the survival mechanism of HRS cells.^d All genes of known function within regions of gain or loss identified by

^dThe potential role of tumour suppressor genes (ie p53) should also be considered in the pathogenesis of cHL.

our array-CGH analysis were examined and any with known involvement in apoptotic pathways were highlighted as potential candidate genes in cHL.

EBV infection may also enable HRS cells to escape apoptosis since the LMP1 gene in EBV-infected cells is known to upregulate anti-apoptotic proteins (Wang et al 1990). In addition, the EBV genes LMP1 and LMP2A mimic CD40 and BCR, respectively, which may enable EBV-infected HRS cells to bypass the apoptotic mechanism in the germinal centre.

From our array-CGH analysis of cHL-derived cell lines, we also identified many genes with known function in cell cycle regulation and DNA repair mechanisms. Changes in cell cycle regulation are common in human neoplasia. To date, only one study has directly examined the expression of cell cycle genes in cHL samples (Tzankov et al 2003). By tissue microarray analysis, overexpression of the cyclin E1 (CCNE1) gene was reported in 84% (212/253) cHL samples. The identification of DNA repair genes located within regions of chromosomal imbalance is not unexpected since the many insertions and deletions detected in HRS cell DNA will be introducing double- and single-strand breaks. In addition, Ig gene recombination, identified in HRS cells, will introduce DNA strand breaks and, therefore, stimulate DNA repair mechanisms.

Selected genes located within the regions of gain and loss in cHL-derived cell line DNA can be further investigated using FICTION or FISH analysis of metaphase chromosomes from cHL cell lines and biopsies. The amplification techniques of multiplex ligation-dependent probe amplification (MLPA) and multiplex amplification

and probe hybridisation (MAPH) could also be used to analyse the copy number of these genes (Sellner & Taylor 2004). Both techniques involve the amplification of specifically bound probes using universal primers. These methods are very cost effective since numerous targets can be amplified simultaneously and fluorescent detection only requires one fluorescent primer. For MAPH, genomic DNA is fixed onto a membrane and hybridisation takes place using a set of specific probes. In MPLA, hybridisation takes place in a solution of genomic DNA and target-specific probe sets. The latter is a more reliable, high throughput, contamination-free method than MAPH. Also only 100-200 ng of DNA is required for optimal MLPA, compared with 1 µg of DNA for MAPH (Sellner & Taylor 2004).

High-density oligoarrays, or single-nucleotide polymorphic allele (SNP)-arrays, are now available for analysing these recurrent chromosomal changes to a higher resolution (150-200 kb) than was possible with CGH-arrays (Bignell et al. 2004; Matsuzaki et al. 2004; Wong et al. 2004; Zhao et al. 2004). MDA is the method of choice for preparation of samples for SNP-array hybridisation since it can be used to generate thousands of high-molecular weight copies of genomic DNA without thermocycling or ligation of DNA adaptors (Dean et al. 2002; Hosono et al. 2003), and with a low incidence of non-specific amplification artefacts or bias among alleles. We performed a number of preliminary experiments (data not shown) to test laser microdissected samples amplified by MDA, using the GenomiPhi (Applied Biosystems) and Repli-gTM (Molecular Staging, New Haven, CT) kits. However, samples were found to be of insufficient quality to be used for hybridisations. The failure of MDA to amplify moderately degraded DNA from formalin-fixed samples has been reported (Wang et al. 2004) and it is possible that some degradation of our

cHL case samples had occurred during sample transport and processing. It may be that snap-freezing biopsy samples on arrival at the laboratory and laser microdissecting HRS cells directly from subsequent frozen tissue sections will preserve the quality of the DNA within these cells. However, this would mean a trade-off between obtaining whole cells and maintaining the quality of the DNA.

7.3 CONCLUSION

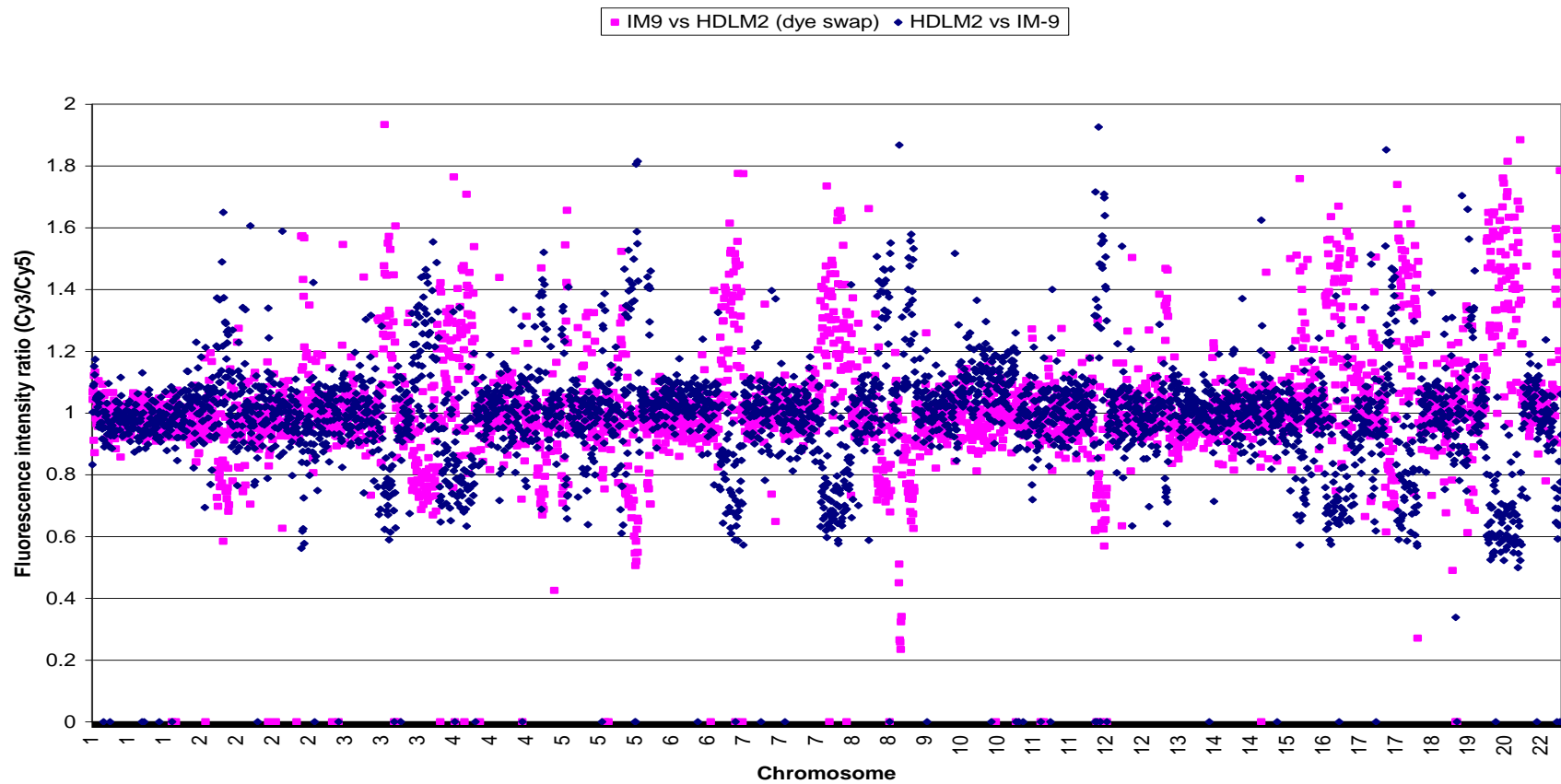
The techniques optimised during this project will continue to be used to assay other cHL cases within the Leukemia Research Fund (LRF) Virus Centre, at Glasgow University. Our analysis of six cHL-derived cell lines and a cHL cell line using array-CGH has led to the identification of regions of chromosomal imbalance which may influence the pathogenesis of cHL. Functional genes located within these regions require further investigation in order to confirm any involvement in this disease.

APPENDICES

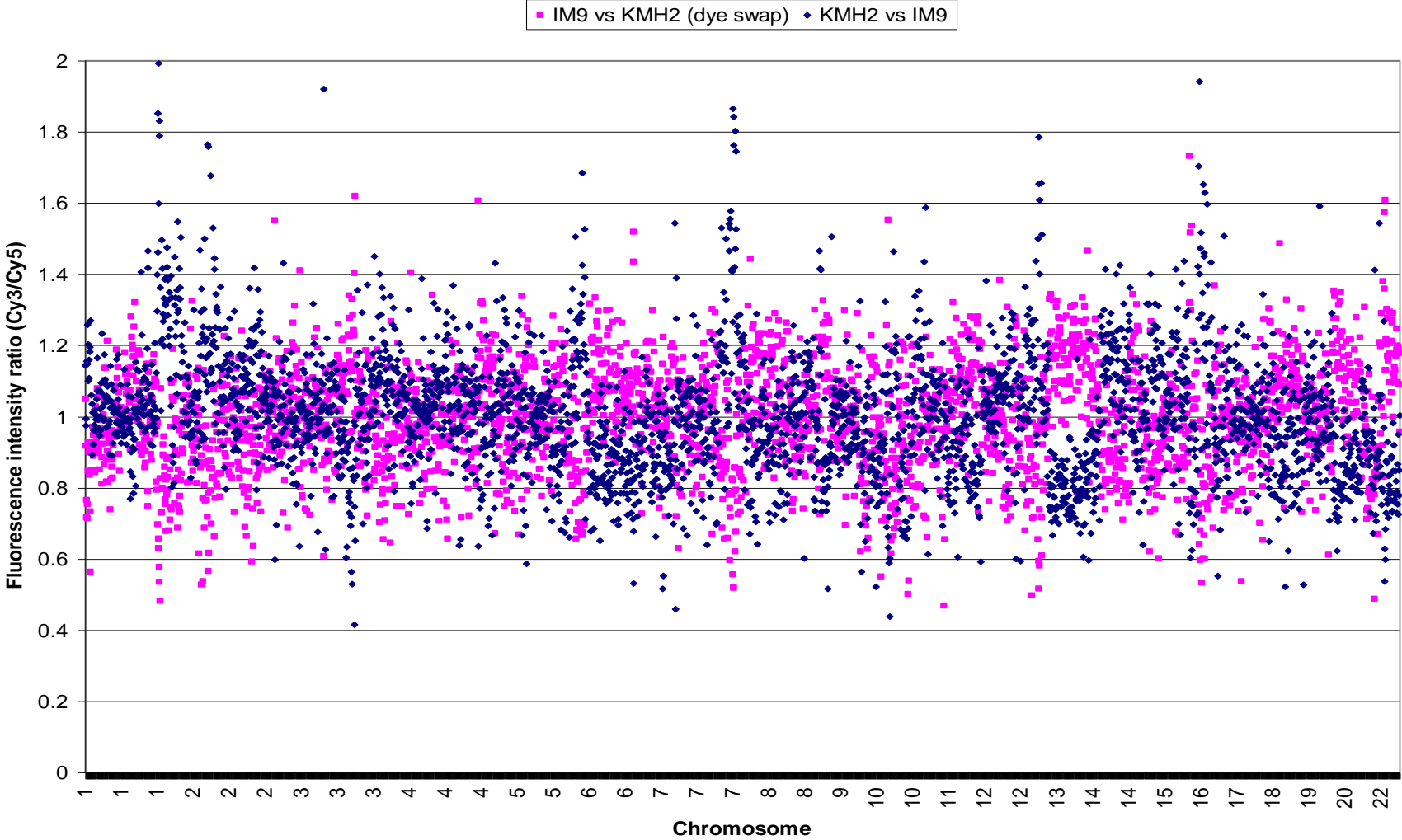
APPENDIX A

Combined hybridisation charts of cHL-derived cell lines

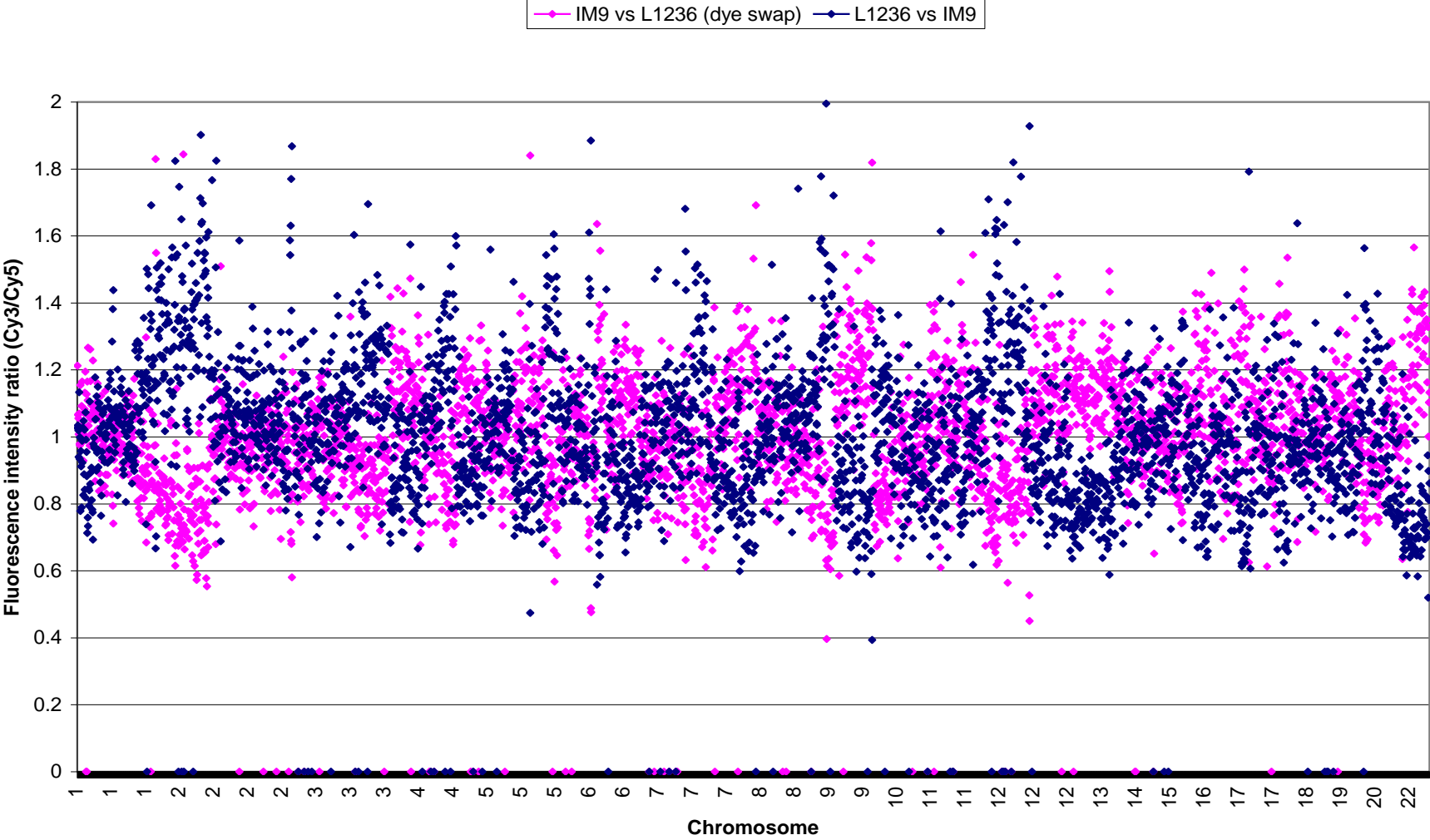
a) HDLM2 versus IM9



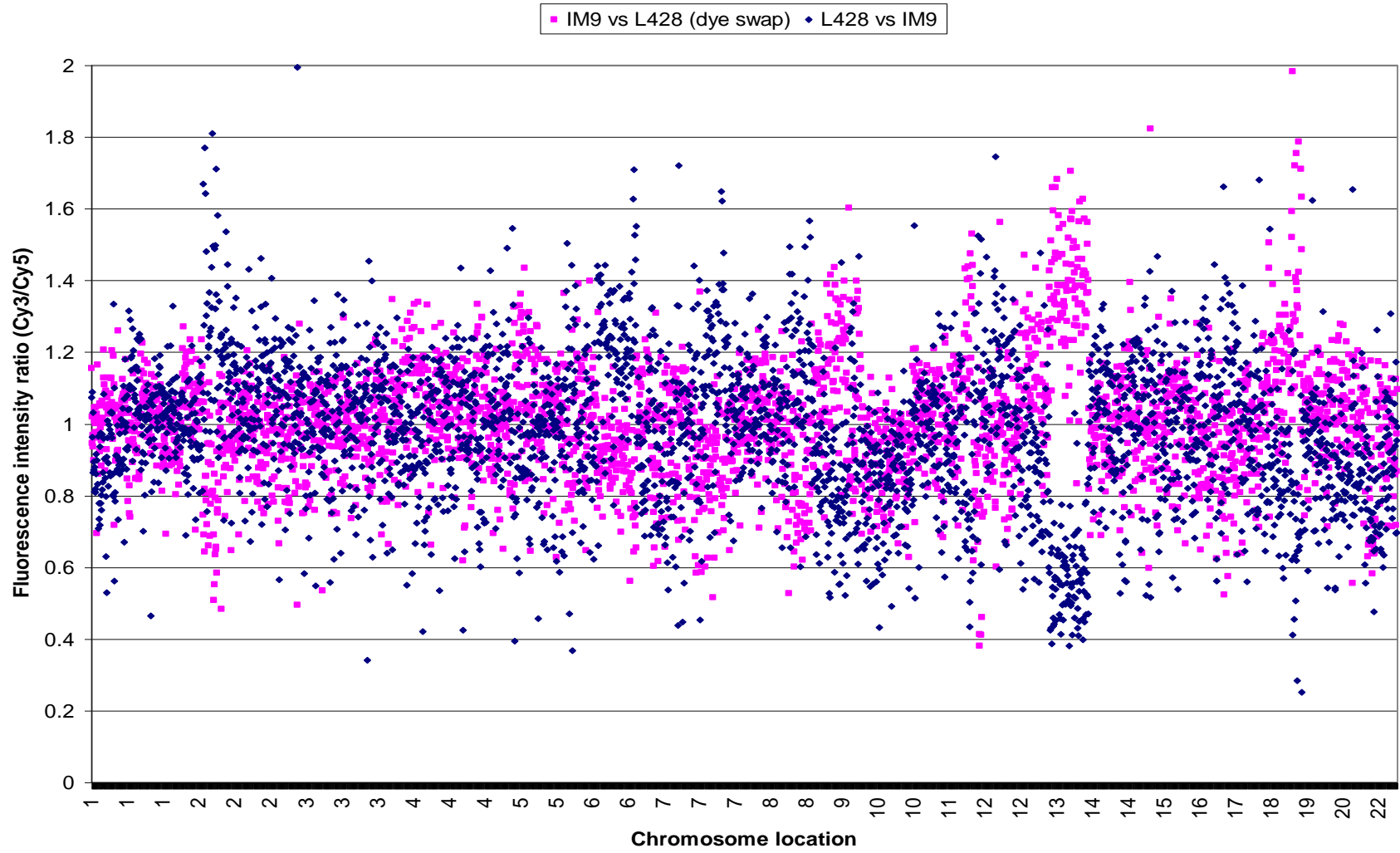
b) KMH2 versus IM9



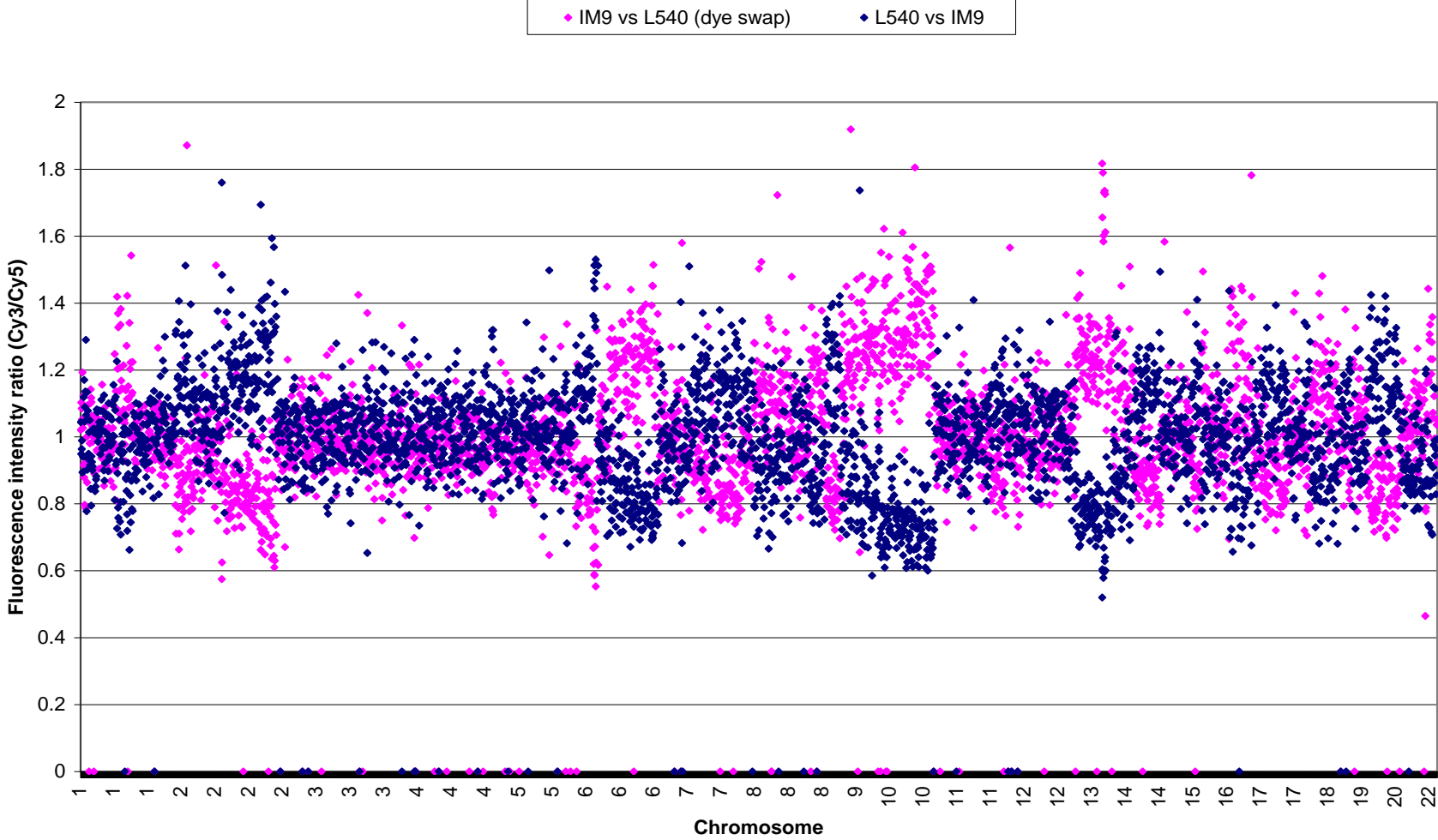
c) L1236 versus IM9



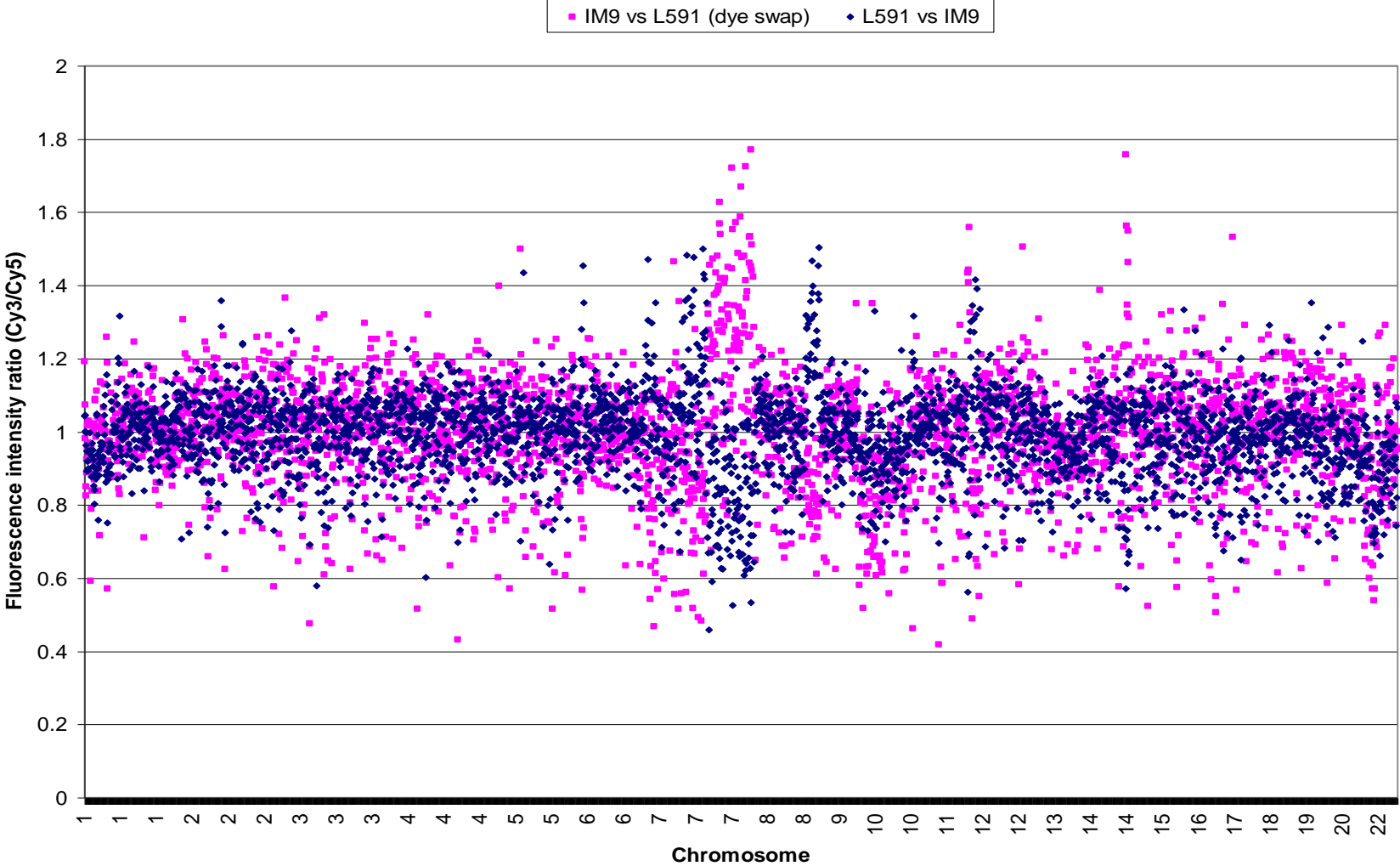
d) L428 versus IM9



e) L540 versus IM9



f) L591 versus IM9



APPENDIX B

Chromosome regions containing known functional genes in which gains were identified in three or more cHL-derived cell lines.

No copy number variations within these genome regions were reported on the Genome Variation Database website (<http://projects.tcag.ca/variation/>; last checked November 2007). Colours at the top of each column correspond to those used for each cell line in Figure 5.3. Shaded rows highlight alternate chromosomes for ease of viewing.

Clone ID	Location	Genes	HDLM2	KMH2	L1236	L428	L540	L591
RP11-19A8	2p16.3	FSHR	Y	Y	Y	Y	N	N
RP11-27C22	2p21	PRKCE	Y	Y	Y	Y	N	N
RP11-304A15	2p13.3	ARHGAP25, BMP10	N	Y	Y	Y	N	N
RP11-373L24	2p16.1	REL	N	Y	Y	Y	N	N
RP11-436L21	2p16.3	FSHR	Y	Y	Y	Y	N	N
RP11-440P5	2p16.1	BCL11A	N	Y	Y	Y	N	N
RP11-457F14	2p22.1	SLC8A1	Y	N	Y	Y	N	N
RP11-477P16	3q26.31	NLGN1	Y	Y	Y	Y	N	N
RP11-84G22	4p15.31	KCIP4	Y	N	Y	N	Y	N
CTC-1480C2	5q22.2	APC	N	N	Y	N	Y	Y
RP11-520O10	5q35.3	COL23A1	Y	Y	N	Y	N	N
RP3-444C7	6p22.3	CDKAL1	Y	N	Y	N	Y	N
RP4-625H18	6p22.3	ID4	Y	Y	Y	N	Y	N
RP11-68J15	6p22.3	FAM8A1, NUP153	Y	Y	Y	N	Y	N

RP1-13D10	6p22.3	MYLIP	Y	Y	Y	N	Y	Y
RP11-221G19	7q33	CALD1	N	Y	N	Y	Y	N
RP11-311I10	7q21.13	PFTK1	N	N	Y	Y	Y	Y
RP11-22A24	8q24.12	ENPP2, TAF2	Y	Y	N	Y	N	N
RP11-48M17	9p24.3-p24.2	SMARCA2	Y	N	Y	Y	Y	Y
RP11-320E16	9p24.2	VLDLR	Y	N	Y	Y	Y	Y
RP11-503K16	9p22.1	ATL1	Y	N	Y	N	Y	N
RP11-15P13	9p21.3	MLLT3	Y	N	N	N	Y	Y
RP11-27J8	9p21.2	MOBKL2B, IFNK	Y	Y	Y	N	Y	Y
RP11-136I14	11q23.3	IGSF4	N	N	Y	N	Y	Y
RP11-419F8	11q25	OPCML	N	N	Y	Y	N	Y
RP11-567M21	11q24.3	PRDM10, APLP2	N	N	Y	Y	Y	Y
RP11-127B1	12p12.3	PIK3C2G	Y	N	Y	N	Y	N
RP11-144O23	12p13.2	TAS2R7, TAS2R8, TAS2R9, TAS2R10, PRR4, TAS2R14, PRH1	Y	N	Y	N	Y	Y
RP11-437F6	12p12.1	SOX5	N	N	Y	Y	Y	N
RP11-474N8	12q13.3	ADMR, ZBT39, TAC3, MYO1A	N	Y	Y	Y	N	N
RP11-296I10	16q22.1	AARS	Y	Y	Y	N	N	N
RP11-515O17	17q22	HLF, MMD	Y	N	Y	N	Y	N

APPENDIX C

Chromosome regions containing known functional genes in which losses were identified in three or more cHL-derived cell lines.

No copy number variations within these genome regions were reported on the Genome Variation Database website (<http://projects.tcag.ca/variation/>; last checked November 2007). Colours at the top of each column correspond to those used for each cell line in Figure 5.4. Shaded rows indicate alternate chromosomes for ease of viewing.

Clone ID	Location	Genes	HDLM2	KMH2	L1236	L428	L540	L591
RP11-148L24	4q34.1	FBX08	Y	N	Y	Y	N	N
RP11-21K15	5q14.1	ARSB	N	Y	Y	N	N	Y
RP11-24O11	5q14.3	MEF2C	N	Y	Y	Y	N	N
RP1-23D17	6q15	SPACA1, CNR1	N	Y	Y	N	Y	N
RP1-142L7	6q21	WISP3, TUBE1, LAMA4	N	Y	Y	N	Y	N
RP11-386H19	6q24.2	UTRN	N	Y	Y	N	Y	N
RP11-545I5	6q24.3	FBXO30, SHPRH	N	Y	N	Y	Y	N
RP4-596O9	7p15.1	CREB5	Y	Y	N	N	Y	N
RP11-177H2	8p23.1	PINX1, XKR6	Y	N	Y	N	Y	Y
RP11-561E1	8p21.2	ADAMDEC1, ADAM7	Y	Y	N	N	N	Y
RP11-138J2	8p21.2	PTK2B	Y	N	N	N	Y	Y
RP11-356F24	8p21.1	EXTL3	Y	N	N	N	Y	Y
RP11-473A17	8p12	PURG, WRN	Y	N	N	N	Y	Y
RP11-301H15	8p12	NRG1	Y	N	N	N	Y	Y
RP11-362L2	9q21.31	TLE4	N	Y	N	Y	Y	N
RP11-31J20	9q31.1	ABCA1	N	N	Y	Y	Y	N
RP11-388N6	9q31.3	PTPN3	N	N	Y	Y	Y	N
RP11-470J20	9q31.3	PALM2	N	N	Y	Y	Y	N
RP11-143H20	9q34.13	LAMC3	N	N	Y	Y	Y	N
RP11-83N9	9q34.3	BTBD14A, LHX3, QSCN6L1	N	N	Y	Y	Y	N

RP11-574P20	10q22.3	RAI17	N	Y	Y	N	Y	N
RP11-110K8	13q12.11	EFHA1	N	Y	Y	Y	Y	N
RP11-187L3	13q12.11	CRYL1	N	N	Y	Y	Y	N
RP11-760M1	13q12.12	TNFRSF19	N	Y	Y	Y	Y	N
RP11-44J9	13q12.13	WASF3	N	Y	Y	Y	N	N
RP11-111G7	13q12.13	ATP8A2	N	Y	Y	Y	Y	N
RP11-125I23	13q12.2	GTF3A	N	Y	Y	Y	Y	N
RP11-218E6	13q12.3	SLC7A1	N	Y	Y	Y	Y	N
RP11-550P23	13q12.3	HMGB1	N	Y	Y	Y	Y	N
RP11-98D3	13q13.3	NBEA, MAB21L1	N	Y	Y	Y	Y	N
RP11-10M8	13q13.3	POSTN, TRPC4	N	Y	Y	Y	Y	N
RP11-131P10	13q13.3	UFM1	N	Y	N	Y	Y	N
RP11-2P5	13q14.11	ELF1, WBP4	N	Y	Y	Y	Y	N
RP11-185C18	13q14.2	SETDB2, PHF11, RCBTB1	N	Y	Y	Y	Y	N
RP11-327P2	13q14.3	ATP7B	N	N	Y	Y	Y	N
RP11-431O22	13q14.3	LECT1, PCDH8	N	Y	N	Y	Y	N
RP11-359P14	13q21.2	TDRD3	N	Y	Y	Y	Y	N
RP11-552M6	13q22.1	KLF12	N	N	Y	Y	Y	N
RP11-332E3	13q22.2	LMO7	N	Y	Y	Y	Y	N
RP11-226E21	13q22.3	MYCBP2	N	Y	Y	Y	Y	N
13 RP11-74A12	13q32.1	ABCC4	N	Y	Y	Y	Y	N
RP11-383H17	13q32.2	RANBP5	N	N	Y	Y	Y	N
RP11-564N10	13q33.1	FGF14	N	Y	Y	Y	Y	N
RP11-480K16	13q34	TUBGCP3	N	Y	Y	Y	N	N
RP11-302G2	15q22.31	RAB11A	N	Y	N	Y	Y	N
RP11-305A7	16q12.1	ZNF423	Y	Y	Y	N	N	N
RP11-87G24	17q25.2	MGAT5B	Y	N	Y	N	Y	N
RP11-323N12	17q25.3	PSCD1, UBP36, TIMP2	N	Y	Y	N	Y	N
RP11-525L23	17q25.3	FOXK2, WDR45L, RAB40B	Y	N	Y	N	Y	N
RP11-146G7	18p11.31	ARHGAP28, LAMA1	Y	Y	Y	N	N	N
RP11-350K6	18q21.32	SEC11L3	N	Y	N	Y	Y	N
RP11-28F1	18q21.33	BCL2, FVT1	N	Y	N	Y	Y	N
RP11-154H12	18q23	CTDP1	N	N	Y	Y	Y	N
RP11-526K24	20p12.1	CT006	Y	Y	N	Y	N	N

RP5-1096J16	20p11.23	CT026	Y	Y	N	Y	N	N
RP5-1071L10	20q13.13	BCAS4, TMSL6	Y	Y	N	Y	N	N
RP5-1075G21	20q13.2	CYP24A	Y	Y	Y	Y	N	N
CTA-228A9	22q13.1	PLA2G6, SLC16A8	N	Y	Y	N	Y	N
RP1-172B20	22q13.1	CACNA1I	N	Y	Y	N	Y	N
RP3-437M21	22q13.2	ARFGAP3	Y	N	Y	N	Y	N
22 CTA-268H5	22q13.31	NUP50, UPK3A, SMC1L2	Y	Y	Y	N	N	N
RP3-398C22	22q13.31	ATXN10	Y	Y	Y	N	N	N

APPENDIX D

Gene expression array analysis results for the EBV-positive cHL cell line KMH2

Top 20 upregulated genes in KMH2			
Probe set ID	Public ID	UniGene ID	Gene Symbol
205403_at	NM_004633	Hs.25333	IL1R2
1566126_at	AK097242	Hs.519719	FABP6
210650_s_at	BC001304	Hs.12376	PCLO
223340_at	AF131801	Hs.241503	SPG3A
204687_at	NM_015393	Hs.105460	DKFZP564O0823
217853_at	NM_022748	Hs.520814	TENS1
214945_at	AW514267	Hs.368516	NY-REN-7 /// LOC389347
203420_at	NM_016255	Hs.95260	FAM8A1
212344_at	AW043713	Hs.409602	SULF1
231883_at	BF306374	Hs.435466	FBXW8
220559_at	NM_001426	Hs.271977	EN1
203354_s_at	AW117368	Hs.434255	PSD3
212607_at	N32526	Hs.498292	AKT3
204083_s_at	NM_003289	Hs.300772	TPM2
223501_at	AW151360	Hs.525157	TNFSF13B
209582_s_at	H23979	Hs.79015	CD200
201566_x_at	D13891	Hs.180919	ID2 /// ID2B
226602_s_at	T30183	Hs.531306	BCR /// LOC440820
219511_s_at	NM_005460	Hs.426463	SNCAIP
223063_at	BC004870	Hs.520494	FLJ14525

Top 20 downregulated genes in KMH2			
Probe set ID	Public ID	UniGene ID	Gene Symbol
208690_s_at	BC000915	Hs.368525	PDLIM1
211555_s_at	AF020340	Hs.77890	GUCY1B3
224657_at	AL034417	Hs.11169	MIG-6
1565162_s_at	D16947	Hs.389700	MGST1
208524_at	NM_005290	Hs.159900	GPR15
202464_s_at	NM_004566	Hs.195471	PFKFB3
203987_at	NM_003506	Hs.292464	FZD6
205114_s_at	NM_002983	Hs.514107	CCL3 /// CCL3L1 /// CCL3L3
221286_s_at	NM_016459	Hs.409563	PACAP
208018_s_at	NM_002110	Hs.126521	HCK
204639_at	NM_000022	Hs.407135	ADA
1559425_at	AL512701	Hs.333907	PRKCH
219159_s_at	NM_021181	Hs.517265	SLAMF7
218241_at	NM_005113	Hs.104320	GOLGA5
1552497_a_at	NM_052931	Hs.492348	SLAMF6
221942_s_at	AI719730	Hs.24258	GUCY1A3
204608_at	NM_000048	Hs.442047	ASL
230673_at	AV706971	Hs.170128	PKHD1L1
203185_at	NM_014737	Hs.379970	RASSF2
1552296_at	NM_153274	Hs.302513	VMD2L2

APPENDIX E

Gene expression array analysis results for the EBV-positive cHL cell line L428

Top 20 upregulated genes in L428			
Probe set ID	Public ID	UniGene ID	Gene Symbol
203824_at	NM_004616	Hs.170563	TSPAN8
205403_at	NM_004633	Hs.25333	IL1R2
206118_at	NM_003151	Hs.80642	STAT4
238553_at	BG426581	Hs.499605	LOC399753 /// LOC399768 /// LOC439983
203354_s_at	AW117368	Hs.434255	PSD3
203835_at	NM_005512	Hs.151641	LRRC32
204483_at	NM_001976	Hs.224171	ENO3
203420_at	NM_016255	Hs.95260	FAM8A1
205141_at	NM_001145	Hs.283749	ANG /// RNASE4
207194_s_at	NM_001544	Hs.386467	ICAM4
1560074_at	AL119889	Hs.531704	PRKCA
230769_at	AI916261	Hs.127350	FLJ37099
212797_at	BE742268	Hs.485195	SORT1
243937_x_at	BF436377	Hs.499605	LOC399768 /// LOC439983
210695_s_at	U13395	Hs.549163	WWOX
203335_at	NM_006214	Hs.498732	PHYH
218910_at	NM_018075	Hs.457131	FLJ10375
203814_s_at	NM_000904	Hs.533050	NQO2
1555464_at	BC046208	Hs.163173	IFIH1
205165_at	NM_001407	Hs.533070	CELSR3

Top 20 downregulated genes in L428			
Probe set ID	Public ID	UniGene ID	Gene Symbol
208690_s_at	BC000915	Hs.368525	PDLIM1
224657_at	AL034417	Hs.11169	MIG-6
211555_s_at	AF020340	Hs.77890	GUCY1B3
1565162_s_at	D16947	Hs.389700	MGST1
207826_s_at	NM_002167	Hs.76884	ID3
202022_at	NM_005165	Hs.155247	ALDOC
205114_s_at	NM_002983	Hs.514107	CCL3 /// CCL3L1 /// CCL3L3
219159_s_at	NM_021181	Hs.517265	SLAMF7
208018_s_at	NM_002110	Hs.126521	HCK
204639_at	NM_000022	Hs.407135	ADA
208524_at	NM_005290	Hs.159900	GPR15
1569607_s_at	BC016022	Hs.522178	ANKRD20A /// C21orf81 /// LOC440841 /// LOC441425 /// LOC441430
230673_at	AV706971	Hs.170128	PKHD1L1
203921_at	NM_004267	Hs.8786	CHST2
1552497_a_at	NM_052931	Hs.492348	SLAMF6
1559425_at	AL512701	Hs.333907	PRKCH
219821_s_at	NM_018988	Hs.484686	GFOD1
204281_at	NM_003213	Hs.94865	TEAD4
202464_s_at	NM_004566	Hs.195471	PFKFB3
208690_s_at	BC000915	Hs.368525	PDLIM1

APPENDIX F

Gene expression array analysis results for the EBV-positive cHL cell line L591

Top 20 upregulated genes in L591			
Probe set ID	Public ID	UniGene ID	Gene Symbol
209369_at	M63310	Hs.480042	ANXA3
241942_at	AA927870	Hs.444882	PXDNL
233052_at	AW270168	Hs.520106	DNAH8
205403_at	NM_004633	Hs.25333	IL1R2
209582_s_at	H23979	Hs.79015	CD200
206707_x_at	NM_015864	Hs.484915	C6orf32
212169_at	AL050187	Hs.103934	FKBP9
1553044_at	NM_032602	Hs.334499	CX62
217853_at	NM_022748	Hs.520814	TENS1
217336_at	AL118510	Hs.512535	RPS10 /// LOC158104 /// LOC388885 /// LOC389127 /// LOC390842 /// LOC401817
205719_s_at	NM_000277	Hs.325404	PAH
206414_s_at	NM_003887	Hs.467662	DDEF2
202336_s_at	NM_000919	Hs.369430	PAM
209676_at	J03225	Hs.516578	TFPI
208450_at	NM_006498	Hs.531776	LGALS2
203665_at	NM_002133	Hs.517581	HMOX1
203498_at	NM_005822	Hs.440168	DSCR1L1
201566_x_at	D13891	Hs.180919	ID2 /// ID2B
205079_s_at	NM_003829	Hs.169378	MPDZ
212797_at	BE742268	Hs.485195	SORT1

Top 20 downregulated genes in L591			
Probe set ID	Public ID	UniGene ID	Gene Symbol
211555_s_at	AF020340	Hs.77890	GUCY1B3
224657_at	AL034417	Hs.11169	MIG-6
205114_s_at	NM_002983	Hs.514107	CCL3 /// CCL3L1 /// CCL3L3
207826_s_at	NM_002167	Hs.76884	ID3
1569607_s_at	BC016022	Hs.522178	ANKRD20A /// C21orf81 /// LOC440841 /// LOC441425 /// LOC441430
1552531_a_at	NM_145007	Hs.375039	NALP11
1559425_at	AL512701	Hs.333907	PRKCH
204281_at	NM_003213	Hs.94865	TEAD4
201522_x_at	NM_003097	Hs.525700	SNRPN /// SNURF
203921_at	NM_004267	Hs.8786	CHST2
209694_at	M97655	Hs.503860	PTS
226301_at	AV729072	Hs.347144	C6orf192
1561336_at	CA449306	Hs.476453	DNASE1L3
1553528_a_at	NM_139052	Hs.96103	TAF5
201487_at	NM_001814	Hs.128065	CTSC
201367_s_at	AI356398	Hs.503093	ZFP36L2
208524_at	NM_005290	Hs.159900	GPR15
204472_at	NM_005261	Hs.345139	GEM
220205_at	NM_013315	Hs.122986	TPTE
208962_s_at	BE540552	Hs.503546	FADS1

REFERENCE LIST

Cancer Research UK: Hodgkin Lymphoma incidence statistics. 2007.

Alexander FE, Jarrett RF, Cartwright RA, Armstrong AA, Gokhale DA, Kane E, Gray D, Lawrence DJ, Taylor GM. Epstein-Barr Virus and HLA-DPB1-*0301 in young adult Hodgkin's disease: evidence for inherited susceptibility to Epstein-Barr Virus in cases that are EBV(+ve). *Cancer Epidemiol Biomarkers Prev* 2001; 10: 705-709.

Alexander FE, Jarrett RF, Lawrence D, Armstrong AA, Freeland J, Gokhale DA, Kane E, Taylor GM, Wright DH, Cartwright RA. Risk factors for Hodgkin's disease by Epstein-Barr virus (EBV) status: prior infection by EBV and other agents. *Br J Cancer* 2000; 82: 1117-1121.

Alexander FE, Lawrence DJ, Freeland J, Krajewski AS, Angus B, Taylor GM, Jarrett RF. An epidemiologic study of index and family infectious mononucleosis and adult Hodgkin's disease (HD): evidence for a specific association with EBV+ve HD in young adults. *Int J Cancer* 2003; 107: 298-302.

Alexander FE, Ricketts TJ, McKinney PA, Cartwright RA. Community lifestyle characteristics and incidence of Hodgkin's disease in young people. *Int J Cancer* 1991; 48: 10-14.

Allan GJ, Inman GJ, Parker BD, Rowe DT, Farrell PJ. Cell growth effects of Epstein-Barr virus leader protein. *J Gen Virol* 1992; 73 (Pt 6): 1547-1551.

Allander T, Andreasson K, Gupta S, Bjerkner A, Bogdanovic G, Persson MA, Dalianis T, Ramqvist T, Andersson B. Identification of a third human polyomavirus. *J Virol* 2007; 81: 4130-4136.

Allday MJ, Farrell PJ. Epstein-Barr virus nuclear antigen EBNA3C/6 expression maintains the level of latent membrane protein 1 in G1-arrested cells. *J Virol* 1994; 68: 3491-3498.

Ambinder RF. Gammaherpesviruses and "Hit-and-Run" oncogenesis. *Am J Pathol* 2000; 156: 1-3.

Anagnostopoulos I, Hansmann ML, Franssila K, Harris M, Harris NL, Jaffe ES, Han J, van Krieken JM, Poppema S, Marafioti T, Franklin J, Sextro M, Diehl V, Stein H. European Task Force on Lymphoma project on lymphocyte predominance Hodgkin disease: histologic and immunohistologic analysis of submitted cases reveals 2 types of Hodgkin disease with a nodular growth pattern and abundant lymphocytes. *Blood* 2000; 96: 1889-1899.

Armstrong AA, Shield L, Gallagher A, Jarrett RF. Lack of involvement of known oncogenic DNA viruses in Epstein-Barr virus-negative Hodgkin's disease. *Br J Cancer* 1998; 77: 1045-1047.

Atwood WJ, Amemiya K, Traub R, Harms J, Major EO. Interaction of the human polyomavirus, JCV, with human B-lymphocytes. *Virology* 1992; 190: 716-723.

Bargou RC, Emmerich F, Krappmann D, Bommert K, Mapara MY, Arnold W, Royer HD, Grinstein E, Greiner A, Scheidereit C, Dorken B. Constitutive nuclear factor-kappaB-RelA activation is required for proliferation and survival of Hodgkin's disease tumor cells. *J Clin Invest* 1997; 100: 2961-2969.

Bargou RC, Leng C, Krappmann D, Emmerich F, Mapara MY, Bommert K, Royer HD, Scheidereit C, Dorken B. High-level nuclear NF-kappa B and Oct-2 is a common feature of cultured Hodgkin/Reed-Sternberg cells. *Blood* 1996; 87: 4340-4347.

Barth TF, Martin-Subero JI, Joos S, Menz CK, Hasel C, Mechttersheimer G, Parwaresch RM, Lichter P, Siebert R, Mooller P. Gains of 2p involving the REL locus correlate with nuclear c-Rel protein accumulation in neoplastic cells of classical Hodgkin lymphoma. *Blood* 2003; 101: 3681-3686.

Benharroch D, Shemer-Avni Y, Levy A, Myint YY, Ariad S, Rager B, Sacks M, Gopas J. New candidate virus in association with Hodgkin's disease. *Leuk Lymphoma* 2003; 44: 605-610.

Benharroch D, Shemer-Avni Y, Myint YY, Levy A, Mejirovsky E, Suprun I, Shendler Y, Prinsloo I, Ariad S, Rager-Zisman B, Sacks M, Gopas J. Measles virus: evidence of an association with Hodgkin's disease. *Br J Cancer* 2004; 91: 572-579.

Berneman ZN, Torelli G, Luppi M, Jarrett RF. Absence of a directly causative role for human herpesvirus 7 in human lymphoma and a review of human herpesvirus 6 in human malignancy. *Ann Hematol* 1998; 77: 275-278.

Boiocchi M, Carbone A, De R, V, Dolcetti R. Is the Epstein-Barr virus involved in Hodgkin's disease? *Tumori* 1989; 75: 345-350.

Boriskin Y, Bogomolova NN, Koptyaeva IB, Giraudon P, Wild TF. Measles virus persistent infection: modification of the virus nucleocapsid protein. *J Gen Virol* 1986; 67 (Pt 9): 1979-1985.

Breitling R, Armengaud P, Amtmann A, Herzyk P. Rank products: a simple, yet powerful, new method to detect differentially regulated genes in replicated microarray experiments. *FEBS Lett* 2004; 573: 83-92.

- Brousset P, Meggetto F, Chittal S, Bibeau F, Arnaud J, Rubin B, Delsol G. Assessment of the methods for the detection of Epstein-Barr virus nucleic acids and related gene products in Hodgkin's disease. *Lab Invest* 1993; 69: 483-490.
- Cabannes E, Khan G, Aillet F, Jarrett RF, Hay RT. Mutations in the I κ B α gene in Hodgkin's disease suggest a tumour suppressor role for I κ B α . *Oncogene* 1999; 18: 3063-3070.
- Caldwell RG, Wilson JB, Anderson SJ, Longnecker R. Epstein-Barr virus LMP2A drives B cell development and survival in the absence of normal B cell receptor signals. *Immunity* 1998; 9: 405-411.
- Carbone M, Stach R, Di R, I, Pass HI, Rizzo P. Simian virus 40 oncogenesis in hamsters. *Dev Biol Stand* 1998; 94: 273-279.
- Carbone PP, Kaplan HS, Musshoff K, Smithers DW, Tubiana M. Report of the Committee on Hodgkin's Disease Staging Classification. *Cancer Res* 1971; 31: 1860-1861.
- Caspersson T, Farber S, Foley GE, et al. Chemical differentiation along metaphase chromosomes. *Exp Cell Res* 1968; 49: 219-222.
- Caspersson T, Zech L, Johansson C. Differential banding of alkylating fluorochromes in human chromosomes. *Exp Cell Res* 1970; 60: 315-319.
- Chadwick N, Bruce IJ, Schepelmann S, Pounder RE, Wakefield AJ. Measles virus RNA is not detected in inflammatory bowel disease using hybrid capture and reverse transcription followed by the polymerase chain reaction. *J Med Virol* 1998; 55: 305-311.

Chang ET, Zheng T, Weir EG, Borowitz M, Mann RB, Spiegelman D, Mueller NE. Childhood social environment and Hodgkin's lymphoma: new findings from a population-based case-control study. *Cancer Epidemiol Biomarkers Prev* 2004; 13: 1361-1370.

Chang MC, Chang YT, Tien YW, Sun CT, Wu MS, Lin JT. Distinct chromosomal aberrations of ampulla of Vater and pancreatic head cancers detected by laser capture microdissection and comparative genomic hybridization. *Oncol Rep* 2005; 14: 867-872.

Chatterjee M, Weyandt TB, Frisque RJ. Identification of archetype and rearranged forms of BK virus in leukocytes from healthy individuals. *J Med Virol* 2000; 60: 353-362.

Chui DT, Hammond D, Baird M, Shield L, Jackson R, Jarrett RF. Classical Hodgkin lymphoma is associated with frequent gains of 17q. *Genes Chromosomes Cancer* 2003; 38: 126-136.

Clark DA, Alexander FE, McKinney PA, Roberts BE, O'Brien C, Jarrett RF, Cartwright RA, Onions DE. The seroepidemiology of human herpesvirus-6 (HHV-6) from a case-control study of leukaemia and lymphoma. *Int J Cancer* 1990; 45: 829-833.

Cole CN. Polyomavirinae: The viruses and their replication. In: Knipe DM, Howley PM, Griffin DE, Lamb RA, Martin MA, Roizman B, Straus SE, eds. *Fields Virology*. Philadelphia: Lippincott, Williams & Wilkins, 2001.

Corallini A, Altavilla G, Cecchetti MG, Fabris G, Grossi MP, Balboni PG, Lanza G, Barbanti-Brodano G. Ependymomas, malignant tumors of pancreatic islets, and

osteosarcomas induced in hamsters by BK virus, a human papovavirus. *J Natl Cancer Inst* 1978; 61: 875-883.

Cossman J, Messineo C, Bagg A. Reed-Sternberg cell: survival in a hostile sea. *Lab Invest* 1998; 78: 229-235.

Countryman J, Jenson H, Seibl R, Wolf H, Miller G. Polymorphic proteins encoded within BZLF1 of defective and standard Epstein-Barr viruses disrupt latency. *J Virol* 1987; 61: 3672-3679.

Daigo Y, Chin SF, Gorringer KL, Bobrow LG, Ponder BA, Pharoah PD, Caldas C. Degenerate oligonucleotide primed-polymerase chain reaction-based array comparative genomic hybridization for extensive amplicon profiling of breast cancers : a new approach for the molecular analysis of paraffin-embedded cancer tissue. *Am J Pathol* 2001; 158: 1623-1631.

De Mattei M, Martini F, Corallini A, Gerosa M, Scotlandi K, Carinci P, Barbanti-Brodano G, Tognon M. High incidence of BK virus large-T-antigen-coding sequences in normal human tissues and tumors of different histotypes. *Int J Cancer* 1995; 61: 756-760.

Deacon EM, Pallesen G, Niedobitek G, Crocker J, Brooks L, Rickinson AB, Young LS. Epstein-Barr virus and Hodgkin's disease: transcriptional analysis of virus latency in the malignant cells. *J Exp Med* 1993; 177: 339-349.

Dean FB, Hosono S, Fang L, Wu X, Faruqi AF, Bray-Ward P, Sun Z, Zong Q, Du Y, Du J, Driscoll M, Song W, Kingsmore SF, Egholm M, Lasken RS. Comprehensive human genome amplification using multiple displacement amplification. *Proc Natl Acad Sci U S A* 2002; 99: 5261-5266.

Devergne O, Hatzivassiliou E, Izumi KM, Kaye KM, Kleijnen MF, Kieff E, Mosialos G. Association of TRAF1, TRAF2, and TRAF3 with an Epstein-Barr virus LMP1 domain important for B-lymphocyte transformation: role in NF-kappaB activation. *Mol Cell Biol* 1996; 16: 7098-7108.

Diamandopoulos GT, Enders JF. Studies on transformation of Syrian hamster cells by simian virus 40 (SV40): acquisition of oncogenicity by virus-exposed cells apparently unassociated with the viral genome. *Proc Natl Acad Sci U S A* 1965; 54: 1092-1099.

Dietmaier W, Hartmann A, Wallinger S, Heinmoller E, Kerner T, Endl E, Jauch KW, Hofstadter F, Ruschoff J. Multiple mutation analyses in single tumor cells with improved whole genome amplification. *Am J Pathol* 1999; 154: 83-95.

Dohner H, Bloomfield CD, Frizzera G, Frestedt J, Arthur DC. Recurring chromosome abnormalities in Hodgkin's disease. *Genes Chromosomes Cancer* 1992; 5: 392-398.

Dorries K, Vogel E, Gunther S, Czub S. Infection of human polyomaviruses JC and BK in peripheral blood leukocytes from immunocompetent individuals. *Virology* 1994; 198: 59-70.

Drexler HG. Recent results on the biology of Hodgkin and Reed-Sternberg cells. II. Continuous cell lines. *Leuk Lymphoma* 1993; 9: 1-25.

Drexler HG, Dirks WG, Macleod RA. False human hematopoietic cell lines: cross-contaminations and misinterpretations. *Leukemia* 1999; 13: 1601-1607.

Eby MT, Jasmin A, Kumar A, Sharma K, Chaudhary PM. TAJ, a novel member of the tumor necrosis factor receptor family, activates the c-Jun N-terminal kinase

pathway and mediates caspase-independent cell death. *J Biol Chem* 2000; 275: 15336-15342.

Emmerich F, Meiser M, Hummel M, Demel G, Foss HD, Jundt F, Mathas S, Krappmann D, Scheidereit C, Stein H, Dorken B. Overexpression of I kappa B alpha without inhibition of NF-kappaB activity and mutations in the I kappa B alpha gene in Reed-Sternberg cells. *Blood* 1999; 94: 3129-3134.

Enam S, Del Valle L, Lara C, Gan DD, Ortiz-Hidalgo C, Palazzo JP, Khalili K. Association of human polyomavirus JCV with colon cancer: evidence for interaction of viral T-antigen and beta-catenin. *Cancer Res* 2002; 62: 7093-7101.

Engels EA, Chen J, Hartge P, Cerhan JR, Davis S, Severson RK, Cozen W, Viscidi RP. Antibody responses to simian virus 40 T antigen: a case-control study of non-Hodgkin lymphoma. *Cancer Epidemiol Biomarkers Prev* 2005; 14: 521-524.

Evans AS, Gutensohn NM. A population-based case-control study of EBV and other viral antibodies among persons with Hodgkin's disease and their siblings. *Int J Cancer* 1984; 34: 149-157.

Fahey JL, Buell DN, Sox HC. Proliferation and differentiation of lymphoid cells: studies with human lymphoid cell lines and immunoglobulin synthesis. *Ann N Y Acad Sci* 1971; 190: 221-234.

Falzetti D, Crescenzi B, Matteuci C, Falini B, Martelli MF, Van Den BH, Mecucci C. Genomic instability and recurrent breakpoints are main cytogenetic findings in Hodgkin's disease. *Haematologica* 1999; 84: 298-305.

Feng, H., Shuda, M. Chang, Y., Moore, P.S. Clonal integration of a polyomavirus in human Merkel cell carcinoma. *Science* 2008; 2008; 19(5866):1096-100. Epub 2008 Jan 17.

Fernandez-Munoz R, Celma ML. Measles virus from a long-term persistently infected human T lymphoblastoid cell line, in contrast to the cytotoxic parental virus, establishes an immediate persistence in the original cell line. *J Gen Virol* 1992; 73 (Pt 9): 2195-2202.

Feys T, Poppe B, De Preter K, Van Roy N, Verhasselt B, De Paepe P, De Paepe A, Speleman F. A detailed inventory of DNA copy number alterations in four commonly used Hodgkin's lymphoma cell lines. *Haematologica* 2007a; 92: 913-920.

Feys T, Poppe B, Verhasselt B, De Paepe P, Menten B, Vandesompele J, Van Roy N, De Paepe A, Speleman F. Array CGH analysis of subnanogram quantities of DNA using whole genome amplification: opportunities for detection of copy number alterations in Hodgkin's lymphoma. 7th International Symposium on Hodgkin Lymphoma (3-4th November 2007) 2007b; abs 097.

Fiegler H, Carr P, Douglas EJ, Burford DC, Hunt S, Scott CE, Smith J, Vetrie D, Gorman P, Tomlinson IP, Carter NP. DNA microarrays for comparative genomic hybridization based on DOP-PCR amplification of BAC and PAC clones. *Genes Chromosomes Cancer* 2003; 36: 361-374.

Flavell K, Constandinou C, Lowe D, Scott K, Newey C, Evans D, Dutton A, Simmons S, Smith R, Crocker J, Young LS, Murray P. Effect of material deprivation on Epstein-Barr virus infection in Hodgkin's disease in the West Midlands. *Br J Cancer* 1999; 80: 604-608.

Flemming W. Zellsubstanz, Kern und Zellteilung. 1882.

Ford CE, Hamerton JL. A colchicine, hypotonic citrate, squash sequence for mammalian chromosomes. *Stain Technol* 1956a; 31: 247.

Ford CE, Hamerton JL. The chromosomes of man. *Nature* 1956b; 178: 1020-1023.

Gall JG, Pardue ML. Formation and detection of RNA-DNA hybrid molecules in cytological preparations. *Proc Natl Acad Sci U S A* 1969; 63: 378-383.

Gallagher A, Perry J, Freeland J, Alexander FE, Carman WF, Shield L, Cartwright R, Jarrett RF. Hodgkin lymphoma and Epstein-Barr virus (EBV): no evidence to support hit-and-run mechanism in cases classified as non-EBV-associated. *Int J Cancer* 2003; 104: 624-630.

Gallagher A, Perry J, Shield L, Freeland J, MacKenzie J, Jarrett RF. Viruses and Hodgkin disease: no evidence of novel herpesviruses in non-EBV-associated lesions. *Int J Cancer* 2002; 101: 259-264.

Garcia JF, Camacho FI, Morente M, Fraga M, Montalban C, Alvaro T, Bellas C, Castano A, Diez A, Flores T, Martin C, Martinez MA, Mazorra F, Menarguez J, Mestre MJ, Mollejo M, Saez AI, Sanchez L, Piris MA. Hodgkin and Reed-Sternberg cells harbor alterations in the major tumor suppressor pathways and cell-cycle checkpoints: analyses using tissue microarrays. *Blood* 2003; 101: 681-689.

Gardner SD, Field AM, Coleman DV. New human papovavirus (BK) isolated from urine after renal transplantation. *Lancet* 1971; 1: 1253-1257.

Garson JA, van den Berghe JA, Kemshead JT. Novel non-isotopic in situ hybridization technique detects small (1 Kb) unique sequences in routinely G-banded

human chromosomes: fine mapping of N-myc and beta-NGF genes. *Nucleic Acids Res* 1987; 15: 4761-4770.

Gaynor AM, Nissen MD, Whiley DM, Mackay IM, Lambert SB, Wu G, Brennan DC, Storch GA, Sloots TP, Wang D. Identification of a novel polyomavirus from patients with acute respiratory tract infections. *PLoS Pathog* 2007; 3: e64.

Gires O, Kohlhuber F, Kilger E, Baumann M, Kieser A, Kaiser C, Zeidler R, Scheffer B, Ueffing M, Hammerschmidt W. Latent membrane protein 1 of Epstein-Barr virus interacts with JAK3 and activates STAT proteins. *EMBO J* 1999; 18: 3064-3073.

Gjerdrum LM, Hamilton-Dutoit S. Laser-assisted microdissection of membrane-mounted sections following immunohistochemistry and in situ hybridization. *Methods Mol Biol* 2005; 293: 139-149.

Glaser SL. Regional variation in Hodgkin's disease incidence by histologic subtype in the US. *Cancer* 1987; 60: 2841-2847.

Glaser SL, Keegan TH, Clarke CA, Trinh M, Dorfman RF, Mann RB, DiGiuseppe JA, Ambinder RF. Exposure to childhood infections and risk of Epstein-Barr virus--defined Hodgkin's lymphoma in women. *Int J Cancer* 2005; 115: 599-605.

Glaser SL, Lin RJ, Stewart SL, Ambinder RF, Jarrett RF, Brousset P, Pallesen G, Gulley ML, Khan G, O'Grady J, Hummel M, Preciado MV, Knecht H, Chan JK, Claviez A. Epstein-Barr virus-associated Hodgkin's disease: epidemiologic characteristics in international data. *Int J Cancer* 1997; 70: 375-382.

Glaser SL, Swartz WG. Time trends in Hodgkin's disease incidence. The role of diagnostic accuracy. *Cancer* 1990; 66: 2196-2204.

Gledhill S, Gallagher A, Jones DB, Krajewski AS, Alexander FE, Klee E, Wright DH, O'Brien C, Onions DE, Jarrett RF. Viral involvement in Hodgkin's disease: detection of clonal type A Epstein-Barr virus genomes in tumour samples. *Br J Cancer* 1991; 64: 227-232.

Gopas J, Itzhaky D, Segev Y, Salzberg S, Trink B, Isakov N, Rager-Zisman B. Persistent measles virus infection enhances major histocompatibility complex class I expression and immunogenicity of murine neuroblastoma cells. *Cancer Immunol Immunother* 1992; 34: 313-320.

Graham B, Gibson SB. The two faces of NFkappaB in cell survival responses. *Cell Cycle* 2005; 4: 1342-1345.

Griffin DE. Measles Virus. In: Knipe DM, Howley PM, Griffin DE, Lamb RA, Martin MA, Roizman B, Straus SE, eds. *Fields Virology*. Philadelphia: Lippincott, Williams & Wilkins, 2001.

Grote D, Russell SJ, Cornu TI, Cattaneo R, Vile R, Poland GA, Fielding AK. Live attenuated measles virus induces regression of human lymphoma xenografts in immunodeficient mice. *Blood* 2001; 97: 3746-3754.

Gruss HJ, Kadin ME. Pathophysiology of Hodgkin's disease: functional and molecular aspects. *Baillieres Clin Haematol* 1996; 9: 417-446.

Gulley ML, Eagan PA, Quintanilla-Martinez L, Picado AL, Smir BN, Childs C, Dunn CD, Craig FE, Williams JW, Jr., Banks PM. Epstein-Barr virus DNA is abundant and monoclonal in the Reed-Sternberg cells of Hodgkin's disease: association with mixed cellularity subtype and Hispanic American ethnicity. *Blood* 1994; 83: 1595-1602.

Gutensohn N, Cole P. Childhood social environment and Hodgkin's disease. *N Engl J Med* 1981; 304: 135-140.

Gutensohn NM. Social class and age at diagnosis of Hodgkin's disease: new epidemiologic evidence for the "two-disease hypothesis". *Cancer Treat Rep* 1982; 66: 689-695.

Hansmann ML, Kaiserling E. The lacunar cells and its relationship to interdigitating reticulum cells. *Virchows Arch B Cell Pathol Incl Mol Pathol* 1982; 39: 323-332.

Harris NL, Jaffe ES, Diebold J, Flandrin G, Muller-Hermelink HK, Vardiman J, Lister TA, Bloomfield CD. The World Health Organization classification of neoplastic diseases of the haematopoietic and lymphoid tissues: Report of the Clinical Advisory Committee Meeting, Airlie House, Virginia, November 1997.

Histopathology 2000; 36: 69-86.

Harris NL, Jaffe ES, Stein H, Banks PM, Chan JK, Cleary ML, Delsol G, Wolf-Peeters C, Falini B, Gatter KC, . A revised European-American classification of lymphoid neoplasms: a proposal from the International Lymphoma Study Group. *Blood* 1994; 84: 1361-1392.

Hayami T, Shukunami C, Mitsui K, Endo N, Tokunaga K, Kondo J, Takahashi HE, Hiraki Y. Specific loss of chondromodulin-I gene expression in chondrosarcoma and the suppression of tumor angiogenesis and growth by its recombinant protein in vivo. *FEBS Lett* 1999; 458: 436-440.

Haybittle JL, Hayhoe FG, Easterling MJ, Jelliffe AM, Bennett MH, Vaughan HG, Vaughan HB, MacLennan KA. Review of British National Lymphoma Investigation

studies of Hodgkin's disease and development of prognostic index. *Lancet* 1985; 1: 967-972.

Henle G, Henle W. Immunofluorescence in cells derived from Burkitt's lymphoma. *J Bacteriol* 1966; 91: 1248-1256.

Herbst H, Samol J, Foss HD, Raff T, Niedobitek G. Modulation of interleukin-6 expression in Hodgkin and Reed-Sternberg cells by Epstein-Barr virus. *J Pathol* 1997; 182: 299-306.

Herbst H, Steinbrecher E, Niedobitek G, Young LS, Brooks L, Muller-Lantzsch N, Stein H. Distribution and phenotype of Epstein-Barr virus-harboring cells in Hodgkin's disease. *Blood* 1992; 80: 484-491.

Hirose Y, Aldape K, Takahashi M, Berger MS, Feuerstein BG. Tissue microdissection and degenerate oligonucleotide primed-polymerase chain reaction (DOP-PCR) is an effective method to analyze genetic aberrations in invasive tumors. *J Mol Diagn* 2001; 3: 62-67.

Hjalgrim H, Askling J, Rostgaard K, Hamilton-Dutoit S, Frisch M, Zhang JS, Madsen M, Rosdahl N, Konradsen HB, Storm HH, Melbye M. Characteristics of Hodgkin's lymphoma after infectious mononucleosis. *N Engl J Med* 2003; 349: 1324-1332.

Hodgkin T. On some morbid appearances of the absorbent glands and spleen. *Medical Chirurgical Transactions* 1832; 17: 68-114.

Holman CD, Matz LR, Finlay-Jones LR, Waters ED, Blackwell JB, Joyce PR, Kelsall GR, Shilkin KB, Cullity GJ, Williams KE, Matthews ML, Armstrong BK. Inter-

observer variation in the histopathological reporting of Hodgkin's disease: an analysis of diagnostic subcomponents using kappa statistics. *Histopathology* 1983; 7: 399-407.

Houff SA, Major EO, Katz DA, Kufta CV, Sever JL, Pittaluga S, Roberts JR, Gitt J, Saini N, Lux W. Involvement of JC virus-infected mononuclear cells from the bone marrow and spleen in the pathogenesis of progressive multifocal leukoencephalopathy. *N Engl J Med* 1988; 318: 301-305.

Hsu TC. Mammalian chromosomes in vitro: I. The karyotype of man. *J Hered* 1952; 43: 167-172.

Huang Q, Sacks PG, Mo J, McCormick SA, Iacob CE, Guo L, Schaefer S, Schantz SP. A simple method for fixation and microdissection of frozen fresh tissue sections for molecular cytogenetic analysis of cancers. *Biotech Histochem* 2005a; 80: 147-156.

Huang Q, Sacks PG, Mo J, McCormick SA, Iacob CE, Guo L, Schaefer S, Schantz SP. A simple method for fixation and microdissection of frozen fresh tissue sections for molecular cytogenetic analysis of cancers. *Biotech Histochem* 2005b; 80: 147-156.

Huang Q, Schantz SP, Rao PH, Mo J, McCormick SA, Chaganti RS. Improving degenerate oligonucleotide primed PCR-comparative genomic hybridization for analysis of DNA copy number changes in tumors. *Genes Chromosomes Cancer* 2000; 28: 395-403.

Huen DS, Henderson SA, Croom-Carter D, Rowe M. The Epstein-Barr virus latent membrane protein-1 (LMP1) mediates activation of NF-kappa B and cell surface phenotype via two effector regions in its carboxy-terminal cytoplasmic domain. *Oncogene* 1995; 10: 549-560.

Hughes S, Lim G, Beheshti B, Bayani J, Marrano P, Huang A, Squire JA. Use of whole genome amplification and comparative genomic hybridisation to detect chromosomal copy number alterations in cell line material and tumour tissue. *Cytogenet Genome Res* 2004; 105: 18-24.

Hummel KB, Vanchiere JA, Bellini WJ. Restriction of fusion protein mRNA as a mechanism of measles virus persistence. *Virology* 1994; 202: 665-672.

Hurst CD, Fiegler H, Carr P, Williams S, Carter NP, Knowles MA. High-resolution analysis of genomic copy number alterations in bladder cancer by microarray-based comparative genomic hybridization. *Oncogene* 2004; 23: 2250-2263.

Iafate AJ, Feuk L, Rivera MN, Listewnik ML, Donahoe PK, Qi Y, Scherer SW, Lee C. Detection of large-scale variation in the human genome. *Nat Genet* 2004; 36: 949-951.

Jacobson S, McFarland HF. Measles virus persistence in human lymphocytes: a role for virus-induced interferon. *J Gen Virol* 1982; 63: 351-357.

Jarrett AF, Armstrong AA, Alexander E. Epidemiology of EBV and Hodgkin's lymphoma. *Ann Oncol* 1996; 7 Suppl 4: 5-10.

Jarrett RF. Viruses and Hodgkin's lymphoma. *Ann Oncol* 2002; 13 Suppl 1: 23-29.

Jarrett RF, Johnson D, Wilson KS, Gallagher A. Molecular methods for virus discovery. *Dev Biol (Basel)* 2006; 123: 77-88.

Jarrett RF, Krajewski AS, Angus B, Freeland J, Taylor PR, Taylor GM, Alexander FE. The Scotland and Newcastle epidemiological study of Hodgkin's disease: impact

of histopathological review and EBV status on incidence estimates. *J Clin Pathol* 2003; 56: 811-816.

Joos S, Granzow M, Holtgreve-Grez H, Siebert R, Harder L, Martin-Subero JI, Wolf J, Adamowicz M, Barth TF, Lichter P, Jauch A. Hodgkin's lymphoma cell lines are characterized by frequent aberrations on chromosomes 2p and 9p including REL and JAK2. *Int J Cancer* 2003; 103: 489-495.

Joos S, Kupper M, Ohl S, von Bonin F, Mechttersheimer G, Bentz M, Marynen P, Moller P, Pfreundschuh M, Trumper L, Lichter P. Genomic imbalances including amplification of the tyrosine kinase gene JAK2 in CD30+ Hodgkin cells. *Cancer Res* 2000; 60: 549-552.

Joos S, Menz CK, Wrobel G, Siebert R, Gesk S, Ohl S, Mechttersheimer G, Trumper L, Moller P, Lichter P, Barth TF. Classical Hodgkin lymphoma is characterized by recurrent copy number gains of the short arm of chromosome 2. *Blood* 2002; 99: 1381-1387.

Joos S, Otano-Joos MI, Ziegler S, Bruderlein S, du MS, Bentz M, Moller P, Lichter P. Primary mediastinal (thymic) B-cell lymphoma is characterized by gains of chromosomal material including 9p and amplification of the REL gene. *Blood* 1996; 87: 1571-1578.

Joseph BS, Lampert PW, Oldstone MB. Replication and persistence of measles virus in defined subpopulations of human leukocytes. *J Virol* 1975; 16: 1638-1649.

Josting A, Wolf J, Diehl V. Hodgkin disease: prognostic factors and treatment strategies. *Curr Opin Oncol* 2000; 12: 403-411.

Jungnickel B, Staratschek-Jox A, Brauninger A, Spieker T, Wolf J, Diehl V, Hansmann ML, Rajewsky K, Kuppers R. Clonal deleterious mutations in the IkappaBalpha gene in the malignant cells in Hodgkin's lymphoma. *J Exp Med* 2000; 191: 395-402.

Kallioniemi A, Kallioniemi OP, Sudar D, Rutovitz D, Gray JW, Waldman F, Pinkel D. Comparative genomic hybridization for molecular cytogenetic analysis of solid tumors. *Science* 1992; 258: 818-821.

Kallioniemi OP, Kallioniemi A, Piper J, Isola J, Waldman FM, Gray JW, Pinkel D. Optimizing comparative genomic hybridization for analysis of DNA sequence copy number changes in solid tumors. *Genes Chromosomes Cancer* 1994; 10: 231-243.

Kanzler H, Hansmann ML, Kapp U, Wolf J, Diehl V, Rajewsky K, Kuppers R. Molecular single cell analysis demonstrates the derivation of a peripheral blood-derived cell line (L1236) from the Hodgkin/Reed-Sternberg cells of a Hodgkin's lymphoma patient. *Blood* 1996a; 87: 3429-3436.

Kanzler H, Kuppers R, Hansmann ML, Rajewsky K. Hodgkin and Reed-Sternberg cells in Hodgkin's disease represent the outgrowth of a dominant tumor clone derived from (crippled) germinal center B cells. *J Exp Med* 1996b; 184: 1495-1505.

Karin M. How NF-kappaB is activated: the role of the IkappaB kinase (IKK) complex. *Oncogene* 1999; 18: 6867-6874.

Kawashima H, Mori T, Takekuma K, Hoshika A, Hata M, Nakayama T. Polymerase chain reaction detection of the hemagglutinin gene from an attenuated measles vaccine strain in the peripheral mononuclear cells of children with autoimmune hepatitis. *Arch Virol* 1996; 141: 877-884.

Kaye KM, Izumi KM, Kieff E. Epstein-Barr virus latent membrane protein 1 is essential for B-lymphocyte growth transformation. *Proc Natl Acad Sci U S A* 1993; 90: 9150-9154.

Kistler A, Avila PC, Rouskin S, Wang D, Ward T, Yagi S, Schnurr D, Ganem D, DeRisi JL, Boushey HA. Pan-viral screening of respiratory tract infections in adults with and without asthma reveals unexpected human coronavirus and human rhinovirus diversity. *J Infect Dis* 2007; 196: 817-825.

Klein G, Giovanella BC, Lindahl T, Fialkow PJ, Singh S, Stehlin JS. Direct evidence for the presence of Epstein-Barr virus DNA and nuclear antigen in malignant epithelial cells from patients with poorly differentiated carcinoma of the nasopharynx. *Proc Natl Acad Sci U S A* 1974; 71: 4737-4741.

Klimm B, Schnell R, Diehl V, Engert A. Current treatment and immunotherapy of Hodgkin's lymphoma. *Haematologica* 2005; 90: 1680-1692.

Kluiver J, Kok K, Pfeil I, de Jong D, Blokzijl T, Harms G, van d, V, Diepstra A, Atayar C, Poppema S, Kuppers R, van den BA. Global correlation of genome and transcriptome changes in classical Hodgkin lymphoma. *Hematol Oncol* 2007; 25: 21-29.

Knoll A, Stoehr R, Jilg W, Hartmann A. Low frequency of human polyomavirus BKV and JCV DNA in urothelial carcinomas of the renal pelvis and renal cell carcinomas. *Oncol Rep* 2003; 10: 487-491.

Kornberg A, Baker TA. DNA replication. San Francisco: W.H.Freeman and Company, 1992.

Krynska B, Del Valle L, Croul S, Gordon J, Katsetos CD, Carbone M, Giordano A, Khalili K. Detection of human neurotropic JC virus DNA sequence and expression of the viral oncogenic protein in pediatric medulloblastomas. *Proc Natl Acad Sci U S A* 1999; 96: 11519-11524.

Kuchiki H, Saino M, Nobukuni T, Yasuda J, Maruyama T, Kayama T, Murakami Y, Sekiya T. Detection of amplification of a chromosomal fragment at 6p21 including the cyclin D3 gene in a glioblastoma cell line by arbitrarily primed polymerase chain reaction. *Int J Cancer* 2000; 85: 113-116.

Kuppers R, Brauning A, Muschen M, Distler V, Hansmann ML, Rajewsky K. Evidence that Hodgkin and Reed-Sternberg cells in Hodgkin disease do not represent cell fusions. *Blood* 2001; 97: 818-821.

Kuppers R, Hansmann ML. The Hodgkin and Reed/Sternberg cell. *Int J Biochem Cell Biol* 2005; 37: 511-517.

Kuppers R, Rajewsky K, Zhao M, Simons G, Laumann R, Fischer R, Hansmann ML. Hodgkin disease: Hodgkin and Reed-Sternberg cells picked from histological sections show clonal immunoglobulin gene rearrangements and appear to be derived from B cells at various stages of development. *Proc Natl Acad Sci U S A* 1994; 91: 10962-10966.

Langer-Safer PR, Levine M, Ward DC. Immunological method for mapping genes on *Drosophila* polytene chromosomes. *Proc Natl Acad Sci U S A* 1982; 79: 4381-4385.

Lee W, Langhoff E. Polyomavirus in human cancer development. *Adv Exp Med Biol* 2006; 577: 310-318.

Leoncini L, Vindigni C, Megha T, Funto I, Pacenti L, Musaro M, Renieri A, Seri M, Anagnostopoulos J, Tosi P. Epstein-Barr virus and gastric cancer: data and unanswered questions. *Int J Cancer* 1993; 53: 898-901.

Levine PH, Ablashi DV, Berard CW, Carbone PP, Waggoner DE, Malan L. Elevated antibody titers to Epstein-Barr virus in Hodgkin's disease. *Cancer* 1971; 27: 416-421.

Lindahl T, Klein G, Reedman BM, Johansson B, Singh S. Relationship between Epstein-Barr virus (EBV) DNA and the EBV-determined nuclear antigen (EBNA) in Burkitt lymphoma biopsies and other lymphoproliferative malignancies. *Int J Cancer* 1974; 13: 764-772.

Lister TA, Crowther D, Sutcliffe SB, Glatstein E, Canellos GP, Young RC, Rosenberg SA, Coltman CA, Tubiana M. Report of a committee convened to discuss the evaluation and staging of patients with Hodgkin's disease: Cotswolds meeting. *J Clin Oncol* 1989; 7: 1630-1636.

Liu H, Ippolito GC, Wall JK, Niu T, Probst L, Lee BS, Pulford K, Banham AH, Stockwin L, Shaffer AL, Staudt LM, Das C, Dyer MJ, Tucker PW. Functional studies of BCL11A: characterization of the conserved BCL11A-XL splice variant and its interaction with BCL6 in nuclear paraspeckles of germinal center B cells. *Mol Cancer* 2006; 5: 18.

Lones MA, Heerema NA, Le Beau MM, Sposto R, Perkins SL, Kadin ME, Kjeldsberg CR, Meadows A, Siegel S, Buckley J, Abromowitch M, Kersey J, Bergeron S, Cairo MS, Sanger WG. Chromosome abnormalities in advanced stage lymphoblastic lymphoma of children and adolescents: a report from CCG-E08. *Cancer Genet Cytogenet* 2007; 172: 1-11.

Longnecker R, Kieff E. A second Epstein-Barr virus membrane protein (LMP2) is expressed in latent infection and colocalizes with LMP1. *J Virol* 1990; 64: 2319-2326.

Ludecke HJ, Senger G, Claussen U, Horsthemke B. Cloning defined regions of the human genome by microdissection of banded chromosomes and enzymatic amplification. *Nature* 1989; 338: 348-350.

Lukes RJ, Butler JJ. The pathology and nomenclature of Hodgkin's disease. *Cancer Res* 1966; 26: 1063-1083.

Mabuchi H, Fujii H, Calin G, Alder H, Negrini M, Rassenti L, Kipps TJ, Bullrich F, Croce CM. Cloning and characterization of CLLD6, CLLD7, and CLLD8, novel candidate genes for leukemogenesis at chromosome 13q14, a region commonly deleted in B-cell chronic lymphocytic leukemia. *Cancer Res* 2001; 61: 2870-2877.

MacKenzie J, Greaves MF, Eden TO, Clayton RA, Perry J, Wilson KS, Jarrett RF. The putative role of transforming viruses in childhood acute lymphoblastic leukemia. *Haematologica* 2006; 91: 240-243.

MacKenzie J, Wilson KS, Perry J, Gallagher A, Jarrett RF. Association between simian virus 40 DNA and lymphoma in the United Kingdom. *J Natl Cancer Inst* 2003; 95: 1001-1003.

MacMahon B. Epidemiology of Hodgkin's disease. *Cancer Res* 1966; 26: 1189-1201.

Maggio E, Benharroch D, Gopas J, Dittmer U, Hansmann ML, Kuppers R. Absence of measles virus genome and transcripts in Hodgkin-Reed/Sternberg cells of a cohort of Hodgkin lymphoma patients. *Int J Cancer* 2007; 121: 448-453.

Magrath I. The pathogenesis of Burkitt's lymphoma. *Adv Cancer Res* 1990; 55: 133-270.

Major EO, Vacante DA. Human fetal astrocytes in culture support the growth of the neurotropic human polyomavirus, JCV. *J Neuropathol Exp Neurol* 1989; 48: 425-436.

Mancao C, Altmann M, Jungnickel B, Hammerschmidt W. Rescue of "crippled" germinal center B cells from apoptosis by Epstein-Barr virus. *Blood* 2005; 106: 4339-4344.

Marafioti T, Hummel M, Foss HD, Laumen H, Korbjuhn P, Anagnostopoulos I, Lammert H, Demel G, Theil J, Wirth T, Stein H. Hodgkin and reed-sternberg cells represent an expansion of a single clone originating from a germinal center B-cell with functional immunoglobulin gene rearrangements but defective immunoglobulin transcription. *Blood* 2000; 95: 1443-1450.

Martin-Subero JJ, Gesk S, Harder L, Sonoki T, Tucker PW, Schlegelberger B, Grote W, Novo FJ, Calasanz MJ, Hansmann ML, Dyer MJ, Siebert R. Recurrent involvement of the REL and BCL11A loci in classical Hodgkin lymphoma. *Blood* 2002; 99: 1474-1477.

Martin-Subero JJ, Klapper W, Sotnikova A, Callet-Bauchu E, Harder L, Bastard C, Schmitz R, Grohmann S, Hoppner J, Riemke J, Barth TF, Berger F, Bernd HW, Claviez A, Gesk S, Frank GA, Kaplanskaya IB, Moller P, Parwaresch RM, Rudiger T et al. Chromosomal breakpoints affecting immunoglobulin loci are recurrent in Hodgkin and Reed-Sternberg cells of classical Hodgkin lymphoma. *Cancer Res* 2006; 66: 10332-10338.

McAulay KA, Higgins CD, Macsween KF, Lake A, Jarrett RF, Robertson FL, Williams H, Crawford DH. HLA class I polymorphisms are associated with development of infectious mononucleosis upon primary EBV infection. *J Clin Invest* 2007; 117: 3042-3048.

McKinney PA, Alexander FE, Ricketts TJ, Williams J, Cartwright RA. A specialist leukaemia/lymphoma registry in the UK. Part 1: Incidence and geographical distribution of Hodgkin's disease. Leukaemia Research Fund Data Collection Study Group. *Br J Cancer* 1989; 60: 942-947.

McQuaid S, Cosby SL. An immunohistochemical study of the distribution of the measles virus receptors, CD46 and SLAM, in normal human tissues and subacute sclerosing panencephalitis. *Lab Invest* 2002; 82: 403-409.

Merk K, Bjorkholm M, Rengifo E, Gavilondo J, Holm G, Rivas H. Epidemiological study of Hodgkin's disease in Cuba and Sweden. *Oncology* 1990; 47: 246-250.

Messineo C, Jamerson MH, Hunter E, Braziel R, Bagg A, Irving SG, Cossman J. Gene expression by single Reed-Sternberg cells: pathways of apoptosis and activation. *Blood* 1998; 91: 2443-2451.

Minagawa T, Sakuma T. Growth of measles virus in various human lymphoid cell lines. *Microbiol Immunol* 1977; 21: 23-31.

Monni O, Joensuu H, Franssila K, Knuutila S. DNA copy number changes in diffuse large B-cell lymphoma--comparative genomic hybridization study. *Blood* 1996; 87: 5269-5278.

Morandi L, Marucci G, Foschini MP, Cattani MG, Pession A, Riva C, Eusebi V.

Genetic similarities and differences between lobular in situ neoplasia (LN) and invasive lobular carcinoma of the breast. *Virchows Arch* 2006; 449: 14-23.

Morohara K, Nakao K, Tajima Y, Nishino N, Yamazaki K, Kaetsu T, Suzuki S, Tsunoda A, Kawamura M, Aida T, Tachikawa T, Kusano M. Analysis by comparative genomic hybridization of gastric cancer with peritoneal dissemination and/or positive peritoneal cytology. *Cancer Genet Cytogenet* 2005; 161: 57-62.

Mota HC. Infantile Hodgkin's disease: remission after measles. *Br Med J* 1973; 2: 421.

Munoz N, Davidson RJ, Witthoff B, Ericsson JE, De The G. Infectious mononucleosis and Hodgkin's disease. *Int J Cancer* 1978; 22: 10-13.

Muschen M, Rajewsky K, Brauninger A, Baur AS, Oudejans JJ, Roers A, Hansmann ML, Kuppers R. Rare occurrence of classical Hodgkin's disease as a T cell lymphoma. *J Exp Med* 2000a; 191: 387-394.

Muschen M, Re D, Brauninger A, Wolf J, Hansmann ML, Diehl V, Kuppers R, Rajewsky K. Somatic mutations of the CD95 gene in Hodgkin and Reed-Sternberg cells. *Cancer Res* 2000b; 60: 5640-5643.

Nagel S, Scherr M, Quentmeier H, Kaufmann M, Zaborski M, Drexler HG, Macleod RA. HLXB9 activates IL6 in Hodgkin lymphoma cell lines and is regulated by PI3K signalling involving E2F3. *Leukemia* 2005; 19: 841-846.

Nickeleit V, Hirsch HH, Binet IF, Gudat F, Prince O, Dalquen P, Thiel G, Mihatsch MJ. Polyomavirus infection of renal allograft recipients: from latent infection to manifest disease. *J Am Soc Nephrol* 1999; 10: 1080-1089.

Niedobitek G. LPA signalling stimulates Hodgkin research. *Blood* 2006; 106: 1898-1899.

Niedobitek G, Kremmer E, Herbst H, Whitehead L, Dawson CW, Niedobitek E, von Ostau C, Rooney N, Grasser FA, Young LS. Immunohistochemical detection of the Epstein-Barr virus-encoded latent membrane protein 2A in Hodgkin's disease and infectious mononucleosis. *Blood* 1997; 90: 1664-1672.

Nogova L, Rudiger T, Engert A. Biology, clinical course and management of nodular lymphocyte-predominant Hodgkin lymphoma. *Hematology Am Soc Hematol Educ Program* 2006; 266-272.

Nonkwelo C, Skinner J, Bell A, Rickinson A, Sample J. Transcription start sites downstream of the Epstein-Barr virus (EBV) Fp promoter in early-passage Burkitt lymphoma cells define a fourth promoter for expression of the EBV EBNA-1 protein. *J Virol* 1996; 70: 623-627.

Olsson AY, Feber A, Edwards S, Te PR, Giddings I, Merson S, Cooper CS. Role of E2F3 expression in modulating cellular proliferation rate in human bladder and prostate cancer cells. *Oncogene* 2007; 26: 1028-1037.

Orlic M, Spencer CE, Wang L, Gallie BL. Expression analysis of 6p22 genomic gain in retinoblastoma. *Genes Chromosomes Cancer* 2006; 45: 72-82.

Padgett BL, Walker DL. Prevalence of antibodies in human sera against JC virus, an isolate from a case of progressive multifocal leukoencephalopathy. *J Infect Dis* 1973; 127: 467-470.

Padgett BL, Walker DL, Zu Rhein GM, Eckroade RJ, Dessel BH. Cultivation of papova-like virus from human brain with progressive multifocal leukoencephalopathy. *Lancet* 1971; 1: 1257-1260.

Pallesen G, Hamilton-Dutoit SJ, Rowe M, Young LS. Expression of Epstein-Barr virus latent gene products in tumour cells of Hodgkin's disease. *Lancet* 1991; 337: 320-322.

Patsouris E, Noel H, Lennert K. Cytohistologic and immunohistochemical findings in Hodgkin's disease, mixed cellularity type, with a high content of epithelioid cells. *Am J Surg Pathol* 1989; 13: 1014-1022.

Pavone V, Guarini A, Liso V. Early autologous stem cell transplantation in Hodgkin disease in partial remission or in relapse. *Haematologica* 1997; 82: 638-639.

Peng DF, Sugihara H, Mukaisho K, Ling ZQ, Hattori T. Genetic lineage of poorly differentiated gastric carcinoma with a tubular component analysed by comparative genomic hybridization. *J Pathol* 2004; 203: 884-895.

Peng DF, Sugihara H, Mukaisho K, Tsubosa Y, Hattori T. Alterations of chromosomal copy number during progression of diffuse-type gastric carcinomas: metaphase- and array-based comparative genomic hybridization analyses of multiple samples from individual tumours. *J Pathol* 2003; 201: 439-450.

Peng KW, Ahmann GJ, Pham L, Greipp PR, Cattaneo R, Russell SJ. Systemic therapy of myeloma xenografts by an attenuated measles virus. *Blood* 2001; 98: 2002-2007.

Phillips JL, Hayward SW, Wang Y, Vasselli J, Pavlovich C, Padilla-Nash H, Pezullo JR, Ghadimi BM, Grossfeld GD, Rivera A, Linehan WM, Cunha GR, Ried T. The consequences of chromosomal aneuploidy on gene expression profiles in a cell line model for prostate carcinogenesis. *Cancer Res* 2001; 61: 8143-8149.

Pileri SA, Ascani S, Leoncini L, Sabattini E, Zinzani PL, Piccaluga PP, Pileri A, Jr., Giunti M, Falini B, Bolis GB, Stein H. Hodgkin's lymphoma: the pathologist's viewpoint. *J Clin Pathol* 2002; 55: 162-176.

Pinkel D, Se Graves R, Sudar D, Clark S, Poole I, Kowbel D, Collins C, Kuo WL, Chen C, Zhai Y, Dairkee SH, Ljung BM, Gray JW, Albertson DG. High resolution analysis of DNA copy number variation using comparative genomic hybridization to microarrays. *Nat Genet* 1998; 20: 207-211.

Pollack JR, Perou CM, Alizadeh AA, Eisen MB, Pergamenschikov A, Williams CF, Jeffrey SS, Botstein D, Brown PO. Genome-wide analysis of DNA copy-number changes using cDNA microarrays. *Nat Genet* 1999; 23: 41-46.

Poppema S, van den Berg A. Interaction between host T cells and Reed-Sternberg cells in Hodgkin lymphomas. *Semin Cancer Biol* 2000; 10: 345-350.

Poppema S, van Imhoff G, Torensma R, Smit J. Lymphadenopathy morphologically consistent with Hodgkin's disease associated with Epstein-Barr virus infection. *Am J Clin Pathol* 1985; 84: 385-390.

Poppema S, Visser L. Epstein-Barr virus positivity in Hodgkin's disease does not correlate with an HLA A2-negative phenotype. *Cancer* 1994; 73: 3059-3063.

Portis T, Dyck P, Longnecker R. Epstein-Barr Virus (EBV) LMP2A induces alterations in gene transcription similar to those observed in Reed-Sternberg cells of Hodgkin lymphoma. *Blood* 2003; 102: 4166-4178.

Portis T, Ikeda M, Longnecker R. Epstein-Barr virus LMP2A: regulating cellular ubiquitination processes for maintenance of viral latency? *Trends Immunol* 2004; 25: 422-426.

Pyakurel P, Montag U, Castanos-Velez E, Kaaya E, Christensson B, Tonnies H, Biberfeld P, Heiden T. CGH of microdissected Kaposi's sarcoma lesions reveals recurrent loss of chromosome Y in early and additional chromosomal changes in late tumour stages. *AIDS* 2006; 20: 1805-1812.

Rajewsky K. Clonal selection and learning in the antibody system. *Nature* 1996; 381: 751-758.

Rambaldi A, Bettoni S, Tosi S, Giudici G, Schiro R, Borleri GM, Abbate M, Chiaffarino F, Colotta F, Barbui T, . Establishment and characterization of a new granulocyte-macrophage colony-stimulating factor-dependent and interleukin-3-dependent human acute myeloid leukemia cell line (GF-D8). *Blood* 1993; 81: 1376-1383.

Rencic A, Gordon J, Otte J, Curtis M, Kovatich A, Zoltick P, Khalili K, Andrews D. Detection of JC virus DNA sequence and expression of the viral oncoprotein, tumor antigen, in brain of immunocompetent patient with oligoastrocytoma. *Proc Natl Acad Sci U S A* 1996; 93: 7352-7357.

Reynolds GM, Billingham LJ, Gray LJ, Flavell JR, Najafipour S, Crocker J, Nelson P, Young LS, Murray PG. Interleukin 6 expression by Hodgkin/Reed-Sternberg cells is associated with the presence of 'B' symptoms and failure to achieve complete remission in patients with advanced Hodgkin's disease. *Br J Haematol* 2002; 118: 195-201.

Ricci-Vitiani L, Conticello C, Zeuner A, De Maria R. CD95/CD95L interactions and their role in autoimmunity. *Apoptosis* 2000; 5: 419-424.

Rickinson AB, Kieff E. Epstein-Barr virus. In: Fields BN, Knipe DM, Howley PM, eds. *Fields Virology*. Philadelphia: Lippincott, Williams & Wilkins, 2001: 2511-2573.

Rima BK, Davidson WB, Martin SJ. The role of defective interfering particles in persistent infection of Vero cells by measles virus. *J Gen Virol* 1977; 35: 89-97.

Rocchi G, Tosato G, Papa G, Ragona G. Antibodies to Epstein-Barr virus-associated nuclear antigen and to other viral and non-viral antigens in Hodgkin's disease. *Int J Cancer* 1975; 16: 323-328.

Rodig SJ, Savage KJ, Nguyen V, Pinkus GS, Shipp MA, Aster JC, Kutok JL. TRAF1 expression and c-Rel activation are useful adjuncts in distinguishing classical Hodgkin lymphoma from a subset of morphologically or immunophenotypically similar lymphomas. *Am J Surg Pathol* 2005; 29: 196-203.

Rollison DE, Helzlsouer KJ, Halsey NA, Shah KV, Viscidi RP. Markers of past infection with simian virus 40 (SV40) and risk of incident non-Hodgkin lymphoma in a Maryland cohort. *Cancer Epidemiol Biomarkers Prev* 2005; 14: 1448-1452.

Roscic-Mrkic B, Schwendener RA, Odermatt B, Zuniga A, Pavlovic J, Billeter MA, Cattaneo R. Roles of macrophages in measles virus infection of genetically modified mice. *J Virol* 2001; 75: 3343-3351.

Rowe M, Lear AL, Croom-Carter D, Davies AH, Rickinson AB. Three pathways of Epstein-Barr virus gene activation from EBNA1-positive latency in B lymphocytes. *J Virol* 1992; 66: 122-131.

Rustigian R. Persistent infection of cells in culture by measles virus. II. Effect of measles antibody on persistently infected HeLa sublines and recovery of a HeLa clonal line persistently infected with incomplete virus. *J Bacteriol* 1966; 92: 1805-1811.

Santos GC, Zielenska M, Prasad M, Squire JA. Chromosome 6p amplification and cancer progression. *J Clin Pathol* 2007; 60: 1-7.

Satterwhite E, Sonoki T, Willis TG, Harder L, Nowak R, Arriola EL, Liu H, Price HP, Gesk S, Steinemann D, Schlegelberger B, Oscier DG, Siebert R, Tucker PW, Dyer MJ. The BCL11 gene family: involvement of BCL11A in lymphoid malignancies. *Blood* 2001; 98: 3413-3420.

Schaadt E, Baier B, Mautner J, Bornkamm GW, Adler B. Epstein-Barr virus latent membrane protein 2A mimics B-cell receptor-dependent virus reactivation. *J Gen Virol* 2005; 86: 551-559.

Schaadt M, Burrichter H, Pfreundschuh M, Schell-Frederick E, Tesch H, Fonatsch C, Stein H, Diehl V. Biology of Hodgkin cell lines. *Recent Results Cancer Res* 1989; 117: 53-61.

Schattner A. Therapeutic role of measles vaccine in Hodgkin's disease. *Lancet* 1984; 1: 171.

Schlegelberger B, Weber-Matthiesen K, Himmler A, Bartels H, Sonnen R, Kuse R, Feller AC, Grote W. Cytogenetic findings and results of combined immunophenotyping and karyotyping in Hodgkin's disease. *Leukemia* 1994; 8: 72-80.

Schmid C, Pan L, Diss T, Isaacson PG. Expression of B-cell antigens by Hodgkin's and Reed-Sternberg cells. *Am J Pathol* 1991; 139: 701-707.

Schraders M, Pfundt R, Straatman HM, Janssen IM, van Kessel AG, Schoenmakers EF, van Krieken JH, Groenen PJ. Novel chromosomal imbalances in mantle cell lymphoma detected by genome-wide array-based comparative genomic hybridization. *Blood* 2005; 105: 1686-1693.

Schrock E, Veldman T, Padilla-Nash H, Ning Y, Spurbeck J, Jalal S, Shaffer LG, Papenhausen P, Kozma C, Phelan MC, Kjeldsen E, Schonberg SA, O'Brien P, Biesecker L, du MS, Ried T. Spectral karyotyping refines cytogenetic diagnostics of constitutional chromosomal abnormalities. *Hum Genet* 1997; 101: 255-262.

Schuler F, Dolken SC, Hirt C, Dolken MT, Mentel R, Gurtler LG, Dolken G. No evidence for simian virus 40 DNA sequences in malignant non-Hodgkin lymphomas. *Int J Cancer* 2006; 118: 498-504.

Schwering I, Brauninger A, Distler V, Jesdinsky J, Diehl V, Hansmann ML, Rajewsky K, Kuppers R. Profiling of Hodgkin's lymphoma cell line L1236 and germinal center B cells: identification of Hodgkin's lymphoma-specific genes. *Mol Med* 2003a; 9: 85-95.

Schwering I, Brauninger A, Klein U, Jungnickel B, Tinguely M, Diehl V, Hansmann ML, Dalla-Favera R, Rajewsky K, Kuppers R. Loss of the B-lineage-specific gene expression program in Hodgkin and Reed-Sternberg cells of Hodgkin lymphoma.

Blood 2003b; 101: 1505-1512.

Seitz V, Hummel M, Marafioti T, Anagnostopoulos I, Assaf C, Stein H. Detection of clonal T-cell receptor gamma-chain gene rearrangements in Reed-Sternberg cells of classic Hodgkin disease. Blood 2000; 95: 3020-3024.

Shah KV. SV40 and human cancer: a review of recent data. Int J Cancer 2007; 120: 215-223.

Silins SL, Sculley TB. Modulation of vimentin, the CD40 activation antigen and Burkitt's lymphoma antigen (CD77) by the Epstein-Barr virus nuclear antigen EBNA-4. Virology 1994; 202: 16-24.

Skinnider BF, Elia AJ, Gascoyne RD, Patterson B, Trumper L, Kapp U, Mak TW. Signal transducer and activator of transcription 6 is frequently activated in Hodgkin and Reed-Sternberg cells of Hodgkin lymphoma. Blood 2002; 99: 618-626.

Sleckman BG, Mauch PM, Ambinder RF, Mann R, Pinkus GS, Kadin ME, Sherburne B, Perez-Atayde A, Thior I, Mueller N. Epstein-Barr virus in Hodgkin's disease: correlation of risk factors and disease characteristics with molecular evidence of viral infection. Cancer Epidemiol Biomarkers Prev 1998; 7: 1117-1121.

Smith RD, Galla JH, Skahan K, Anderson P, Linnemann CC, Jr., Ault GS, Ryschkewitsch CF, Stoner GL. Tubulointerstitial nephritis due to a mutant polyomavirus BK virus strain, BKV(Cin), causing end-stage renal disease. J Clin Microbiol 1998; 36: 1660-1665.

Snijders AM, Nowak N, Se Graves R, Blackwood S, Brown N, Conroy J, Hamilton G, Hindle AK, Huey B, Kimura K, Law S, Myambo K, Palmer J, Ylstra B, Yue JP, Gray JW, Jain AN, Pinkel D, Albertson DG. Assembly of microarrays for genome-wide measurement of DNA copy number. *Nat Genet* 2001; 29: 263-264.

Solinas-Toldo S, Lampel S, Stilgenbauer S, Nickolenko J, Benner A, Dohner H, Cremer T, Lichter P. Matrix-based comparative genomic hybridization: biochips to screen for genomic imbalances. *Genes Chromosomes Cancer* 1997; 20: 399-407.

Solomou EE, Sfikakis PP, Kotsi P, Papaioannou M, Karali V, Vervessou E, Hoffbrand AV, Panayiotidis P. 13q deletion in chronic lymphocytic leukemia: characterization of E4.5, a novel chromosome condensation regulator-like guanine nucleotide exchange factor. *Leuk Lymphoma* 2003; 44: 1579-1585.

Speicher MR, Gwyn BS, Ward DC. Karyotyping human chromosomes by combinatorial multi-fluor FISH. *Nat Genet* 1996; 12: 368-375.

Staal SP, Ambinder R, Beschorner WE, Hayward GS, Mann R. A survey of Epstein-Barr virus DNA in lymphoid tissue. Frequent detection in Hodgkin's disease. *Am J Clin Pathol* 1989; 91: 1-5.

Staratschek-Jox A, Kotkowski S, Belge G, Rudiger T, Bullerdiek J, Diehl V, Wolf J. Detection of Epstein-Barr virus in Hodgkin-Reed-Sternberg cells : no evidence for the persistence of integrated viral fragments in Latent membrane protein-1 (LMP-1)-negative classical Hodgkin's disease. *Am J Pathol* 2000; 156: 209-216.

Stein H, Hummel M, Marafioti T, Anagnostopoulos I, Foss HD. Molecular biology of Hodgkin's disease. *Cancer Surv* 1997; 30: 107-123.

Stokke T, DeAngelis P, Smedshammer L, Galteland E, Steen HB, Smeland EB, Delabie J, Holte H. Loss of chromosome 11q21-23.1 and 17p and gain of chromosome 6p are independent prognostic indicators in B-cell non-Hodgkin's lymphoma. *Br J Cancer* 2001; 85: 1900-1913.

Struski S, Helias C, Gervais C, Audhuy B, Zamfir A, Herbrecht R, Lessard M. 13q deletions in B-cell lymphoproliferative disorders: frequent association with translocation. *Cancer Genet Cytogenet* 2007; 174: 151-160.

Sui LF, Williamson J, Lowenthal RM, Parker AJ. Absence of simian virus 40 (SV40) DNA in lymphoma samples from Tasmania, Australia. *Pathology* 2005; 37: 157-159.

Taguchi F, Kajioka J, Miyamura T. Prevalence rate and age of acquisition of antibodies against JC virus and BK virus in human sera. *Microbiol Immunol* 1982; 26: 1057-1064.

Tanke HJ, Wiegant J, van Gijlswijk RP, Bezrookove V, Pattenier H, Heetebrij RJ, Talman EG, Raap AK, Vrolijk J. New strategy for multi-colour fluorescence in situ hybridisation: COBRA: COmbined Binary RATIO labelling. *Eur J Hum Genet* 1999; 7: 2-11.

Taqi AM, Abdurrahman MB, Yakubu AM, Fleming AF. Regression of Hodgkin's disease after measles. *Lancet* 1981; 1: 1112.

Telenius H, Carter NP, Bebb CE, Nordenskjold M, Ponder BA, Tunnacliffe A. Degenerate oligonucleotide-primed PCR: general amplification of target DNA by a single degenerate primer. *Genomics* 1992; 13: 718-725.

Thorbecke GJ, Amin AR, Tsiagbe VK. Biology of germinal centers in lymphoid tissue. *FASEB J* 1994; 8: 832-840.

Tijo JH, Levan A. The chromosome number in man. *Hereditas* 1956; 42: 1-6.

Tilly H, Bastard C, Delastre T, Duval C, Bizet M, Lenormand B, Dauce JP, Monconduit M, Piguet H. Cytogenetic studies in untreated Hodgkin's disease. *Blood* 1991; 77: 1298-1304.

Tosi S, Giudici G, Rambaldi A, Scherer SW, Bray-Ward P, Dirscherl L, Biondi A, Kearney L. Characterization of the human myeloid leukemia-derived cell line GF-D8 by multiplex fluorescence in situ hybridization, subtelomeric probes, and comparative genomic hybridization. *Genes Chromosomes Cancer* 1999; 24: 213-221.

Truant AL, Hallum JV. Detection of mumps virus antigens in Hodgkin's disease tissues. *Oncology* 1976; 33: 241-245.

Tsubosa Y, Sugihara H, Mukaisho K, Kamitani S, Peng DF, Ling ZQ, Tani T, Hattori T. Effects of degenerate oligonucleotide-primed polymerase chain reaction amplification and labeling methods on the sensitivity and specificity of metaphase- and array-based comparative genomic hybridization. *Cancer Genet Cytogenet* 2005; 158: 156-166.

Tzankov A, Zimpfer A, Lugli A, Krugmann J, Went P, Schraml P, Maurer R, Ascani S, Pileri S, Geley S, Dirnhofer S. High-throughput tissue microarray analysis of G1-cyclin alterations in classical Hodgkin's lymphoma indicates overexpression of cyclin E1. *J Pathol* 2003; 199: 201-207.

Uchida J, Yasui T, Takaoka-Shichijo Y, Muraoka M, Kulwichit W, Raab-Traub N, Kikutani H. Mimicry of CD40 signals by Epstein-Barr virus LMP1 in B lymphocyte responses. *Science* 1999; 286: 300-303.

Van Roosbroeck K, Lahortiga I, Cools J, Vandenberghe P, Marynen P, De Wolfe-Peeters C, Wlodarska I. A novel t(4;9)(q21;p24) fuses SEC31A to JAK2 in nodular-sclerosis Hodgkin lymphoma. 7th International Symposium on Hodgkin Lymphoma 2007.

Verma RS, Lubs HA. Variation in human acrocentric chromosomes with acridine orange reverse banding. *Humangenetik* 1975; 30: 225-235.

Vilchez RA, Madden CR, Kozinetz CA, Halvorson SJ, White ZS, Jorgensen JL, Finch CJ, Butel JS. Association between simian virus 40 and non-Hodgkin lymphoma. *Lancet* 2002; 359: 817-823.

Vockerodt M, Belge G, Kube D, Irsch J, Siebert R, Tesch H, Diehl V, Wolf J, Bullerdiek J, Staratschek-Jox A. An unbalanced translocation involving chromosome 14 is the probable cause for loss of potentially functional rearranged immunoglobulin heavy chain genes in the Epstein-Barr virus-positive Hodgkin's lymphoma-derived cell line L591. *Br J Haematol* 2002; 119: 640-646.

Wada M, Okamura T, Okada M, Teramura M, Masuda M, Motoji T, Mizoguchi H. Frequent chromosome arm 13q deletion in aggressive non-Hodgkin's lymphoma. *Leukemia* 1999; 13: 792-798.

Waldeyer W. Karyokinesis and its relation to the process of fertilization. *Q J Microsc Sci* 1890; 30: 159-281.

Waldheyer W. Uber Karyokinese und ihre Beziehung zu den Befruchtungsvorgangen.
Arch Mikrosk Anat 1888; 32: 1.

Wang D, Urisman A, Liu YT, Springer M, Ksiazek TG, Erdman DD, Mardis ER,
Hickenbotham M, Magrini V, Eldred J, Latreille JP, Wilson RK, Ganem D, DeRisi
JL. Viral discovery and sequence recovery using DNA microarrays. PLoS Biol 2003;
1: E2.

Wang F, Gregory C, Sample C, Rowe M, Liebowitz D, Murray R, Rickinson A, Kieff
E. Epstein-Barr virus latent membrane protein (LMP1) and nuclear proteins 2 and 3C
are effectors of phenotypic changes in B lymphocytes: EBNA-2 and LMP1
cooperatively induce CD23. J Virol 1990; 64: 2309-2318.

Wang GJ, Yang P, Xie HG. Gene variants in noncoding regions and their possible
consequences. Pharmacogenomics 2006; 7: 203-209.

Watanabe-Fukunaga R, Brannan CI, Copeland NG, Jenkins NA, Nagata S.
Lymphoproliferation disorder in mice explained by defects in Fas antigen that
mediates apoptosis. Nature 1992; 356: 314-317.

Weber-Matthiesen K, Deerberg J, Poetsch M, Grote W, Schlegelberger B. Numerical
chromosome aberrations are present within the CD30+ Hodgkin and Reed-Sternberg
cells in 100% of analyzed cases of Hodgkin's disease. Blood 1995; 86: 1464-1468.

Weber T, Weber RG, Kaulich K, Actor B, Meyer-Puttlitz B, Lampel S, Buschges R,
Weigel R, Deckert-Schluter M, Schmiedek P, Reifenberger G, Lichter P.
Characteristic chromosomal imbalances in primary central nervous system
lymphomas of the diffuse large B-cell type. Brain Pathol 2000; 10: 73-84.

Weinreb M, Day PJ, Niggli F, Powell JE, Raafat F, Hesselning PB, Schneider JW, Hartley PS, Tzortzatou-Stathopoulou F, Khalek ER, Mangoud A, El Safy UR, Madanat F, Al Sheyyab M, Mpofu C, Revesz T, Rafii R, Tiedemann K, Waters KD, Barrantes JC et al. The role of Epstein-Barr virus in Hodgkin's disease from different geographical areas. *Arch Dis Child* 1996; 74: 27-31.

Weiss LM, Movahed LA. In situ demonstration of Epstein-Barr viral genomes in viral-associated B cell lymphoproliferations. *Am J Pathol* 1989; 134: 651-659.

Wells D, Sherlock JK, Handyside AH, Delhanty JD. Detailed chromosomal and molecular genetic analysis of single cells by whole genome amplification and comparative genomic hybridisation. *Nucleic Acids Res* 1999; 27: 1214-1218.

White MK, Khalili K. Polyomaviruses and human cancer: molecular mechanisms underlying patterns of tumorigenesis. *Virology* 2004; 324: 1-16.

Wilson JB, Bell JL, Levine AJ. Expression of Epstein-Barr virus nuclear antigen-1 induces B cell neoplasia in transgenic mice. *EMBO J* 1996; 15: 3117-3126.

Wolf J, Kapp U, Bohlen H, Kornacker M, Schoch C, Stahl B, Mucke S, von Kalle C, Fonatsch C, Schaefer HE, Hansmann ML, Diehl V. Peripheral blood mononuclear cells of a patient with advanced Hodgkin's lymphoma give rise to permanently growing Hodgkin-Reed Sternberg cells. *Blood* 1996; 87: 3418-3428.

Wood KM, Roff M, Hay RT. Defective IkappaBalpha in Hodgkin cell lines with constitutively active NF-kappaB. *Oncogene* 1998; 16: 2131-2139.

Wu Q, Hoffmann MJ, Hartmann FH, Schulz WA. Amplification and overexpression of the ID4 gene at 6p22.3 in bladder cancer. *Mol Cancer* 2005; 4: 16.

Wu TC, Mann RB, Charache P, Hayward SD, Staal S, Lambe BC, Ambinder RF.

Detection of EBV gene expression in Reed-Sternberg cells of Hodgkin's disease. *Int J Cancer* 1990; 46: 801-804.

Xiao Q, Shen N, Hedvat CV, Moskowitz CH, Sussman LK, Filippa DA, Zelenetz AD, Houldsworth J, Chaganti RS, Teruya-Feldstein J. Differential expression patterns of c-REL protein in classic and nodular lymphocyte predominant Hodgkin lymphoma.

Appl Immunohistochem Mol Morphol 2004; 12: 211-215.

Yan W, Song L, Wei W, Li A, Liu J, Fang Y. Chromosomal abnormalities associated with neck nodal metastasis in nasopharyngeal carcinoma. *Tumour Biol* 2005; 26: 306-312.

Young KK, Heineke BE, Wechsler SL. M protein instability and lack of H protein processing associated with nonproductive persistent infection of HeLa cells by measles virus. *Virology* 1985; 143: 536-545.

Young L, Alfieri C, Hennessy K, Evans H, O'Hara C, Anderson KC, Ritz J, Shapiro RS, Rickinson A, Kieff E, . Expression of Epstein-Barr virus transformation-associated genes in tissues of patients with EBV lymphoproliferative disease. *N Engl J Med* 1989; 321: 1080-1085.

Yunis JJ, Sanchez O. The G-banded prophase chromosomes of man. *Humangenetik* 1975; 27: 167-172.

Zhdanov, V.M. Integration of viral genomes. *Nature* 1975; 256(5517):471-3.

Zhang J, Feuk L, Duggan GE, Khaja R, Scherer SW. Development of bioinformatics resources for display and analysis of copy number and other structural variants in the human genome. *Cytogenet Genome Res* 2006; 115: 205-214.

Zygiert Z. Hodgkin's disease: remissions after measles. *Lancet* 1971; 1: 593.

PUBLICATIONS FROM THESE STUDIES